5. SITE 643: NORWEGIAN SEA[1]

Shipboard Scientific Party[2]

HOLE 643A

Date occupied: 2 August 1985

Date departed: 8 August 1985

Time on hole: 116 hr

Position: 67°42.9′N, 01°02.0′E

Water depth (sea level; corrected m, echo-sounding): 2753

Water depth (rig floor; corrected m, echo-sounding): 2764

Bottom felt (rig floor; m, drill pipe measurement): 2779.8

Distance between rig floor and sea level (m): 11.1

Total depth (rig floor; m): 3345.0

Penetration (m): 565.2

Number of cores (including cores with no recovery): 61*

Total length of cored section (m): 565.2

Total core recovered (m): 449.2

Core recovery (%): 79.5

Oldest sediment cored:
Depth sub-bottom (m): 565.2
Nature: pyroclastic sandstone/mudstone
Age: middle-early(?) Eocene
Measured velocity (km/s): 2.1

Principal drilling results: The Cenozoic sedimentary section at Site 643 comprises five lithologic units, which in general can be correlated with the lithostratigraphic record of Site 642 at the outer Vøring Plateau:

Unit I. 0–49.4 m. Pleistocene to Recent. Glacial-interglacial sedimentary cycles consisting of alternations of dark, relatively carbonate-poor, and light, carbonate-rich layers of muds, sandy muds, and sandy calcareous muds. Moderate slumping is observed.

Unit II. 49.4–100.2 m. Late Miocene to Pleistocene. This unit is affected by slumping. Based on composition, it is subdivided into three subunits. Subunit IIA. 49.4–63.8 m. Pleistocene-Pliocene. Siliceous nannofossil ooze. Subunit IIB. 63.8–81.3 m. Early Pliocene-late Miocene. Predominantly terrigenous, containing siliceous muds and mud with only minor amounts of nannofossil ooze. Subunit IIC. 81.3–100.2 m. Late Miocene. Predominantly diatomaceous nannofossil ooze.

Unit III. 100.2–274.1 m. Early–late Miocene. Primarily diatom oozes.

Unit IV. 274.1–400.7 m. Early Miocene. Monotonous dark, extremely fossil-poor, terrigenous mudstones and minor gray nannofossil chalk.

Unit V. 400.7–565.2 m. Early–middle Eocene to late Oligocene. Predominantly dark greenish gray to dark reddish brown and grayish brown zeolitic mudstones, most of which are intensively compacted and laminated.

The lowermost two cores contain pebble- to cobble-sized basaltic fragments, a polymict conglomerate of pyroclastic rocks, and a dark basaltic conglomerate. We interpret this to indicate that drilling terminated in a basal sequence overlying the oceanic basement.

The two lower units are reflected by distinct changes in bulk density. Except for a few local high-seismic velocity beds, the seismic velocity is low, averaging 1.65 km/s throughout the section.

The Neogene sedimentary sequence contains numerous volcanic ashes that can be correlated with great precision to the air-fall tephra layers found at Site 642.

Site 643 never experienced shallow-water depositional environments and can be considered the deep-water analog to the DSDP sites on the Vøring Plateau and ODP Site 642. However, the sedimentation rates are higher than anticipated, mainly because of the presence of slumped sediment layers. Nevertheless, Site 643 provides a record of the depositional environments under the seaward boundary of the Norwegian Current and from water depths close to the Norwegian Sea basin floors.

SITE 643 SUMMARY

ODP Site 643 was located on the lower slope near the foot of the outer Vøring Plateau, seaward of the dipping reflector sequence and in an area underlain by typical oceanic basement. The site is located just landward of magnetic anomaly 23 near the presumed oldest crust in the Norwegian–Greenland Sea.

The site forms the western end of a paleoenvironmental transect across the outer Norwegian margin. The single-bit Hole 643A penetrated a 565.2-m-thick pelagic and hemipelagic Cenozoic sedimentary sequence. A total of 62 cores were recovered, consisting of 16 hydraulic piston core-barrel (HPC) cores (0–147.8 m) and 46 extended core-barrel (XCB) cores (147.8–565.2 m). Poor hole conditions prevented further drilling as well as the planned logging program.

Drilling results are summarized in a stratigraphic section (Fig. 1).

BACKGROUND AND OBJECTIVES, SITE 643

Site 643 represents the seaward end of the northwest-trending paleoenvironmental site transect. The transect crosses the Vøring Plateau, extending from the central to lower continental slope (Fig. 2). This transect allows us to study the history of one of the most important elements of the Norwegian–Greenland Sea surface-water current regimes, namely the Norwegian Current. In addition to establishing the history of the surface water masses, a major objective is to establish the history of the abyssal

---

[1] Eldholm, O., Thiede, J., Taylor, E., et al., 1987. *Proc., Init. Repts. (Pt. A), ODP*, 104.

[2] Olav Eldholm, (Co-Chief Scientist), University of Oslo, Oslo, Norway; Jørn Thiede (Co-Chief Scientist), Christian-Albrechts-Universität, Kiel, FRG; Elliott Taylor (Staff Scientist), ODP, Texas A&M University, College Station, TX; Colleen Barton, Stanford University, Stanford, CA; Kjell Bjørklund, University of Oslo, Oslo, Norway; Ulrich Bleil, Universität Bremen, Bremen, FRG; Paul R. Ciesielski, University of Florida, Gainesville, FL; Alain Desprairies, Université de Paris Sud, Orsay, France; Diane Donnally, Amoco Production Co., New Orleans, LA; Claude Froget, Faculté des Sciences de Luminy, Marseille, France; Robert Goll, IKU/SINTEF, Trondheim, Norway; Rudiger Henrich, Christian-Albrechts Universität, Kiel, FRG; Eystein Jansen, University of Bergen, Bergen, Norway; Larry Krissek, Ohio State University, Columbus, OH; Keith Kvenvolden, USGS, Menlo Park, CA; Anne LeHuray, Lamont-Doherty Geological Observatory, Palisades, NY; David Love, University of Waterloo, Ontario, Canada; Peter Lysne, Sandia National Laboratory, Albuquerque, NM; Thomas McDonald, Texas A&M University, College Station, TX; Peta Mudie, Geological Survey of Canada, Nova Scotia, Canada; Lisa Osterman, Smithsonian Institution, Washington, DC; Lindsay Parson, Institute of Oceanographic Sciences, Surrey, UK; Joseph Phillips, University of Texas, Austin, TX; Alan Pittenger, Texas A&M University, College Station, TX; Gunnbjørg Qvale, Norsk Hydro, Oslo, Norway; Günther Schönharting, University of Copenhagen, Copenhagen, Denmark; Lothar Viereck, Ruhr Universität, Bochum, FRG.

*Although 62 cores were taken, Core 58 is a miscellaneous core. Therefore, it is treated as a sample and excluded in the core recovery calculation.

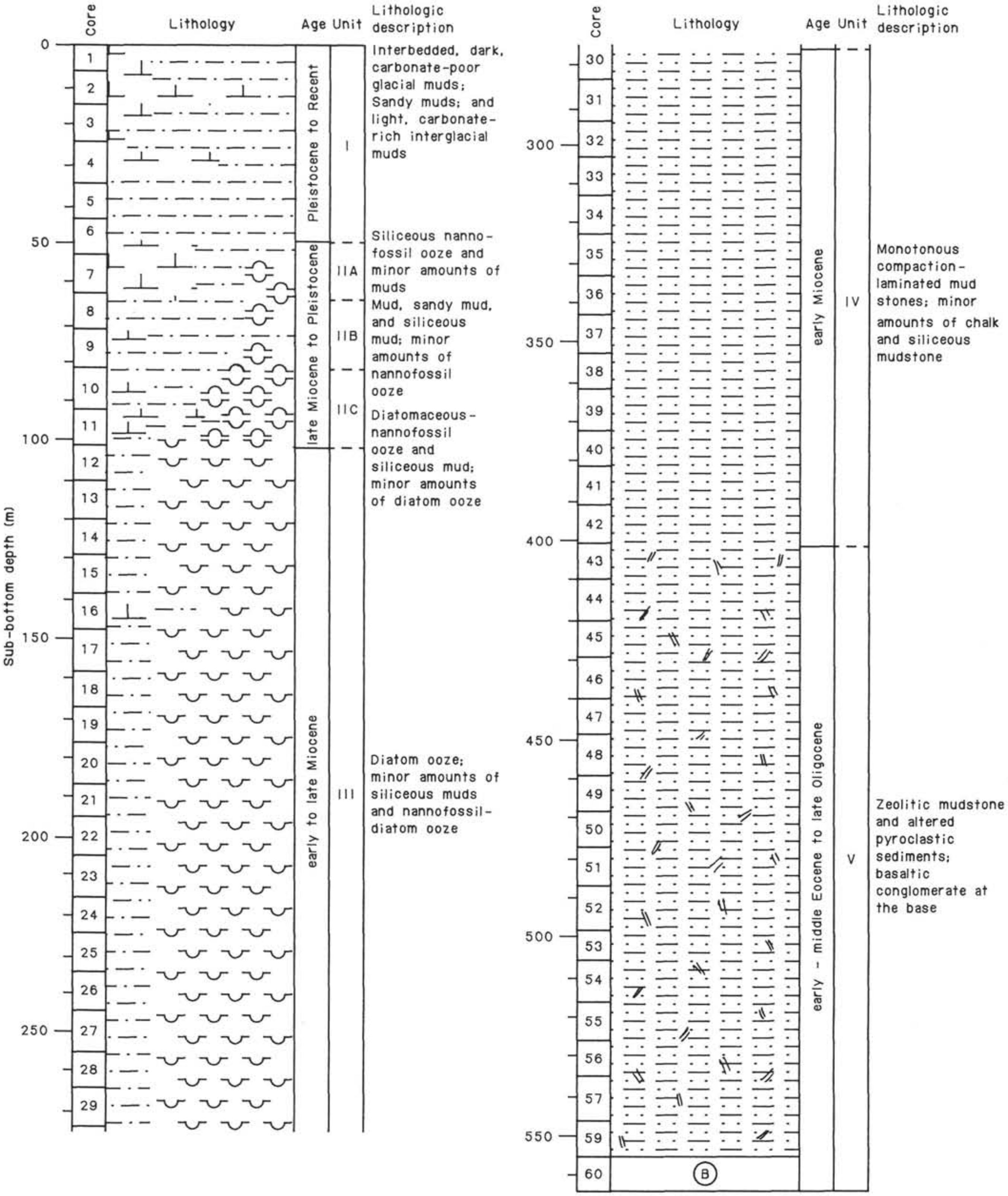

Figure 1. Graphic summary of lithologic units at Site 643. Bedding thicknesses presented are schematic.

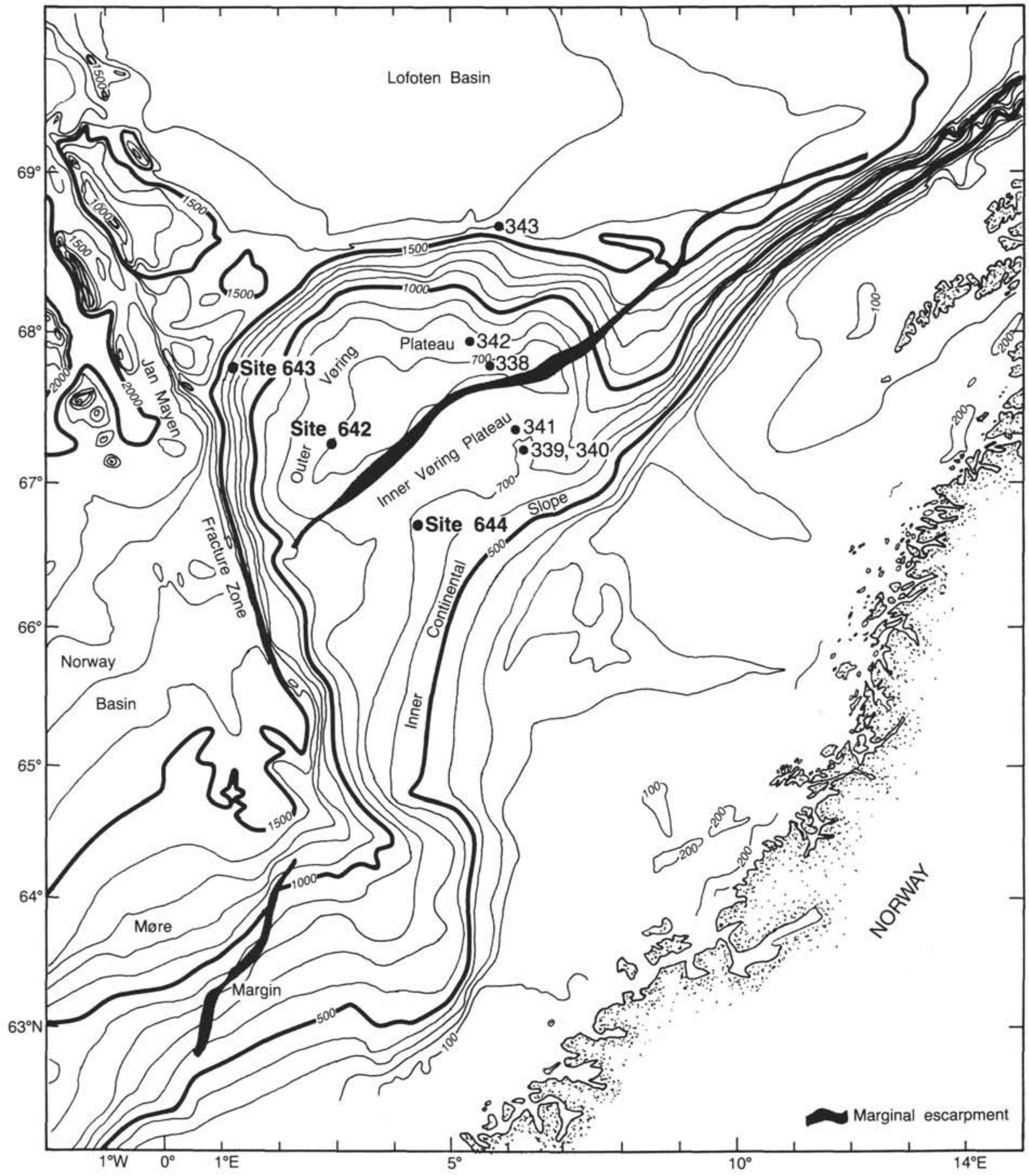

Figure 2. Bathymetry and location of ODP sites on the Vøring Plateau.

Norwegian-Greenland Sea water masses. The modern mode of deep-water formation, mainly in the Greenland Basin, results in a rapid renewal of the bottom-water masses and, therefore, a well-oxygenated seafloor in the Norwegian-Greenland Sea deep basins.

An examination of seismic records in light of having completed Site 642, where a nearly complete Neogene pelagic sediment section and a thick volcanic sequence of probable Eocene age had been penetrated, indicated that a Paleogene pelagic section could be recovered at Site 643. Little is presently known about the Paleogene depositional environments, other than that they are characterized by increasing isolation from the North Atlantic. The poorly understood paleoceanography of this region suggests that a relatively warm and narrow subpolar ocean basin existed during the Paleocene (Thiede, 1980).

Drilling at Site 643 was planned to reach the oceanic basement. Site 643 is located close to magnetic anomaly 23 (Fig. 3) in approximately 2750-m water depth, just above the floor of the adjacent Lofoten Basin. It was considered particularly important to compare the volcanic rocks of this "typical" oceanic

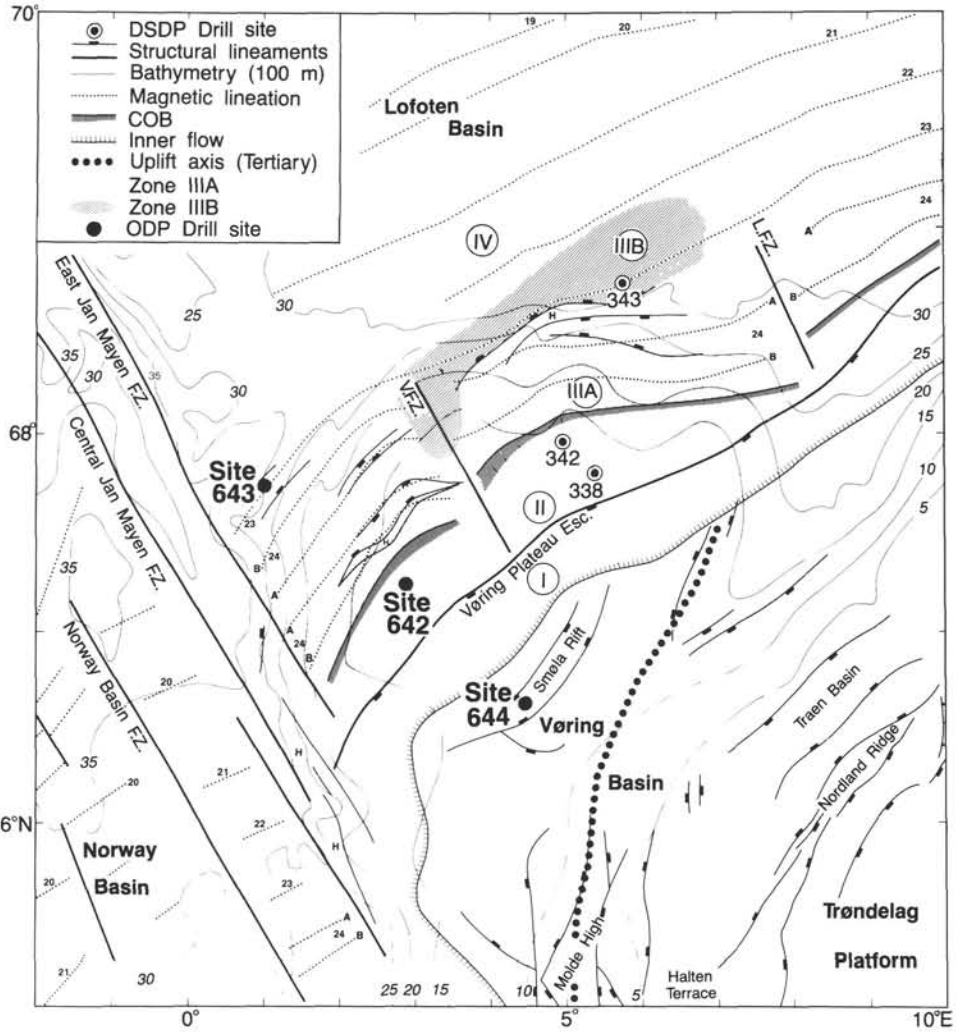

Figure 3. Main structural features, seafloor-spreading magnetic anomalies and simplified bathymetry (hundreds of meters) in the Norwegian-Greenland Sea. Zone III outlines the extent of the seaward-dipping reflectors. From Skogseid and Eldholm (unpublished).

basement of early Eocene age with the basalts encountered at Site 642, and to establish the subsidence history of this region relative to the Vøring Plateau marginal high.

The location of Site 643 in 2750 m of water was selected on MCS line NH-1 (Fig. 4). This seismic reflection profile displays a clear record of oceanic basement beneath the flank of the Vøring Plateau, below a younger stratified pelagic sediment sequence. Within the sediment section, reflectors corresponding to the base-Miocene, mid-Oligocene, base-Oligocene, and base-Eocene have been identified, suggesting a relatively complete sediment section. The selected locality is found near SP 9440, at the seaward flank of a small depression in the underlying basement. This location was determined (1) to avoid the erosion expected to have affected the sedimentary record on top of the basement highs, (2) to avoid the ponded sediments in the basement depressions, and (3) to allow sampling of a sediment section and basement with a single-bit hole.

The scientific objectives of Site 643 were as follows:

1. To sample the Cenozoic (Quaternary to Eocene or older) sedimentary section above the oceanic basement;
2. To obtain samples of the oceanic basement to determine its nature and age, as well as composition and age of the sediment immediately overlying the basement;
3. To help establish the subsidence history of Site 642 and relate it to the subsidence history of the Vøring marginal high;
4. To investigate changes of the Norwegian Current and of Cenozoic Northern Hemisphere paleoceanography through variations of sediments and pelagic, as well as benthic, fossil assemblages;
5. To determine the history of the Norwegian Current water properties;
6. To monitor the paleoclimatic and paleoceanographic variability of the Northern Hemisphere glacial and interglacial cycles during the past 3-6 m.y. and to document the influx, petrology, and possibly source regions of ice-rafted debris;
7. To investigate the onset of Northern Hemisphere glaciations and to establish the nature and properties of the "pre-Glacial"-type depositional environments in the Norwegian-Greenland Sea;
8. To study the problems of endemism of Norwegian-Greenland Sea pelagic floras and faunas and of the impact of the Greenland-Scotland Ridge sill on the biota;
9. To establish stratigraphic type-sections for some of the major oceanic microfossil groups and to correlate the biostratigraphies obtained with a well-defined magnetostratigraphy;
10. To determine the physical and chemical properties of the polar to subpolar sediments and their relationship to the widespread mass wasting and slumping;
11. To establish a tephrachronology of ashes known to occur in the Cenozoic sediment column and, if possible, to relate the volcanic ashes to volcanic provinces;

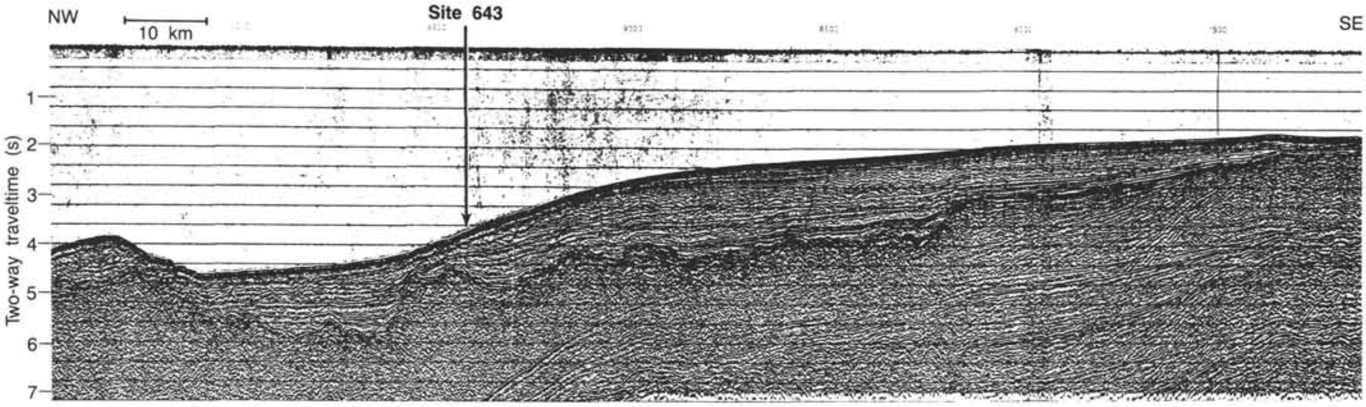

Figure 4. Multichannel seismic line NH-1 with location of Site 643.

12. And finally, to attempt a correlation of paleoceanographic events with the paleoclimatic evolution on nearby land areas through investigations of palynomorphs and of erosional debris derived from the nearby Caledonides.

SITE 643 OPERATIONS

Site 642 to Site 643

August 2, 1985, was a bad day for acoustic beacons. The beacon that had been deployed on the taut wire at Site 642 was lost, along with the taut wire weight, when the wire parted just as the beacon and weight were being hoisted aboard before departure. Good steaming weather permitted preassembly of part of the bottom-hole assembly (BHA), giving us a head start on operations at Hole 643A. We launched an acoustic beacon at 0607 hr, 2 August, just 6 hr after departing the previous site. We retrieved the seismic gear, continued to deploy the BHA, and lowered thrusters and hydrophones as the ship maneuvered onto the drill site at low speed. Upon returning to the drop point we learned that the beacon signal was too weak to use for pipe operations. We then dropped a standby beacon to replace it. The second unit failed completely after about 5 min. We then had to rig and deploy a third beacon (with a third frequency) before satisfactory positioning could be achieved.

Hole 643A—Vøring Plateau, Outer Flank

Because the drill site sloped considerably, there was reason to believe that the precision depth recorder reading of 2764 m was somewhat shallow. We therefore "shot" the first piston core from 2766 m. The correction allowance proved inadequate, however, as we recovered only a "water core." We then advanced the pipe one joint for the next core and established water depth at 2779.8 m from drilling datum.

We took HPC cores to 148 meters below seafloor (mbsf) with good results, primarily in glacial muds. At that depth an overpull of 60,000 lb was required to retract the core barrel from the sediment, and we converted to the XCB. We reduced the circulation rate after the first two XCB attempts produced low recovery. Good core recovery then continued during drilling of the remainder of the hole except for a zone of laminated, terrigenous mudstones between about 300 and 400 mbsf. Both recovery and penetration rates were less through this interval. Cores were considerably more disturbed in general than when using the XCB at Hole 642D.

The hole was nearly lost after a 467-m penetration when the sinker bar assembly parted at the wireline swivel. The nature of the break necessitated fabrication of a special makeshift fishing overshot. Fortunately, the fishing effort was successful on the first attempt, and the sinker bar/jar assembly and a full core barrel were recovered intact from the drill string.

Hole conditions remained excellent to about 530 mbsf, when unstable conditions were encountered without even the warning signal of a low-recovery core. Torquing, sticking, "packing off," and several meters of hole fill, consisting of large chunks of hard mudstone, had to be overcome by pumping polymer mud slugs and "working" the pipe. With the hole apparently stabilized, we continued coring, and began hard drilling at about 558 mbsf. Two short pieces of basalt core were found in the core-catcher. During attempts to take short Navidrill Core Barrel cores with special hard-formation cutter shoes, hole conditions again deteriorated badly. The XCB proved ineffective in the basement material, with low recovery and very low penetration rates. The situation seemed tailor-made for the planned further testing of the NCB system, but the hole could not be stabilized enough to risk deployment of the expensive prototype corer (or any further coring attempts). Coring operations were terminated at 3345 m (565 mbsf). The coring summary for Hole 643A is listed in Table 1.

In preparation for logging operations, we rigged down the top drive and pulled the bit to 2858 m (78 mbsf). We rigged the Schlumberger LSS/DIL/GR logging assembly and ran it into the hole, only to be stopped by an obstruction 70 m below the bit. When we could not advance the logging sonde deeper into the hole, it was retrieved and three stands of drill pipe were added to the string to put the bit at 2945 m. We redeployed the same logging tool and again it was stopped by an obstruction—this time at 2999 m. With operating time running out, we abandoned plans for open-hole logging. Our best odds of recovering useful log data appeared to be with the gamma-spectral-tool (GST) log, which can be recorded through pipe. Because of the good hole conditions during most of the coring operations, we felt that logging through pipe could be conducted fairly safely above the depth of first indications of an unstable hole. Intending to locate the bit at about 3300 m, just above the unstable zone, we ran the pipe back into the hole. After five stands of drill pipe had been added, however, an obstruction in the hole stopped the bit. We added additional pipe, which was bent just above the seafloor, preventing its rotation and effectively preventing any further logging attempts.

We recovered the drill string to the bent interval and laid out nine joints before the lowermost portion of the string could be brought aboard. The ship departed Site 643 at 0200 hr, 8 August.

Table 1. Coring summary, Site 643.

Core no.	Core type[a]	Date	Time (LST)	Sub-bottom depths top (m)	Sub-bottom depths bottom (m)	Length cored (m)	Length recovered (m)	Amount recovered (%)
1	H	AUG-02-1985	1700	0	5.3	5.3	5.3	99.0
2	H	AUG-02-1985	1750	5.3	14.8	9.5	9.8	103.3
3	H	AUG-02-1985	1853	14.8	24.3	9.5	9.8	103.3
4	H	AUG-02-1985	2025	24.3	33.8	9.5	9.9	104.3
5	H	AUG-02-1985	2117	33.8	43.3	9.5	9.4	99.2
6	H	AUG-02-1985	2212	43.3	52.8	9.5	8.7	92.0
7	H	AUG-02-1985	2306	52.8	62.3	9.5	8.2	85.8
8	H	AUG-02-1985	2359	62.3	71.8	9.5	9.5	99.7
9	H	AUG-03-1985	0055	71.8	81.3	9.5	9.9	104.3
10	H	AUG-03-1985	0145	81.3	90.8	9.5	9.5	100.2
11	H	AUG-03-1985	0240	90.8	100.3	9.5	9.9	104.2
12	H	AUG-03-1985	0340	100.3	109.8	9.5	9.3	97.9
13	H	AUG-03-1985	0425	109.8	119.3	9.5	9.8	103.4
14	H	AUG-03-1985	0522	119.3	128.8	9.5	9.1	96.1
15	H	AUG-03-1985	0607	128.8	138.3	9.5	9.4	99.1
16	H	AUG-03-1985	0655	138.3	147.8	9.5	10.1	106.2
17	X	AUG-03-1985	0820	147.8	157.3	9.5	0.7	7.1
18	X	AUG-03-1985	0943	157.3	166.8	9.5	3.7	39.2
19	X	AUG-03-1985	1055	166.8	176.3	9.5	9.5	99.9
20	X	AUG-03-1985	1220	176.3	185.8	9.5	9.7	102.5
21	X	AUG-03-1985	1345	185.8	195.3	9.5	3.8	39.9
22	X	AUG-03-1985	1500	195.3	205.1	9.8	9.8	99.5
23	X	AUG-03-1985	1634	205.1	214.9	9.8	9.8	100.2
24	X	AUG-03-1985	1735	214.9	224.7	9.8	9.8	99.8
25	X	AUG-03-1985	1850	224.7	234.5	9.8	9.9	100.5
26	X	AUG-03-1985	2005	234.5	244.3	9.8	9.8	100.2
27	X	AUG-03-1985	2120	244.3	254.1	9.8	9.7	99.1
28	X	AUG-03-1985	2235	254.1	263.9	9.8	9.8	99.7
29	X	AUG-03-1985	2347	263.9	273.7	9.8	9.8	100.5
30	X	AUG-04-1985	0120	273.7	283.5	9.8	0.9	9.6
31	X	AUG-04-1985	0330	283.5	293.3	9.8	9.8	100.4
32	X	AUG-04-1985	0535	293.3	303.1	9.8	4.9	49.8
33	X	AUG-04-1985	0720	303.1	312.9	9.8	4.9	49.8
34	X	AUG-04-1985	0818	312.9	322.7	9.8	4.0	41.0
35	X	AUG-04-1985	1120	322.7	332.5	9.8	3.8	38.7
36	X	AUG-04-1985	1315	332.5	342.3	9.8	8.8	90.0
37	X	AUG-04-1985	1505	342.3	352.1	9.8	6.2	62.9
38	X	AUG-04-1985	1642	352.1	361.8	9.7	3.7	37.6
39	X	AUG-04-1985	1820	361.8	371.4	9.6	3.7	38.0
40	X	AUG-04-1985	2045	371.4	381.1	9.7	1.1	11.0
41	X	AUG-05-1985	0010	381.1	390.7	9.6	1.8	19.0
42	X	AUG-05-1985	0240	390.7	400.4	9.7	5.3	54.5
43	X	AUG-05-1985	0425	400.4	410.0	9.6	0.4	4.3
44	X	AUG-05-1985	0555	410.0	419.7	9.7	9.9	101.8
45	X	AUG-05-1985	0710	419.7	429.4	9.7	9.0	92.6
46	X	AUG-05-1985	0830	429.4	439.1	9.7	9.8	101.2
47	X	AUG-05-1985	1005	439.1	448.7	9.6	9.8	102.1
48	X	AUG-05-1985	1125	448.7	458.4	9.7	9.8	101.2
49	X	AUG-05-1985	1630	458.4	468.1	9.7	9.7	100.4
50	X	AUG-05-1985	1910	468.1	477.7	9.6	1.2	12.8
51	X	AUG-05-1985	2100	477.7	487.3	9.6	9.8	102.0
52	X	AUG-05-1985	2240	487.3	497.0	9.7	9.9	101.5
53	X	AUG-06-1985	0026	497.0	506.7	9.7	9.2	94.8
54	X	AUG-06-1985	0241	506.7	516.4	9.7	10.0	102.9
55	X	AUG-06-1985	0430	516.4	526.0	9.6	9.8	102.3
56	X	AUG-06-1985	0650	526.0	535.6	9.6	9.7	101.3
57	X	AUG-06-1985	0850	535.6	545.2	9.6	9.7	100.7
58	M	AUG-06-1985	1110	545.2	545.2	0	8.7	?
59	X	AUG-06-1985	1343	545.2	554.9	9.7	2.0	20.6
60	X	AUG-06-1985	1640	554.9	561.2	6.3	3.7	59.2
61	X	AUG-06-1985	1945	561.2	563.7	2.5	1.8	70.0
62	X	AUG-07-1985	0205	563.7	565.2	1.5	1.7	115.3

[a] H = hydraulic piston; X = extended core barrel; M = re-cored interval.

SEDIMENT LITHOLOGY

Lithologic Summary

The sedimentary sequence drilled at Site 643 has been subdivided into five units: Unit I is a terrigenous-dominated unit of glacial/interglacial depositional cycles, Unit II contains a mixture of terrigenous/siliceous biogenic/calcareous biogenic deposits and has been split into three subunits, Unit III is a siliceous biogenic unit, Unit IV consists of terrigenous mudstones, and Unit V contains terrigenous and volcaniclastic mudstones and coarser sediments. The lithologic divisions are summarized in Table 2 and Figure 1, while the smear-slide compositional data for these units are included in the barrel sheets and summarized in Figure 5. Shipboard carbonate analyses are presented in Figure 6. Additional compositional data were obtained by semi-quantitative X-ray diffraction (XRD) analysis of pressed pow-

Table 2. Summary of lithologic units, Site 643.

Unit	Dominant lithology	Interval depth (mbsf)	Age	Occurrence (core 104-)
I	Interbedded, dark, carbonate-poor glacial muds; sandy muds; and light, carbonate-rich interglacial muds	0–49.42	Pleistocene to Recent	643A-1H to 6H-5, 12 cm
IIA	Siliceous nannofossil ooze and minor amounts of muds	49.42–63.80	Pleistocene	643A-6H-05, 12 cm to 643A-8H-01, 150 cm
IIB	Mud, sandy mud, and siliceous mud; minor amounts of nannofossil ooze	63.80–81.30	to	643A-8H-02, 1 cm to 643A-9H-CC, 34 cm
IIC	Diatomaceous-nannofossil ooze and siliceous mud; minor amounts of diatom ooze	81.30–100.15	late Miocene	643A-10H-01, 1 cm to 643A-11H-07, 35 cm
III	Diatom ooze, minor amounts of siliceous muds, and nannofossil-diatom ooze	100.15–274.05	late Miocene to early Miocene	643A-11H-07, 35 cm to 643A-30H-CC, 35 cm
IV	Monotonous compaction-laminated mudstones, minor amounts of chalk, and siliceous mudstone	274.05–400.70	early Miocene	643A-30H-CC, 35 cm to 643A-43H-CC, 43 cm
V	Zeolitic mudstone and altered pyroclastic sediments; basaltic conglomerate at the base	400.70–565.20	late Oligocene to early-middle Eocene	643A-43H-CC, 43 cm to 643A-62H-CC, 28 cm

ders (see "Explanatory Notes" chapter, "Shipboard X-Ray Diffraction Analysis," this volume, for a more complete explanation of this method); these results are shown in Figure 7. Distal air-fall tephra deposits are a minor to common component within Units I through III; these are considered separately below.

Unit I: Section 104-643A-1H-1 to Section 104-643A-5H-7, 12 cm (0–49.42 m sub-bottom)

Age: Pleistocene to Recent.

Unit I is a 50-m-thick sequence of glacial-interglacial sedimentary cycles, characterized by repeated alternations of dark, relatively carbonate-poor, and light, carbonate-rich layers. Intervals containing closely spaced, dark subunits represent glacial stages, while interglacial stages are represented by widely spaced, dark subunits. Both dark and light layers at Site 643 generally contain higher carbonate contents than the corresponding lithologies at Site 642. The dark layers are also much thicker at Site 643. The lowermost 7 m of Unit I at Site 643 has been affected by downslope slumping.

Unit I consists predominantly of muds, sandy muds, and sandy calcareous muds that display a repeated alternation of dark and light layers similar to the pattern observed at Site 642 (Figs. 5, 8, and 9; compare with "Lithologic Summary," Site 642 chapter, this volume). The light layers at Site 643 exhibit slight differences relative to the light layers at Site 642, however, in that grayish brown (2.5YR 5/2) and dark brownish gray (2.5Y 4/2) dominate gray (5Y 5/1), olive gray (5Y 5/2, 5Y 4/2), and greenish gray (5GY 5/1). These light layers consist of 3%–40% quartz (about 30% average), 0%–5% feldspar (about 2%), 10%–70% clay (about 40%), 0%–30% other minerals (especially detrital carbonates), 0%–55% foraminifers (about 22%), and 0%–10% nannofossils (trace). Results of XRD analyses indicate that illite is relatively more common than chlorite in the light layers. The clay mineral assemblage suggests the influence of a continental source. Bioturbation is common in the light layers, especially in the form of small burrow tubes approximately 2 mm in diameter. Foraminifer and carbonate contents (Figs. 5 and 6) are generally higher in the light layers than at Site 642, and a similar relationship is also observed for the glacial periods at these sites. A general trend of decreasing carbonate downcore is observed in the sediments of Site 643 (Figs. 5–7).

The dark layers in Unit I at Site 643 display a variety of lithofacies types. The most important of these is the lithologic change that may represent the termination of a glacial maximum stage and the transition to an interglacial period. This transition is recorded by a specific sequence of deposits, which consists of a basal, very dark gray sandy mud with scattered dropstones, grading upward into a laminated, dark olive-gray mud, commonly sand-rich, and overlain by a carbonate-rich, extensively bioturbated, light-colored horizon. The basal subunit may record times of maximum glaciation and complete pack-ice coverage, the laminated subunit may represent most of the deglaciation event, and the uppermost horizon may have been deposited during an interglacial or interstadial period. Unit I contains approximately 22 to 24 of these major deglaciation units.

Additional lithofacies within the dark layers include very dark gray (5Y 3/1) to black layers (5Y 2/1) with both sharp bases and tops, and dark olive gray (5Y 3/2), laminated sandy muds. The very dark gray beds may represent relatively short-term cooling events within a longer glacial period, and thereby reflect minor climatic oscillations. The dark olive gray laminated horizons may indicate short-term warming periods, associated with minor changes in climatic conditions within the longer glacial periods.

The composition of the dark layers at Site 643 consists of 5%–60% quartz (average about 42%), 0%–5% feldspar (about 2%), 30%–70% clay (about 42%), 0%–20% other minerals (about 10%), 0%–15% foraminifers (about 1%), and 0%–5% nannofossils (about 1%). Results of the XRD analyses confirm the presence of less carbonate, more feldspar, and a clay mineral assemblage dominated by chlorite within the dark layers. The abundance of chlorite and illite suggests that a continental source was also predominant during deposition of the dark layers.

The abundance and characteristics of dark layers vary from Site 643 to Site 642. The total number of dark layers observed at Site 643 is much smaller than at Site 642, while the average thickness of individual beds is much larger at Site 643 (Figs. 8 and 9; compare with "Sediment Lithology," Site 642 chapter, this volume). These variations suggest that the climatic record observed in the alternating dark and light layers may be overprinted by regional changes across the Vøring Plateau related to proximity to the continental sediment source and intensity of

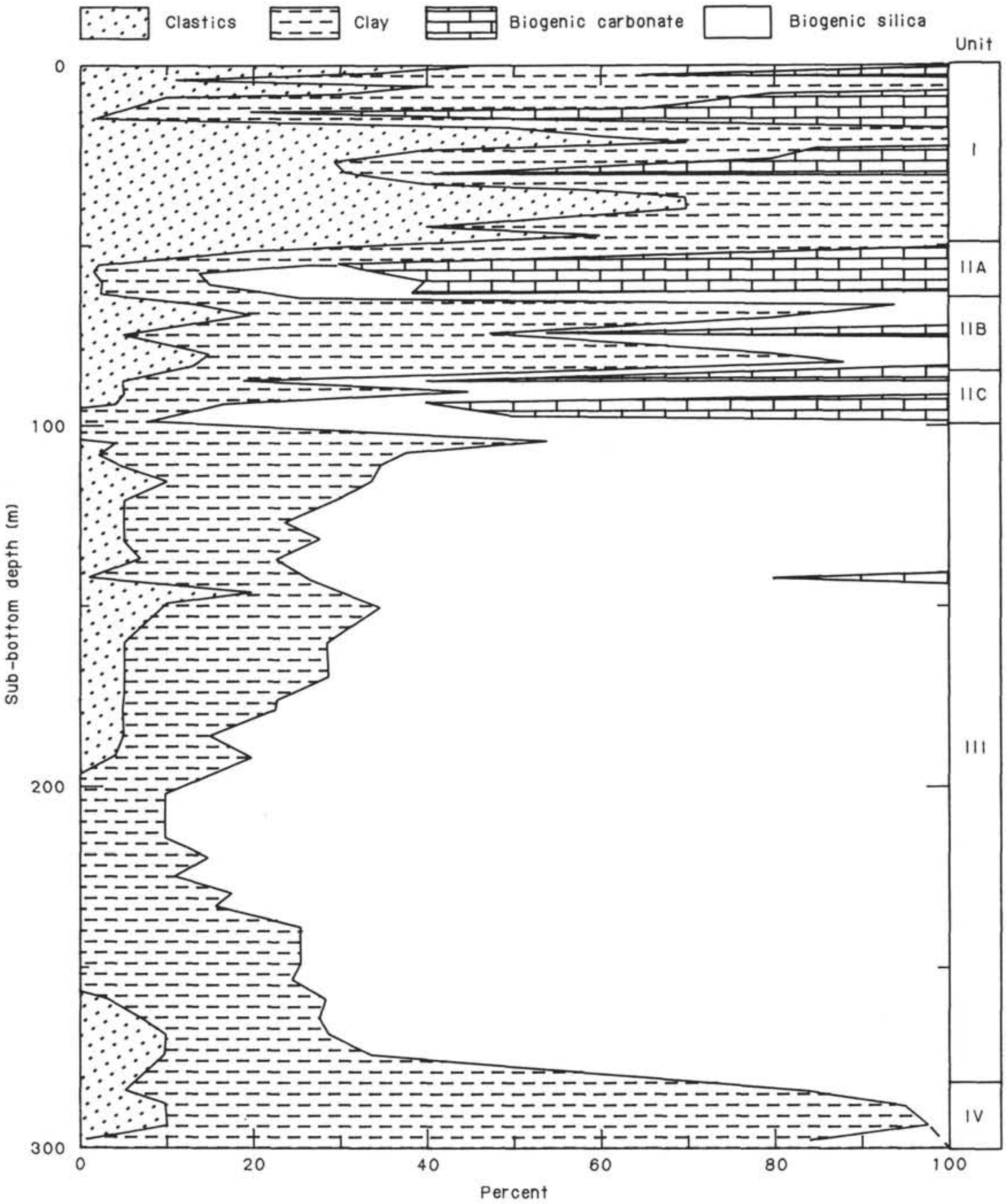

Figure 5. Summary of the composition of major lithologies at Site 643 from shipboard smear-slide data. The compositions of Units IV and V are essentially constant down to the base of Site 643.

iceberg drift. This overprinting may complicate preliminary attempts to trace the climatic record in this region, based solely on the distribution of dark sediment layers.

Despite the potential complications, the dark layers at Sites 642 and 643 can be correlated quite well over the respective Unit Is (compare Figs. 8 and 9 with the "Sediment Lithology" section, Site 642 chapter, this volume). The correlation becomes less convincing in the lowermost portion of Unit I, where the previously mentioned slumping appears to disrupt the pattern at Site 643 relative to Site 642. Within this lower interval, the major anomaly is a pronounced peak in the thickness of individual black layers (Fig. 8) and in the areal coverage of dark layers (Fig. 9). This anomalous increase is the only major reversal observed within the general downcore pattern of decreasing dark layer amplitude and increasing dark layer frequency observed at both Sites 642 and 643 (compare Figs. 8 and 9 with "Sediment Lithology" section, Site 642 chapter, this volume).

The uppermost, obviously slumped, sediment section is located at 42.7-43.3 m sub-bottom. Between this interval and the base of Unit I, two major dark layers contribute to the anomalous increase in dark layer thickness and areal coverage. Each of these layers consists of a predominant black horizon, overlain by a dark gray to dark greenish gray deposit that contains numerous large, reworked dark olive gray, dark gray, and dark greenish gray mudstone clasts interpreted as a debris flow deposit. In addition, an overconsolidated olive gray mud to mud-

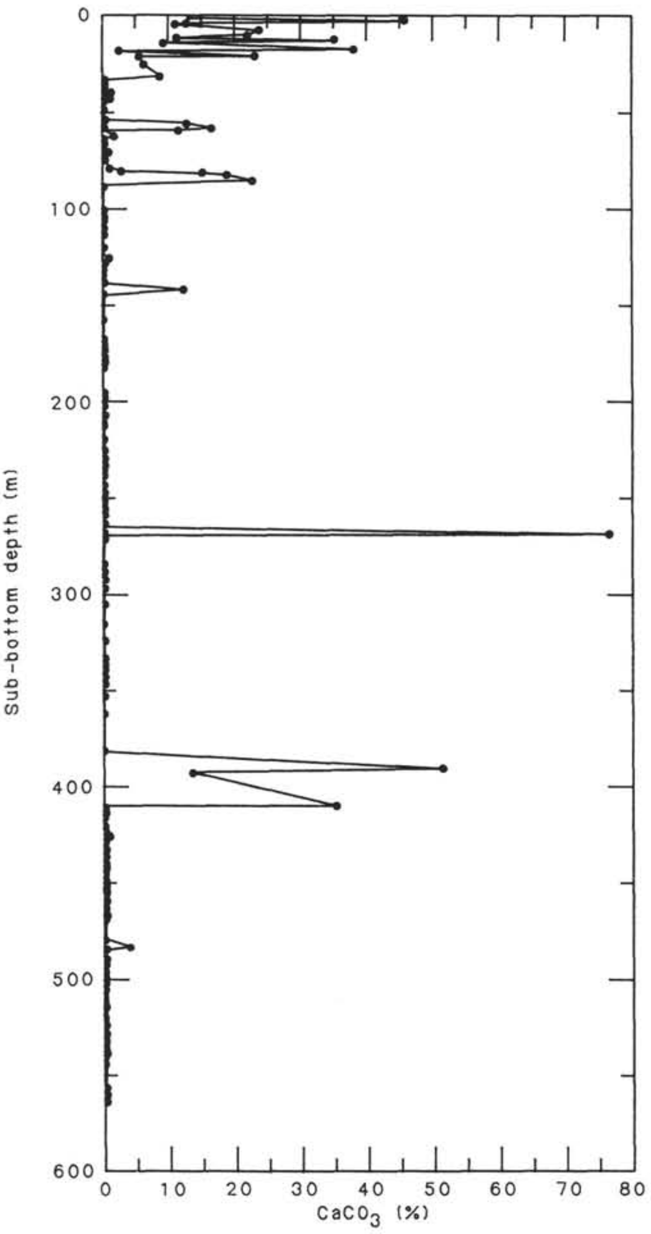

Figure 6. Carbonate contents at Site 643, determined by shipboard analysis.

stone, interbedded between very dark gray layers at 49.35 m sub-bottom, can be interpreted as the basal surface of a slump block. Two explanations can be advanced to account for the presence of these four horizons. The first suggests that multiple small-scale slumps and debris flows have affected the lowermost 7 m of Unit I. The second explanation interprets the horizon at 49.35 m as the basal surface of a larger slump block extending from 49.35 to 42.7 m because of the overconsolidated nature of the lowermost horizon. Detailed examination of physical structures and chronostratigraphic data from this interval should provide a better understanding of the depositional mechanisms active during the deposition of lower Unit I.

The distribution of calcium carbonate with depth exhibits three distinct patterns within Unit I (Fig. 6). The uppermost interval (0–20.5 m) contains high-frequency/high-amplitude fluctuations in carbonate content, and records rapid and pronounced

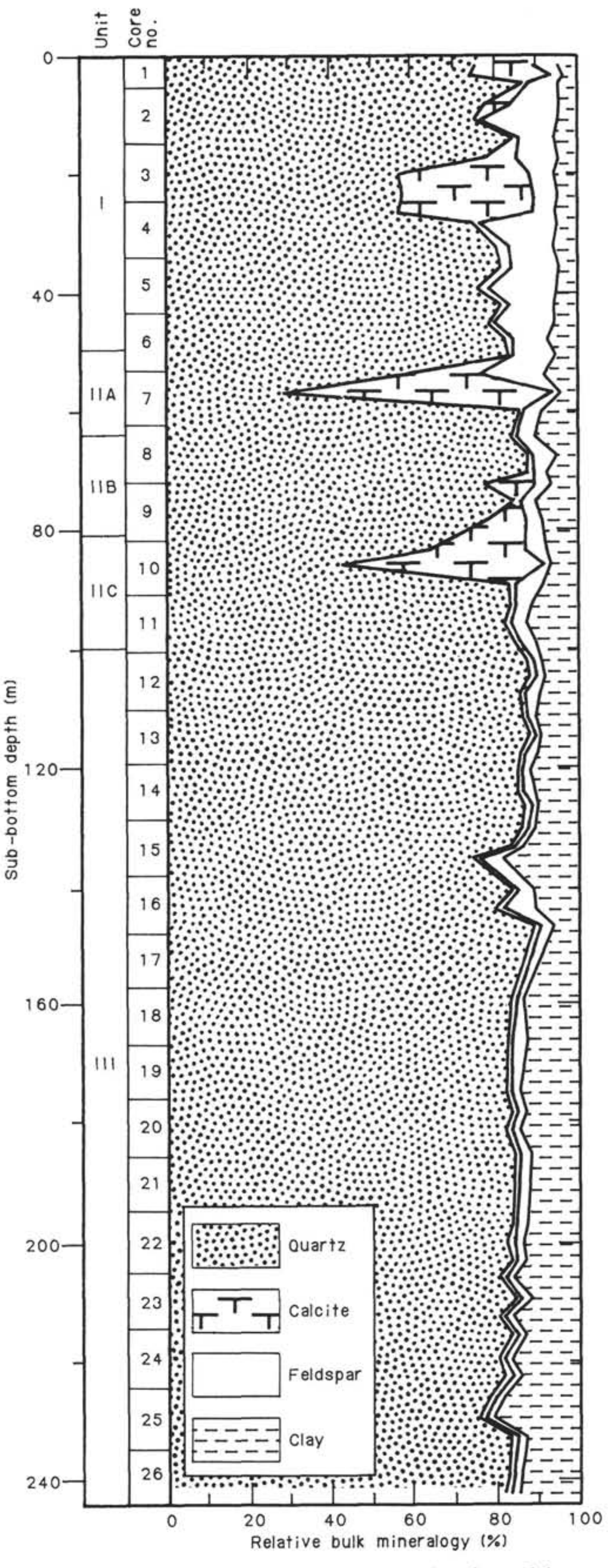

Figure 7. Semiquantitative estimates of the bulk mineralogy of the major lithologic units at Hole 643, based on X-ray-diffraction peak area ratios.

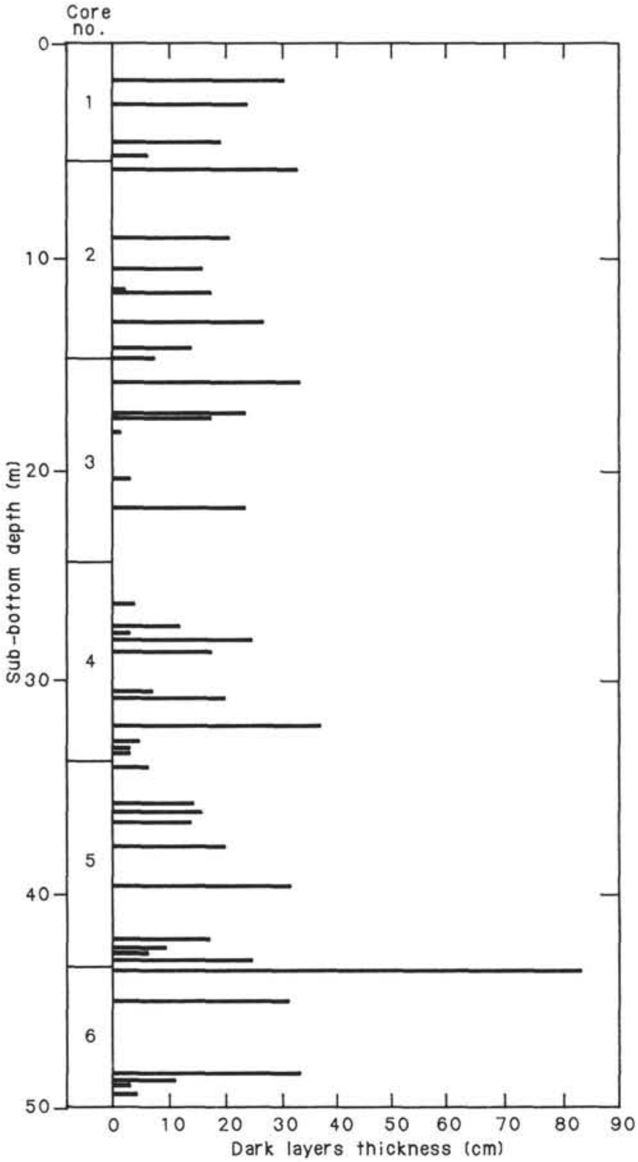

Figure 8. Thickness (cm) of individual dark layers in Unit I, plotted as a function of sub-bottom depth for Site 643. These dark layers record periods of maximum glaciation; note general decrease in intensity and increase in frequency downcore.

climatic fluctuations. Low carbonate contents are developed during glacials, and high carbonate contents are developed during interglacials. Similar patterns are evident in the smear-slide and XRD data (Figs. 5 and 7). This interval includes at least six interglacials. The second interval (20.5-31.5 m) appears to record a long period of warmer, more temperate climate. The third interval (31.5-49.4 m), almost carbonate-free, may record very low amplitude climatic fluctuations, indicating overall cold, unproductive environments during both glacials and interglacials.

In summary, the available data provide consistent patterns of dark layer thickness and occurrence (Figs. 9 and 10), carbonate content (Fig. 6), and bulk sediment and composition (Figs. 5 and 7) over the entire section of Unit I. We interpret these patterns to indicate a well-preserved Pleistocene/upper Pliocene glacial/interglacial sequence, with a high stratigraphic resolution of climatic changes in the upper portion of the section. This record may be disturbed by slumping in the lowest 7 m of Unit I, but the effects of this disturbance are not yet evaluated. The relationship of the sequence recovered at Site 642 to Pliocene-Pleistocene material recovered from the Vøring Plateau during DSDP Leg 38 (Talwani, Udintsev, et al., 1976a) has been discussed in Chapter 4 (this volume).

Unit II: Section 104-643A-5H-7, 12 cm, to Section 104-643A-11H-7, 35 cm (49.42–100.15 m sub-bottom)

Age: late Miocene to Pleistocene.

Unit II is 50 m thick and has been subdivided into three subunits on the basis of composition. Subunit IIA is a siliceous nannofossil ooze with minor amounts of mud and sandy mud. Subunit IIB is highly terrigenous in nature, containing siliceous muds and muds, with only minor amounts of nannofossil ooze. Subunit IIC consists of mixed siliceous-calcareous sediments, predominantly diatomaceous nannofossil oozes. Unit II has been more intensely affected by downslope slumping than Unit I, making lithologic correlation of subunits with Site 642 somewhat problematic. Major slumps occur at 68.3–70.3 m (104-643A-8H-5, 5 cm, to 104-643A-8H-6, 48 cm), 79.85–80.57 m (104-643A-9H-6, 55–127 cm), 86.16–86.87 m (104-643A-10H-4, 36–107 cm, including a debris flow), and 88.0–89.1 m (104-643A-10H-5, 70–110 cm) sub-bottom. Despite the comparison difficulties, parts of Subunits IIA and IIC appear to correlate with the general sequence of lithologies developed in Subunits IIA and IID at Site 642.

Subunit IIA: Section 643A-5H-7, 16 cm, to Section 643A-8H-1, 150 cm (49.42–63.80 m sub-bottom)

Age: Pleistocene–early Miocene.

Subunit IIA consists of gray (5Y 5/1), greenish gray (5GY 5/1), and olive gray (5Y 4/2), mottled and bioturbated nannofossil oozes, siliceous nannofossil oozes, and minor amounts of siliceous muds. Minor dark gray ash lenses occur in Subunit IIA; these are considered in the section on distal air-fall tephra deposits (this chapter). The siliceous muds have a compositional range of 55%–90% clay, 10%–30% quartz, and 5%–10% biogenic siliceous components (predominantly sponge spicules). The nannofossil oozes and siliceous nannofossil oozes contain 15%–35% clay, 50%–70% nannofossils, and 5%–25% biogenic siliceous components (predominantly sponge spicules). Subunit IIA contains the first major occurrence of carbonate below the glacial/interglacial cyclic sequence (compare Figs. 6–8), and can be correlated with Subunit IIA at Site 642 on the basis of composition and stratigraphic position (see "Sediment Lithology," Chapter 4, this volume).

Subunit IIB: Section 643A-8H-2 to Section 643A-9H, CC, 34 cm (63.8–81.3 m sub-bottom)

Age: early Pliocene to late Miocene.

Subunit IIB is a highly terrigenous sequence, predominantly composed of muds, sandy muds, and siliceous muds, with an intercalated siliceous nannofossil ooze layer at 62.3–63.3 m sub-bottom. Several dark-gray discrete and disseminated ash layers occur in Subunit IIB; these are discussed in the section on distal air-fall tephra deposits (this chapter). Important colors in Subunit IIB are dusky yellow green (5GY 5/2), olive gray (5Y 5/2), and minor dark olive gray (5Y 3/2) to dark greenish gray (10GY 5/2). Most of the sediments in this interval are mottled and contain abundant faint pyritized burrow tubes. Faint color banding on a scale of 1–10 cm is occasionally visible within this interval, suggesting repeated fluctuations in depositional processes or sediment composition. The cause of this banding is not obvious from bulk sediment characteristics.

Compositional data for Subunit IIB are summarized in Figures 5, 6, and 7. The siliceous nannofossil oozes contain 50%–62% nannofossils, 7%–15% biogenic siliceous components, and 15%–30% clay. The muds and sandy muds contain 70%–80%

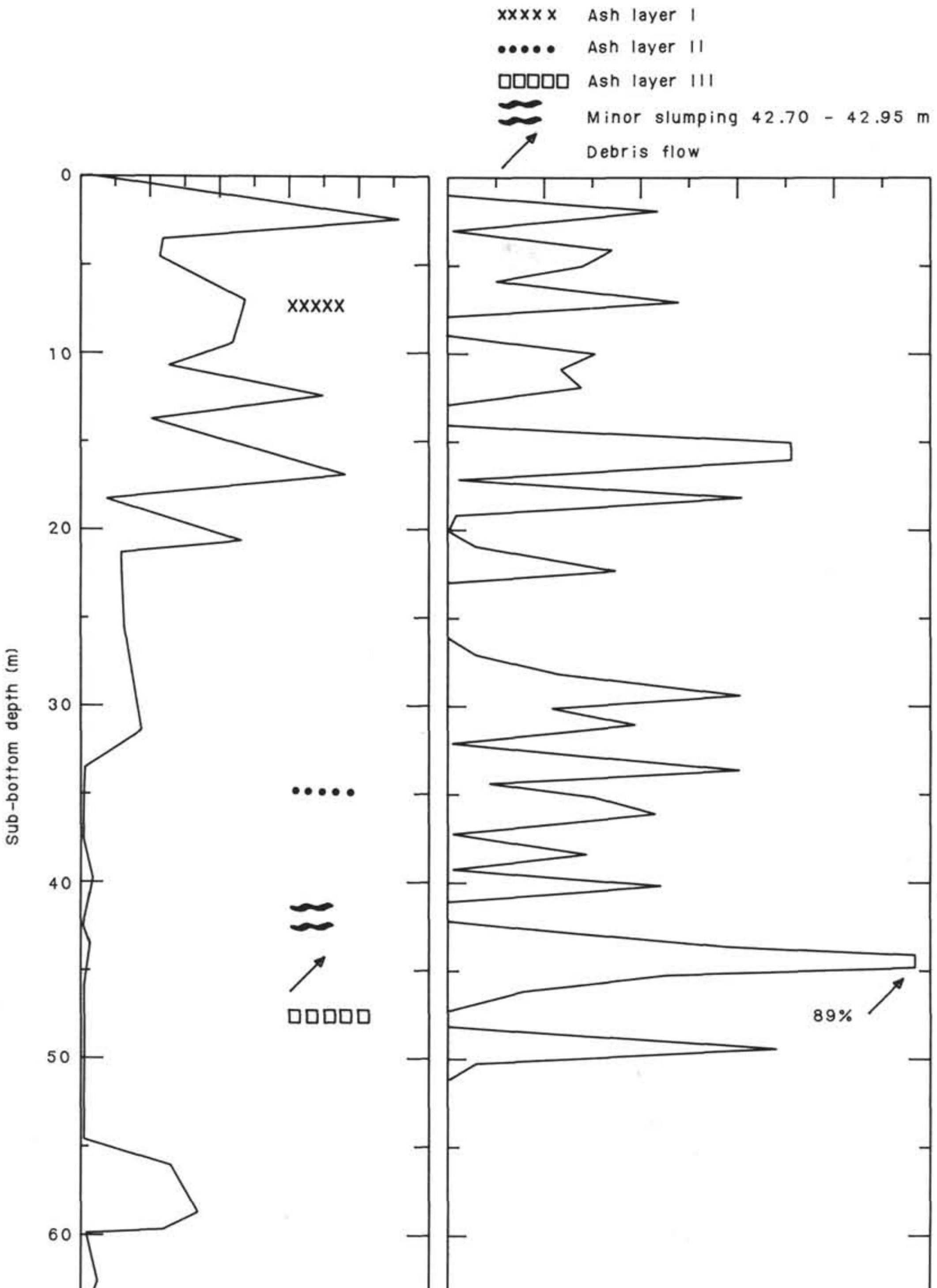

Figure 9. Preliminary profiles of calcium carbonate content and percent of core surface (per meter of core length) covered by dark layers in Unit I, plotted as a function of sub-bottom depth for Site 643. Note inverse correlation of the two curves, absence of carbonate below 35 m, and change in dark layer nature (decreased coverage and increased fluctuation rate) downcore.

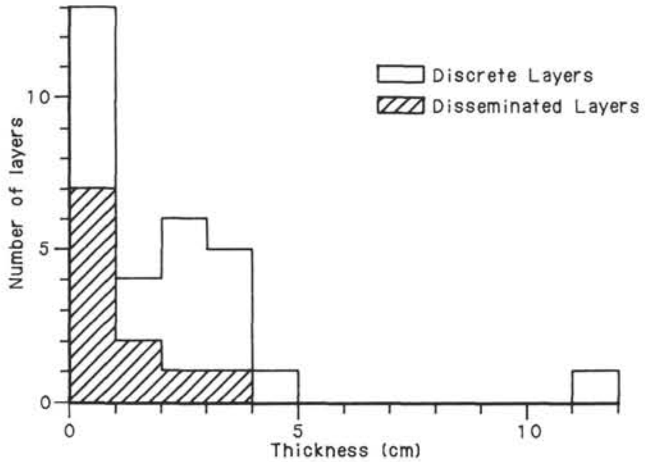

Figure 10. Number of layers vs. thickness of ash layers at Site 643. Thirty tephra layers were examined.

clay, 5%-25% quartz, 1%-2% feldspar, and 2%-10% biogenic siliceous components, while the siliceous muds contain 60%-82% clay, 10%-20% biogenic siliceous components (predominantly sponge spicules and diatoms), 5%-15% quartz, and 0%-2% nannofossils. Carbonate and XRD data (Figs. 6 and 7) reflect the carbonate-poor nature of the major lithologies, while the presence of illite, chlorite, and kaolinite in the clay minerals suggests a terrigenous source for the clay fraction.

Subunit IIB has been extensively disturbed by slumping (68.3-70.38 and 79.85-80.57 m sub-bottom), and several debris flows have been identified in this interval. Because of these complications, we are unable to suggest a correlation between Subunit IIB and the lithologic units at Site 642.

Subunit IIC: Section 104-642A-10H-1 to Section 104-643A-11H-7, 35 cm (81.3-100.15 m sub-bottom)

Age: late Miocene.

Subunit IIC consists predominantly of extensively mottled and bioturbated diatomaceous nannofossil oozes of gray (5Y 5/1), olive gray (5Y 5/2), and dark olive gray (5Y 3/2) color. Siliceous muds and diatom oozes are present in minor amounts (Fig. 5). Subunit IIC also contains the highest number of discrete and disseminated ash layers in Unit II. These are discussed in the section on distal air-fall tephra deposits (this chapter).

The diatomaceous nannofossil oozes in Subunit IIC contain 45%-60% nannofossils, 0%-1% foraminifers, 18%-42% biogenic siliceous components (predominantly diatoms), 8%-24% clay and 1%-5% quartz. The compositional range of the siliceous muds is 50%-80% clay, 5%-10% quartz, and 10%-40% biogenic siliceous components. The mixed carbonate-siliceous nature of Subunit IIC is apparent in the smear slide, carbonate, and XRD data (Figs. 5-7). This subunit is the first major occurrence of a mixed calcareous-siliceous lithofacies below the cyclic glacial/interglacial sequence. On the basis of its composition and stratigraphic location, Subunit IIC at Site 643 is correlated lithologically with portions of Subunit IID at Site 642.

In summary, Unit II at Site 643A contains two intervals with pronounced peaks of carbonate content, separated by terrigenous-dominated sediments. This general pattern of lithologies can be correlated easily and directly with Subunits IIA and IID at Site 642. Unit II at Site 643 is 50 m thick, while Unit II at Site 642 is approximately 100 m thick. This difference may be explained, however, either by the loss of sediment at Site 643 by downslope slumps, or by a considerable difference in net sedimentation rate (deposition and/or erosion effects) at the two sites. A combination of these two factors may be the most probable cause of the observed difference in sediment thickness. The lithologic changes identified in Unit II reflect major changes in the paleoceanographic and paleoclimatic conditions at Site 643 during late Miocene to Pleistocene time. Stepwise cooling events, induced and accelerated by increased deep-water circulation, may account for the multiple changes documented in the sediments of Unit II at both Sites 642 and 643. Changes in bottom-water circulation patterns and intensity during this time may have affected the area of Site 643 more strongly than Site 642, thereby contributing to the low sedimentation rates observed at Site 643. In addition, fluctuations in the level of the CCD may have had a greater influence on deposition in deeper water environments (i.e., Site 643) than on the shallower parts of the Vøring Plateau. This increase in dissolution would account for the lower amount of carbonate accumulation at Site 643.

Previous drilling on the outermost Vøring Plateau and the Plateau slope (DSDP Leg 38, Sites 338, 342, and 343; Talwani, Udintsev, et al., 1976b) recovered only isolated portions of the middle Miocene to lower Pliocene sedimentary sequence in this area. As a result, detailed relationships between Leg 38 stratigraphic descriptions and the section recovered at Site 643 are unclear. Several general observations by Caston (1976), however, are relevant to this region. On the basis of lithologic and age changes across an uncored interval at Site 343, an unconformity is interpreted to have occurred sometime during early Miocene to middle Pliocene time on the outer Vøring Plateau. Although the proposal of this hiatus is quite general, it does agree with one of the mechanisms described earlier to account for differences in sedimentation rates at Sites 642 and 643. In addition, Caston (1976) noted that the predominant biogenic siliceous component at Sites 338 and 342 changed from diatoms in the early Miocene to sponge spicules in the middle to middle/late Miocene, suggesting an increased terrigenous influence through this time. This change in sediment input may, in turn, account for an increase in opal dissolution. A similar shift is observed from Subunit IIC to Subunit IIA, suggesting that the increase in terrigenous input extended across the Vøring Plateau and onto the slope. Finally, minor amounts of nannofossil ooze and calcareous (nannofossil) mud were recovered from sediments dated as "Pliocene-Pleistocene" at Site 343 (Caston, 1976), suggesting that the discontinuous pattern of carbonate accumulation in Unit II at Site 643 is representative of sedimentation elsewhere on the slope, and does not result simply from slumping effects. Because the nannofossil ooze at Site 343 contains no siliceous biogenic components (Talwani, Udintsev, et al., 1976b), it may correlate with Subunit IIA at Site 643.

Unit III: Section 104-643A-11H-7, 35 cm, to Section 104-643A-30H, CC, 35 cm (100.15-274.05 m sub-bottom)

Age: early to late Miocene.

Unit III consists of 174 m of highly siliceous sediments, predominantly diatom oozes, and appears to correlate with the siliceous oozes and siliceous muds of Unit III at Site 642. The composition of Unit III at Site 643 indicates that terrigenous input at this site was significantly lower than at Site 642 during the deposition of these units.

This unit consists of grayish green (10GY 5/2) to dark olive gray (5Y 3/2), extensively mottled and bioturbated diatom oozes and minor amounts of siliceous muds throughout its length (Fig. 5). Bioturbation is developed predominantly as intensive mottling or as indistinct large burrows (possibly *Zoophycos* feeding traces). A diffuse color-banding in green to brown on a scale of 1-10 cm is quite common locally. The only minor lithologies observed are a nannofossil diatom ooze at 141.3-142.8 m sub-bottom and several dark-gray ash bodies, present as discrete or disseminated layers or pockets and lenses. The ashes are discussed separately in the section on distal air-fall tephra deposits (this chapter).

The diatom oozes contain 60%-82% biogenic siliceous components (40%-60% diatoms, 5%-10% radiolarians, 10%-20% sponge spicules, and trace silicoflagellates), 10%-20% clay, and 5%-10% quartz. The nannofossil diatom ooze contains 53% biogenic siliceous components (40% diatoms, 2% radiolarians, 10% sponge spicules, and 1% silicoflagellates), 20% nannofossils, 24% clay, and 1% quartz. Carbonate analyses (Fig. 6) and XRD results (Fig. 7) illustrate the low carbonate content of Unit III, and the XRD results indicate that the clay minerals are predominantly smectites, with minor amounts of chlorite and illite. This assemblage suggests a terrigenous source for the clays throughout Unit III.

On the basis of general composition and stratigraphic occurrence, Unit III at Site 643 is correlated with Unit III at Site 642. The total thickness and the apparent (preliminary) sedimentation rate of Unit III at Site 643, however, are approximately twice as high as those values for Unit III at Site 642. In addition, the terrigenous input at Site 643 is lower than at Site 642, as indicated by the presence of diatom oozes at Site 643 and siliceous muds at Site 642. This pattern may be best explained by the more distal position of Site 643 relative to a terrigenous source, while the higher apparent total sedimentation rate may reflect significantly higher productivity of surface waters overlying the Vøring Plateau slope at this time. The apparent lateral change in surface-water productivity may record regionally confined zones of upwelling along the margin of the Vøring Plateau, or may reflect a more discontinuous record at Site 642. In the latter case, Unit III at Site 643 may be much more complete than Unit III at Site 642, where multiple minor, presently unidentified, hiatuses may produce a relatively low sedimentation rate and total thickness.

A major and complete shift in apparent (preliminary) sedimentation rates, sediment thicknesses, and patterns of carbonate accumulation is obvious in Units II and III at Sites 642 and 643, with Unit II being thicker at Site 642 and Unit III being thicker at Site 643. This change may result from a general reorganization of surface- and bottom-water circulation during major cooling pulses in the early to late Miocene. A stepwise cooling event might have been initiated at this time and been recorded by the occurrence of the first carbonate peak in the uppermost portions of Unit III at each site. The transition in accumulation patterns may also be modified by mass movement events within Unit II at Site 643.

A similar shift—from siliceous-dominated to terrigenous and terrigenous-calcareous sediments—has previously been observed at this time on the Vøring Plateau and at the base of its slope, from DSDP Leg 38 results (Talwani, Udintsev, et al., 1976a; Caston, 1976). Terrigenous content fluctuates throughout the Miocene siliceous section at Site 342, suggesting that local processes were the dominant control on the importance of clastic input. If this interpretation is correct, then a locally variable upwelling may have been the dominant mechanism driving high surface-water productivity at this time.

Unit IV: Section 104-643A-30H, CC, 35 cm, to Section 104-643A-43X, CC, 43 cm (274.05-400.7 m sub-bottom)

Age: early Miocene.

Unit IV is composed of monotonous dark olive gray (5Y 3/2), dark greenish gray (5GY 5/2) to dark gray (5Y 4/1), extremely fossil-poor, terrigenous mudstones, with minor amounts of yellow brownish (10YR 5/4) calcareous mudstones and gray (5Y 6/1) nannofossil chalk. The mudstones contain 73%-97% clay, 0%-10% quartz, and trace amounts of glauconite (Fig. 5). Within the upper 10 m of Unit IV, 5%-16% biogenic siliceous components are also present. The nannofossil chalks contain 65%-90% nannofossils, 20%-30% clay, and 5%-10% quartz. Pyrite impregnations and concretions are quite common.

All lithologies in Unit IV exhibit an unusually high degree of consolidation and appear to have experienced complex early diagenetic alteration. Most of these sediments are extensively compaction-laminated, some are completely lithified, and some of the nannofossil oozes have been almost entirely altered by early diagenetic dissolution and recalcification. Units III and IV show an obvious difference in consolidation history, and this transition presently occurs at the relatively shallow burial depth of 300 m sub-bottom. As a result, we conclude that a significant tectonic and/or erosional event has developed a major unconformity between Units III and IV.

Unit V: Section 104-643A-43X, CC, 43 cm, to Section 104-643A-62X, CC (400.7-565.2 m sub-bottom)

Age: early-middle Eocene to late Oligocene.

Unit V consists predominantly of dark greenish gray (5GY 5/1), dark reddish brown (5YR 3/2, 7.5YR 3/2) to very dark grayish brown (10YR 3/2) zeolitic mudstones, most of which are extensively compaction-laminated. These mudstones only rarely show relict sedimentary structures; those structures that are preserved tend to be diffuse indicators of bioturbation. The greenish zeolitic mudstones contain 1%-15% volcanic glass, 2%-5% quartz, 70%-80% clay, and 5%-15% zeolites, while the reddish mudstones consist of 50%-90% clay, 10%-30% opaque minerals (predominantly goethite), and 2%-10% quartz. Minor lithologies include light gray (2.5Y 7/2) calcareous mudstones, light greenish gray (5GY 7/1) sandy muds, and grayish brown (2.5Y 5/2) mudstones rich in altered volcanic glass. The latter mudstones occasionally contain biogenic opal. Pyrite concretions are common.

Increasing amounts of altered volcanic ash beds, reworked pyroclastic rocks, and thick welded and compacted pumicestones occur in the basal portion of Unit V. Colors in these rocks vary between greenish gray (5G 5/1, 5GY 5/1), dark greenish gray (5G 4/1), dark reddish brown (5YR 4/2), and dark reddish gray (5YR 4/2). The uppermost ash beds range from several centimeters to 20 cm thick, and form a bluish gray (5B 4/2) (plastic) mudstone. The major changes downcore are increases in the frequency of occurrence, the thickness, and the grain size of these ash beds. The basal 30 m of Unit V consists of thick, compaction-laminated sandy mudstones, alternating with reworked pyroclastic mudstones and welded pumicestones(?).

Most of the sediments in Unit V contain extensive compaction laminations that were also highly disturbed during drilling. As a result, sedimentary structures are only observable in the less-disturbed "drilling biscuits." The lowermost 10 m of Unit V shows better preservation, with some well-developed sedimentary structures. These include horizontal stratification, graded ash beds, welded and compacted pumicestones, angular reworking surfaces within pyroclastic rocks, and rare bioturbation.

Cores 104-643A-61X and 104-643A-62X contain pebble- to cobble-sized basaltic fragments, a polymict conglomerate of pyroclastic rocks, and a dark greenish gray (5GY 4/1) to dusky green (5G 3/2) basaltic conglomerate. Within the basaltic conglomerate, which occurs at the base of Core 104-643A-62X, clasts are weathered and well-rounded, with an average diameter of approximately 2 cm. The clasts are predominantly basaltic (about 80%), although a pyroclastic mudstone pebble was also observed. The matrix appears to be basaltic in composition, having been crushed and weathered.

A similar set of lithologies of early Eocene age was recovered in a 1.2-m-thick horizon of thin-bedded turbidites immediately overlying basalt at Site 343 (Talwani, Udintsev, et al., 1976b).

Although drilling deformation prevented identification of turbidite sequences, the lowermost 5 m recovered at Site 643 does contain abundant evidence of vigorous sedimentary reworking. This suggests that Site 643 was terminated within the pyroclastic unit directly overlying basaltic basement. Depth to basement, however, remains uncertain. In addition, the basal ages at Sites 343 and 643 indicate that terrigenous sedimentation began during the early Eocene at both sites. The transition to siliceous sedimentation, however, occurred during the middle to late Eocene at Site 343 (Caston, 1976), the early Miocene at Site 643, the late Eocene at Site 338 (Caston, 1976), and the early Miocene at Site 642 (Site 642 and summary chapters). The variability in this timing across the VØring Plateau region suggests that complex oceanographic and/or tectonic controls have influenced depositional patterns throughout the region since the Paleogene.

Conclusions

1. The deep-water sedimentary section recovered at Site 643 contains a high-resolution climatic signal within the glacial/interglacial cycles of lithologic Unit I. The general trend within Unit I is a stepwise change downcore in the amplitude and frequency of glacial/interglacial oscillations. The youngest interval contains a high-amplitude pattern and is preceded by a period of more equitable temperate conditions. The oldest interval exhibits low-amplitude oscillations, with almost no carbonate present in the sediments.

2. The major changes in lithologies from Unit III to Unit II suggest a stepwise transition from high-productivity regimes with rapid accumulation of siliceous biogenic ooze in the lower portions of Unit III to low-productivity, terrigenous-dominated conditions during the deposition of Unit II. The increasing frequency of slowly accumulating nannofossil oozes, beginning in the upper portion of Unit III, suggests a series of stepwise cooling events within the surface waters. The accompanying episodic increase in terrigenous input reflects the development of the more vigorous oceanic circulation driven by these cooling events.

3. Preliminary estimates of sedimentation rates of biogenic silica within the lower part of Unit III are relatively high and indicate that highly productive surface-water conditions existed along the margin of the VØring Plateau during the early to middle Miocene, most probably in response to the development of continental margin upwelling regimes.

4. The obvious differences in the consolidation and the early diagenetic histories of Units III and IV indicate that a significant tectonic and/or erosional event developed a major unconformity between these two units. Future investigation of the nature of this event may provide valuable insight into the tectonic and/or sedimentologic evolution of the VØring Plateau.

5. Compositional differences within the volcaniclastic sequences of Unit V at Site 643 and Unit IV at Site 642, especially the presence of glauconite only at Site 642, indicate that these two sites experienced different sequences of depositional environments. These differences most probably reflect variations in proximity to a volcaniclastic source, as well as differences in the bathymetric conditions required for glauconite formation. Differences in the tectonic histories of the interior of the VØring Plateau and its slope to the Lofoten Basin may also have significantly influenced the development of these volcaniclastic sequences.

Quaternary and Neogene Air-fall Tephra Layers

Fresh tephra was recovered within Units I, II, and III at Site 643. No discrete ash layers were identified in the consolidated sediments of Units IV and V, below 274.05 m. As at Site 642, the 58 occurrences of fresh tephra can be classified as discrete (19) or disseminated (11) layers, enriched ooze (8), and pocket fillings and ash lenses (20). See Figure 10. In two instances pocket fillings were associated with a discrete or disseminated ash layer, so that 56 distinct tephra horizons are represented.

The data presented are based on microscopic studies of 65 smear slides, using the standard procedure for shipboard smear slide description. Shard sizes were measured on 53 slides. Shipboard X-ray refraction (XRF) analyses were not available. The criteria used for chemical classification of the tephra, as well as a detailed description of the different lithologic forms of tephra occurrence, are given in the Site 642, "Sediment Lithology," section (this volume).

Description

The tephra occurs in the sediment pile as well-sorted, sandy layers that have often been reworked and/or strongly bioturbated, and are only preserved in pockets or lenses. In all, the ash occurrences make up 0.27% of the stratigraphic sequence formed by Units I, II, and III (Miocene to Recent). Trace amounts of fresh glass shards are present throughout all sediments drilled. The tephra layers consist of fresh glass shards and are essentially vitric ashes free of lithics, but at times contain a few crystals (alkali feldspar, plagioclase, quartz, zircon, and hornblende). Three compositionally different types can be distinguished (Fig. 11 and Table 3). Type A consists of colorless shards of rhyolitic composition. Types B and C are distinguished by whether colorless or olive green to brown shards are the dominant shard type and are referred to as icelandites and tholeiitic andesites, respectively.

Discrete and disseminated layers range in thickness from less than 1 to 5 cm (Fig. 10), with a frequency maximum at less than or equal to 1 cm. One layer reaches 11 cm in thickness (104-643A-15H-04, 139-150 cm). The average median shard size is about 110 μm (112 ± 41 μm), but layers of Type C have an average of less than 100 μm. The average maximum size of the three largest shards in each layer is 471 ± 169 μm for 35 layers of Types A and B and 244 ± 84 μm for 15 layers of Type C (not including the Type C layer at 104-643A-27X-04, 44-45 cm). In two layers the largest shard reaches the extraordinary size of more than 1 mm (104-643A-11H-01, 103-106 cm, Type B, and 104-643A-27X-4, 44-45 cm, Type C).

Discrete layers of Types A and B always show a sharp base and a gradational top. Three layers also exhibit a sharp upper boundary (104-643A-9H-02, 23-24 cm; 104-643A-22X-01, 132-134 cm; and 104-643A-22X-03, 126-128 cm). At 170.72 m, a tephra layer overlies an irregular erosion surface (104-643A-19X-3, 92-96 cm). The ash layers are variable in color, depending on the composition of the constituent shards. Layers of icelanditic to rhyolitic composition (Types B and A, respectively, in Table 3 and Fig. 11) are white to gray. Tephra layers of Type C are dark gray or brown. Intense coating of shards by pyrite (indicated in Table 3) results in dark gray to black coloring of all three types. Two ash layers are cemented by pyrite (104-643A-12H-5, 98-99 cm, and 104-643A-27X-4, 44-45 cm). Although layers of Type C are more uniform in color, layers of Types A and B are graded from white to gray or light gray to dark gray, respectively. The lighter colored base generally represents one-tenth, and rarely as much as one-third, of the total thickness. The change in color is caused by a decrease in median and maximum grain size by about 40% and 50%-60%, respectively. This color change is also associated with an increase in pyrite coating on the shards.

Discussion

All well-sorted ash layers described earlier are thought to be of air-fall origin and to be derived from plinian eruptions on Iceland (for a detailed discussion, see "Sediment Lithology," Site 642 chapter, this volume). The grain-size characteristics show that layers of less-differentiated composition have a smaller maximum and median grain size than those of more-differentiated

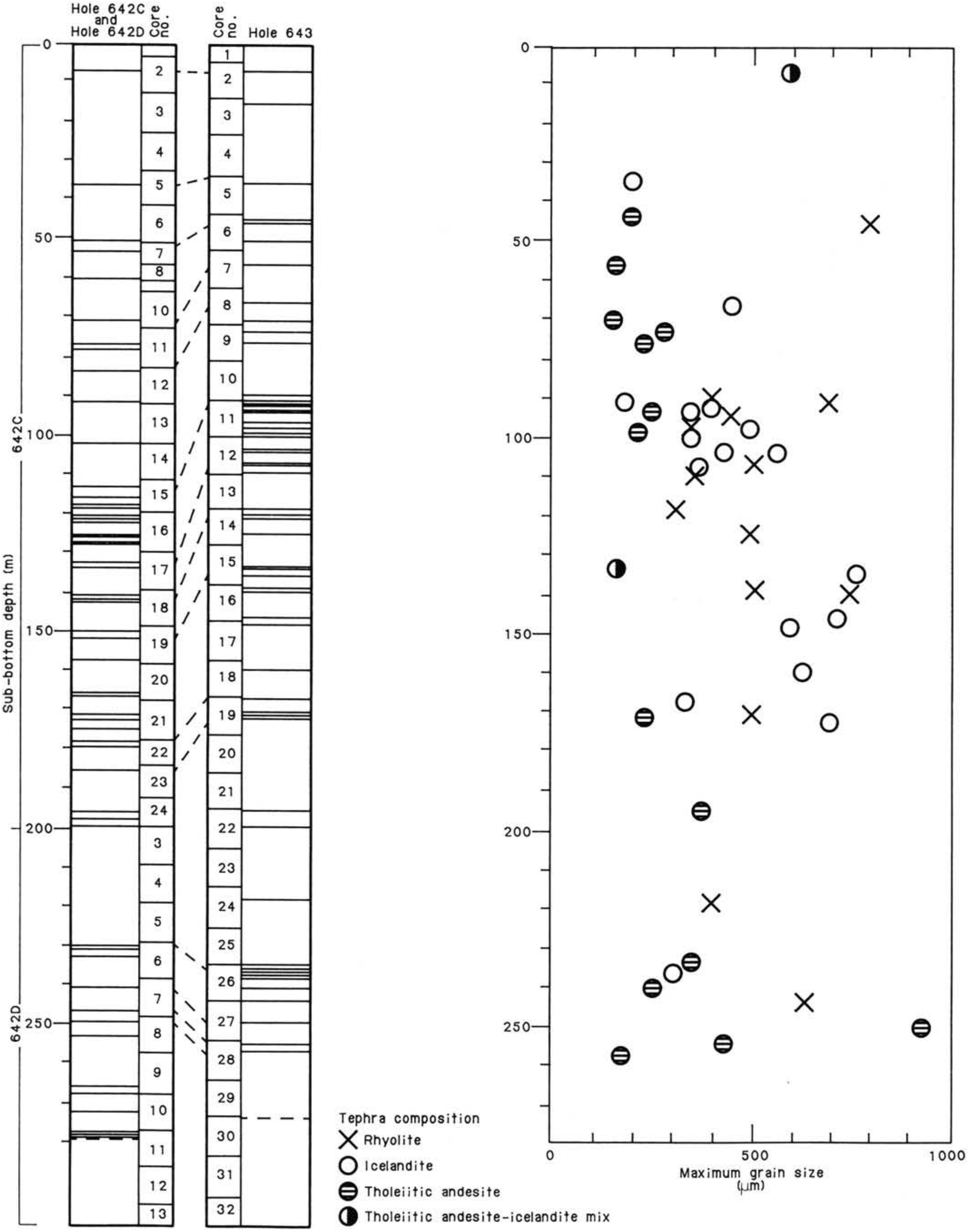

Figure 11. Occurrence, composition, and correlation of tephra layers at Sites 642 and 643.

Table 3. Tephra horizons at Site 643.

Depth (mbsf)	Core-section-interval (cm)	Type of sediment[a]	Petrographic type[b]	Remarks
7.52	02-03, 72–74.5	L	B/C	
14.98	03-01, 18–18.5	P	?	
35.37	05-02, 107–114	E	A/B	
44.53	06-01, 123–125	P	C	
46.54	06-03, 24–27	D	A	
50.27	06-05, 97–101	D	?	
56.46	07-03, 66–66.3	P	C	
66.59	08-03, 129–130	P	B/A	zircon
70.63	08-06, 83–84	E	C	
73.53	09-02, 23–24	L	C	pyrite 45%
76.43	09-04, 13–14	P	C	
76.77	09-04, 47–48	E	C	pyrite 50%
90.31	10-07, 01–03	P	A	pyrite 60%
90.89	11-01, 09–10	P	B	
91.83	11-01, 103–106	L	A	pyrite 25%
92.58	11-02, 28–29	P	A/B	
92.95	11-02, 65–66	P	C	
93.06	11-02, 76–78	L	B	
93.71	11-02, 141–146	L	A	zircon
96.86	11-05, 06–10	L	A	
99.15	11-06, 85–86	P	B	
99.45	11-06, 115–116	P	C	pyrite 15%
99.89	11-07, 08–10	L	A/B	
103.88	12-03, 58–60	P	B	
104.42	12-03, 112–113	P	B	pyrite 15%
107.01	12-05, 98–99	D	A	lithified by pyrite
107.14	12-05, 111–112	P	A/B	
110.06	13-01, 26–27	P	A	pyrite
119.11	13-CC, 11–12	D	A/B	
120.23	14-01, 93–94	E	C	
121.56	14-02, 76–77	P	B/C	
125.06	14-04, 126–127	L	A	pyrite 60%
133.24	15-03, 144–145	L	C	
134.69	15-04, 139–150	L	B	
134.89	15-05, 09–10	P	B	
135.85	15-05, 105–106	P	B	
139.64	16-01, 134–135	D	A	
140.00	16-02, 20–21	L	A	
146.24	16-06, 44–48	L	B/A	
148.20	17-01, 40–44	L	B	
160.04	18-02, 124–125.5	D	B	pyrite 80%
160.07	18-02, 127–128	D	B	pyrite
167.28	19-01, 48–50	L	B/C	pyrite
170.72	19-03, 92–96	L	A	hornblende, zircon
171.34	19-04, 04–12	P	C	pyrite
172.48	19-04, 118–119	L	B/A	
196.62	22-01, 132–134.5	L	B	pyrite
199.56	22-03, 126–128	L	C	FSP, ZR, hornblende pyrite 50%
218.08	24-03, 18–20	D	A	
234.25	25-CC, 11–11.7	D	C	pyrite 80%
236.45	26-02, 45–46	E	A	pyrite 40%
236.70	26-02, 70–73	D	B	pyrite 40%
237.42	26-02, 142–143	E	B	
240.18	26-04, 118–118.5	D	C	pyrite 25%
243.16	26-06, 116–117	L	A	
249.24	27-04, 44–45	P	C	lithified by pyrite
254.77	28-01, 67–68	E	C	
257.08	28-02, 148–150	E	C	

[a] L = discrete layer, P = pocket filling and lenses, D = disseminated layer, E = enriched ooze.

[b] A = tephra composed of colorless shards of rhyolitic composition, B = tephra composed of colorless to pale shards of icelanditic composition, C = tephra composed of green to brown shards of tholeiitic composition.

Table 4. Correlation of ash layers between Site 643 and Holes 642C and 642D.

Site 643 Sample				Site 642 Sample		
Core section	Interval depth (cm)	Depth (mbsf)		Depth (mbsf)	Core section	Interval depth (cm)
	643				642C	
02-03,	72–74.5	7.52		8.78	02-04,	88–98
05-02,	107–114	35.37		36.82	05-03,	92–94
06-03,	24–27	46.54		52.23	07-01,	133–140
07-03,	66–66.3	56.46		71.05	10-06,	05–08
08-03,	129–130	66.59		84.30	12-02,	30–32
11-01,	103–106	91.83		113.32	15-02,	82–87
12-05,	98–99	107.01		132.55	17-02,	105–108
13-CC,	11–12	119.11		142.71	18-03,	21–22
15-04,	139–150	134.69		152.67	19-03,	67–68
19-01,	48–50	167.28		177.65	22-01,	15–18
			or	178.14	22-01,	64–69
19-04,	118–119	172.48		186.20	23-02,	40–41
					642D	
26-02,	45–46	236.45		230.05	6-02,	05–06
27-04,	44–45	249.24		241.00	7-02,	130–136
28-01,	67–68	254.77		246.32	7-06,	62–74
28-02,	148–150	257.08		249.00	8-01,	120–121

composition (Fig. 11). This agrees with the general observation that the area of dispersal of tephra resulting from plinian eruptions increases with increasing degree of differentiation. A slight downhole increase in the maximum grain size of Type C layers is also apparent (Fig. 11). This is not obviously indicated by tephra at Core 104-643A-27X-4, 44–45 cm.

Petrographic criteria and grain-size characteristics were used to correlate the tephra layers at Site 643 and Site 642 (Holes 642C and 642D, Table 4, Fig. 11). Ash layers are rare in the Pliocene/Pleistocene sediments at both sites. Both sites, however, do exhibit a 20-m-thick stratigraphic interval characterized by a high frequency of ash layers. This interval occurs at 90–110 m at Site 643 and at 113–133 m at Site 642C. Fifteen layers have currently been correlated among these sites. Because of their distinct characteristics, two of these layers may be useful for regional correlations throughout the Norwegian–Greenland Sea. The first layer occurs in Core 104-643A-11H-01, 103–106 cm, at a depth of 91.8 m and at 113.3 m at Site 642, in Core 104-642C-15H-2, 82–87 cm, and Core 104-642B-13H, CC, 9–13 cm. This tephra layer is rhyolitic in composition, is color-zoned from white to gray, and is graded, the size of the largest clast being approximately 1 mm. The layer occurs at the upper end of the high-frequency ash layer interval and has an age of about 6.0 Ma according to the paleomagnetic data of Site 642. The second layer occurs at Site 643 at a depth of 134.7 m (Core 104-643-15H-4, 139–150 cm) and at 152.7 m at Hole 642C (Core 104-643C-19H-3, 67–78 cm). This layer cannot be correlated to Hole 642B. The layer is icelanditic in composition and color-zoned from gray to dark gray. It is 11–12 cm thick and graded, with a maximum grain size (average of 3 largest shards) of 770 μm at the base and 300 μm in the upper half. This layer has a probable age of about 13 Ma.

The correlation between Sites 642 and 643 indicates:

1. A lower sedimentation rate at Site 643 in the interval 0–120 m. This is especially pronounced in Unit II, which has a biostratigraphic age of upper Miocene to Pleistocene.
2. A higher sedimentation rate at Site 643 for the interval 175–235 m (Cores 104-643A-19X to 643A-25X, early Miocene).

BIOSTRATIGRAPHY

Introduction

The primary biostratigraphic objectives at Site 643 were as follows: (1) to determine the age of the sediment deposits, (2) to interpret the paleoceanographic and paleoclimatic history of this high-latitude subpolar region, and (3) to study the Cenozoic evolution of the subpolar marine flora and fauna. Summaries of the initial results for each microfossil group, followed by a synthesis of initial biostratigraphic and paleoenvironmental findings, are presented here.

Diatom Stratigraphy

Methods

All Hole 643 core-catcher (CC) samples were examined for their diatom content using whole-fraction sediments. Sieved sediment preparations were also examined from Cores 104-643A-1H through 104-643A-30X. Five additional samples from Cores 104-643A-8H through 104-643A-11H were examined to determine the upper limit of diatom preservation and to check for the possibility of an unconformity in this interval. References to the absolute ages of datums mentioned here may also be found in Figure 9, Chapter 2, this volume.

Abundance and Preservation

Diatoms are absent from Samples 104-643A-1H, CC through 104-643A-7H, CC (5.3-62.3 m). The first diatoms were encountered in Sample 104-643A-8H-5, 70 cm (78.5 m). Between this sample and Sample 104-643A-11H, CC (100.3 m), diatoms are moderately diverse, common, and moderately to poorly preserved. Sample 643A-12H, CC records a major downhole increase in species diversity and abundance. Diatoms are common to abundant, moderately well preserved, and exhibit large diversity among Samples 104-643A-12H, CC through 104-643A-30X, CC (109.8-283.5 m).

Only a few unaltered diatoms were found from 283.5 m to the base of the hole (565.2 m). The interval between Cores 104-643A-30X and 104-643A-31X (283.5-293.3 m) appears as a sharp diagenetic boundary separating the diverse and abundant diatom assemblages above from sparse and altered assemblages below. The abrupt loss of unaltered biogenic opal at this level and the accompanying changes in physical properties are reasons to suspect the presence of an unconformity. Conformable sequences seldom, if ever, record such an abrupt and permanent loss of biogenic opal.

Below 283.5 m unaltered diatoms are very rare; however, manganese-encrusted diatoms are frequent to common in some cores. The highest concentration of altered diatoms occurs between Samples 104-643A-31X, CC and 104-643A-43X, CC, whereas diatoms are almost completely absent below this level. Manganese-encrusted diatoms are completely opaque, making species identification impossible.

Results

Sample 104-643A-8H-5, 70 cm (78.5 m) contains rare *Denticulopsis hustedtii* and is above the last *Actinocylus ingens*. This sample appears to be younger than either the last common occurrence of *D. hustedtii* (5.8 Ma) and the last appearance datum (LAD) of *Actinocyclus ingens* (~5.9 Ma). The LAD of *D. hustedtii* is ~5.5 Ma in Site 642; therefore, we inferred the age of this sample to be between 5.9 and 5.5 Ma. Correlation of this interval with the zonation of Schrader and Fenner (1976) places this zone within the lower *Coscinodiscus marginatus* Zone. Correlations of this sample with other zonations is not possible because of the absence of indicator species; however, Site 642 results indicate correlation with the *Nitzschia porteri–N. miocenica* Interval Zone of Baldauf (1984) and with the *D. hustedtii* Zone, Subzone B of Barron (1985).

The last common occurrence of *Denticulopsis hustedtii* occurs in Sample 104-643A-9H-4, 47 cm. At Site 642 this datum occurs at ~115 m and has an assigned age of 6.2 Ma. This sample is assigned to the *D. hustedtii* Zone of Schrader and Fenner (1976). Sample 104-643A-10H-1, 83 cm, has a similar assemblage as the previous sample and is assigned to the *D. hustedtii* Zone.

Samples 104-643A-10H, CC and 104-643A-11H, CC are tentatively correlated to the *D. hustedtii* Zone and *Cymatosira biharensis* Zone of Schrader and Fenner (1976). This interval appears to correlate with the section between 120 and 130 m of Site 642 and may also represent some of the late Miocene section missing in the hiatus of that site.

A major stratigraphic break is indicated between core-catcher Samples 104-643A-11H and 104-643A-12H at Site 643. Diatoms are much more abundant and diverse in Core 104-643A-12H, with many species exhibiting their last occurrences. The joint last occurrences of *D. lauta* and *D. nicobarica* in Core 104-643A-12H indicate that the upper range of *D. lauta* has been truncated. Sample 104-643A-12H, CC can be no younger than the age of the last *D. nicobarica*, which occurs in the base of Subzone B of the *Denticulopsis hustedtii* Zone (NNPD5). Using the age of the Subzone B base, an age of ~13.3 Ma was assigned to the base of Core 104-643A-12H.

The change in diatom assemblages between Core 104-643A-12H, CC and 104-643A-11H, CC is strong evidence for an unconformity from 90.8 to 100.3 m. Absent between these cores are Subzones C and D of the *D. hustedtii–D. lauta* Zone (NNPD5) and Subzone A of the *D. hustedii* Zone (NNPD6). This unconformity represents approximately the same time interval as the unconformity at ~130 m of Site 642.

The last occurrence of *Coscinodiscus lewisianus* in Core 104-643A-13H, CC is used to approximate the Subzone A/B boundary of the *D. hustedtii–D. lauta* Zone (Barron, 1985). The first occurrences of both *D. hustedtii* and *D. lauta* in Core 104-643A-14H, CC indicate the presence of another unconformity between Core 104-643A-14H, CC and Core 104-643A-15H, CC. Missing between these cores is the *D. lauta* Zone (NNPD4) and possibly portions of the upper *Actinocyclus ingens* Zone (NNPD3) and lowermost *D. hustedtii/D. lauta* Zone (NNPD5).

Underlying this last unconformity is the *A. ingens* Zone (NNPD3), which extends to the first occurrence of *A. ingens* in Core 104-643A-16H, CC (147.8 m). The age for this datum is 16.8 Ma and correlates with a depth of 207 m at Site 642.

Conformable with the *A. ingens* Zone is the *Thalassiosira fraga* Zone (NNPD2), which is recognized in Cores 643A-16H, CC through Core 104-643A-30X, CC (148-283.5 m). Barron (1985) assigns an age of 19.5 to 16.8 Ma for this zone. At Site 643 the base of the zone occurs at an abrupt diagenetic boundary at ~284 m, below which depth very few diatoms are found. Thus, the base of the zone at this site probably does not represent true evolutionary first appearance of *T. fraga* and may be younger than 19.5 Ma.

The thickness of the early Miocene *T. fraga* Zone is ~150 m, in great contrast to the ~55-m thickness of this zone at Site 642. The higher early Miocene sedimentation rates indicated at Site 643 are also confirmed by silicoflagellate assemblages (see "Silicoflagellate Biostratigraphy," this section).

Paleoenvironment

Diatoms are absent to common in the Eocene to Miocene of Cores 104-643A-31X through 104-643A-62X (293-565 m); however, all but a few specimens are encrusted with manganese. The opaque condition of these diatoms prevents any detailed paleoenvironmental conclusions. Significant diatom productivity appears likely during this interval; however, most biogenic opal has apparently undergone diagenesis to opal (cristobalite-tridymite).

The extremely high abundance and diversity of diatoms in the early Miocene (Samples 104-643A-15H, CC through 104-643A-30X, CC; 138-293 m) is indicative of high diatom productivity. Sea-surface water temperatures were significantly warmer than during the remainder of the Neogene. Some of the species and genera in this section, which are common in temporally equivalent sections of the low- to mid-latitudes, include *Asterolampra* spp., *Asteromphalus* spp., *Craspedodiscus coscinodiscus, Coscinodiscus blysmos*, and *Brunia mirabilis*. Comparison of the early Miocene between Sites 642 and 643 reveals higher biogenic opal concentrations and higher sedimentation rates at Site 643, indicative of higher siliceous biogenic productivity at the latter site.

Without further detailed studies, little can be inferred about middle to late Miocene paleoenvironmental conditions because of the condensed section (~68–157 m) representing this 16.0- to 5.2-Ma interval. In addition, much of the middle Miocene and early Miocene appears to be unrepresented because of a hiatus in Core 104-643A-15H. Lower Miocene assemblages below the hiatus may represent warmer surface waters than the upper Miocene, based on higher diversities and characteristics of the overall assemblage. Upper Miocene assemblages are less diverse but still have some moderate water temperature indicators such as *Hemidiscus cuneiformis* and *Brunia mirabilis*.

No Pliocene or Quaternary diatoms were noted. We do not know if this interval is entirely present; therefore, we could make no inferences regarding its paleoenvironment. Middle to upper Pliocene assemblages were well-preserved at Site 642, suggesting the possibility of a hiatus of similar age at Site 643.

Silicoflagellate Biostratigraphy

Methods

All core-catcher samples within Hole 643A were examined for their silicoflagellate content within the whole-sediment fractions. Sieved fraction preparations were also examined from Cores 104-643A-1H through 104-643A-30X. Five additional samples were examined in Cores 104-643A-8H through 104-643A-11H to determine the upper limit of silicoflagellate preservation and to determine the possibility of an unconformity within this interval.

A complete discussion of zonal definitions, ages, and correlations to other microfossil zonations is given in "Silicoflagellate Biostratigraphy" in the "Biostratigraphy" section of the Site 642 chapter (this volume).

Abundance and Preservation

Silicoflagellates are absent from Samples 104-643A-1H, CC through 104-643A-7H, CC (5.3–62.3 m). The first silicoflagellates were encountered in Sample 104-643A-8H-5, 70 cm. Between this sample and Sample 104-643A-12H, CC, species diversity and abundance is low and preservation is poor. Sample 104-643A-13H, CC records a major increase in species abundance and diversity. Silicoflagellates are common to abundant, well preserved, and of moderate diversity between Samples 104-643A-13H, CC and 104-643A-30X, CC. Below Sample 643A-30X, CC silicoflagellates are absent, except for three specimens found in Cores 104-643A-33X and 104-643A-34X.

Results

Sample 104-643A-8H-5, 70 cm, is assigned to the *Mesocena diodon* Zone on the basis of a few poorly preserved *M. diodon* and the absence of *Mesocena circulus*. If these few specimens are not reworked, the age of this sample is between 6.4 and 4.4 Ma.

Samples 104-643A-9H-4, 47 cm, through 104-643A-10H, CC contain few to frequent *M. diodon* and *M. circulus*, indicative of the *M. circulus/M. diodon* concurrent range zone. This interval is assigned a late Miocene age, and suggests correlation with a portion of the interval between lower Chron C-3A through basal Chron C-4A (between 6.4 and 8.7 Ma).

Core-catcher Samples 104-643A-11H and 104-643A-12H of Hole 643A contain a sparse assemblage of silicoflagellates. The presence of *M. diodon* in the absence of *M. circulus* suggests that this interval represents the upper portion of the *Corbisema triacantha* Zone of Martini (1971a). Martini and Müller (1976) report *M. diodon* below the first-appearance datum (FAD) of *M. circulus* at Site 338. At Site 642 *M.* cf. *diodon* had its FAD in Core 642C-20H, immediately below the first *M. circulus* in Core 642C-19H. The tenuous correlations based on this sparse assemblage are used to infer a middle-middle to late-middle Miocene age.

The interval between Sample 104-643A-13H, CC and 104-643A-27X, CC (119.3 and 244.3 m) is equivalent to the the *Corbisema triacantha* Zone of Martini (197la), defined here as the interval from the last *Naviculopsis quadrangula* to the first *M. circulus*. The assemblage of this interval is identical to that encountered at Site 642 between ~163 and 233.5 m, with the most common species being *Distephanus crux, D. crux parvus, D. longispinus, D. speculum hemisphaericus, Mesocena apiculata*, and *M. apiculata curvata*. Through correlations of this assemblage with the age vs. depth curve of Site 642, the base of the interval is ~17.5 Ma. The last occurrence of *M. apiculata* and *M. apiculata curvata* in Sample 104-643A-15H, CC provides stratigraphic control for the upper portion of the interval. Ages for these datums at Site 642 are ~13.2 to 13.7 Ma, respectively.

Silicoflagellate assemblages between 119 and 244 m range in age from 17.5 Ma to no younger than 13.2 Ma. The estimated sedimentation rate for this middle Miocene section is approximately 30 m/m.y., in contrast to a sedimentation rate of 18 m/m.y. during the same interval at Site 642.

Further comparisons with Site 642 suggest the presence of a similar middle-middle Miocene to middle-upper Miocene unconformity at Site 643. Poor preservation of silicoflagellates in Samples 642B-12H, CC and 643A-13H, CC prevents a definitive identification of the possible position of the unconformity. The presence of an unconformity does seem likely, however, because of middle-middle Miocene assemblages (>13.2 Ma) in Core 104-643A-13H and an upper Miocene assemblage in Core 104-643A-10H (<9.0 Ma). The ages of these cores are similar to the bracketing ages of the proposed unconformity at Site 642.

Samples 104-643A-28X, CC through 104-643A-30X, CC are assigned to the *Naviculopsis navicula* Zone and are characterized by the presence of the typical lower Miocene species *Naviculopsis navicula, N. quadrangula*, and *N. iberica*. The age of the upper boundary of the zone was correlated with approximately the NN3/NN4 boundary by Martini (1971a) and with the upper NN2 by Martini (1979). Correlations of this boundary with Site 642 yield an age of ~17.5 Ma, which supports Martini and Müller's (l976) correlation with the NN3/NN4 boundary.

The base of the zone (~284 m) is marked by a sudden diagenetic transition to sediments almost entirely barren of siliceous microfossils. It appears that the true base of the *N. navicula* Zone, the evolutionary first appearance of this species, is not represented because of diagenesis, thus making the age of this abrupt loss of biogenic opal at ~284 m younger than the ~21-Ma age of the base of the zone. This conclusion is supported by the age of the diatom assemblage at this boundary ("Diatom Stratigraphy," this section).

Three specimens of *Distephanus crux* and *D. longispinus* occur in Samples 104-642A-33X, CC and 104-643A-34X, CC. *D. longispinus* does not appear to range below the lower Miocene. Cores 104-643A-35X through 643A-62X are completely barren of silicoflagellates.

Paleoenvironment

Early to middle Miocene assemblages reveal few major changes in overall assemblage composition or species dominance. The disappearance and gradual decrease in the abundance of

Mesocena apiculata and *M. apiculata curvata* between 14 and 13 Ma may be interpreted as representative of a decline in surface-water temperature. Sporadic occurrences of *Dictyocha* spp. in Cores 104-643A-13H, 104-643A-11H, and 104-643A-10H indicate nonglacial conditions during portions of the middle(?) and late Miocene.

Radiolarian Stratigraphy

Introduction

Radiolarians preserved in the recovery from Site 643 range in age from early Miocene to early Pliocene, and their occurrence is confined to the interval between 104-643A-8H-5 and 104-643A-29X, CC (69.5-273.7 m). The absence of radiolarians in the glacial marine sediments above Core 104-643A-9H is consistent with the absence of these and other siliceous microfossils in such sediments from many other regions of the Norwegian Sea. Siliceous microfossil preservation declines abruptly below Core 104-643A-30X, where the lithology grades from siliceous muds and ooze of the upper section into fissile shale below. The loss of siliceous microfossils at this horizon may have resulted from a silica phase change associated with lithification. This interpretation is supported by the occurrence of abundant siliceous microfossils in sediments of earliest Miocene and late Oligocene age at Site 338 (Bjørklund, 1986). The absence of radiolarians in the Eocene sediments at Site 643 (477.7-565 m), which have a more typically hemipelagic aspect, is difficult to explain. Other Eocene sediments from the Vøring Plateau and adjacent regions of the Norway and Lofoten basins are composed of radiolarian oozes. Their absence in coeval sediments on this distal portion of the plateau (Site 643), as well as at Sites 345, 346, and 348 through 350, suggests that the zone of Eocene high productivity on the Vøring Plateau, and perhaps in the Norwegian Sea in general, was longitudinally restricted to a narrow area.

Abundance and Preservation

Much of the skeletal opal in the sediments between Cores 104-643A-8H and 104-643A-29H has abnormally high indices of refraction, and the quality of preservation of the radiolarians is only moderately good. Radiolarians are much less frequent in the lower Pliocene and Miocene diatomaceous oozes of Site 643 than they are in coeval sediments at Site 642. This dissimilarity in radiolarian abundance at two closely spaced localities can be partially explained by the complex age relationships of the sediments at these sites. With respect to the relative paucity of radiolarians compared to diatoms, these sediments are similar to the shales of the Miocene/Pliocene Monterey Formation of central California, which were deposited under conditions of intensified coastal upwelling.

Results

The biosiliceous interval ranges from biozones NSR2 to NSR9. The upper Miocene section is only 50 m thick and contains two extensive hiatuses. Alternatively, the lower Miocene biosiliceous interval is approximately 210 m thick and comprises the most complete section of this age and lithology presently available from the Norwegian Sea. Sedimentation at Site 643 appears to have been reasonably continuous from upper NSR2 to lower NSR7 time, whereas the coeval section at Site 642 is cut by two hiatuses. Consequently, recovery from these two sites can be integrated to form a composite section for much, but not all, of the Neogene.

The true base of the NSR2 Zone is not present in Hole 643A. The base of this zone is at the bottom of Core 104-643A-29X, and coincides with the level of degraded opal preservation. The NSR2/NSR3 boundary occurs in Section 104-643A-27X-5 (251 mbsf). This boundary is marked by the first appearance of the precursor to *Clathospyris sandellae*, and Site 643 contains the only section in which this event is recorded. The NSR3/NSR4 boundary is located in Section 104-643A-22X, CC (205 mbsf), and it is marked by the first appearance of *C. sandellae* sensu stricto. Again, this biostratigraphic event is not recorded at Site 642. Biozones NSR3 and NSR4 are represented by 47 and 55 m of highly compacted sediment at Site 643. These two provisional zones are strong candidates for further subdivision.

The top and base of NSR5 are located in Sections 104-643A-16H-2 (140.3 m) and 104-643A-17X-1 (148.3 m), respectively. Site 643 contains the most "complete" NSR5 biozone of any known locality, but the continuity of deposition at the base of NSR5 is doubtful. The base of this biozone is marked by the evolutionary first appearance of *Actinomma* sp. The abrupt first occurrence of this species, without an obvious precursor, in Site 643 recovery suggests either a pronounced zoogeographic shift or a hiatus. We have no other evidence of a hiatus, however. The biozonal boundary between NSR6 and NSR7 is located in Section 104-643A-13H-6 (117 m), which is correlative with Section 104-642B-22X-2 (18.9 m). The NSR7/NSR8 boundary is located in Section 104-643A-12H-3 (108 m) and is represented by a hiatus, which also occurs at Site 642. Biozone NSR8 is very short in Hole 643A, and is represented by only 8 m of sediments (Sections 104-643A-11H-3 to 643A-12H-3). The NSR8/NSR9 boundary is also represented by a hiatus at Site 643 that correlates with the upper hiatus at Site 642. Biozone NSR9 extends up to the top of Core 104-643A-9H, which represents the approximate top of biosiliceous sedimentation at Site 643. Thus, neither the true top of NSR9 nor sediments assignable to NSR10-13 are present at Site 643.

Paleoenvironment

The status of our research on Leg 104 radiolarians is too preliminary in nature to permit a well-documented presentation. Noticeable, however, is the presence in NSR5-NSR7 of significant concentrations of species (i.e., *Collosphaera* sp., *Aerosphaera spinosa*, and *Cyclampterium*(?) *neatum*) that indicate relatively warm surface water. These occurrences show that at least a few species that evolved in tropical environments were preadapted to the pelagic ecosystem of the Norwegian Sea during latest early Miocene and middle Miocene time, and that conduits existed to allow the episodic circulation of warm water into this region.

Calcareous Nannofossil Biostratigraphy

Zone Definitions

The standard Martini (1971b) nannofossil zonation was followed to some extent, but because of the absence of many marker species, various zones had to be combined into longer-ranging zones. The nannofossil assemblages presented here are similar to those compiled in Leg 38 (Müller, 1976), with the exception of the interval containing *Cyclococcolithus floridanus*, which is presented here in Table 5 and in the Site 642 "Biostratigraphy" section (see Table 11).

Emiliania huxleyi and *Gephyrocapsa oceanica* Zone (NN21/20)
Bottom: LAD *Pseudoemiliania lacunosa*
Age: middle to late Quaternary

Interval with *P. lacunosa* (NN19/16)
Top: LAD *P. lacunosa*
Bottom: LAD *Reticulofenestra pseudoumbilica*

Interval with *R. pseudoumbilica* (NN15/7)
Top: LAD *R. pseudoumbilica*
Bottom: LAD *Cyclococcolithus floridanus*
Age: middle Miocene to early Pliocene

Table 5. Calcareous nannofossil biostratigraphy, Site 643.

Depth (msbf) Sample	Nannofossil zonation	Zonal marker	Age (Ma)	Species present
27/ 4H-2, 123 cm	*Emiliania huxleyi-Gephyrocapsa oceanica* (NN21/20)	LAD *P. lacunosa*	upper to middle Quaternary (0–0.47 m)	*E. huxleyi*?, *Gephyrocapsa* sp., *Coccolithus pelagicus*, small *Reticulo fenestra* sp., *Coronocyclus nitescens*, *Cyclococcolithus leptoporus*, *Dictyococcites* sp., *Discolithina* sp., *Helicosphaera* sp.
74/ 9H-2, 125 cm	*Pseudoemiliania lacunosa* (NN19-16)	LAD *R. pseudoumbilica*	early Quat. to late Miocene (0.47–3.2)	same as *G. oceanica* Zone except add *P. lacunosa*
90.8/ 10H, CC	*Reticulofenestra pseudoumbilica* (NN15-7)	LAD *C. floridanus*	late Miocene (3.2–13.5)	*C. pelagicus*, small *Reticulofenestra*, *R. pseudoumbilica*, *C. leptoporus*, *Dictyococcites* sp.
Barren from 90.8 to 301.1 m				
<400.4/ 34X, CC	*Cyclocargolithus floridanus* (NN6-1)	LAD *D. enormis*	late Miocene early Miocene (13.5–24.8)	*C. floridanus*, *C. pelagicus*, *Dictyococcites* sp., *Helicosphaera* sp., *R. pseudoumbilica*, *Reticulofenestra* sp., *Coccolithus abisectus*
Barren from 400.4 to 410 m				
410/ 43X, CC	*Discolithina enormis* (NP25)	FAD *D. enormis*	late Oligocene (24.8–27.8)	same as *C. floridanus* Zone except add *D. enormis*

Note: LAD = last occurrence datum.

Interval with *C. floridanus* (NN6/1)
Top: LAD *C. floridanus*
Bottom: LAD *Discolithina enormis*
Age: early Miocene

Interval with *D. enormis* (NP25)
Top: LAD *D. enormis*
Bottom: FAD *D. enormis*
Age: latest Oligocene

Abundance and Preservation

The abundance of nannofossils at Site 643 is generally poor, except for a few rich intervals in the upper Pliocene–Pleistocene intervals. The interval from 91 m sub-bottom to total depth is mostly barren, with the exception of a few scattered samples that contained a generally small-diversity assemblage.

Preservation of nannofossils here is never good and is generally poor to moderate, often making identification difficult.

Reworked specimens of older nannofossils are commonly present down to a sub-bottom depth of about 30 m. The reworking consists primarily of Cretaceous nannofossils, but Paleogene reworking is also found to a lesser extent. The reworked specimens often comprise more than 50% of the assemblage.

Results

Cores 104-643A-1H through 104-643A-3H contain an assemblage of dominantly *Gephyrocapsa*. *E. huxleyi*, the marker for NN21, could not be determined without scanning electron microscopy (SEM). Thus, this interval is designated as the upper to middle Pleistocene Zone NN21/20.

The marker for the upper Pliocene to lower Pleistocene Zone NN19/16, *P. lacunosa*, is first observed at 27 m, but could occur higher due to its rarity in the area. Thus, the NN20/19 boundary is not precisely determined.

Cores 104-643A-5H through 104-643A-8H are barren or contain insufficient nannofossils to designate a nannofossil zone.

Cores 104-643A-9H and 104-643A-10H both contain *R. pseudoumbilica*. This is the marker for Zone NN15/7, which is followed by a long barren interval from Cores 104-643A-11H through 104-643A-31X.

Core 104-643A-34X contains a few nannofossils, including *C. floridanus*. No Oligocene nannofossils, such as *D. enormis*, were observed. This designates NN6/1, which is lower Miocene. The upper limit of NN6/1 could not be determined because of the barren interval present above the *C. floridanus* found there.

Cores 104-643A-35X through 104-643A-41X are barren or contain only rare, poorly preserved nannofossils, insufficient for determining nannofossil zones.

Core 104-643A-42X contains the same assemblage as Core 643A-32X, as well as a few small specimens of *C. abisectus*, although not enough to be considered the acme present in the upper Oligocene. *D. enormis* is also missing. This interval is thus considered a continuation of NN6-1.

D. enormis is observed in Core 104-643A-43X, which designates the late Oligocene NP25 Zone.

Cores 104-643A-45X through 104-643A-47X all contain few to rare occurrences of nannofossils, and no positive age determinations are possible. *C. floridanus*, which ranges from late Eocene to early Miocene, is observed, but none of the upper Eocene to lower Oligocene markers from Leg 38, such as *Istmolithus recurvus* or *Reticulofenestra umbilica*, are observed.

Cores 104-643A-48X through 104-643A-62X are barren of nannofossils.

Paleoenvironment

The sediments at Site 643, as a general rule, contain relatively few calcareous nannofossils and those that are present are of low diversity. The specimens present are typically high-latitude species, such as *Coccolithus pelagicus*. The lower- to middle-latitude species (sphenoliths, ceratoliths, and discoasters) are missing.

Planktonic Foraminifer Stratigraphy

Methods

Shipboard study was limited to core-catcher samples. Additional shore-based investigations of every second section were performed. Results are listed in Table 6.

The same informal zonal scheme and zonal definitions were applied for the Neogene section as were used for Site 642. See Chapter 4, this volume. Two additional Paleogene zones were identified and are defined next. As these zones are restricted by barren intervals, they are regarded as preliminary assemblage zones.

Results

The interval from the top of the hole through Sample 104-643A-6H, CC is highly dominated by *Neogloboquadrina pachyderma* sin. in the heavily encrusted morphotype. This correlates to Zone NSPF6 of Site 642. Other species found in minor amounts in this interval are *N. pachyderma* dex. and *Globigerina quinqueloba*. Significant amounts of *N. pachyderma* dex. were identified in Samples 104-643A-2H-3, 76-80 cm, and 104-643A-2H-5, 76-80 cm, indicating warmer interglacial to interstadial environments. A long barren zone comparable to that found in the upper parts of Site 642 is present in Cores 104-643A-5H and 104-643A-6H.

Core 104-643A-8H is barren, while a completely different fauna appears in Cores 104-643A-9H, 643A-10H, and 643A-11H. *N. pachyderma* sin. appears in minor amounts in its reticulate, more open and less compressed form. The dominant species are *N. pachyderma* dex., *N. acostaensis*, and *N. continuosa*, whereas *N. atlantica* dex. occurs in some samples. These assemblages correlate to zone NSPF3, Site 642, indicating a major hiatus between Cores 104-643A-7H and 104-643A-9H, where large portions of the Pliocene are apparently missing from the section.

The interval from Samples 104-643A-12H, CC through 104-643A-29X, CC is barren in planktonic foraminifers and consists mainly of siliceous muds and oozes. A limited number of unidentifiable globigerinids are present in Sample 104-643A-30X, CC. Then, a new barren interval comprises Cores 104-643A-31X to 104-643A-41X, CC.

Samples 104-643A-41X, CC, 643A-43X, CC, and 643A-44X, CC contain small amounts of planktonic foraminifers in hard and thin calcareous layers interbedded in noncalcareous sediments. The small number of specimens and problems with disaggregation of the samples make identification of the species difficult. Thus, only preliminary species assignments can be given in this report. The species are identified as *Globigerina anguliofficinalis* Blow, *G. angiporoides* Hornibrook, *G. linaperta* Finlay s.l., and some unidentified small forms of globigerinids. According to Blow (1969, 1979) and Stainforth et al. (1975) the concurrent ranges of the species of this assemblage are from P17 to P19 (late Eocene to late Oligocene). The very restricted assemblage in Sample 104-643A-41X, CC may range into P21 (=N2, latest Oligocene) based on the absence of *G. angiporoides*. *G. anguliofficinalis* is believed to be an especially good Oligocene marker (Blow, 1969).

The samples 104-643A-45X, CC through 104-643A-51X, CC are barren in planktonic foraminifers. The assemblages encountered in Samples 104- 643A-52X, CC, 643A-54X, CC, 643A-55X, CC, 643A-56X, CC, and 643A-59, CC are different from those found in the nonbarren interval mentioned earlier. *G. officinalis* Subbotina and *G. linaperta* s.l. are the most common species. A number of small unidentifiable globigerinids also occur. The occurrence of *G. officinalis* indicates a middle to late Eocene age (Blow, 1969, 1979).

The lowermost samples (beneath Core 104-643A-59X) are barren in planktonic foraminifers.

Table 6. Planktonic foraminifers in Hole 643A.

Core/sec/int (cm)	*N. pachyderma* (sin)	*N. pachyderma* (dex)	*N. atlantica* (sin)	*N. atlantica* (dex)	*N. acostaensis*	*N. continuosa*	*G. bulloides*	*G. falconensis*	*G. quinqueloba*	*Globigerina* spp.	*G. officinalis*	*G. linaperta*	*G. angiporoides*	*G. anguliofficinalis*	Zone
1-1, 74-78	A														
1-3, 74-78	R														
2-1, 76-80	R														
2-3, 76-80	A	C							R						
2-5, 76-80	A														
2-CC, 10-14	F	C							R						
3-2, 74-78	A														
3-4, 74-78	F														
3-6, 74-78	A														
3-CC, 9-13	A														
4-2, 70-74	R														NSPF6
4-4, 73-77	A														
4-6, 71-75	F														
4-CC, 18-22	Barren														
5-2, 67-71	Barren														
5-4, 72-76	Barren														
5-6, 72-76	Barren														
6-1, 75-79	Barren														
6-3, 75-79	Barren														
6-5, 75-79	Barren														
6-CC, 14-19	R	R													
7-2, 74-78	R		R												NSPF 5-4
7-4, 74-78	R	R	R												
7-CC, 9-12	Barren														
8-2, 74-78	Barren														
8-4, 74-78	Barren														
8-6, 74-78	Barren														
9-1, 73-77		C			R										
9-3, 73-77	Barren														
9-5, 73-77		R			R										
9-CC, 15-17	Barren														
10-2, 73-78	Barren														
10-4, 73-78		R		R	R	A	R		R						NSPF3
10-6, 73-77	Barren														
11-1, 75-79	Barren														
11-3, 75-79						R									
11-5, 75-79					C										
Rest of Core 11 and Cores 12 through 29 barren															
30-CC, 46-48										R					
Cores 31 through 40 barren															
41-CC, 18-21										R				R	
Cores 42 through 44-5 barren															NSPF2
44-CC, 10-14										R		R	R		
Cores 45 through 52-5 barren															
52-CC, 18-22										R	R		R		
Cores 53 through 54-5 barren															NSPF1
54-CC, 18-22										R		R			
Cores 55 through 61 barren															

A = abundant, F = frequent, C = common, R = rare.

Preliminary Planktonic Foraminifer Zones

Zones NSPF3 through 6 were defined in the biostratigraphic section, Chapter 4, this volume.

Zone NSPF1

Assemblage zone defined by the occurrence of *G. linaperta* s.l. Finlay and *G. officinalis* Subbotina.

Age estimate: late Oligocene (P19-P21).

Zone NSPF2

Assemblage zone defined by the occurrence of *G. anguliofficinalis* Blow and *G. angiporoides* Hornibrook.

Age estimate: middle to late Eocene.

Discussion

The zonation of Site 643 correlates to that of Site 642 in Figure 45 (see "Biostratigraphy" section, Chapter 4, this volume).

The total dominance of sinistral *N. pachyderma* in the uppermost zone implies that mainly deposits reflecting glacial environments were encountered in the samples analyzed. No assemblages belonging to Zones NSPF4 and 5 were found at Site 643, which indicates a significant hiatus spanning the lower Pliocene and the upper Miocene.

The Paleogene planktonic foraminifers are found in thin calcareous beds within barren clay-rich sediments. It is difficult to assign this pattern to a rapidly shifting environment with rapid and short-lived changes from noncarbonate deposition to carbonate deposition and vice versa. Changes between autochthonous and allochthonous deposition seem a more likely explanation.

Benthic Foraminifer Stratigraphy

Introduction

Benthic foraminifers from core-catcher samples at Site 643 were analyzed and showed assemblages ranging from the Eocene to the Pleistocene. Correlation to Site 642 was somewhat hampered in the upper interval because of apparent slumps and/or hiatuses, and the fact that some core-catcher samples were not analyzed due to time constraints. From 0 to 440 mbsf the fauna in the samples were poor, and barren intervals were frequent (Table 7). Preservation was poor to moderate except in Samples 104-643A-1H, CC and 104-643A-5H, CC. Calcareous specimens were absent in most samples below Core 104-643A-11H (100 mbsf). Benthics dominated the total foraminifer assemblage in all samples except 104-643A-1H, CC, 643A-3H, CC, and 643A-9H, CC.

Core Zonation

Hole 634A was divided into seven benthic foraminiferal zones and subzones, some of which represent deep-water equivalents to Site 642. The uppermost Zone A (0–72 mbsf) is divided into two subzones. Subzone A1 (0–53 mbsf) is characterized by the presence of a calcareous benthic foraminifer assemblage of *Eponides umbonatus, Epistimonella exigua*, and *Pyrgo murrhina* along with ice rafted detritus. The species composition differs slightly from Site 642, Zone A1, *Cassidulina laevigata*, and reflects the deeper water conditions of this site. Subzone A2 (53–72 mbsf) contains only rare benthic foraminifers and is undifferentiated at this time.

Zone B (72–100 mbsf) contains a calcareous assemblage consisting of *Melonis zaandamae* and *Cassidulina subglobosa*, which we believe correlates to Zone B of Site 642.

There appears to be a large hiatus at Site 643, as suggested by the absence of the Site 642, Zone C1, *Martinottiella communis* assemblage. At Site 643 the arenaceous Zone C (100–293 mbsf) is represented only by Subzone C2. This subzone contains a rare assemblage of *Spirosigmoilinella* spp. in a sediment rich in biogenic silica similar to the oldest benthic foraminiferal Subzone C2 of Site 642.

Zone C2 is separated from Zone D by a barren interval from 293 to 323 mbsf. Zone D (323–497 mbsf) is characterized by the presence of *Cyclammina amplectens* and can be divided into two subzones. Subzone D1 is characterized by poor samples that contain mostly arenaceous forms. Calcareous foraminifers were encountered in the calcium-carbonate-rich sediment of Sample 104-643A-43X, CC, which contains a rather diverse assemblage dominated by *Cibicides grimsdalei, Anomalinoides alazanensis*, and *Turrilina alsatica*. Several additional calcium-carbonate-rich layers occur in Zone D and may contain calcareous foraminifers. Core-catcher Samples 104-643A-45X, CC and 104-643A-46X, CC are barren. In Subzone D2 samples are richer, and tube-shaped forms such as *Rhabdammina* and *Hyperammina* are common.

Zone E (497–555 mbsf) comprises a unit that contains an even more abundant arenaceous assemblage than Zones C and D. Most samples contain a rather diverse fauna including *Haplophragmoides* sp., *Cribrostomoides* sp., *Ammodiscus* sp., and tube-shaped forms such as *Rhabdammina* and *Hyperammina*. The lower part of Zone E is characterized by small specimens of *Spiroplectammina spectabilis*.

Age of Deposits

The upper 290 m (Zones A1, A2, B, and C2) of Site 643 can be correlated to the same zones at Site 642. The sequence cored at this site, however, appears to have more disturbances in the upper section, and portions of the lower Pliocene, upper Miocene, and the entire middle Miocene are missing (Fig. 12). The lower section of the hole below 333 mbsf (Zones D and E) penetrates into Oligocene- and Eocene-aged deposits. The calcareous species in Sample 104-643A-43X, CC are of Oligocene age and have been described from the Bay of Biscay and Rockall Plateau (Berggren, 1972; Schnitker, 1979). *Turrilina alsatica* ranges from the uppermost upper Eocene to upper Oligocene in the North Sea area (King, 1983), and was found in Oligocene sediments on Leg 38 (Talwani, Udintsev, et al., 1976a).

The lowermost part of the cored sequence at Site 643 contains foraminifers that range in age from early to middle Eocene in other areas, but these ranges may be too old for this site. *Cyclammina amplectens*, the dominant species in Zone D, characterizes the late early Eocene deposits in the North Sea, but also ranges into the middle Eocene (King, 1983). The dominant species in the lower part of Zone E, *Spiroplectammina spectablis*, occurs in Paleocene deposits in the North Sea (King, 1983). On Leg 38, however, this species occurred frequently in deposits of Eocene age, and its presence was used to define the Oligocene/Eocene boundary at Sites 338 and 343 (Talwani, Udintsev, et al., 1976a). The same assemblage of arenaceous species as in Zone E has also been reported from Eocene deposits of the Bay of Biscay (Murray, 1979; Schnitker, 1979) and the Rockall Plateau (Berggren, 1972).

Paleoenvironment

The presence of a deep-water arenaceous assemblage, including *Bathysiphon* sp. and *Abyssammina* spp., in the oldest foraminifer-bearing sediments (Zone E) indicates that this site has been in relatively deep water since the early Eocene. The lack of calcareous foraminifers may indicate deposition near or below the CCD (Berggren, 1972). The arenaceous facies appear characteristically associated with turbidite sequences and basinal infilling.

A major faunal change exists across the Eocene/Oligocene boundary, which results in a more restricted benthic foraminifer assemblage at this site. Berggren (1977) proposed that this was caused by a cooling of world bottom water by as much as 5°C, which may or may not apply in the Norwegian Sea. The occurrence of the calcareous foraminifers in Zone D1 does indicate that basin infilling slowed at times to allow the deposition of calcareous-rich sediments (Berggren, 1977). Arenaceous assemblages continued to dominate during times of increased sediment input.

The lower and upper Miocene sediments (Zone C2) contain a rare undiagnostic arenaceous assemblage. No paleoenvironmental interpretation is attempted on this unit at this time. Lower Pliocene and upper Miocene sediments (Zone B) contain calcar-

Table 7. Distribution (percent of total benthic foraminifers of the most important benthic-foraminifer species) in core-catcher samples from Site 643.

																											Other fossils					
Core	*Eponides umbonatus*	*Pyrgo murrhina*	*Cibicides wuellerstorfi*	*Cassidulina reniforme*	*C. subglobosa*	*Stainforthia loeblichi*	*Epistominella exigua*	*Melonis zaandamae*	*Cibicides* spp.	*C. grimsdalei*	*Anomalinoides alazanensis*	*Bathysiphon* sp.	*Rhabdammina* sp.	*Cribrostomoides* sp.	*Spiroplectammina spectabilis*	*Recurvoides* sp.	*Ammodiscus* sp.	*Haplophragmoides* sp.	*Trochammina* sp.	*Cyclammina* spp.	*C. amplectus*	*Spirosigmoilinella* spp.	Other species	% Benthic foram.	Abundance	Preservation	Siliceous fossils	Ostracodes	*Bolboforma*	Other	Reworking	Benthic foram zonation
1	59	10		6																			25	4	F	G		X		Ec Bv	Shelf transp	A_1
3			11		4	26	47																12	1	F	G				Ec		
5																									—		R, Sp			Ec	X	
6																									—							
7																									—		Sp			Fi		A_2
8																							X		R		D, Sp					
9	6				23		2	17	7													2	43	38	R	P	R, Sp, D		X	Pt		B
10	46							39	4													2	9	100	R	G	R, D, Sp		X			
11					X																	X	X	70	R	M	D, R, Sp					
13																						X		100	R	P	D, R, Sp					C_2
15																						X	X	~100	R	P	D, Sp, R					
17																						X	X	100	R		D, R					
18																									—		D, R					
19																									—		D, R					
20																									—		R(D)					
21																									—		D, R, Sp			W		
23																						X		100	R	M	D, R					
25																						X		100	R		R					
27																									—		R					
29																						X		100	R		D, R, Sp					
30																									—		D					
31																							X	100	R							
32																									—							
34																									—							D_1
35																				X				100	R	M				W		
37																									—							
39																							X	100	R	P				Fi		
41																									—							
																									?							
42																							X	100	R	P						
43										X	X												X	~100	R	M						
44																X	X	X	X				X	92	F	P						
45																									—							
46																									—							
47																		XX			XX		X	100	F	P						D_2
48														X							XX		X	100	F	M						
49																		X			XX		X	100	F	P						
50																					XX		X	100	F	M						
51														X		X		X			XX		X	~99	F	M				Fi		
52														X		X	X	X		X	X		X	~90	F	M			X	Fi		
53													X			X							X	100	R							E
54																							X	~75	F	P			X			
55																							X	~75	R	P						
56														XX			X			X			X	100	R	P						
57														X	XXX			X	X		X		X	100	F	P						
58												X						X		X			X	100	F	P				Fi		
59												XX			X		X	X	X	X				100	R	P	R, D			Fi		
60																									—							Barren
61																									—							
62																									—							

Abbreviations: R = rare, C = common, P = poor, M = moderate, G = good, D = diatoms, R = radiolarians, Sp = sponge spicules, Ec = echinoderm remains, Bv = bivalves, Pt = pteropods, W = wood fragments, Fi = fish remains, Q = quartz, Se = sedimentary rock fragments, Mi = mica, V = tephra, Z = zeolite, Dol = dolomite concretions, Gl = glauconite, X = occurrence in sample.

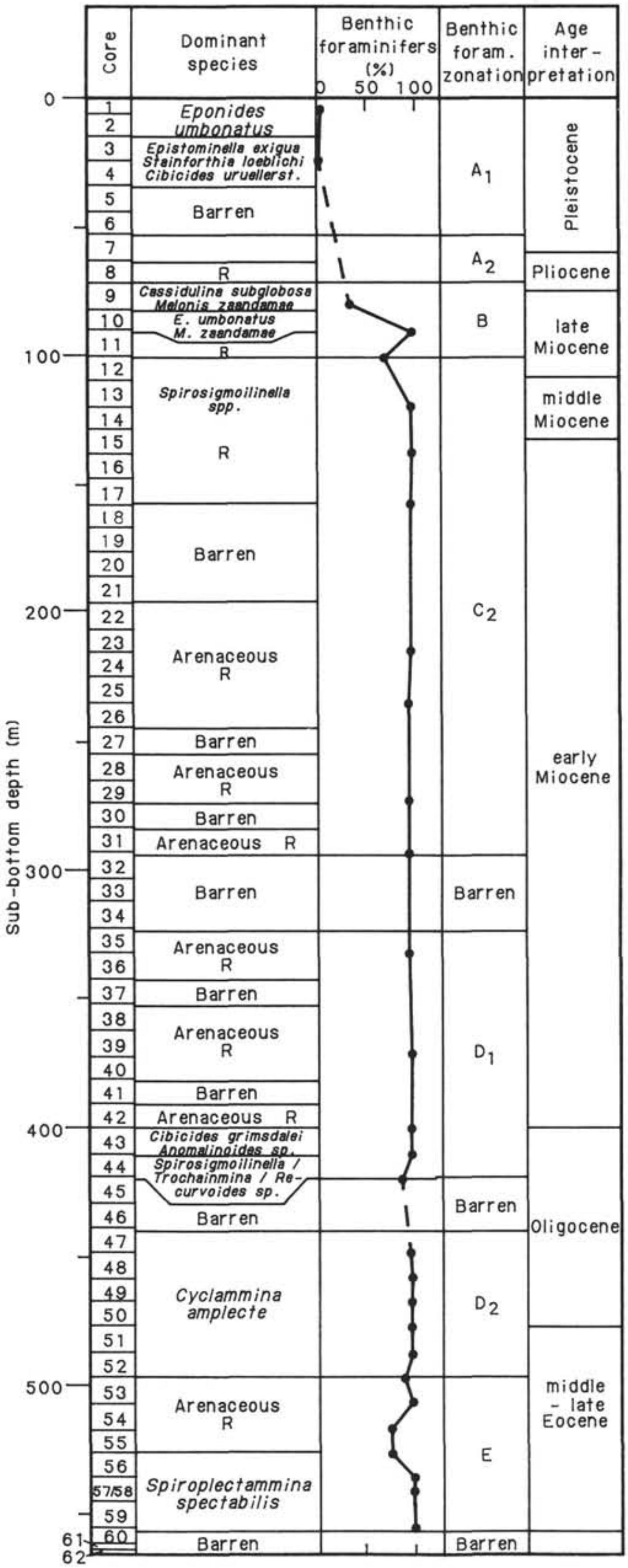

Figure 12. Core intervals in Hole 643A. The characteristic species/species group and the frequency of benthic foraminifers (in percent of total foraminifers) indicated for each core refer to the core-catcher sample. The benthic foraminifer zonation is shown on the right side of the diagram. The age interpretations are based on all stratigraphic information from this site.

eous foraminifers, which are similar in composition to those of Zone B for Site 642; however, paleoenvironmental determination must await further shore-based analysis of this unit.

The uppermost Pleistocene (Zone A1) sediments reflect a glacial environment (see "Sedimentary Lithology" section, this chapter). The occurrence of *Cibicides wuellerstorfi* in Sample 104-643A-5H, CC indicates interglacial conditions (Streeter et al., 1982). Sample 104-643A-1H, CC contains *Elphidium excavatum* transported from the neighboring shelf, which represents a glacial episode.

Palynology

Palynomorph Content and Preservation

Dinocysts (dinoflagellate cysts) and sporomorphs (pollen and spores) were identified and counted in 29 core-catcher samples from Hole 643A. We also estimated the palynodebris composition of those samples (% amorphogen, wood fragments, and coaly particles) and the presence of reworked palynomorphs. Most samples contained common to rare dinocysts and a few sporomorphs. The relative rarity of pollen and spores is indicated by the Dinocyst Index values (D/P = ratio of total dinocysts to pollen and spores) shown in Figure 13. Preservation of dinocysts and sporomorphs is generally moderate to good in the muddy glaciogenic and diatomaceous sediment units down to about 300 mbsf; moderate to poor in the banded gray mudstone from about 300 to 560 m; and excellent just above the basaltic conglomerate at the base of the hole. A tentative palynostratigraphy is presented (Fig. 13), based on the same criteria used for Site 642 (this volume), but note that this zonation will undoubtedly be modified when detailed onshore studies have been completed. Initial data from these onshore studies were used to clarify the zonation of the Paleogene–lower Miocene sediments, as outlined in the following description of the zonation.

Zonation

0–5.4 m. Subzone PM1a, the upper Pleistocene *Spiniferites elongatus* range zone, was recognized by the same group of species found in this subzone at Site 642. The base of this subzone corresponds to the Jaramillo subchron (0.94 m.y.). Subzone PM1b was not recognized in Hole 643A because of the apparent absence of *Filisphaera filifera* in the core-catcher samples.

20–42 m. Zone PM2/3. The top of the *Achomosphaera ramulifera* range zone, PM2, was recognized by the LAD of *A. ramulifera* in Sample 104-643A-3H, CC at 20 mbsf. This datum probably marks the Olduvai Event (1.6 Ma) at Site 643. However, many of the characteristic species found at Site 642 and in other parts of the North Atlantic are not present at Site 643, and a barren interval (Sample 104-643A-4H, CC) truncates the assemblage zone, as shown in Figure 13. Sample 104-643A-5H, CC contained abundant *Palaeostomocystis* species that form an acme zone at the base of Zone PM3. Similar dinocyst assemblages mark the Pontian Stage at Site 642 and elsewhere in the northeast Atlantic. Therefore, the base of Zone PM2/3 probably has a late Miocene age of 8.8–6.8 Ma.

42–81.3 m. Samples 104-643A-6H, CC to 104-643A-9H, CC comprise a barren interval that appears to truncate the base of the Pontian Stage sediment. Siliceous microfossils also indicate a large hiatus between Samples 104-643A-8H, CC and 104-643A-9H, CC, so that sediments found in Hole 642B from the top of 104-Core 642B-10H to the middle of Core 104-642B-15H are missing in Hole 643A. This hiatus explains the apparent absence of Zone PM3 at Site 643.

81.3–100.8 m. Zone PM4 is the upper-middle lower-upper Miocene *Nematosphaeropsis aquaeducta* range zone. The LAD of *N. aquaeducta* correlates with P15/16 (ca. 10 Ma) at the

Gram-type section. *Pyxidiella* sp. A reaches an acme in this zone in Hole 643A, although it is rare at Site 642. This taxon has an age range of about 13.0–7.5 Ma at DSDP Site 611 (Mudie, 1987).

100–176.3 m. Zone PM4/5. The top of this interval is marked by the FAD of *N. aquaeducta* in Sample 104-643A-12H, CC and it lies just below the LAD of *Ascostomocystis* sp. 1 of Manum (1976), which last occurred in the middle Miocene at DSDP Site 338. The base of the zone is marked by the LAD of several species that characterize the underlying *Systematophora ancyrea-Pentadinium laticinctum* Zone, which has an early Miocene age at Site 642. However, at Site 643, the FAD of *Operculodinium crassum* and *Achomosphaera andalousiense* also occur at the base of this zone. At the type-section of *A. andalousiense* and at the Gram stratotype, the FAD of this species correlates with NN10 (ca. 11 Ma). Hence, the exact age of the lower Miocene Zone PM4/5 is presently uncertain.

176–410.0 m. Zone PM6, the *Systematophora ancyrea-Pentadinium laticinctum* acme zone is marked by approximately the same assemblages as those found in the lower Miocene interval at Site 642. In addition, the LAD of *Apteodinium spiridoides* is found at the top of this zone; this species has an early Miocene LAD at DSDP Site 338. Zone PM6 has an early Miocene age of about 23–16 Ma. The range of *Systematophora placacantha* is found in this zone at both Sites 643 and 642. The range of *Pentadinium laticinctum* is also found in this zone. This species has a LAD in upper Eocene-Oligocene sediments of the western North Atlantic (Williams and Bujak, 1977), but extends to the top of the middle Miocene interval at DSDP Site 552 in the eastern North Atlantic (Edwards, 1984). The presence of *Hystrichosphaeropsis obscurum* in Zone PM6 indicates Miocene age, according to Manum (pers. comm., 1986). The presence of typical Eocene species, e.g., *Batiacasphaera compta* and *Hystrichosphaeridium tubiferum*, in the lower part of this zone (Samples 104-643A-32X, CC to 104-643A-43X, CC, 303.1–410 mbsf) is probably due to reworking.

410–520 m. Zone PM7, the *Chiropteridium dispersum* range zone, contains mostly a sparse flora at Site 643. Barren intervals exist near the top (Samples 104-643A-42X, CC to 104-643A-44X, CC), middle (Samples 104-643A-50X, CC and 104-643A-52X, CC), and base (Samples 104-643A-54X, CC and 104-643A-55X, CC) of the zone. Therefore, the zone is tentatively subdivided into Subzones PM7A (Samples 104-643A-43X, CC to 104-643A-50X,CC, 410–477.7 mbsf) and PM7B (Samples 104-643A-51X, 0–1 cm, to 104-643A-54X, CC, 487.3–516.4 mbsf). Subzone PM7A contains the range of *Chiropteridium* sp. according to the onshore work of Manum (pers. comm., 1986). This subzone is quite definitely of late Oligocene age. Rare occurrences of middle-upper Eocene species, such as *Homotryblium oceanicum*, are probably due to reworking. The boundary between the upper Oligocene and lower Miocene sediments, therefore, was provisionally placed at Sample 104-643A-43X, CC (410 mbsf), which also agrees with sporomorph ranges found in onshore studies by Boulter (pers. comm., 1986).

Subzone PM7B (104-643A-50X, CC to 104-643A-55X-2, 30–32 cm) is marked by the LAD of two Eocene dinocyst index species, *Areosphaeridium multicornutum* and *Svalbardella cooksoniae* in Sample 104-643A-51X-4, 30–32 cm. The base of this subzone is marked by the LAD of *Diphyes colligerum* and *H. oceanicum* in Core 104-643A-55X-2, 30–32 cm (520 mbsf). These species probably mark the boundary between middle and lower Eocene sediments in Hole 643A, according to the onshore studies of Manum (pers. comm., 1986).

520–565.2 m. Zone PM9, the *Cerebrocysta bartonensis* partial range zone, is similar to the corresponding zone at Site 642. At Site 643, a very rich palynoflora is found in Sample 104-643-57X, CC, which contains well-preserved specimens of *Cordosphaeridium cantharellum, Homotryblium oceanicum, H. pallidum*, and *Wetzeliella homomorpha*, in addition to the characteristic species of this zone. All the species mentioned previously are found in the upper middle Eocene Barton Beds. Onshore studies of a species-rich Sample 104-643A-60X-2, 31–33 cm, also shows the presence of other good middle Eocene markers, e.g., *Rottnestia borussica* and *Hystrichokolpoma cinctum*; therefore, a middle Eocene age is assigned to this palynozone.

Paleoecological Interpretation

At Site 643, approximately the same range of palynological events is evident from the Dinocyst Index (D/P) values found at Site 642. These events can also tentatively be correlated with those reported by Manum (1976) for DSDP Sites 336 through 348. The events shown in Figure 13 are identified as follows: (1) late Pliocene–Pleistocene fluctuations in sea level and influx of ice-rafted debris; (2) early to mid-Miocene subsidence of the Iceland-Faeroe Ridge, marking the stabilization of oceanic conditions and flow of warm North Atlantic surface water into the Norwegian Sea; (3) opening of the Greenland Sea and the inception of a Northern Hemispheric cool climatic interval in the late Eocene–Oligocene; (4) early-middle Eocene (Anomaly 24–25) opening of the Norwegian Sea; and (5) early Eocene volcanogenesis and marine transgressions and regressions on the Vøring Plateau and in eastern Greenland.

It is interesting that "palynoevents" 1, 3, 4, and 5 were recognized at both Sites 643 and 642 because some notable differences exist in the palynofloras at the two sites. These differences are (1) lower concentrations of pollen and spores in most parts of the stratigraphic section above Zone PM9 and below Zone PM2/3 at Site 643, (2) more species diversity in the Miocene and older dinocyst assemblages at Site 643, and (3) a much better preserved Eocene dinocyst flora at Site 643, suggesting deeper water and less oxidizing marine conditions than at the shallower Site 642 on the top of the Vøring Plateau.

Biostratigraphic Synthesis

Stratigraphic conclusions from the different fossil groups are summarized in this section. The biostratigraphic interpretation of this site was seriously hampered by intervals barren of one or more microfossil groups, thus limiting biostratigraphic resolution. As a result of these factors, unequivocal age interpretation is not possible at this time. Individual zonal assignments and the age interpretations for individual fossil groups are summarized in Figure 14. The age column in this figure gives the best preliminary age estimate, taking all available data into consideration.

Upper Pliocene–Quaternary Biostratigraphy

Only limited age control exists for the glacial interval corresponding with lithologic Unit I. NN21/20 (0–0.47 Ma) is present above Sample 104-643A-3H, CC (24.3 m). NN19/16 (0.47–3.2 Ma) is present in Sample 104-643A-4H, CC (33.8 m). The FAD of *A. ramulifera*, a marker for the Olduvai Event, appears in Core 104-643A-3H, suggesting that the NN20/NN19 boundary is situated above 33.8 m. This is in accordance with the paleomagnetic interpretation, which places the Brunhes/Matuyama boundary at about 16 m (see "Paleomagnetics" section, this chapter). From this placement we infer a lower sedimentation rate for the upper Quaternary at Site 643 than at Site 642.

Age control for the upper Pliocene is poor. As at Site 642, the base of the planktonic foraminiferal *N. pachyderma* sin. s.s. Zone and benthic foraminiferal Zone A roughly coincide with the base of the barren biosiliceous zones and with the boundary between lithostratigraphic Units I and II (glacial to nonglacial sediments, 49.42 m). Correlations of tephra layers between Sites 642 and 643 also support this conclusion. However, palynologi-

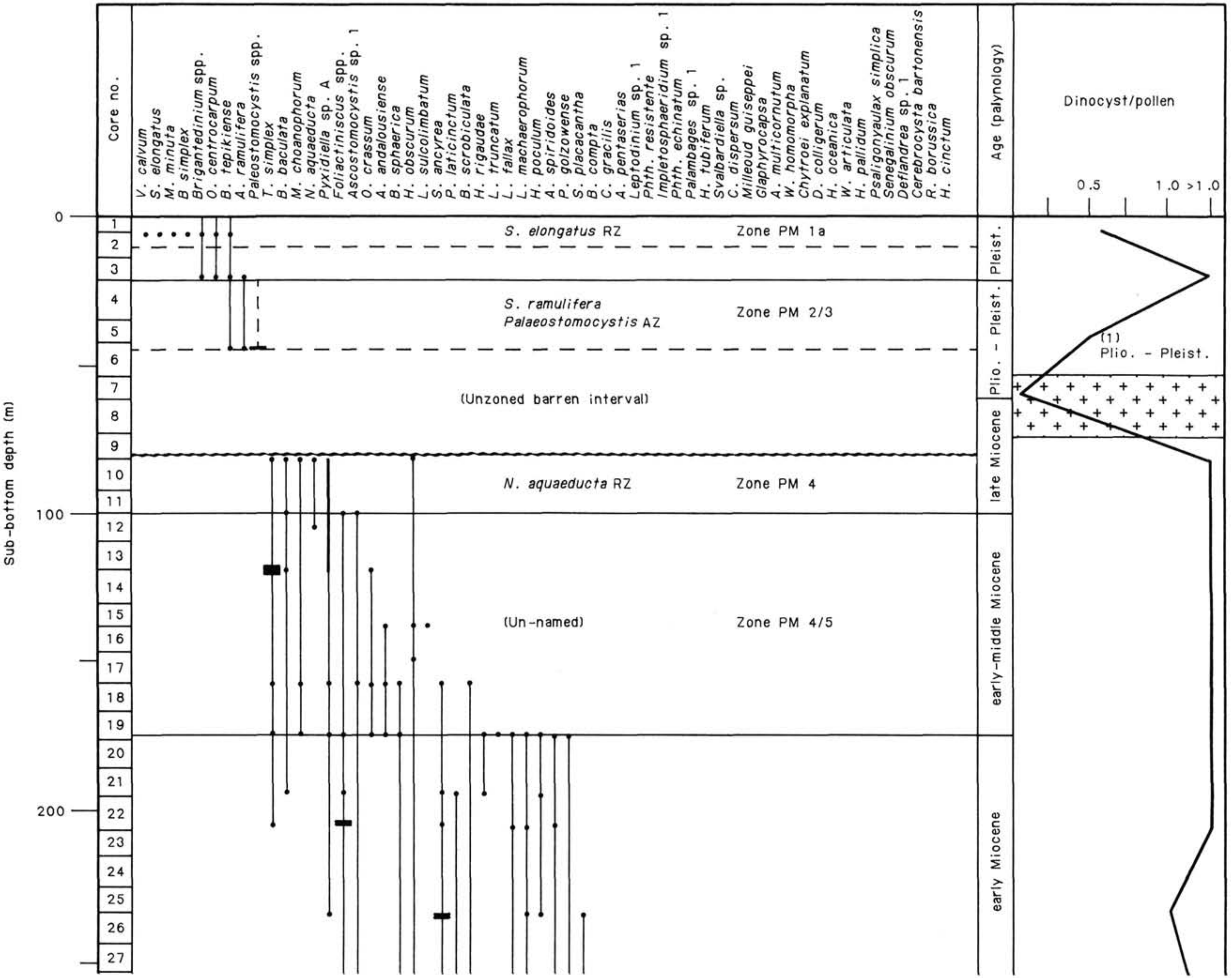
Core no.
V. calvum
S. elongatus
M. minuta
B simplex
Brigantedinium spp.
O. centrocarpum
B. tepikiense
A. ramulifera
Paleostomocystis spp.
T. simplex
B. baculata
M. choanophorum
N. aquaeducta
Pyxidiella sp. A
Foliactiniscus spp.
Ascostomocystis sp. 1
O. crassum
A. andalousiense
B. sphaerica
H. obscurum
L. sulcolimbatum
S. ancyrea
P. laticinctum
B. scrobiculata
H. rigaudae
L. truncatum
L. fallax
L. machaerophorum
H. poculum
A. spiridoides
P. golzowense
S. placacantha
B. compta
C. gracilis
A. pentaserias
Leptodinium sp. 1
Phth. resistente
Impletosphaeridium sp. 1
Phth. echinatum
Palambages sp. 1
H. tubiferum
Svalbardiella sp.
C. dispersum
Milleoud guiseppei
Glaphyrocapsa
A. multicornutum
W. homomorpha
Chytroei explanatum
D. colligerum
H. oceanica
W. articulata
H. pallidum
Psaligonyaulax simplica
Senegalinium obscurum
Deflandrea sp. 1
Cerebrocysta bartonensis
R. borussica
H. cinctum
Age (palynology)
Dinocyst/pollen
0.5
1.0 >1.0
0
100
200
Sub-bottom depth (m)
1
2
3
4
5
6
7
8
9
10
11
12
13
14
15
16
17
18
19
20
21
22
23
24
25
26
27
S. elongatus RZ
Zone PM 1a
S. ramulifera
Palaeostomocystis AZ
Zone PM 2/3
(Unzoned barren interval)
N. aquaeducta RZ
Zone PM 4
(Un-named)
Zone PM 4/5
Pleist.
Plio. - Pleist.
late Miocene
early-middle Miocene
early Miocene
(1)
Plio. - Pleist.

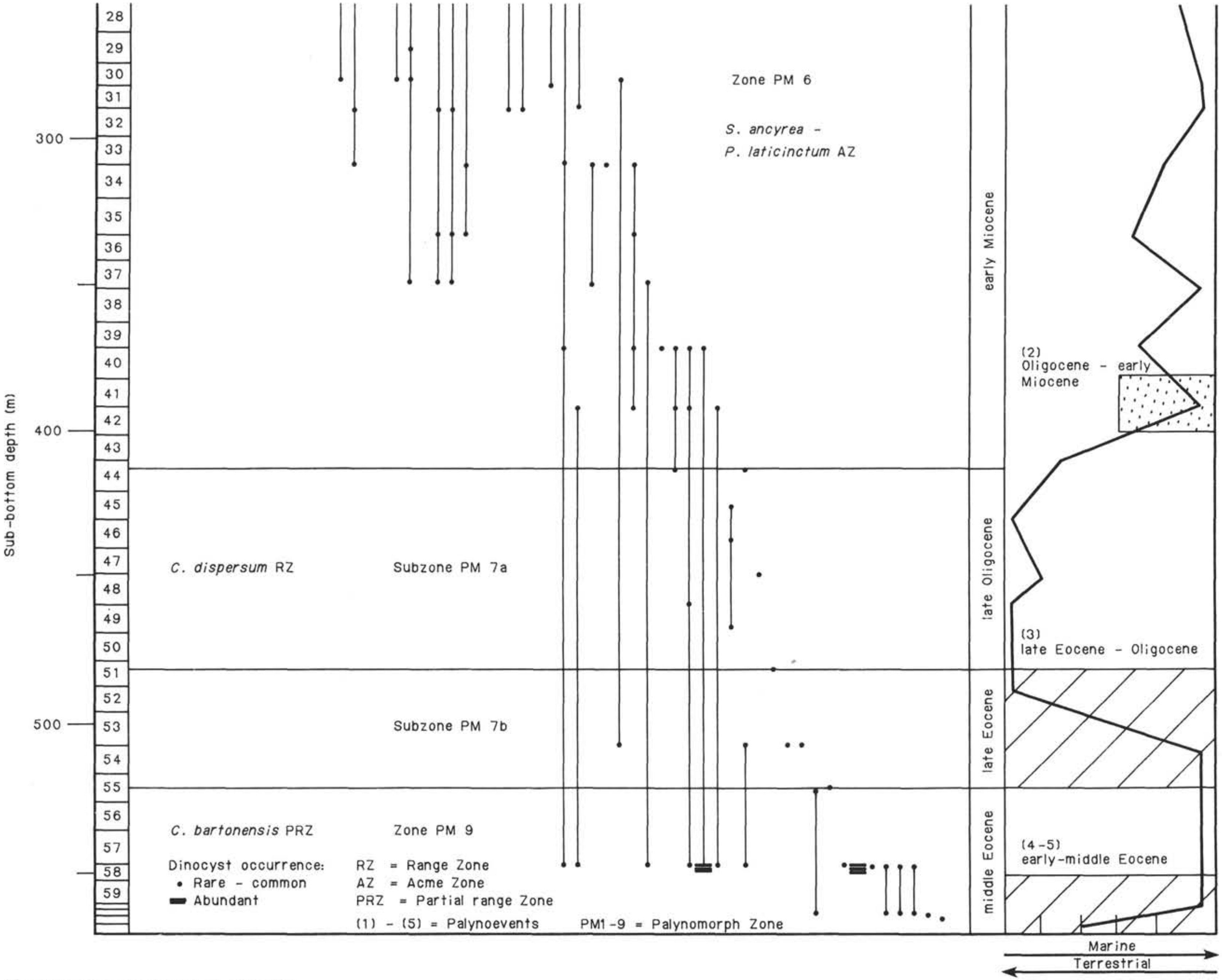

Figure 13. Dinocyst range chart, Site 643A.

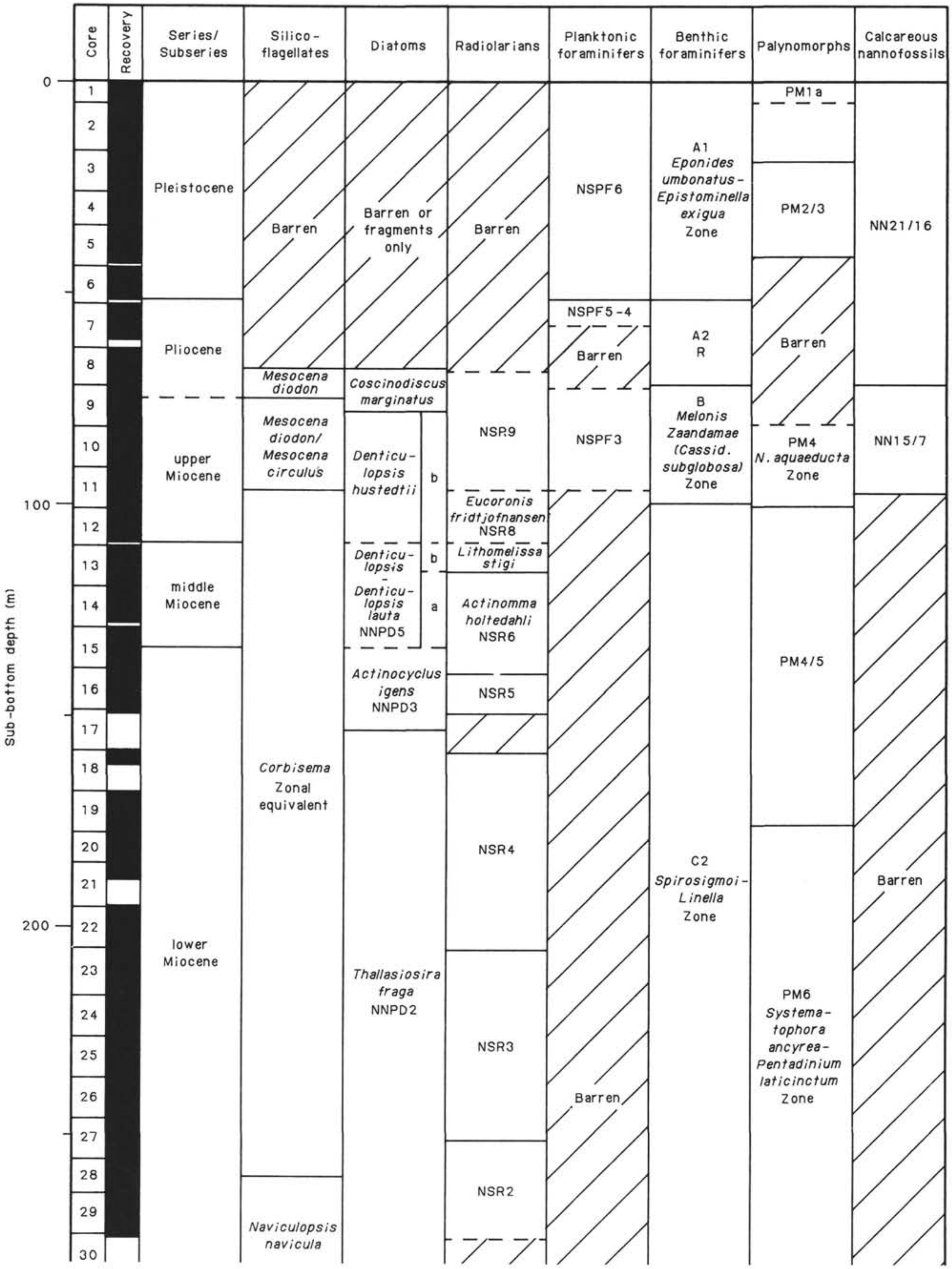

Figure 14. Composite biozone diagram.

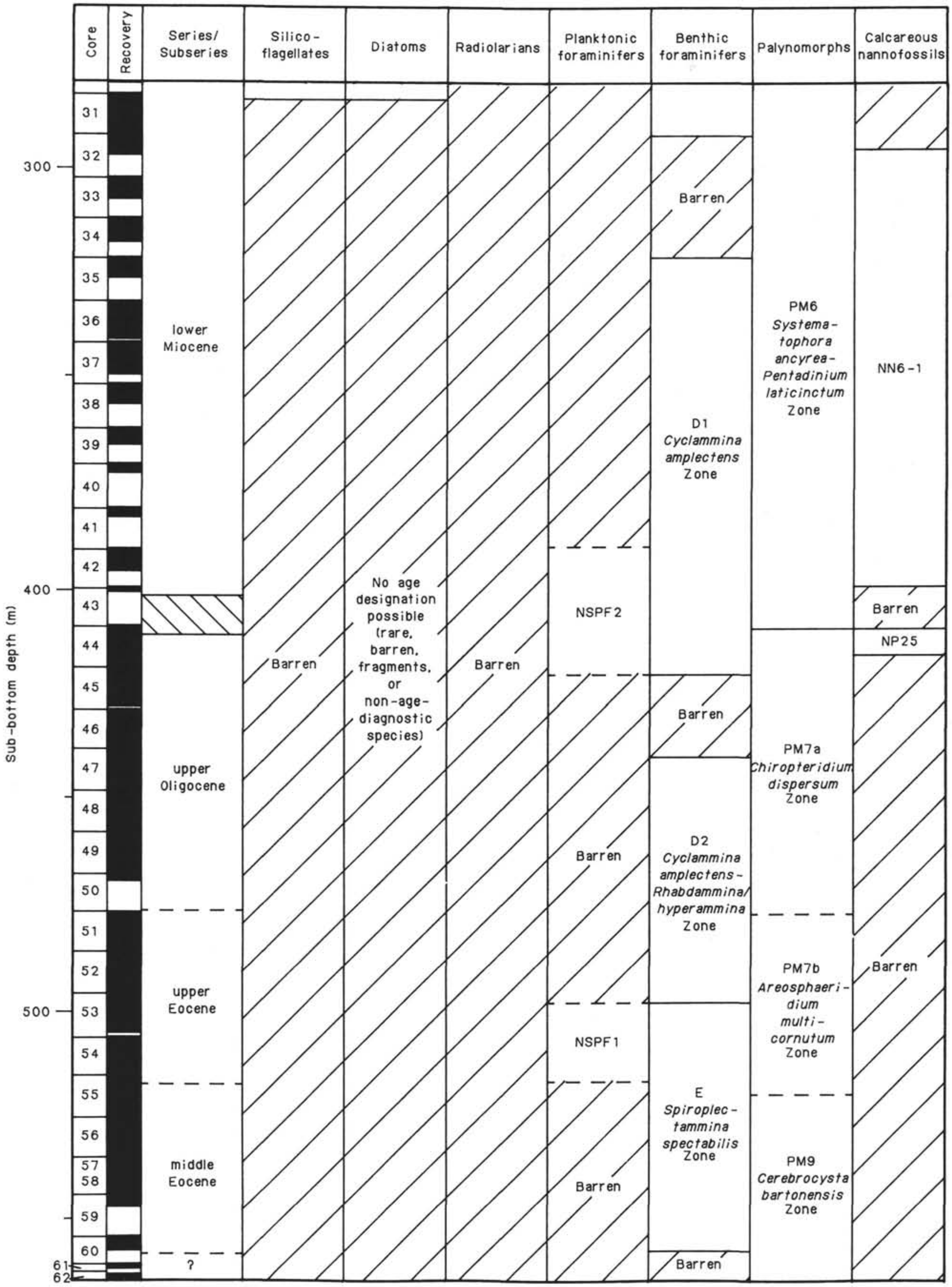

Figure 14 (continued).

cal data give the youngest age as the base of the Pontian Stage (6.8 Ma).

Middle Miocene–Pliocene Biostratigraphy

Samples 104-643A-7H, CC and 104-643A-8H, CC are barren in most microfossil groups. Section 104-643A-8H-5 contains a diatom assemblage belonging to the *D. marginatus* Zone and a silicoflagellate assemblage belonging to the *M. diodon* Zone. This indicates an age between 6 and 5.5 Ma (late Miocene). Several fossil groups give middle to late Miocene ages for Samples 104- 643A-9H, CC, 643A-10H, CC, and 643A-11H, CC. Calcareous nannofossils are from within NN15–NN7 (3.2–13.5 Ma). The top of the dinocyst *Pyxidiella* sp. acme (palynomorphs) (~7.7 Ma) is found in Core 104-643A-9H. Planktonic foraminifers from Samples 104-643A-9H, CC and 104-643A-11H, CC represent the NSPF3 planktonic foraminiferal zone, which indicates a middle to late Miocene age. Benthic foraminiferal assemblages in these samples correlate with Zone B (middle to late Miocene) from Site 642. Silicoflagellate assemblages from this interval belong to the late Miocene *M. circulus*/*M. diodon* Zone and diatom assemblages representative of the late Miocene *D. hustedtii* Subzone B also occur. These fossil groups are consistent with a late Miocene age. In contrast, the radiolarian assemblages in Samples 643A-10H, CC and 643A-11H, CC are assigned to the NSR9 Zone, which had a late Miocene age at Site 642. Except for occurrence of Pontian Stage palynomorphs in Sample 643A-5H, CC, these data suggest that major parts of the Pliocene and possibly parts of the upper Miocene are missing from the section. This unconformity is probably located between 60 and 80 m within lithostratigraphic Unit II, which is only about one-half as thick at this site as it is at Site 642 (see "Sediment Lithology" section, this chapter).

Middle–Lower Miocene Biostratigraphy

The radiolarian evidence indicates the presence of two extensive unconformities in Cores 104-643A-11H and 104-643A-12H that correlate with unconformities in Cores 104-642B-16H/642C-17H and 104-642B-19H/642C-20H. Missing zones from the same interval at Site 642 are also indicated by diatoms (parts of the *D. hustedtii*/*D. lauta* and *D. hustedtii* Zones), silicoflagellates (*M. circulus* Zone), and benthic foraminifers (Zone C1). The unconformity probably located in Cores 104-643A-12H seems to be of similar age as the unconformity/low sedimentation rate interval at Site 642, but it may include older sediments. The diatom stratigraphy shows evidence for an additional unconformity in Core 104-643A-15H, indicated by the absence of the *D. lauta* Zone. The presence of *A. holtedahli* above Core 104-643A-15H might be evidence against an unconformity here.

The lower Miocene to lower middle Miocene section of Site 643 is expanded in comparison with Site 642 (150 vs. 55 m). Biostratigraphic control from the siliceous microfossil groups disappears beneath the boundary between lithologic Units III and IV (274.05 m). By comparison with Site 642, the lowermost diatom and silicoflagellate zones at Site 642 are absent at Site 643, suggesting that the marked lithologic break at Site 643 is younger than the boundary to the altered volcanic sands at Site 642. Alternatively, diagenesis of siliceous microfossils may have destroyed assemblages correlative with the basal siliceous assemblages of Site 642 in which case the lithologic break may be of similar or older age.

Both palynomorphs and well-preserved siliceous microfossils provide consistent age determinations of early Miocene age down to 283.5 m. Between 283.5 and 400.4 m, calcareous nannofossils and palynomorphs give consistent Miocene ages. No age control can be derived from siliceous microfossils in this interval because they are absent.

Oligocene Biostratigraphy

The biostratigraphic age control for the interval 283.5 to 320 m is poor, with long barren zones. Lower Neogene calcareous nannofossils are found in Samples 104-643A-30X, CC (283.5 m) and 104-643A-42X, CC (400.4 m). Core 104-643A-43X (410 m) contains the zonal marker for NP25 (uppermost Oligocene, 24.8–24.7 Ma), placing the Oligocene/Miocene boundary between 400.4 and 410 m. Arenaceous benthic foraminiferal assemblages from Zone D correlate to the Oligocene deposits from Site 338, Leg 38 (Talwani, Udintsev, et al. 1976b). An Oligocene-Miocene age is also confirmed from planktonic foraminifers in Cores 104-643A-41X to 104-643A-44X (P16–P19) (381–419.7 m). Dinoflagellates in Zone PM7A (Cores 104-643A-30X to 104-643A-33X) have a late Eocene age, which agrees well with an Oligocene/Miocene boundary being placed in Core 104-643A-42X.

Eocene Biostratigraphy

Benthic foraminiferal Zone D2 (Samples 104-643A-46X, CC to 104-643A-52X, CC, 439.1–497.0 m) correlates to early and middle Eocene faunas in the North Sea. At the Vøring Plateau, these species seem to indicate younger ages, according to dating by palynomorphs and results from DSDP Sites 338 and 343. Planktonic foraminifers indicate a middle to late Eocene age (P13–P16) for Samples 104-643A-53X through 104-643A-56X (506.7–545.2 m). Palynomorph Zone PM7B coincides with this core interval and gives a late early Eocene age for Samples 104-643A-51X, CC to 104-643A-54X, CC. Cores 104-643A-57X and 104-643A-59X contain a well-preserved middle Eocene dinocyst flora. No specific microfossil age can be assigned for the basaltic conglomerate at the bottom of the hole, but an early or middle Eocene age is most likely.

Paleoecological Synthesis

In this paleoenvironmental synthesis of the microfossil assemblages at Site 643, one must assume that the composite biostratigraphic ages are approximately correct. All paleoecological interpretations can only be tentative until better dating control is available for Site 643. Several salient features (summarized here) are evident, however, based on more detailed descriptions given previously in this section.

Water Chemistry, Paleodepth, and Microfossil Diagenesis

All microfossil groups are absent from the basaltic conglomerate at the base of the hole, probably due to unfavorable environmental and preservation conditions. Most planktonic siliceous microfossils are also absent from the Paleogene sediments. This may indicate that the surface water was depleted in silica during this time interval, as interpreted for the Oligocene interval at DSDP Site 338. Alternatively, diagenetic factors may require a different interpretation. However, the first pulse of opal accumulation is found in middle-upper Eocene sediments on the Vøring Plateau and at other DSDP sites in the Norwegian Sea. This initial accumulation corresponds to the widening of the North Atlantic Ocean and connection to the Norwegian Sea (Thiede, 1980). Furthermore, abundant arenaceous benthic foraminifers are present in the lower-middle Eocene sediments at Site 643 (ca. 560–440 mbsf). The presence of benthic foraminifers in lithologic Unit V (zeolitic mudstone and overconsolidated pyroclastic sediments) suggests relatively deep water. Evidence from the concurrent presence of planktonic foraminifers and peaks in dinocysts, shown by the Dinocyst Index (D/P) in Unit V, also indicates oceanic conditions. Therefore, the total absence of siliceous microfossils more likely indicates that opal preservation was unfavorable in the water column and/or sediments.

The presence of arenaceous foraminifers in Unit IV indicates relatively deep water during the late Paleogene at Site 643. This suggests that the low D/P values between 500 and 400 mbsf reflect increased influx of terrigenous sediments. Note that in both Units IV and V, carbonate deposits are associated with marine incursions, as indicated by the peaks in the D/P values; however, the carbonate layers may only indicate local conditions of better carbonate preservation.

The lower Miocene Unit III at Site 643 is marked by moderate to good preservation of all siliceous and organic-walled microfossils and by poor preservation of calcareous microfossils.

The upper Neogene and Quaternary interval at Site 643 shows a turnover of oceanic conditions: siliceous planktonic and arenaceous benthic microfossils become replaced largely by calcareous species. In the Pleistocene interval, this change may be due to decreased primary productivity and, consequently, lower rates of biogenic silica fixation associated with ice cover during the glacial intervals.

Hiatuses

Several microfossil groups indicate unconformities in the sedimentary record of this site (Fig. 14). Lack of planktonic foraminifers in Zone NSPF4 indicates a Pliocene hiatus in Core 104-643A-8H. Presently, no data are available from the other fossil groups to substantiate this hiatus.

Radiolarian and diatom data show evidence for as much as three middle to late Miocene unconformities that may correlate with unconformities recorded at Site 642. A hiatus in Cores 104-643A-12H to 104-643A-13H is confirmed by both diatoms and radiolarians. Radiolarian data indicate an unconformity in Core 104-643A-11H, which at the present is not confirmed by other siliceous microfossils. Evidence for an unconformity in Core 643A-15H comes from diatom data, but is at present not confirmed by radiolarians. The apparently conflicting evidence will have to be addressed in further post-cruise studies. A major Paleogene unconformity present between Cores 104-643A-51X and 643A-49X is documented by a change from late Eocene to late Oligocene dinocyst assemblages.

Paleotemperature and Bioevolution

Little is known about the paleotemperature requirements of the Paleogene microfossil assemblages on which to base interpretations. However, calcareous nannofossils throughout Hole 643A are dominated by small-diversity, high-latitude assemblages, and low- to mid-latitude species are observed. This contrasts with the onshore flora, as indicated by the sporomorphs at Site 643. The middle Eocene flora contains thermophilous tree pollen species, including *Juglans, Platycarya*, and *Tilia*, and boreal forest indicators are rare. Bottom- and surface-water conditions (indicated by arenaceous benthics and dinocysts, respectively) also resemble middle-latitude assemblages found from Rockall Bank to the Bay of Biscay, about 30° latitude farther south. The pollen floras changed to cool temperate boreal associations during the interval between the late Eocene and early Miocene. Dinocyst species diversity also decreased at this time, suggesting the occurrence of a major cooling event. Silicoflagellates show decreased diversity from the base to the top of the upper Miocene interval. All microfossil groups in Unit I show small diversity, as expected for glacial sediment intervals.

PALEOMAGNETICS

The shipboard paleomagnetics of the 526.5-m-thick Quaternary to lower-middle Eocene sediments of Hole 643A consisted exclusively of analyses of the natural remanent magnetization (NRM) properties. The pass-through cryogenic magnetometer was used to measure the archive halves of all cores. Shore-based measurements, including a systematic alternating-field (AF) demagnetization, are presently available only for Cores 104-643A-1H through 104-643A-18X.

Because of a number of yet unresolved correlation problems between the paleomagnetic results and the paleontological and sedimentological records, this report gives only a tentative interpretation of the uppermost section of Hole 643A and a short outline of the more important features comparable to those at Site 642. Further detailed shore-based studies of a large number of discrete samples should allow us to evaluate a more complete magnetostratigraphy for the upper and middle part of the section at a later stage. It appears doubtful, however, whether a magnetostratigraphy can ever be established for the lower 250 m because of highly disturbed cores and also because of probable remagnetization effects throughout extended portions of Units IV and V.

The downhole variation in stable inclination and NRM intensity is shown in Figure 15 and Table 8. For the uppermost two cores, the polarity of the sediments is normal, indicating that they accumulated within the present geomagnetic Brunhes Epoch.

Note that in this report, as in that for Site 642, the magnetostratigraphic nomenclature used is the traditional epoch scheme. The new chron terminology (Harland et al., 1982; Tauxe et al., 1984) will be applied, however, for all subsequent shore-based work. Numerical ages for the Earth's magnetic field reversal history are based on the Berggren et al. (1985) time scale.

Core 104-643A-3H is fairly disturbed due to vertical water flow in the center of the core during the coring or retrieving operations. The polarity distribution of this core is not clear. For this reason, our interpretation identifies the boundary between the Brunhes and Matuyama Epochs (0.73 m.y.) only in Section 104-643A-4H-2 at 26.56 mbsf. The reduced depth of the Matuyama Epoch relative to Site 642 indicates a somewhat reduced sedimentation rate away from the shelf during the Brunhes Epoch (about 50 m/m.y at Site 642, as compared with about 36 m/m.y. at Site 643).

The Jaramillo Event also occurs within Core 104-643A-4H between 29.94 and 31.46 mbsf. The second major normal event within the reversed Matuyama Epoch extends from 49.71 mbsf (Section 104-643A-6H-5) to 54.71 mbsf (Sections 104-643A-7H-1/2). The Matuyama/Gauss is interpreted at about 63.20 mbsf in Section 104-643A-8H-1. The Gauss/Gilbert boundary would then be recognized at about 77.86 mbsf (Sections 104-643A-9H-4/5).

According to this paleomagnetic model, the sedimentation rates during the Matuyama Epoch would amount to about 21 m/m.y. and to about 16 m/m.y. during the Gauss Epoch, respectively. However, the peculiar reversal pattern representing the polarity fine structure of the Gauss Epoch strongly suggests highly variable sediment accumulation conditions. This variability is not surprising, as frequent slumping-type deformation is recorded for the entire core interval between 43 and 110 mbsf.

The admittedly vague magnetostratigraphic interpretation below the Gauss/Gilbert transition is based mainly on a correlation with paleomagnetic findings at Site 642. We established that at Site 642 high-NRM intensity values of about 10^{-5} Gauss persist to about the base of the Gilbert Epoch, followed by a sharp decrease to about 10^{-7} Gauss. A similar decrease is observed in Hole 643A at about 87 mbsf. For this reason, the Gilbert/Epoch 5 boundary in Hole 643A was identified at 87.11 mbsf (Sections 104-643A-10H-4/5). This implies, however, a remarkably lower sedimentation rate of less than 5 m/m.y., about the same as that observed at Site 642 at this level. Details of the tentative correlation between the Hole 643A downhole inclination pattern and the Earth's field polarity sequence since the uppermost Miocene are outlined in Figure 16 (see also Table 9).

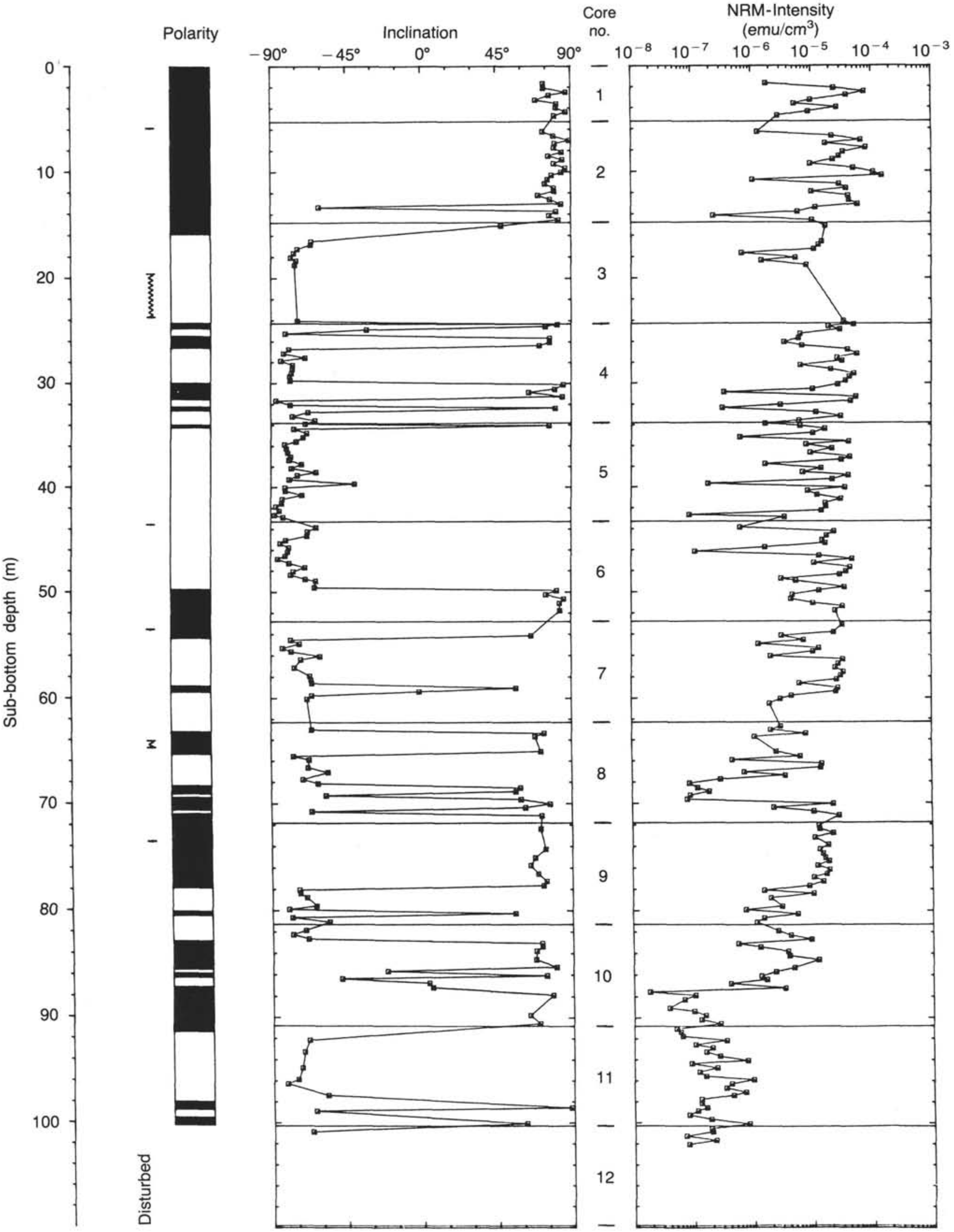

Figure 15. Stratigraphic sequence of the upper about 100 m of Hole 643A, showing the variations in inclination of the characteristic remanent magnetization and in NRM intensity. Horizontal lines indicate core boundaries. The paleomagnetic polarity log is based on stable inclinations, black being normal and white being reversed polarity. Disturbed intervals are indicated next to the polarity curve.

Table 8. Paleomagnetic properties of Hole 643A sediments.

Sample interval (cm)	Sub-bottom depth (m)	J (NRM)[a] (Gauss)	NRM[a]		AF			MDF (Oe)
			I	D	I	D	Pol.	
1-2, 16–18	1.67	1.77 E-6	+69.2	134.4	+73.5	136.9	N	283
1-2, 60–62	2.11	2.39 E-5	+69.4	77.1	+73.7	79.2	N	227
1-2, 96–98	2.47	7.66 E-5	+84.7	130.5	+87.4	186.2	N	250
1-2, 130–132	2.81	3.86 E-5	+76.9	77.2	+77.1	72.1	N	299
1-3, 25–27	3.26	9.86 E-6	+63.1	179.4	+69.0	72.9	N	177
1-3, 60–62	3.61	5.24 E-6	+77.7	129.7	+81.6	133.5	N	274
1-3, 96–98	3.97	2.68 E-5	+77.4	104.1	+81.2	94.1	N	277
1-3, 135–137	4.36	9.02 E-6	+88.2	298.4	+87.1	304.3	N	279
1-4, 25–27	4.76	2.77 E-6	+86.8	118.2	+80.2	275.2	N	141
*2-1, 55–57	5.86	2.00 E-5	+74.9	231.4	+72.4	240.2		239
2-1, 95–97	6.26	1.27 E-6	+57.3	94.7	+73.1	100.0	N	156
2-1, 135–137	6.66	2.19 E-5	+83.9	335.5	+79.5	280.2	N	145
2-2, 24–26	7.05	6.61 E-5	+89.2	233.5	+88.9	196.2	N	248
2-2, 55–57	7.36	1.70 E-5	+79.6	67.3	+80.3	70.6	N	148
2-2, 95–97	7.76	8.07 E-5	+80.6	236.0	+80.0	241.5	N	278
2-2, 135–137	8.16	3.40 E-5	+86.4	251.4	+84.6	274.5	N	290
2-3, 24–26	8.55	2.92 E-5	+77.5	311.1	+76.5	313.3	N	158
2-3, 55–57	8.86	2.31 E-5	+85.6	145.1	+85.1	219.4	N	202
2-3, 95–97	9.26	9.68 E-6	+61.2	107.3	+79.9	94.5	N	285
2-3, 135–137	9.66	5.04 E-5	+86.6	16.8	+86.7	324.5	N	218
2-4, 24–26	10.05	1.08 E-4	+84.8	294.8	+84.3	300.4	N	276
2-4, 55–57	10.36	1.49 E-4	+77.5	294.7	+78.5	294.6	N	274
2-4, 95–97	10.76	1.04 E-6	+63.6	200.0	+76.0	287.4	N	276
2-4, 135–137	11.16	2.92 E-5	+75.6	287.2	+74.4	291.2	N	284
2-5, 24–26	11.55	3.80 E-5	+82.1	278.6	+79.8	285.9	N	267
2-5, 55–57	11.86	1.01 E-5	+75.1	179.5	+80.0	11.0	N	164
2-5, 95–97	12.26	4.11 E-5	+70.8	75.3	+70.2	77.1	N	217
2-5, 135–137	12.66	4.24 E-5	+81.8	63.2	+77.4	6.9	N	213
2-6, 24–26	13.05	5.90 E-5	+86.5	255.7	+84.0	270.8	N	266
2-6, 55–57	13.36	1.18 E-5	+62.2	191.0	−61.1	187.9		92
2-6, 95–97	13.76	5.95 E-6	+81.0	203.8	+81.2	267.6	N	176
2-6, 135–137	14.16	2.32 E-7	+74.8	351.8	+76.9	188.2	N	232
2-7, 24–26	14.55	1.03 E-5	+81.9	258.3	+82.5	261.0	N	238
3-1, 29–31	15.10	1.72 E-5	+47.3	189.5	+48.1	203.7	N	239
3-2, 25–27	16.56	1.49 E-5	−60.6	165.2	−65.8	166.0	R	215
3-2, 55–57	16.86	1.31 E-5	−72.5	139.3	−66.2	122.9	R	267
3-2, 95–97	17.26	1.10 E-5	−79.6	246.6	−74.2	311.3	R	200
3-2, 135–137	17.66	6.79 E-7	−55.5	180.8	−76.3	216.4	R	388
3-3, 25–27	18.06	5.40 E-6	−67.0	97.3	−78.1	51.8	R	328
3-3, 55–57	18.36	1.45 E-6	−69.4	23.6	−74.9	322.5	R	493
3-3, 95–97	18.76	8.23 E-6	−50.0	124.5	−75.5	131.8	R	230
*3-4, 25–27	19.56	3.26 E-6	−3.2	345.1	−60.1	111.3		30
*3-4, 55–57	19.86	3.65 E-6	+31.5	186.7	−59.9	141.4		262
*3-4, 95–97	20.26	6.79 E-6	+38.4	30.4	−27.7	142.0		36
*3-4, 135–137	20.66	3.81 E-6	−29.8	136.8	−51.4	74.8		94
*3-5, 25–27	21.06	1.88 E-6	+17.3	105.8	−75.2	53.5		389
*3-5, 55–57	21.36	2.01 E-5	−58.5	189.5	−65.1	175.9		99
*3-5, 95–97	21.76	2.35 E-5	+36.7	208.4	+39.5	208.4		223
*3-5, 135–137	22.16	1.59 E-5	−50.8	164.3	−75.9	171.2		190
*3-6, 25–27	22.56	3.96 E-6	−41.1	143.6	−74.8	155.1		272
*3-6, 55–57	22.86	3.66 E-5	+53.0	85.1	+52.0	93.3		44
*3-6, 95–97	23.26	1.35 E-6	+1.0	202.5	−78.4	213.6		280
*3-6, 135–137	23.66	3.61 E-6	−51.6	128.9	−70.7	193.4		102
3-7, 25–27	24.06	3.39 E-5	−66.6	107.1	−74.1	108.9	R	142
3-7, 54–56	24.35	5.05 E-5	+15.9	345.5	+81.7	343.2	N	285
4-1, 25–27	24.56	1.91 E-5	+72.3	199.4	+74.6	206.1	N	289
4-1, 55–57	24.86	2.98 E-5	+18.5	106.5	−32.6	97.3	R	48
4-1, 95–97	25.26	6.44 E-6	−75.0	194.5	−81.3	154.7	R	331
4-1, 135–137	25.66	6.06 E-6	+80.9	132.1	+77.1	343.3	N	321
4-2, 25–27	26.06	3.46 E-6	+36.5	193.3	+77.1	168.2	N	446
4-2, 55–57	26.36	6.95 E-6	+52.7	126.5	+70.8	139.3	N	399
4-2, 95–97	26.76	3.99 E-5	−79.9	353.8	−79.2	355.4	R	307
4-2, 135–137	27.16	5.71 E-5	−83.3	351.9	−82.4	349.3	R	305
4-3, 25–27	27.56	2.65 E-5	−68.5	30.1	−69.5	25.0	R	302
4-3, 55–57	27.86	3.21 E-5	−80.2	73.1	−84.1	61.4	R	273
4-3, 95–97	28.26	6.46 E-6	−75.5	267.3	−76.9	342.7	R	395
4-3, 135–137	28.66	2.07 E-5	−81.6	41.3	−77.1	352.3	R	288
4-4, 25–27	29.06	5.06 E-5	−78.6	20.4	−77.8	0.6	R	289
4-4, 55–57	29.36	4.25 E-5	−61.9	308.7	−78.7	347.9	R	262
4-4, 95–97	29.76	3.67 E-5	−75.0	59.9	−78.4	49.5	R	306
4-4, 131–133	30.12	2.75 E-5	+84.0	211.8	+85.3	186.1	N	281
4-5, 25–27	30.56	1.04 E-5	+67.8	326.9	+80.1	123.7	N	181
4-5, 55–57	30.86	3.46 E-7	+28.6	121.9	+64.5	126.7	N	46
4-5, 95–97	31.26	5.51 E-5	+87.7	163.3	+84.7	144.5	N	235
4-5, 135–137	31.66	4.47 E-5	−79.3	93.0	−86.9	94.1	R	335
4-6, 25–27	32.06	3.01 E-6	−39.3	113.8	−78.4	130.2	R	175
4-6, 55–57	32.36	3.23 E-7	+64.0	144.9	+80.3	144.5	N	132
4-6, 95–97	32.76	1.18 E-5	−58.3	129.6	−67.8	112.1	R	248
4-6, 135–137	33.16	3.07 E-5	−70.2	57.4	−77.2	32.8	R	353
4-7, 25–27	33.56	6.17 E-6	+70.5	102.9	−63.6	21.3	R	88
4-7, 55–57	33.86	1.68 E-6	+65.2	254.3	−69.5	357.8	R	41
5-1, 25–27	34.06	6.43 E-6	+56.5	95.2	+76.7	95.5	N	127
5-1, 55–57	34.36	1.65 E-5	−66.3	140.2	−76.3	153.6	R	364
5-1, 95–97	34.76	1.04 E-5	−58.6	137.1	−68.6	141.7	R	230
5-1, 135–137	35.16	6.35 E-7	−27.3	83.8	−70.8	325.3	R	442
5-2, 25–27	35.56	4.19 E-5	−71.7	116.4	−74.8	118.5	R	285
5-2, 55–57	35.86	8.14 E-6	−80.7	116.7	−81.8	121.0	R	303
5-2, 95–97	36.26	2.20 E-5	−79.4	98.2	−80.6	114.5	R	285
5-2 135–137	36.66	9.57 E-6	−76.6	100.8	−79.8	103.6	R	309
5-3, 25–27	37.06	4.39 E-5	−72.6	94.9	−78.2	102.2	R	330
5-3, 55–57	37.36	3.15 E-5	−76.4	99.1	−79.2	114.4	R	310
5-3, 95–97	37.76	1.68 E-6	−55.0	109.9	−71.6	67.9	R	281
5-3, 135–137	38.16	1.45 E-5	−78.7	179.3	−77.8	185.9	R	228
5-4, 25–27	38.56	7.15 E-6	−38.0	110.6	−63.0	72.4	R	149
5-4, 55–57	38.86	4.14 E-5	−72.0	103.7	−74.2	106.7	R	313

Table 8 (continued).

Sample interval (cm)	Sub-bottom depth (m)	J (NRM)[a] (Gauss)	NRM[a]		AF			MDF (Oe)
			I	D	I	D	Pol.	
5-4, 95–97	39.26	2.22 E-5	−78.7	99.0	−79.1	99.5	R	304
5-4, 135–137	39.66	1.89 E-7	+36.8	84.8	−39.8	260.5	R	>500
5-5, 24–26	40.05	3.63 E-5	−78.8	112.2	−81.6	123.9	R	260
5-5, 54–56	40.35	8.65 E-6	−80.4	268.7	−81.5	237.1	R	327
5-5, 94–96	40.75	1.25 E-5	−73.6	166.2	−71.5	204.9	R	219
5-5, 134–136	41.15	3.10 E-5	−84.4	119.5	−83.2	124.2	4	285
5-6, 25–27	41.56	1.72 E-5	−85.9	127.6	−83.5	136.0	R	258
5-6, 55–57	41.86	1.76 E-5	−86.0	159.0	−86.9	158.0	R	324
5-6, 95–97	42.26	1.48 E-5	−82.7	156.4	−85.0	202.5	R	296
5-6, 135–137	42.66	9.28 E-8	−86.3	54.8	−87.8	358.4	R	235
5-7, 7–9	42.88	3.57 E-6	−84.6	190.6	−82.7	106.5	R	345
*6-1, 25–27	43.56	1.35 E-7	+25.5	124.4	−64.0	72.6		>500
6-1, 54–56	43.85	6.43 E-7	−10.9	133.6	−63.0	105.1	R	>500
6-1, 94–96	44.25	2.39 E-5	−63.8	106.3	−68.1	81.1	R	377
6-1, 134–136	44.65	1.79 E-5	−56.3	94.6	−68.4	101.6	R	367
6-2, 25–27	45.06	1.51 E-5	−74.4	37.7	−81.2	39.8	R	319
6-2, 55–57	45.36	1.71 E-5	−89.2	305.3	−84.5	58.7	R	351
6-2, 95–97	45.76	1.66 E-6	−20.6	13.7	−79.3	18.8	R	>600
6-2, 135–137	46.16	1.14 E-7	−24.9	94.8	−80.0	118.7	R	>500
6-3, 25–27	46.56	1.34 E-5	−68.6	99.1	−81.3	108.4	R	323
6-3, 55–57	46.86	4.81 E-5	−83.2	118.3	−85.8	83.8	R	286
6-3, 95–97	47.26	1.10 E-5	−80.3	19.2	−78.9	40.3	R	291
6-3, 135–137	47.66	4.45 E-5	−60.0	113.6	−69.5	104.2	R	295
6-4, 25–27	48.06	3.78 E-5	−63.4	114.6	−76.5	117.8	R	243
6-4, 55–57	48.36	2.98 E-5	−64.0	86.2	−78.1	63.8	R	388
6-4, 95–97	48.76	3.11 E-6	−61.8	89.5	−69.3	58.1	R	147
6-4, 113–115	48.94	5.50 E-6	−44.2	89.4	−63.1	63.8	R	163
6-5, 25–27	49.56	3.55 E-5	−59.4	75.4	−63.8	80.1	R	252
6-5, 55–57	49.86	1.34 E-5	+58.8	110.8	+81.3	211.3	N	397
6-5, 95–97	50.26	4.79 E-6	−9.7	126.1	+74.8	209.6	N	471
6-5, 135–137	50.66	4.53 E-6	+17.8	85.6	+85.5	211.2	N	339
6-6, 25–27	51.06	1.06 E-5	+40.8	147.1	+82.9	249.0	N	483
6-6, 55–57	51.36	3.30 E-5	+75.9	119.1				
6-6, 95–97	51.76	2.47 E-5	+87.5	129.4	+83.1	238.2	N	358
7-1, 30–32	53.11	3.27 E-5	+76.5	61.1				
*7-1, 72–74	53.53	4.54 E-5	+78.3	95.7	+78.1	91.8		305
7-1, 101–103	53.82	2.35 E-5	+63.7	73.0				
7-1, 133–135	54.14	3.15 E-6	+44.1	97.8	+65.9	78.3	N	462
7-2, 23–25	54.54	7.39 E-6	−87.7	281.4	−78.1	245.2	R	259
7-2, 59–61	54.90	1.29 E-6	−56.1	176.7	−72.9	208.7	R	>650
7-2, 100–102	55.31	1.32 E-5	−87.3	161.5	−83.1	239.5	R	341
7-2, 132–134	55.63	1.06 E-5	−45.0	103.4	−77.9	160.3	R	61
7-3, 25–27	56.06	2.06 E-6	−17.6	133.3	−60.6	253.2	R	>500
7-3, 57–59	56.38	3.29 E-5	−74.1	249.1	−72.2	265.6	R	332
7-3, 99–101	56.80	2.75 E-5	−70.0	259.6				
7-3, 132–134	57.13	2.44 E-5	−80.4	334.4	−76.1	306.4	R	358
7-4, 23–25	57.54	3.35 E-5	−64.0	3.0				
7-4, 58–60	57.89	3.04 E-5	−71.7	344.9	−66.6	341.5	R	345
7-4, 94–96	58.25	2.61 E-5	−61.8	22.8	−65.9	15.9	R	267
7-4, 128–130	58.59	6.24 E-6	+13.8	159.5	−65.5	220.7	R	236
7-5, 24–26	59.05	2.74 E-5	+53.5	108.2	+56.8	117.0	N	270
7-5, 56–58	59.37	2.54 E-5	+0.3	163.5	−1.3	169.4		369
7-5, 94–96	59.75	4.65 E-6	−55.4	191.1	−65.6	224.0	R	>500
7-5, 126–128	60.07	3.01 E-6	−36.1	94.4	−68.4	275.5	R	>500
7-6, 19–21	60.50	1.98 E-6	−73.2	39.8				
8-1, 40–42	62.71	3.01 E-6	−65.4	336.8				
8-1, 71–73	63.02	2.04 E-6	−44.3	105.3	−65.9	120.0	R	217
8-1, 106–108	63.37	7.99 E-6	+71.0	159.6	+73.6	165.0	N	226
8-1, 137–139	63.68	1.11 E-6	+71.5	193.7	+68.1	202.5	N	171
*8-2, 24–26	64.05	4.71 E-6	+10.3	109.6	−18.3	90.9		292
*8-2, 55–57	64.36	5.62 E-6	+58.9	130.1	+64.5	129.4		328
*8-2, 89–91	64.70	8.37 E-7	+29.5	279.8	+50.2	256.7		>650
8-2, 130–132	65.11	2.55 E-6	+70.7	44.5	+71.5	352.4	N	167
8-3, 24–26	65.55	6.46 E-6	−72.7	75.8	−76.7	67.3	R	246
8-3, 57–59	65.88	4.68 E-7	−31.0	77.7	−67.3	42.2	R	609
8-3, 94–96	66.25	1.47 E-5	−52.8	42.2			R	
8-3, 131–133	66.62	1.40 E-5	−63.0	52.6	−68.0	35.2	R	243
8-4, 24–26	67.05	7.43 E-7	−37.4	78.5	−56.0	52.2	R	611
8-4, 57–59	67.38	3.59 E-6	−66.5	36.2			R	
8-4, 93–95	67.74	2.97 E-7	−58.4	95.9	−71.1	63.8	R	>650
8-4, 131–133	68.12	8.97 E-8	−47.2	93.9	−62.1	83.4	R	143
8-5, 24–26	68.55	1.24 E-7	+55.7	70.2	+59.0	61.5	N	475
8-5, 58–60	68.89	1.94 E-7	+56.5	46.7	+56.4	42.4	N	172
8-5, 93–95	69.24	9.30 E-8	−1.9	111.7	−57.2	53.5	R	328
8-5, 131–133	69.62	8.28 E-8	+32.4	120.2	+59.5	160.0	N	254
8-6, 24–26	70.05	2.26 E-5	+76.0	197.6	+76.8	205.1	N	386
8-6, 57–59	70.38	2.26 E-6	+7.4	118.4	+62.1	155.2	N	364
8-6, 92–94	70.73	1.06 E-5	−63.9	111.9	−65.9	108.8	R	349
8-6, 132–134	71.13	2.80 E-5	+73.7	215.8	+71.7	220.0	N	307
9-1, 25–27	72.06	1.28 E-5	+73.2	119.0				
9-1, 55–57	72.36	1.32 E-5	+66.1	108.7	+71.0	99.2	N	407
9-1, 95–97	72.76	2.23 E-5	+77.4	101.1				
9-1, 135–137	73.16	1.09 E-5	+71.9	89.4				
*9-2, 20–22	73.51	2.00 E-5	+36.7	85.7	+36.4	85.3		391
9-2, 55–57	73.86	1.83 E-5	+72.5	315.8				
9-2, 95–97	74.26	1.33 E-5	+73.4	249.1	+73.9	249.9	N	366
9-2, 135–137	74.66	1.51 E-5	+66.4	25.7				
9-3, 25–27	75.06	1.65 E-5	+70.5	60.0	+67.6	67.7	N	345
9-3, 55–57	75.36	1.91 E-5	+72.6	63.4				
9-3, 95–97	75.76	1.21 E-5	+58.2	72.7	+64.9	70.9	N	350
9-3, 135–137	76.16	1.93 E-5	+69.3	53.4				
9-4, 25–27	76.56	1.73 E-5	+71.0	86.4	+69.5	86.0	N	330
9-4, 55–57	76.86	1.05 E-5	+65.1	1.4				
9-4, 95–97	77.26	1.53 E-5	+76.5	58.5	+74.4	62.9	N	316
9-4, 135–137	77.66	8.80 E-6	+74.1	84.8	+72.5	69.5	N	301

Table 8 (continued).

Sample interval (cm)	Sub-bottom depth (m)	J (NRM)[a] (Gauss)	NRM[a]		AF			MDF (Oe)
			I	D	I	D	Pol.	
9-5, 25-27	78.06	1.52 E-6	+33.4	25.3	-73.8	229.0	R	34
9-5, 55-57	78.36	1.04 E-5	-75.4	252.4	-73.3	249.6	R	360
9-5, 95-97	78.76	1.96 E-6	-73.6	168.5	-69.3	247.5	R	>500
9-6, 25-27	79.56	3.03 E-6	+62.8	100.1	-63.6	222.7	R	88
9-6, 57-59	79.88	7.60 E-7	-14.3	109.3	-80.0	84.9	R	44
9-6, 95-97	80.26	5.61 E-6	+56.9	5.4	+55.6	357.0	N	312
9-6, 135-137	80.66	1.52 E-6	+37.2	97.6	-78.2	90.9	R	53
9-7, 25-27	81.06	1.15 E-6	+48.5	147.8	-55.9	123.9	R	75
10-1, 55-57	81.86	2.59 E-6	-56.6	188.2	-70.2	203.3	R	472
10-1, 95-97	82.26	4.22 E-6	-73.7	166.8	-77.9	190.4	R	383
10-1, 135-137	82.66	9.33 E-6	-64.8	202.0	-68.6	198.4	R	365
10-2, 25-27	83.06	5.60 E-7	+73.9	74.5	+71.3	36.0	N	75
10-2, 55-57	83.36	1.30 E-6	+87.6	15.8	+71.4	26.4	N	97
10-2, 95-97	83.76	3.77 E-6	+70.1	49.0	+67.8	24.8	N	252
10-2, 135-137	84.16	3.97 E-6	+79.1	60.0				
10-3, 25-27	84.56	1.22 E-5	+67.6	12.9	+67.4	10.1	N	325
10-3, 95-97	85.26	4.79 E-6	+77.9	52.3	+79.8	60.3	N	285
10-3, 135-137	85.66	2.35 E-6	+7.5	228.5	-21.4	231.9	R	343
10-4, 25-27	86.06	1.35 E-6	+70.3	333.7	+74.0	307.0	N	82
10-4, 55-57	86.36	1.66 E-6	-36.1	209.8	-48.8	211.5	R	431
10-4, 95-97	86.76	4.15 E-7	+16.5	352.3	+3.6	349.6		264
10-4, 135-137	87.16	3.34 E-6	+22.9	194.2	+5.6	198.1		389
10-5, 25-27	87.56	1.83 E-8	+35.8	91.1				
10-5, 55-57	87.86	1.06 E-7	+70.3	30.6	+77.6	1.9	N	82
10-5, 95-97	88.26	6.93 E-8	+42.7	330.7				
10-6, 25-27	89.06	3.85 E-8	-0.2	269.6				
10-6, 55-57	89.36	1.00 E-7	+24.1	340.2				
10-6, 95-97	89.76	1.54 E-7	+65.3	347.0	+63.8	339.3	N	253
10-6, 135-137	90.16	1.31 E-7	+72.6	3.4				
10-7, 25-27	90.56	2.74 E-7	+74.6	286.9	+69.6	328.7	N	324
11-1, 25-27	91.06	5.07 E-8	+1.3	4.7				
11-1, 55-57	91.36	5.99 E-8	-50.6	212.4				
11-1, 95-97	91.76	6.45 E-8	+4.0	80.7				
11-1, 135-137	92.16	3.50 E-7	-63.9	222.6	-68.5	208.2	R	304
11-2, 25-27	92.56	1.05 E-7	-26.1	291.6				
11-2, 55-57	92.86	2.03 E-7	-53.6	181.7				
11-2, 95-97	93.26	1.59 E-7	-14.3	14.3	-71.5	338.4	R	46
11-2, 135-137	93.66	2.69 E-7	+80.2	272.4				
11-3, 25-27	94.06	7.79 E-7	+26.4	244.3				
11-3, 55-57	94.36	8.98 E-8	-35.5	282.5				
11-3, 95-97	94.76	2.41 E-7	-39.9	151.7	-73.0	160.1	R	298
11-3, 135-137	95.16	1.21 E-7	-50.2	312.7				
11-4, 25-27	95.56	1.56 E-7	-51.6	248.4				
11-4, 55-57	95.86	9.73 E-7	-46.6	113.3	-75.4	21.1	R	>1000
11-4, 95-97	96.26	4.21 E-7	-41.1	104.9	-81.8	42.5	R	139
11-4, 135-137	96.66	3.41 E-7	-52.5	177.5				
11-5, 25-27	97.06	7.23 E-7	+25.3	54.7				
11-5, 55-57	97.36	4.51 E-7	-25.9	79.5	-57.5	33.8	R	142
11-5, 95-97	97.76	1.31 E-7	-41.9	133.5				
11-5, 135-137	98.16	1.30 E-7	+8.5	81.5				
11-6, 25-27	98.56	1.61 E-7	+84.6	80.8	+88.4	264.0	N	46
11-6, 55-57	98.86	1.13 E-7	-38.3	233.8	-64.6	183.7	R	78
11-6, 95-97	99.26	8.08 E-8	-6.7	97.4				
11-6, 135-137	99.66	1.87 E-7	-8.0	107.4				
11-7, 25-27	100.06	8.06 E-7	+27.6	98.2	+61.4	83.0	N	361
12-1, 25-27	100.56	1.87 E-7	-37.7	85.1				
12-1, 55-57	100.86	1.96 E-7	-57.7	46.2	-66.9	11.0	R	>500
12-1, 95-97	101.26	7.15 E-8	+15.2	105.3				
12-1, 135-137	101.66	1.58 E-7	-37.2	63.2	-67.2	45.2	R	197
12-2, 25-27	102.06	7.94 E-8	-27.7	91.7				
12-2, 55-57	102.36	1.64 E-7	+27.8	62.6				
12-2, 95-97	102.76	1.97 E-7	+29.4	75.8	+51.4	32.8	N	189
12-2, 135-137	103.16	1.68 E-7	+28.0	105.3				
12-3, 25-27	103.56	1.04 E-7	+53.8	92.8				
12-3, 55-57	103.86	1.00 E-7	+33.8	49.6	+57.4	46.4	N	327
12-3, 95-97	104.26	1.03 E-7	-56.8	62.7				
12-3, 135-137	104.66	1.21 E-7	-65.8	102.6	-71.4	164.8	R	>500
12-4, 25-27	105.06	5.90 E-8	-33.9	36.9				
12-4, 55-57	105.36	3.27 E-8	+29.4	161.1				
12-4, 95-97	105.76	1.18 E-7	+26.2	86.0				
12-4, 135-137	106.16	1.58 E-7	+61.7	34.4	+56.4	29.1	N	420
12-5, 25-27	106.56	1.38 E-7	+53.2	63.8				
12-5, 55-57	106.86	1.88 E-7	+66.1	64.4	+67.9	46.4	N	612
12-5, 95-97	107.26	1.22 E-7	+49.4	75.3				
12-6, 25-27	108.06	1.65 E-7	+58.0	71.3				
12-6, 55-57	108.36	1.54 E-7	+47.4	44.7	+54.1	28.9	N	305
12-6, 95-97	108.76	1.70 E-7	+23.4	109.7				
12-6, 135-137	109.16	7.35 E-8	-31.9	70.5				
12-7, 26-28	109.57	6.68 E-8	-39.4	82.9	-67.6	103.7	R	239
13-1, 25-27	110.06	2.29 E-7	+26.5	44.0	+72.6	1.5	N	328
13-1, 55-57	110.36	2.47 E-7	+81.0	285.8	+74.1	296.6	N	656
13-1, 95-97	110.76	1.06 E-7	+65.0	31.8				
13-1, 135-137	111.16	6.51 E-8	+8.0	340.9				
13-2, 25-27	111.56	3.57 E-8	+4.4	161.5				
13-2, 54-56	111.85	7.54 E-8	+46.6	58.0	+68.2	44.1	N	312
13-2, 95-97	112.26	3.37 E-8	-33.1	188.8				
13-2, 135-137	112.66	2.36 E-7	-24.0	353.8	-36.4	344.3	R	202
13-3, 25-27	113.06	4.43 E-8	+24.5	13.9				
13-3, 55-57	113.36	4.43 E-8	+54.9	56.7				
13-3, 95-97	113.76	1.18 E-6	+59.9	178.3	+59.3	179.4	N	220
13-3, 135-137	114.16	1.62 E-7	+83.3	136.6				
13-4, 25-27	114.56	8.12 E-8	-77.0	109.8				
13-4, 55-57	114.86	4.13 E-8	-50.4	210.0				
13-4, 95-97	115.26	7.47 E-8	-61.9	233.8	-59.7	229.5	R	>500
13-4, 135-137	115.66	2.59 E-8	-51.8	230.2				

Table 8 (continued).

Sample interval (cm)	Sub-bottom depth (m)	J (NRM)[a] (Gauss)	NRM[a]		AF			MDF (Oe)
			I	D	I	D	Pol.	
13-5, 25-27	116.06	1.18 E-7	-41.3	169.1				
13-5, 55-57	116.36	1.16 E-7	-84.1	113.4	-78.8	212.4	R	>500
13-5, 95-97	116.76	1.34 E-7	-20.6	123.3				
13-6, 25-27	117.56	1.96 E-8	-40.3	133.8				
13-6, 55-57	117.86	6.19 E-8	-49.5	174.2	-47.1	185.8	R	78
13-6, 95-97	118.26	2.99 E-8	-7.0	241.0				
13-6, 135-137	118.66	6.42 E-8	-49.2	105.3				
13-7, 25-27	119.06	6.93 E-8	-55.9	107.5				
14-1, 25-27	119.56	8.37 E-8	-67.1	8.4				
14-1, 57-59	119.88	1.32 E-7	-33.6	18.4				
14-1, 83-85	120.14	1.19 E-7	+4.6	84.6	-52.6	353.6	R	318
14-1, 135-137	120.66	4.96 E-8	+24.5	152.6				
14-2, 25-27	121.06	8.58 E-8	-17.5	336.9				
14-2, 55-57	121.36	1.23 E-7	-74.1	346.4	-74.1	340.5	R	>500
14-2, 95-97	121.76	8.78 E-8	-57.9	249.6				
14-2, 135-137	122.16	1.20 E-7	-24.4	305.2				
14-3, 25-27	122.56	1.18 E-7	-74.8	299.3				
14-3, 55-57	122.86	1.29 E-7	-44.6	306.2	-47.0	304.8	R	>950
14-3, 95-97	123.26	7.87 E-8	-86.9	347.2				
14-3, 135-137	123.66	8.66 E-8	-57.1	259.9				
14-4, 25-27	124.06	2.54 E-8	+15.8	64.3				
14-4, 55-57	124.36	7.09 E-8	-52.6	98.9	-71.3	74.2	R	>700
14-4, 95-97	124.76	5.96 E-8	-60.0	67.5				
14-4, 135-137	125.16	1.59 E-7	-44.9	343.1				
14-5, 24-26	125.55	7.59 E-8	-40.1	301.5				
14-5, 55-57	125.86	1.23 E-7	-50.3	300.6	-61.2	315.6	R	451
14-5, 95-97	126.26	1.07 E-7	-48.7	340.6				
14-5, 135-137	126.66	4.48 E-8	+5.6	178.7				
14-6, 25-27	127.06	7.92 E-8	+56.0	217.7				
14-6, 55-57	127.36	1.08 E-7	-52.5	327.8	-55.7	343.7	R	494
14-6, 95-97	127.76	2.34 E-8	+0.0	347.5				
15-1, 25-27	129.06	5.71 E-8	-8.3	268.5				
15-1, 55-57	129.36	6.63 E-8	-78.8	251.8	-80.6	261.8	R	>400
15-1, 95-97	129.76	4.44 E-8	-20.6	270.4				
15-1, 135-137	130.16	7.76 E-8	-81.0	200.0				
15-2, 25-27	130.56	4.05 E-8	-23.6	210.6				
15-2, 55-57	130.86	1.60 E-8	+23.5	278.5	-54.2	70.1	R	>0
15-2, 95-97	131.26	2.42 E-8	-60.9	252.5	-64.6	262.1	R	>400
15-2, 135-137	131.66	4.14 E-8	-3.0	193.7				
15-3, 25-27	132.06	8.64 E-8	+25.5	221.5				
15-3, 55-57	132.36	6.80 E-8	-17.0	209.5	-55.9	271.4	R	162
15-3, 95-97	132.76	3.18 E-8	-31.2	252.5				
15-3, 135-137	133.16	8.22 E-8	-60.8	296.5				
15-4, 25-27	133.56	3.25 E-8	-37.6	308.6				
15-4, 55-57	133.86	3.17 E-8	+16.5	247.5				
15-4, 95-97	134.26	1.32 E-7	-57.1	272.1				
15-4, 135-137	134.66	1.03 E-7	+80.7	123.3	+73.8	85.4	N	139
15-5, 25-27	135.06	1.90 E-7	+27.6	153.5				
15-5, 55-57	135.36	3.02 E-7	+64.8	46.4				
15-5, 95-97	135.76	8.36 E-7	+86.8	272.0	+88.8	349.3	N	387
15-6, 25-27	136.56	2.33 E-7	+74.8	106.1				
15-6, 55-57	136.86	1.85 E-7	+75.2	347.6	+69.5	4.9	N	152
15-6, 95-97	137.26	9.12 E-8	+2.8	318.7				
15-6, 135-137	137.66	1.85 E-7	+69.3	49.5				
15-7, 25-27	138.06	4.60 E-7	+44.9	315.4	+69.8	322.8	N	360
16-1, 25-27	138.56	1.02 E-7	-26.8	146.2				
16-1, 55-57	138.86	6.10 E-8	+66.0	91.8				
16-1, 95-97	139.26	2.71 E-8	+9.6	236.5				
16-1, 135-137	139.66	1.94 E-7	+47.2	183.1				
16-2, 25-27	140.06	1.16 E-7	+72.1	319.5				
16-2, 51-53	140.32	2.83 E-7	+78.8	322.6				
16-2, 95-97	140.76	2.65 E-7	+87.0	94.0				
16-2, 135-137	141.16	2.48 E-7	+74.4	324.1	+69.4	345.2	N	194
16-3, 25-27	141.56	1.11 E-7	+84.5	306.8				
16-3, 51-53	141.82	1.04 E-7	+71.6	329.2				
16-3, 95-97	142.26	1.23 E-7	+80.4	308.0				
16-3, 135-137	142.66	1.47 E-7	-15.8	73.1	-53.4	72.9	R	154
16-4, 25-27	143.06	1.87 E-7	-43.5	82.1	-80.3	12.2	R	145
16-4, 51-53	143.32	2.25 E-7	-49.1	105.4				
16-4, 95-97	143.76	2.83 E-7	-37.6	104.3				
16-4, 135-137	144.16	2.60 E-7	-50.4	89.2	-59.9	84.1	R	131
16-5, 25-27	144.56	2.22 E-7	-31.0	89.0				
16-5, 51-53	144.82	1.91 E-7	-35.8	86.8				
16-5, 95-97	145.26	1.80 E-7	-27.2	90.4				
16-5, 125-127	145.56	2.74 E-7	-36.7	77.3	-60.3	56.5	R	187
16-6, 25-27	146.06	3.83 E-7	-76.7	130.1				
16-6, 51-53	146.32	3.30 E-7	-57.9	108.8				
16-6, 95-97	146.76	2.96 E-7	-38.1	99.9				
16-6, 135-137	147.16	8.10 E-7	-55.1	107.1	-69.7	103.4	R	201
16-7, 25-27	147.56	1.33 E-6	-47.3	95.9	-64.5	91.1	R	176
17-1, 25-27	148.06	1.55 E-6	+35.0	98.7	+86.0	3.5	N	258
17-1, 55-57	148.36	6.59 E-7	-32.2	116.2	-65.7	97.7	R	147
18-1, 20-22	157.51	8.10 E-6	+55.4	102.6	+55.6	76.8	N	147
18-1, 67-69	157.98	1.94 E-7	-4.3	62.6				
18-1, 125-127	158.56	6.28 E-8	-14.8	87.0				
18-2, 20-22	159.01	9.08 E-8	-15.8	120.3				
18-2, 67-69	159.48	9.89 E-8	-20.9	132.8				
18-2, 125-127	160.06	9.31 E-7	-26.9	102.1	-45.9	106.5	R	135
18-3, 20-22	160.51	6.52 E-7	-42.7	92.8				

[a] J = intensity, I = inclination, D = declination of natural remanent magnetization (NRM) and stable remanence after AF demagnetization; Pol. = polarity, N = normal, R = reversed; MDF = median destructive field.

*Asterisks denote disturbed core intervals.

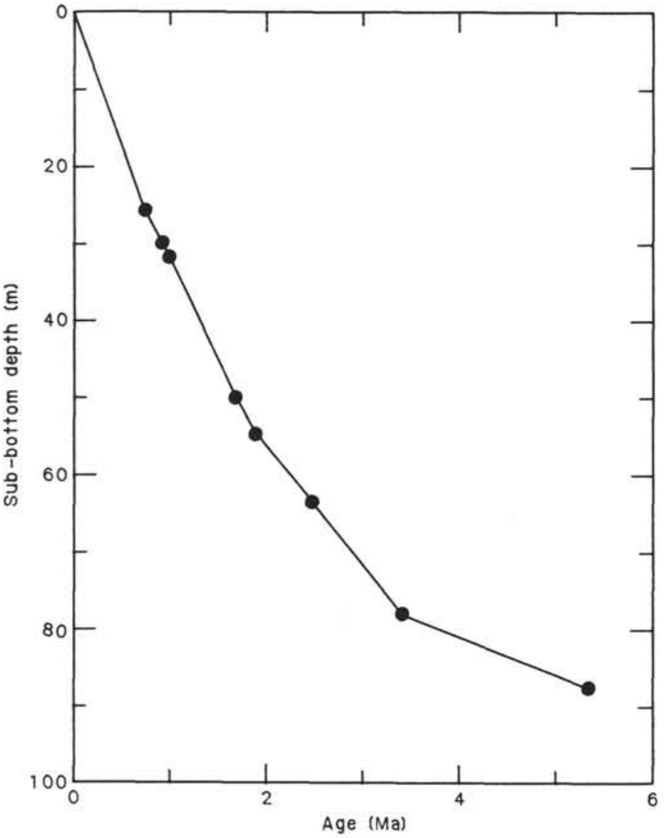

Figure 16. Apparent sediment accumulation at Site 643, derived from the correlation of the downhole pattern in remanent magnetization polarity with the geomagnetic polarity time scale of Berggren et al. (1986).

Table 9. Magnetostratigraphic summary of Hole 643A.

Epoch	Event	Core-section	Interval (cm)	Depth (mbsf)	Age (Ma)
Brunhes Matuyama		4-2 4-2	56 96	26.56	0.73
	Jaramillo, top	4-4 4-4	96 132	29.94	0.91
	Jaramillo, base	4-5 4-5	96 136	31.46	0.98
	Olduvai, top	6-5 6-5	26 56	49.71	1.66
	Olduvai, base	7-1 7-2	134 24	54.34	1.88
Matuyama Gauss		8-1 8-1	72 107	63.20	2.47
Gauss Gilbert		9-4 9-5	136 26	77.86	3.40
Gilbert Epoch 5		10-4 10-5	56 56	87.11	5.35

Below the Gilbert/Epoch 5 boundary, the magnetic record for Hole 643A becomes progressively poorer, preventing a straightforward interpretation of the magnetic record at present. In the two lithological units below about 274 mbsf, the pass-through cryogenic magnetometer NRM record indicates that the paleomagnetic signal is severely diminished and at times even lost because of an increased degree of mechanical disturbance from coring (disking effects as well as fragmentation and irregular rotation of harder beds). In addition, probable remagnetization of the sediments is indicated by increasing fluctuations in intensities and almost exclusively normal polarities. The first basalt fragment was encountered in Core 104-643A-60X and the last two sections (Core 104-643A-61X) also included pieces of basalt. Because of a lack of orientation, no result in terms of polarity could be established for any of the basaltic fragments.

GEOCHEMISTRY

Organic

The strategy for sampling and analyses for organic geochemistry at Site 643 was similar to that adopted for Site 642. Eighteen sediment samples, ranging in age from Pleistocene to early Eocene, were recovered at approximately 30-m intervals from 3.0 to 533.5 m sub-bottom.

Methane

As a test of a routine monitoring procedure, gas was extracted and quantified from a portion of the 18 samples collected at this site. Only methane in low concentrations (0 to 12.8 ppm) was found in these samples (Table 10). Figure 17 shows the gas chromatogram resulting from the analysis of sediment collected at about 495 m sub-bottom. This sample contained the highest amount of methane (12.8 ppm). For comparison, Figure 17 also shows the gas chromatogram of a standard mixture of hydrocarbon gases. The concentrations of methane are similar to those observed at Site 642. At Site 643, the general trend is an increase in the amount of methane with depth, the highest concentrations occurring in lower to middle Eocene sediment (Fig. 18). Although much of the residual methane in the sediments at this site is probably of biological origin, the increasing amounts of methane with depth may result from the effects of early thermal diagenesis.

Carbon

At Site 642, organic carbon was measured on acidified samples using the Elemental Analyzer, and inorganic carbon was determined in nonacidified sediment by means of the carbonate bomb and the Carbonate Carbon apparatus. For Site 643, the procedure was modified in that the acidification step was eliminated, and organic carbon was determined by the difference between the total carbon (from the Elemental Analyzer) and the inorganic carbon (from the Carbonate Carbon Apparatus). We ascertained that this procedure was feasible by reexamining the samples from Site 642, where it was found that for 10 of 13 samples, the organic carbon results obtained by difference and

Table 10. Organic and carbonate carbon, and methane at Site 643.

Core	Section	Depth (mbsf)	Organic carbon (%)	Carbonate carbon (%)	Methane (ppm)
1	2	3.0	0.25	3.51	0.8
4	4	30.3	0.22	0.01	5.2
7	5	60.3	0.42	0.01	1.3
10	5	88.7	0.11	0.02	3.0
13	5	117.3	1.05	0.01	0.9
16	5	145.8	0.19	0.01	1.3
19	5	174.3			2.9
22	4	201.2	0.62	0.01	3.7
25	5	232.2	0.66	0.03	4.0
28	5	261.6	0.73	0.07	9.3
31	5	291.0	0.80	0.04	1.8
34	2	315.8	1.08	0.03	1.1
37	3	346.7	1.78	0.04	5.0
44	5	417.5	0.11	0.09	5.5
46	5	436.9	0.09	0.03	8.9
49	4	464.4	0.05	0.04	4.9
52	5	494.8	0.05	0.02	12.8
56	5	533.5	0	0.05	9.7

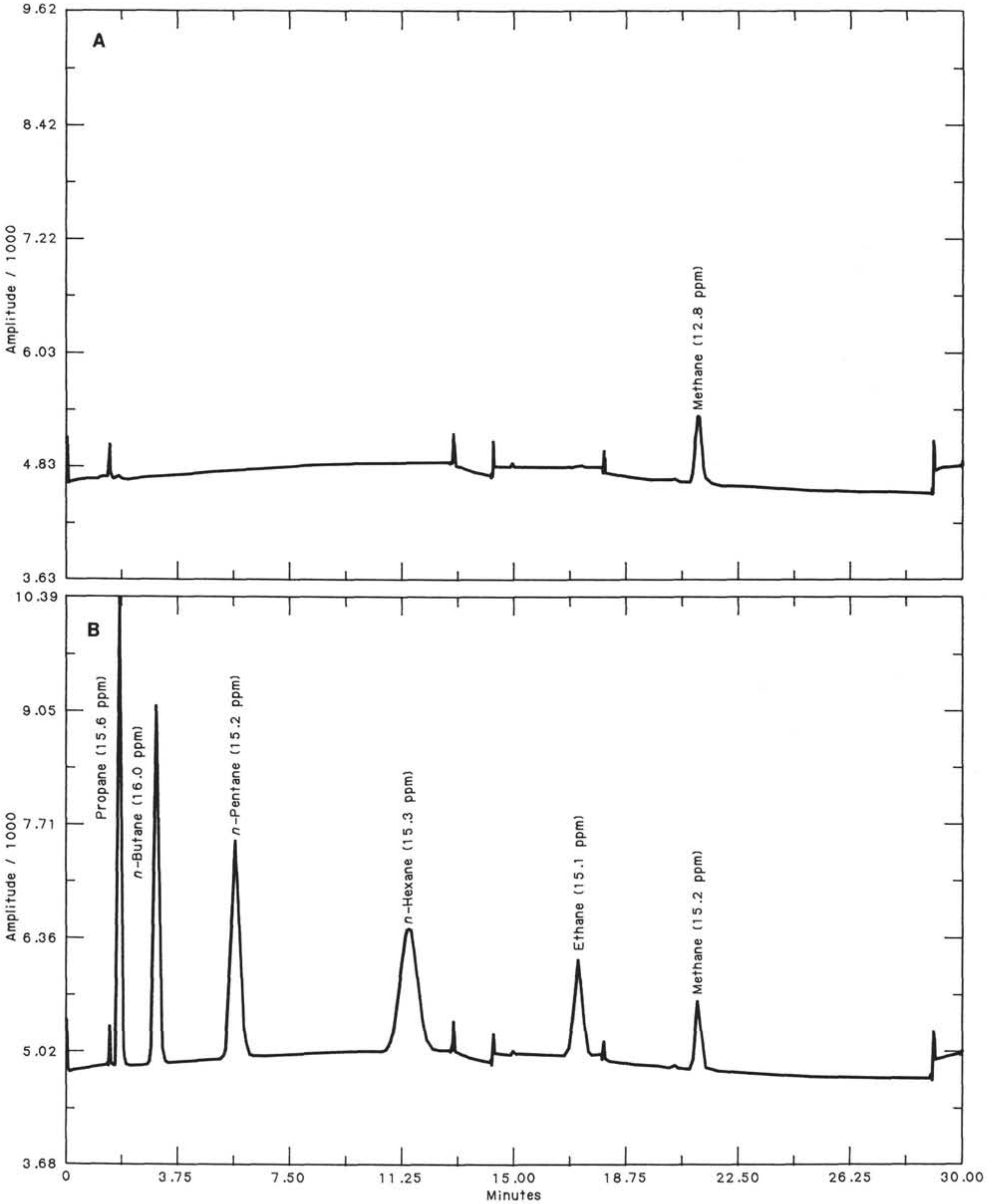

Figure 17. Gas chromatograms of hydrocarbon gases in sample and standard.

by direct measurement of acidified samples were nearly the same. Because acidification is time-consuming and offers abundant opportunity for contamination, we determined organic carbon by difference. This procedure was applied to portions of the same sediment used to determine methane and interstitial water chemistry. The amount of organic carbon (Table 10) increases irregularly with depth, reaching a maximum value in the Oligocene (347 m sub-bottom) of 1.78% (Fig. 18). Underlying Eocene sediments have low carbon contents that average less than 0.1%.

Carbonate carbon (Table 10) in 17 samples at Site 643 shows little variation. The uppermost sediment (3.0 m sub-bottom)

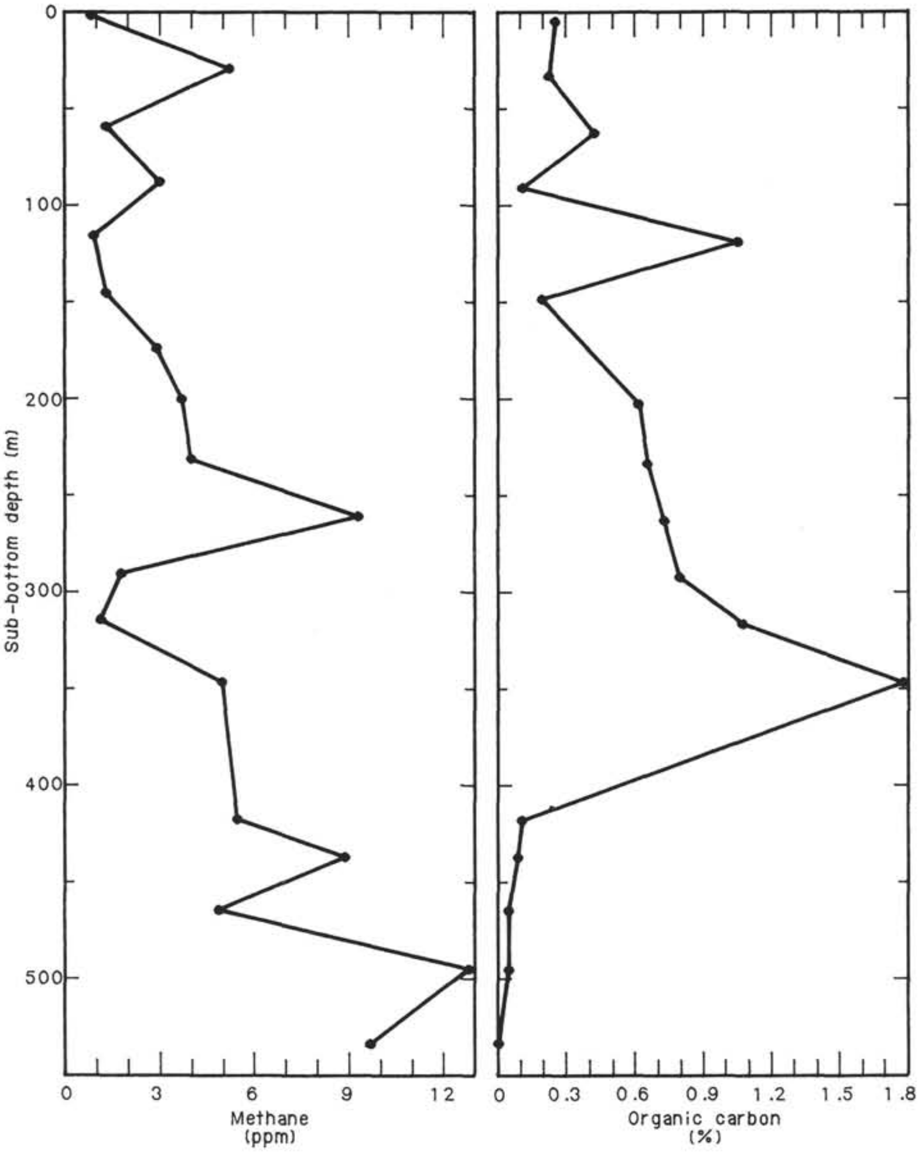

Figure 18. Profiles of methane and organic carbon vs. depth at Site 643.

contains 3.51% carbonate carbon. For all other samples, the carbonate carbon content is less than 0.1% (averaging 0.03%). This monotonous, low-resolution profile of carbonate carbon variation with depth contrasts with the high-resolution profile discussed later.

Organic Matter Characteristics

Rock-Eval pyrolysis was used in an attempt to characterize the organic matter in the sediments at Site 643. Results (Table 11) do not provide a clear understanding of the organic matter. Of interest, however, is that the total organic carbon (TOC) from Rock-Eval and the organic carbon values determined by difference are remarkably similar. These results contrast with the observations at Site 642, where Rock-Eval TOC data could not be used. Sediments in the interval from 89 to 347 m sub-bottom consistently have S_2 values greater than 1.0 mg HC/g sediment. These values show that kerogen in these sediments has the potential to generate some hydrocarbons. The hydrogen and oxygen indices (Table 11), calculated for these sediments, seem reasonable and are plotted in Figure 19. This diagram, comparable to a van Krevelen diagram (Tissot and Welte, 1984), shows that the organic matter in these sediments is generally a mixture of types II and III; that is, a mixture of both marine (oil/gas prone) and terrestrial (gas prone) components. The position of these samples on a van Krevelen-type diagram suggests that the organic matter is immature. The temperature of maximum pyrolysis yield (T_{max}) in part confirms this interpretation.

Inorganic

The chemistry of interstitial water was routinely monitored at Site 643 in the sediments overlying basalts of probable early Eocene age. In addition to the routine inorganic parameters, calcium carbonate was determined for 154 samples from the stratigraphic section; these samples were selected on the basis of sedimentologic considerations.

Interstitial Water

Eighteen 10-cm, full-round sediment core samples for interstitial-water analyses were collected about every third core between sub-bottom depths of 3.0 and 533.5 m. Results are given in Table 12. Figure 20 shows typical ion chromatograms from which we measured concentrations of calcium, magnesium, and

Table 11. Rock-Eval data for Site 643.

Core	Sec.	Depth (mbsf)	T_{max} (°C)	S_1	S_2	S_3	TOC	HI	OI
1	2	3.0	465	0.10	0.08	2.60	0.08	100	3250
4	4	30.3	478	0.12	0.67	0.55	0.11	609	500
7	5	60.3	537	0.08	0.66	0.25	0.06	1100	416
10	5	88.7	595	0.46	1.40	1.31	0.72	194	181
13	5	117.3	588	0.24	1.39	0.58	0.35	397	165
16	5	145.8	488	0.31	1.67	0.48	0.18	927	266
22	4	201.2	561	0.53	2.10	0.82	0.55	381	149
25	5	232.2	400	0.72	2.22	0.83	0.67	331	123
28	5	261.6	435	0.64	2.00	0.86	0.74	270	116
31	5	291.0	403	0.23	1.46	1.23	0.74	197	166
34	2	315.8	406	0.34	1.60	0.97	1.06	150	91
37	3	346.7	416	0.42	3.15	1.29	1.72	183	75
44	5	417.5	568	0.02	0.52	1.61	0.10	520	1610
46	5	436.9	505	0.04	0.92	1.58	0.11	836	1436
49	4	464.4	499	0.01	0.86	2.29	0.08	1075	2862
52	4	494.8	545	0	0.72	2.32	0.06	1200	3866
56	5	533.5	514	0.05	0.84	1.48	0.07	1200	2114

Abbreviations: S_1 (mg HC/g rock) = volatile hydrocarbons; S_2 (mg HC/g rock) = kerogen-derived hydrocarbons; S_3 (mg CO_2/g rock) = organic CO_2 from kerogen; TOC = % total organic carbon; HI (100 S_2/C_{org}) = Hydrogen Index, OI (100 S_3/C_{org}) = Oxygen Index; T_{max} = temperature (°C) of maximum hydrocarbon generation from kerogen.

sulfate ions. Profiles with depth of the concentrations of these ions are given in Figure 21. Trends with depth are generally smooth, except for the values at 30.3 m sub-bottom; these values are anomalous and probably incorrect. Calcium ion concentrations increase, whereas magnesium ion concentrations decrease, from the mud line down at this site. Sulfate ions also decrease with depth. In general, these profiles follow the results generated by Gieskes, Lawrence, and Galleisky (1978). As at Site 642, the chemistry of pore waters at Site 643 suggests that substantial, post-burial, diagenetic changes altered these sediments.

Calcium Carbonate

We sampled 154 discrete sediment intervals and measured them for calcium carbonate between sub-bottom depths of 0.9 and 565 m, using the Carbonate Carbon apparatus. The results gave a high-resolution profile of calcium carbonate content with depth. The data are presented in Table 13. Figure 22 depicts the variations in calcium carbonate content with depth. The percentage of calcium carbonate ranges from 0% at 536.6 m to 76.5% at 268.9 m. The six major fluctuations of calcium carbonate content in the upper 30 m of sediment are probably the result of glacial/interglacial periods in Pliocene-Pleistocene times. Two less-intense fluctuations can be found at 58 and 85

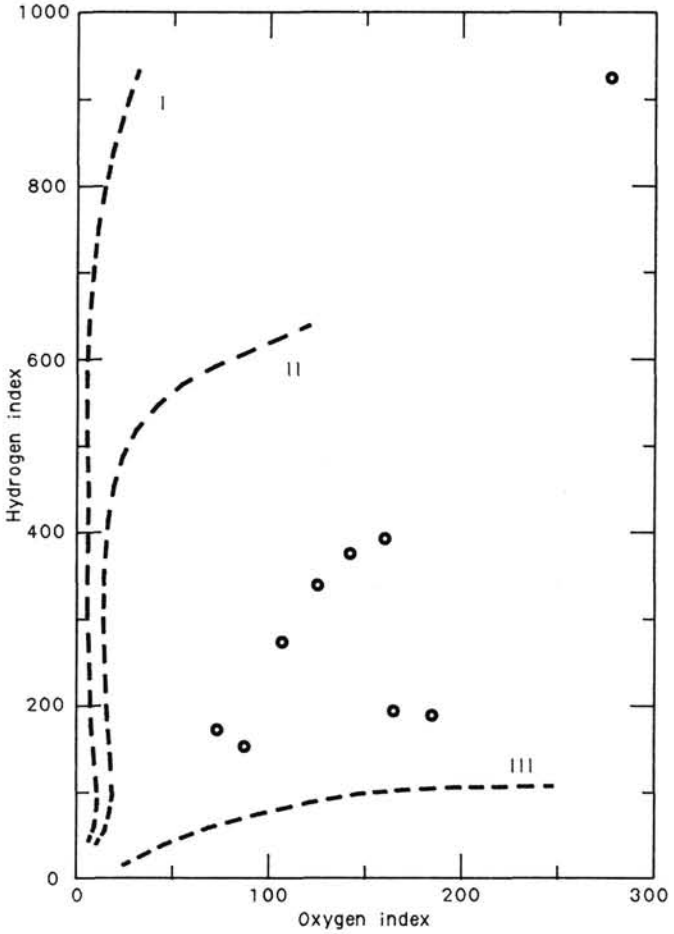

Figure 19. Van Krevelen-type diagram of organic matter at Site 643. Numerals designate organic-matter type.

Table 12. Interstitial-water chemistry for Site 643.

Core	Section	Depth (mbsf)	pH	Alkalinity (meq/L)	Salinity (ppt)	Chlorinity (mmol/L)	Calcium (mmol/L)	Magnesium (mmol/L)	Sulfate (mmol/L)
Seawater		0	7.91	2.55	34.5	560	10	49	27
1	2	3.0	7.42	3.68	35.5	560	16	53	27
4	4	30.3	7.67	5.39	35.2	554	8	14	12
7	5	60.3	8.09	3.51	34.0	553	13	30	24
10	5	88.7	7.79	4.31	33.9	551	11	29	22
13	5	117.3	7.58	4.32	34.2	553	14	29	19
16	5	145.8	7.34	3.82	34.5	560	14	29	17
19	5	174.3	7.50	7.95	33.8	558	15	27	19
22	4	201.2	7.49	7.77	33.8		20	28	17
25	5	232.2	7.60	7.85	33.5	561	21	30	17
28	5	261.6	7.11	3.51	34.9	563	18	23	15
31	5	291.0	7.68	3.93	33.5				
34	2	315.8							
37	3	346.7							
44	5	417.5					27	13	
46	5	436.9			32.5	539	32	14	17
49	4	464.4							
52	5	494.8					36	6	15
56	5	533.5			33.5	556	41	2	8

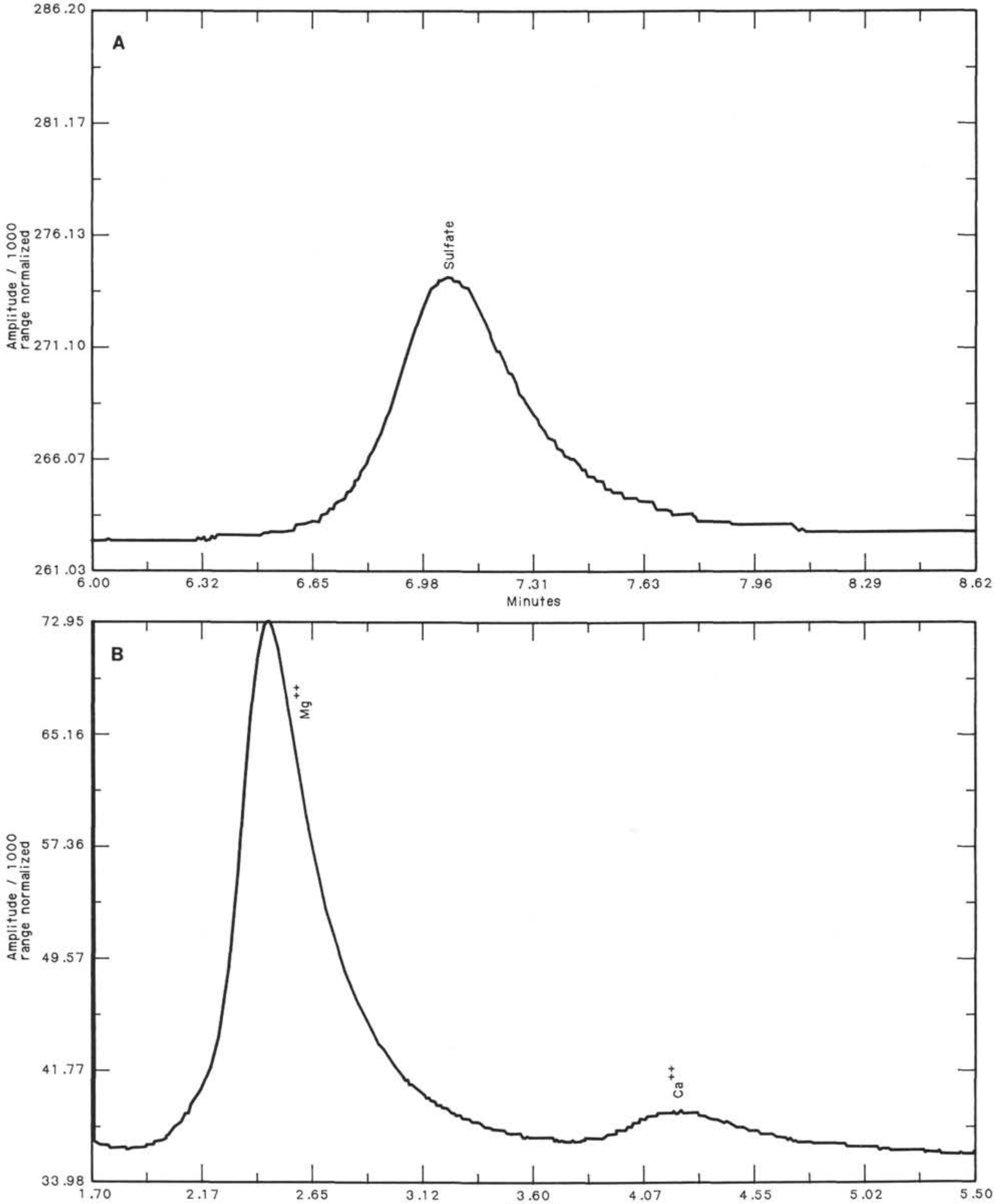

Figure 20. Ion chromatograms of sulfate, magnesium, and calcium for Sample 104-643-56-5, 135–145 cm.

m; these spikes probably represent major periods of ocean cooling with calcium carbonate being derived mainly from nannofossils. The small increase occurring at 145 m may also result from a change in climatic conditions. The lower portion of the sediment column has relatively low amounts of calcium carbonate (about 0.2%) with only three pulses, which are probably due to chalk layers.

PHYSICAL PROPERTIES

Introduction

Coring at Site 643 sampled approximately 530 m of sediments from Recent to early Eocene age. Physical properties measured at the site were index properties, thermal conductivity, and compressional-wave velocity.

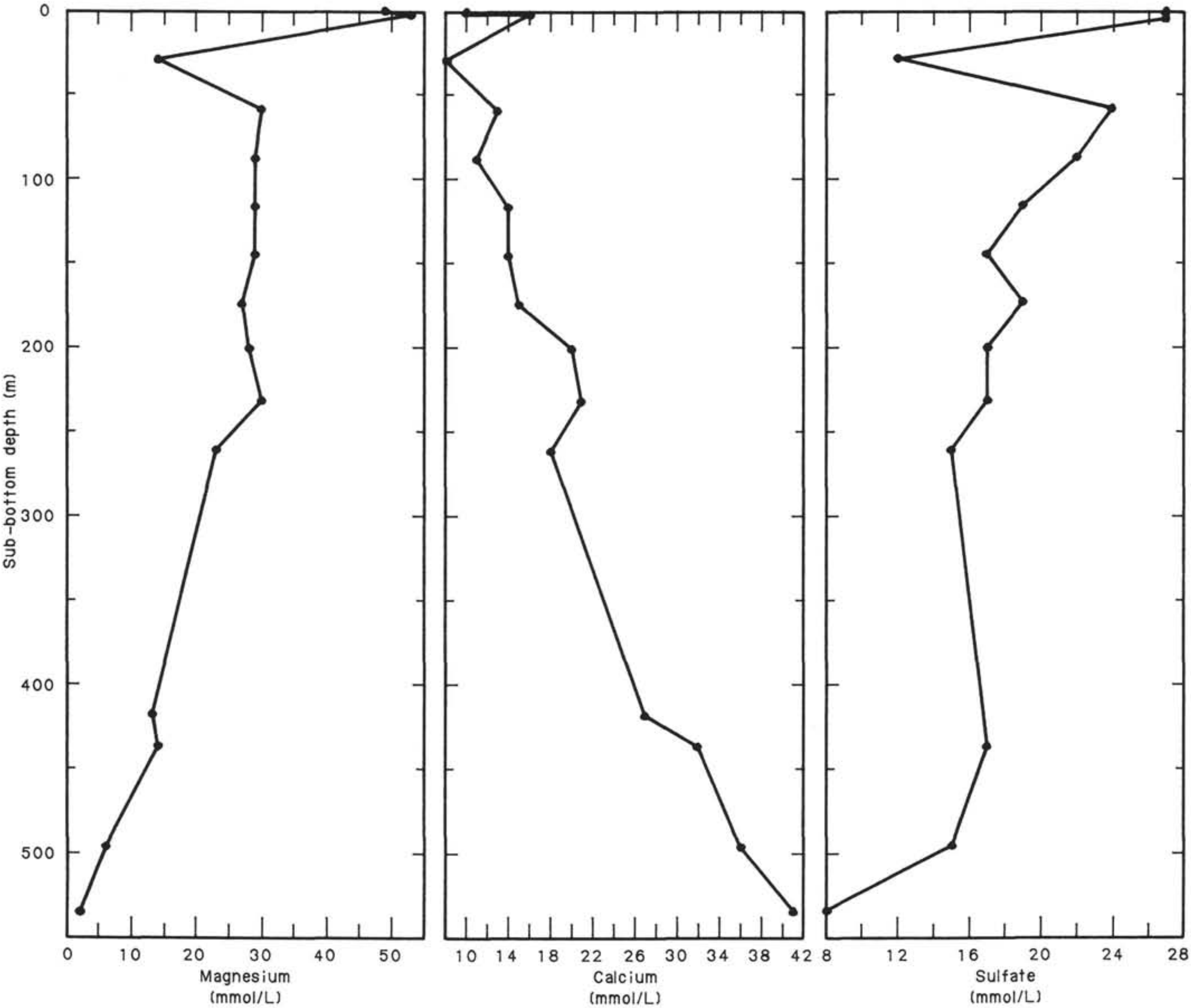

Figure 21. Profiles of magnesium, calcium, and sulfate vs. depth at Site 643.

Hydraulic piston cores in the upper portion of the hole (to 148 mbsf) are relatively undisturbed. Cores from the lower one-half of the section were taken by extended core barrel (XCB) and show considerable disturbance. Both flow along the core liner and "biscuiting" are evident in XCB cores. Consequently, some physical properties, in particular compressional-wave velocity, may not be representative of *in-situ* values.

Index Properties

Index properties (bulk density, water content, and porosity) are plotted relative to sub-bottom depth in Figure 23. All physical properties data from Site 643 are listed in Table 14. As at Site 642, the vertical distribution of these properties closely relates to the lithology, and significant changes in the properties correlate with lithologic unit boundaries. Index property profiles are also similar in trend and magnitude to the profiles for Site 642.

The trends of decreasing bulk density and increasing porosity with depth in lithologic Units II and III at Site 643 were also observed at Site 642. These trends are the reverse of the expected response of sediments to increasing burial and may reflect compositional and textural differences. Composition and texture are more important than diagenetic effects when determining the physical properties of sediments especially at shallow depths of burial (Bennett and Nelsen, 1983).

Unit I is a 50-m-thick sequence of Pleistocene-Recent, glacial and interglacial sediments (see "Sediment Lithology" section, this chapter). Bulk densities in this unit range from 1.39 to 1.93 g/cm^3 and average 1.71 g/cm^3. Index properties variations primarily reflect variable amounts of clastics and carbonate. Positive correlation between bulk density and thermal conductivity, which averages 2.90×10^{-3} cal × °C^{-1} × cm^{-1} × s^{-1} in Unit I, and inverse correlation between bulk density, porosity (averaging 61%), and water content (averaging 55%) is evident from Figure 23.

Unit II is a 50-m section of late Miocene to Pleistocene siliceous and nannofossil oozes divided into three subunits. The contact between Units I and II is characterized by steep physical-properties gradients. The general trend of index properties in Unit II is toward a decreasing gradient.

Subunits IIA and IIC are predominantly calcareous oozes separated by siliceous mud in Subunit IIB. Subunit IIB is characterized by a faster rate of decrease in bulk density, coupled

Table 13. Calcium carbonate content at Site 643.

Core	Section	Depth (mbsf)	$CaCO_3$ (%)
1	1	0.9	13.00
1	2	2.4	45.60
1	3	3.4	12.80
1	3	4.1	11.00
2	1	6.7	23.80
2	3	9.4	22.00
2	4	10.9	11.20
2	5	12.4	35.10
2	6	13.7	9.30
3	2	16.8	38.10
3	3	18.3	2.70
3	4	20.5	23.00
3	5	21.2	5.60
4	1	25.5	6.40
4	5	31.5	8.90
4	7	33.6	0.10
4	CC	33.8	0.16
5	1	35.1	0.31
5	3	37.7	0.14
5	5	39.9	1.53
5	6	42.6	0.09
6	1	43.6	1.35
6	2	46.1	0.18
6	4	48.9	0.08
7	2	54.7	0.65
7	3	56.0	12.80
7	4	58.6	16.70
7	5	59.5	11.60
7	5	59.8	0.45
8	1	62.6	2.17
8	2	64.8	0.21
8	4	67.2	0.45
8	5	68.6	0.33
8	6	71.0	1.12
9	1	72.4	0.63
9	3	75.4	0.57
9	5	78.4	1.36
9	6	80.4	3.20
9	7	81.3	15.20
10	1	82.1	18.80
10	3	85.1	22.70
10	5	88.1	0.39
12	1	101.1	0.10
12	3	104.1	0.22
12	5	107.1	0.45
13	1	110.7	0.16
13	3	113.7	0.39
13	5	116.7	0.15
14	1	120.1	0.45
14	3	123.1	0.09
14	5	126.1	1.41
15	1	129.6	0.58
15	3	132.6	0.27
15	5	135.6	0.08
16	1	139.1	0.22
16	3	142.1	12.30
16	5	145.1	0.37
18	1	158.2	0.24
19	1	167.6	0.10
19	3	170.6	0.11
19	5	173.6	0.32
20	1	177.1	0.15
20	3	180.1	0.32
20	5	183.1	0.23
22	1	195.5	0.25
22	3	199.0	0.22
22	5	202.5	0.17
23	2	207.4	0.42
23	5	211.3	0.13
23	6	213.8	0.13
24	2	216.9	0
24	4	220.3	0.27
24	5	221.9	0.16
25	2	226.3	0.29
25	4	230.1	0.15
25	6	232.3	0.26
26	1	235.5	0.16
26	4	239.1	0.18
26	6	243.0	0.05
27	1	244.9	0.20
27	3	247.9	0.30
27	6	252.0	0.22
28	1	254.9	0.24
28	4	258.7	0.32
28	6	262.6	0.29
29	1	264.6	0.10
29	4	268.9	76.50
29	4	269.4	0.27
29	6	272.5	0.20
31	1	284.1	0.24
31	3	287.1	0.26
31	6	291.6	0.36
32	2	295.6	0.17
33	2	305.2	0.29
34	2	315.0	0.14
35	1	323.6	0.24
36	1	333.1	0.11
36	3	336.1	0.19
36	5	339.1	0.20
37	1	342.9	0.16
37	3	345.9	0.23
38	2	354.2	0.24
39	1	362.5	0.14
41	1	381.8	0.12
41	CC	390.6	51.30
42	2	392.8	13.30
43	CC	409.9	35.30
44	1	411.0	0.29
44	3	414.0	0.30
44	5	417.0	0.26
45	1	420.7	0.29
45	3	423.7	0.28
45	5	426.7	1.10
46	1	430.4	0.37
46	3	433.4	0.32
46	5	436.4	0.23
47	1	440.3	0.33
47	3	443.3	0.33
47	5	446.3	0.31
48	1	449.5	0.16
48	3	452.5	0.41
48	5	455.5	0.35
49	2	460.4	0.25
49	4	464.1	0.38
49	6	467.3	0.52
50	1	468.8	0.36
51	2	479.7	0.31
51	5	484.3	4.24
51	6	485.4	0.36
52	2	489.6	0.21
52	4	492.9	0.21
52	6	495.0	0.24
53	1	498.1	0.16
53	3	501.1	0.27
53	5	504.1	0.26
54	1	507.6	0.10
54	1	507.7	0.16
54	3	510.6	0.21
54	3	510.7	0.15
54	6	515.1	0.88
54	6	515.2	0.48
55	1	517.3	0.25
55	3	520.3	0.28
55	6	524.8	0.28
56	1	526.8	0.11
56	3	529.8	0.32
56	5	532.8	0.16
57	1	536.6	0
57	3	539.6	0.53
57	5	542.6	0
59	1	545.9	0.01
60	2	557.2	0.25
61	1	561.8	0.12
62	1	564.7	0.13

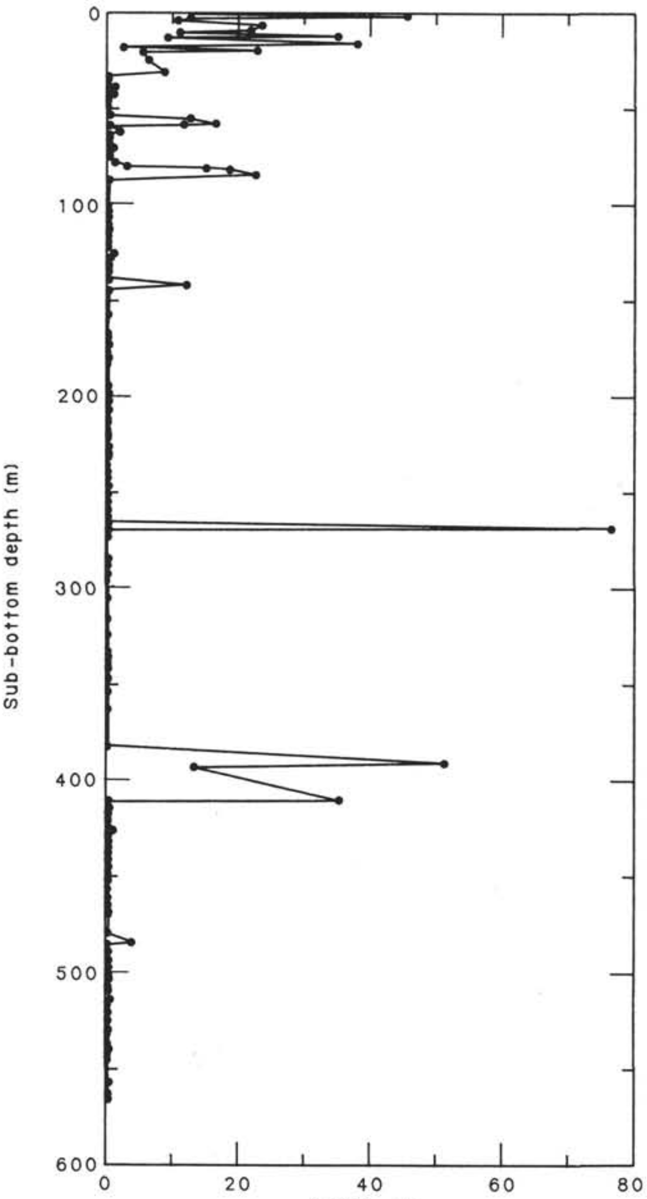

Figure 22. Calcium carbonate at Site 643.

with a smaller range of values relative to the over- and underlying carbonates. The average bulk density for Subunit IIB is 1.41 g/cm^3, compared with an average of 1.43 g/cm^3 for Subunit IIA. Average porosity (83%) and water content (139%) are higher in Subunit IIB than in the carbonate-enriched subunits. Subunit IIA has the following averages: 1.43 g/cm^3 bulk density, 80% porosity, and 126% water content.

Unit III, as at Site 642, shows a slight downhole decrease in bulk density (1.33 g/cm^3 average), with increasing porosity (79% average) and water content (144% average). This trend is interrupted by an approximately 40-m-thick section centered around 165 mbsf. This zone exhibits excursions to higher bulk densities and lower water contents and porosities, and correlates with the interval of highest clay and clastic content for Unit III. The remainder of Unit III consists primarily of lower-upper Miocene, siliceous ooze.

The contact between Units III and IV is marked by a very abrupt, large shift in bulk density (1.86 g/cm^3 average) as well as lower water content (57% average) and porosity (average 58%). Unit V has an average bulk density of 1.86 g/cm^3, 55% porosity, and 44% water content. Units IV and V are composed of lower Miocene to lower Eocene terrigenous mudstones that are well indurated for such shallow burial depths. The sharp contrast in lithologies, degree of consolidation, and the large, abrupt change in all physical properties suggest an unconformity occurs at about 275 mbsf. The trend of physical properties below this boundary is one of generally increasing bulk density and decreasing porosity and water content (normal gradient), as opposed to the overlying Units II and III.

Units IV and V could be subdivided on the basis of physical-properties trends, some of which show reverse gradients, although the overall trend is one of a normally consolidated sequence. The most obvious of these trend reversals coincides with the boundary between Units IV and V.

Undrained Shear Strength

The undrained shear-strength profile is plotted in Figure 24. Shear strength increases almost linearly from 2.77 kPa at the seafloor to 87.58 kPa at 51 mbsf, the base of lithologic Unit I. Below this point, shear strength values become more variable and increase less rapidly with depth to 137 kPa at 146 mbsf in Unit III. A sudden drop to 25 kPa occurs at this depth, followed by a normal (increasing with depth) trend. The break is associated with a change in index properties, as noted earlier, and correlates to a relatively clastic-rich interval in Unit III.

Shear strength could not be measured below 300 mbsf. Cores recovered below this depth are too indurated to permit insertion of the vane. The overall trend at Site 643 is very similar to Site 642 down to 150 mbsf. The uppermost change in gradient at approximately 70 mbsf is observed at both sites and occurs over comparable depths. The shift to much lower values of shear strength is not as abrupt as at Site 642 and occurs at somewhat greater depth (about 175 mbsf). Below 175 mbsf, shear strength increases with depth to a maximum of nearly 250 kPa at 280 mbsf.

The depth at which the shear strength gradient is reduced and below which more variable values of shear strength are measured corresponds to Subunit IIB. In this unit, biogenic silica first becomes a significant compositional component in the section.

Compressional-Wave Velocity and Acoustic Impedance

Compressional-wave velocity generally shows only a slight increase with depth (Fig. 25). Overall, velocities increase downhole by distinct and fairly abrupt shifts to higher average velocities, punctuated by several occurrences of relatively high velocities. Each of these velocity intervals has an associated change in bulk density and acoustic impedance and is also associated with a lithologic unit boundary.

The distribution of both compressional-wave velocity and acoustic impedance is similar to Site 642 down to about 325 mbsf (the base of the sedimentary section at Site 642). Trends, ranges, and peak values of velocity and impedance correlate between the two sites, with similar magnitudes occurring at comparable depths.

Average velocities for Units I, IIA, IIB, and III are 1419.3, 1457.7, 2154.7 and 1591.5 m/s, respectively. The much higher velocity of Subunit IIB is associated with the siliceous muds sandwiched between carbonate units and responsible for a relatively high acoustic impedance. High velocity and impedance values occur within Unit III at about 160 and 200 mbsf. Velocities at these depths are 1789 and 1887 m/s, respectively. The former is associated with other changes in index properties previously mentioned. The 200-mbsf event appears to be associated with an interval of maximum silica and minimum clay and clastic content in Unit III. We observed high velocities (2904 m/s) and acoustic impedance (5779 Mg/m^2/s) at the Unit III/IV

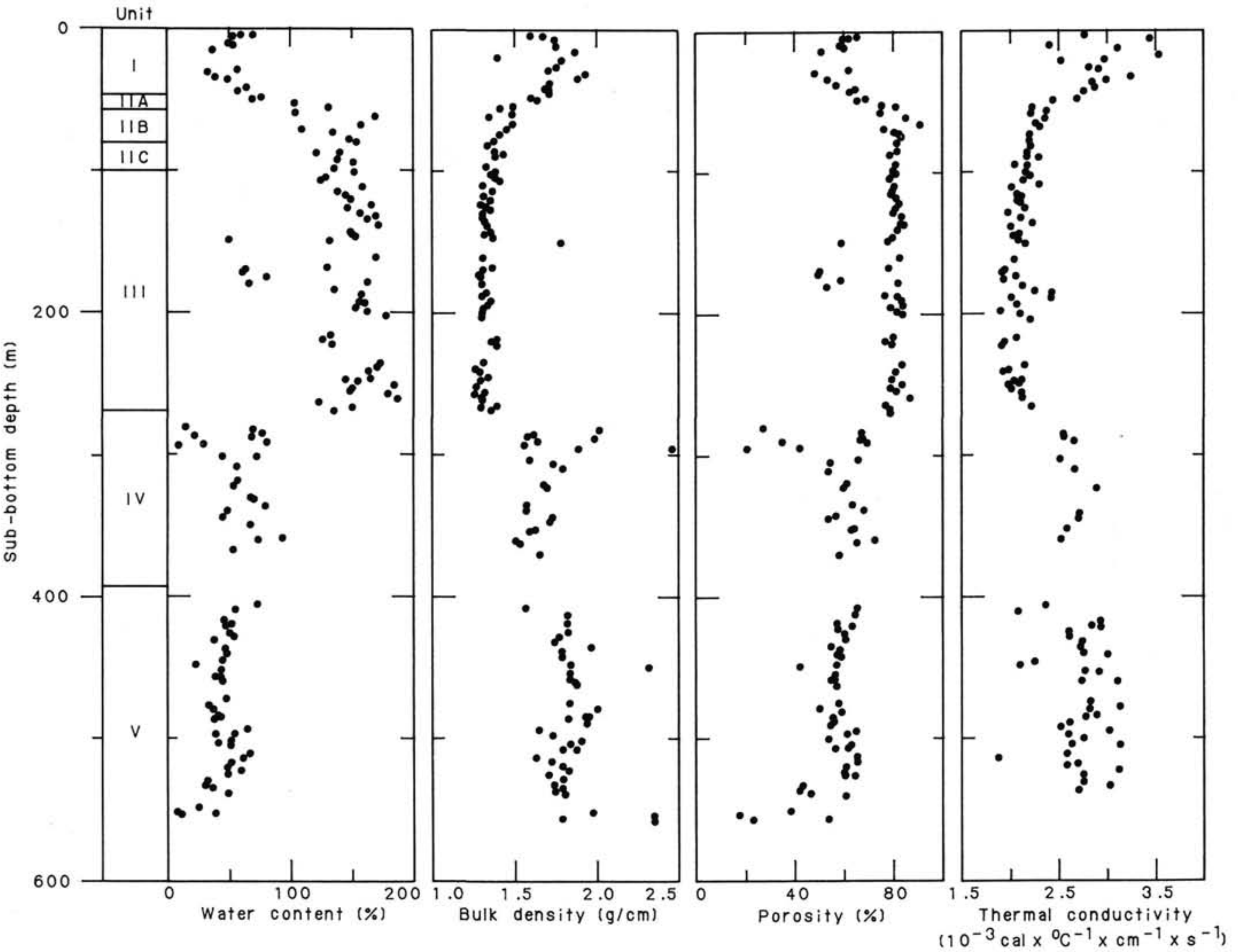

Figure 23. Index properties (water content, bulk density, and porosity) and thermal conductivity profiles for Site 643.

boundary, which may indicate an unconformity. Units IV and V exhibit somewhat greater increases and ranges of velocity and acoustic impedance with depth (Table 14); however, some of the variation may be attributed to core disturbance, which is very common in this portion of the section. The boundary between Units IV and V only approximately correlates with a high-velocity and acoustic-impedance event at 430 mbsf. This peak and a larger one at 500 mbsf correlate with the boundaries between normal and reverse density and porosity gradients noted earlier.

The large acoustic-impedance contrast at 300 mbsf between Units III and IV correlates with a high-amplitude seismic reflector at 0.42 s (two-way traveltime) on NPD Line NH-1-79, if one assumes an average velocity of 1500 m/s for the overlying section.

Thermal Conductivity

Thermal conductivity at Site 643 varies from 1.90 to 3.56 × 10^{-3} cal × °C^{-1} × cm^{-1} × s^{-1} (Fig. 23, Table 14). Overall, thermal conductivity shows an inverse correlation with water content, which is typical of marine sediments (Hamilton, 1974) and a direct correlation in these sediments with bulk density. The profile is similar to that of Site 642, with widely varying values and a rapid rate of decrease to a depth of about 50 mbsf near the base of lithologic Unit I. At this depth, there is an abrupt decrease in the gradient. Conductivity continues to decrease slightly from 3.0 to 2.0 × 10^{-3} cal × °C^{-1} × cm^{-1} × s^{-1} at about 250 mbsf. There is a fairly rapid increase in thermal conductivity from 250 mbsf to about 325 mbsf. This increase is observed at Site 642 as well, although it is more gradual there. Below 325 mbsf, there is a trend toward a much more gradual increase of conductivity, but with a much wider range of values—from about 2.0 to 3.0 × 10^{-3} cal × °C^{-1} × cm^{-1} × s^{-1}.

Summary

Physical-properties profiles (Figs. 23 and 25) at Site 643 are similar in trend and range of values to the sediment section at Site 642 (Fig. 26). The lower one-half of the section at Site 643, below 300 mbsf, is not present at Site 642.

The close correlation between physical properties and sediment type observed at Site 643, including the anomalous trends in bulk density and porosity associated with the diatomaceous oozes, mimics the physical properties in similar lithologies at Site 642 (see "Physical Properties" section, Site 642 chapter, this volume). Changes in physical-properties profiles also appear to be good indicators of lithologic changes, as at Site 642.

SEISMIC CORRELATION

We approached Site 643 along seismic multichannel profile NH-1. The proposed site was located at sp. 9400. Analog single-channel seismic data were recorded between Sites 642 and 643

Table 14. Summary of physical-properties data for sediments from Site 643.

Core	Section	Sample interval		Depth (mbsf)	Bulk density (g/cm^3)	Porosity (%)	Water content (%)	Vane[a] (kPa)	Velocity[b] (m/s)	Thermal conductivity ($10^{-3} \times cal \times °C^{-1} \times cm^{-1} \times s^{-1}$)	Acoustic impedance ($Mg/m^2/s$)
		top (cm)	bottom (cm)								
1	2	48	50	2.00	1.60	66.20	70	2.77		2.76	
1	3	35	37	3.35	1.67	62.80	60	5.24	1454		2428.18
1	4	50	52	5.00	1.73	60.10	53	0.11	1411	3.45	2441.03
2	2	134	136	9.15	1.76	59.00	50	10.87	1336	2.39	2351.36
2	4	99	101	10.80	1.74	60.80	54	21.47	1375	3.11	2392.50
2	6	105	107	13.85	1.87	50.50	37	17.97	1555	3.56	2907.85
3	2	99	101	17.30	1.39			11.02	1412	2.51	1962.68
3	4	49	51	19.80	1.78			13.90	1413	2.97	2515.14
3	6	99	101	23.30	1.75			11.02	1364	2.83	2387.00
4	2	59	61	26.39	1.70	62.90	58	27.69	1559	2.94	2650.30
4	3	112	115	28.42	1.93	48.50	34	52.54	1551	3.26	2993.43
4	6	39	41	32.19	1.88	53.70	40	49.72	1376	3.00	2586.88
5	2	69	72	34.49	1.71	57.40	51	33.90	1394	2.87	2383.74
5	4	99	101	39.30	1.68	66.50	65	42.38		2.89	
5	6	29	31	41.60	1.71	63.30	58	48.59	1518	2.77	2595.78
6	2	29	71	45.50	1.60	70.20	77	38.96	1341	2.71	2145.60
6	4	29	31	48.10	1.63	66.80	69	63.28	1230	2.41	2004.90
6	6	29	31	51.10	1.49	76.40	102	87.58		2.20	
7	1	109	111	53.90	1.41	81.30	130	31.08	1748	2.37	2464.68
7	3	109	111	56.90	1.48	76.30	104	83.62	1406	2.22	2080.88
7	5	79	111	59.90	1.34	85.80	169	59.89	1219	2.35	1633.46
8	2	79	81	64.60	1.47	91.90	157	42.38	1470	2.28	2160.90
8	4	79	81	67.60	1.45	76.70	109	99.88	2494	2.32	3616.30
8	6	79	81	70.60	1.40	81.20	134	99.16	2231	2.22	3123.40
9	1	79	81	72.60	1.41	81.90	134	76.84	2368	2.22	3338.88
9	3	79	81	75.60	1.38	84.10	148	95.49	2664	2.22	3676.32
9	5	79	81	78.60	1.33	82.10	154	86.45	1701	2.21	2262.33
10	2	79	81	83.60	1.38	82.20	140	74.58	1454	2.17	2006.52
10	4	77	80	86.60	1.42	78.60	120	98.31		2.30	
10	6	77	80	89.60	1.38	81.20	138	95.48	1855	2.16	2559.90
11	2	80	82	93.10	1.33	81.70	150	65.54	1547	2.05	2057.51
11	4	79	81	96.10	1.39	80.90	135	83.39	1537	2.16	2136.43
11	6	79	81	99.10	1.35	82.80	151	100.12	1543	2.20	2083.05
12	2	49	51	102.30	1.38	78.70	128	100.34	1512	2.15	2086.56
12	4	49	51	105.30	1.41	79.60	126	107.12	1518	2.31	2140.38
12	6	49	51	108.30	1.30	81.30	159	96.39	1541	2.03	2003.30
13	2	59	61	111.90	1.37	80.90	138	50.40	1484	2.06	2033.08
13	4	59	61	114.90	1.32	79.80	146	77.40	1488	2.11	1964.16
13	6	59	61	117.90	1.34	81.40	148	105.99	1516	2.06	2031.44
14	2	59	61	121.40	1.31	83.20	166	39.32	1471	2.13	1927.01
14	4	59	61	124.40	1.35	81.30	146	116.39	1497	2.15	2020.95
14	6	59	61	127.40	1.30	81.10	156	110.51	1535	1.96	1995.50
15	2	59	61	130.90	1.30	83.60	170	42.94	1467	2.11	1907.10
15	4	59	61	133.90	1.32	83.60	163	94.13	1472	2.26	1943.04
15	6	59	61	136.90	1.33	86.00	173	110.18	1493	2.01	1985.69
16	2	59	61	140.40	1.35	82.20	149	128.03	1486	2.08	2006.10
16	4	59	61	143.40	1.32	80.90	152	128.14	1519	2.02	2005.08
16	6	59	61	146.40	1.38	79.50	131	136.96	1501	2.10	2071.38
18	2	59	61	159.40	1.30	83.40	170	24.63	1786	2.04	2321.80
18	CC	15	17	166.75	1.37	78.60	129	57.52	1507	1.94	2064.59
19	2	59	61	168.90	1.30	50.42	63	54.80	1521	1.92	1977.30
19	4	60	62	171.90	1.28	49.20	62	55.03	1533	2.06	1962.24
19	6	59	61	174.90	1.29	58.10	81	64.18	1482	1.95	1911.78
20	2	60	61	178.40	1.31	82.60	162	44.07	1506	2.13	1972.86
20	4	60	61	181.40	1.31	52.60	67	32.77	1689	2.27	2212.59
20	6	59	61	184.40	1.33	77.90	136	47.80	1553	2.44	2065.49
22	2	59	61	187.40	1.31	81.90	157	45.20	2423	2.43	3174.13
22	4	59	61	190.40	1.35	83.60	155	40.68	1244	2.00	1679.40
22	6	59	61	193.40	1.34	84.50	160	66.67	1882	2.06	2521.88
23	2	59	61	196.40	1.31	80.60	152	76.84	1433	1.90	1877.23
23	4	59	61	199.40	1.31	82.40	162	51.98	1181	2.11	1547.11
23	6	59	61	202.40	1.30	84.50	177	118.65	1531	2.21	1990.30
24	2	59	61	216.99	1.39	80.70	133	64.41	1683	2.10	2339.37
24	4	59	61	219.99	1.36	77.00	126	42.38	1563	1.93	2125.68
24	6	59	61	222.99	1.39	81.10	134	62.51	1526	1.90	2121.14
25	2	59	61	226.80	1.28	81.00	164	35.03	1520	2.03	1945.60
25	4	59	61	229.80	1.27	83.90	184	23.73	1708	2.01	2169.16
25	6	59	61	232.80	1.32	80.80	149	57.63	1463	2.00	1931.16
26	2	59	61	236.60	1.30	83.70	173	88.71	1887	2.15	2453.10
26	4	59	61	239.60	1.27	81.40	170	75.71	1509	1.99	1916.43
26	6	59	61	242.59	1.29	81.90	163	99.44	1492	1.92	1924.68
27	2	59	61	246.39	1.33	79.80	144	76.84	1492	2.12	1984.36
27	4	59	61	249.98	1.32	81.40	153	42.94	1740	2.08	2296.80
27	6	59	61	252.39	1.32	80.40	148	101.70	1473	1.99	1944.36
28	2	59	61	255.60	1.30	78.90	147	73.45	1514	2.03	1968.20

Table 14 (continued).

Core	Section	Sample interval		Depth (mbsf)	Bulk density (g/cm^3)	Porosity (%)	Water content (%)	Vane[a] (kPa)	Velocity[b] (m/s)	Thermal conductivity ($10^{-3} \times$ cal $\times$ °C^{-1} $\times$ cm^{-1} $\times$ s^{-1})	Acoustic impedance (Mg/m^2/s)
		top (cm)	bottom (cm)								
28	4	59	61	258.60	1.26	82.30	177	75.71	1528	2.12	1925.28
28	6	59	61	261.60	1.31	87.40	187	77.97	3340	2.13	4375.40
29	2	59	61	266.00	1.39	77.70	122	74.58	1551	2.23	2155.89
29	4	59	61	269.00	1.31	80.00	149	70.96	1552		2033.12
29	6	59	61	272.00	1.37	80.20	134	81.59	1529		2094.73
30	CC	39	41	283.30	2.03	26.10	15	117.63	3367		6835.01
31	2	59	61	285.60	1.62	67.20	70	226.00	1549	2.57	2509.38
31	4	59	61	288.60	1.57	68.60	77		1538	2.59	2414.66
31	5	83	85	290.35	1.99	35.10	22		2904		5778.96
31	6	59	61	291.60	1.64	66.70	68		1566	2.71	2568.24
32	2	59	61	295.40	1.56	70.40	81		1495		2332.20
32	2	140	142	296.20	1.89	42.60	29		2623		4957.47
32	3	146	148	297.75	2.49	20.00	9		4000		9960.00
33	2	59	61	305.20	1.60	66.90	71		1586	2.53	2537.60
33	3	43	45	306.55	1.73	54.50	46		2180	2.51	3771.40
34	1	70	72	313.60	1.80	52.70	57		2216	2.71	3988.80
34	CC	46	48	322.40	1.68	60.80	57		1743		2928.24
35	3	20	22	325.90	1.71	60.30	54		1607	2.93	2747.97
36	2	59	61	334.60	1.58	64.20	68		1604		2534.32
36	4	60	62	337.60	1.58	64.80	69		1683		2659.14
36	6	59	61	340.60	1.57	69.00	78		1615		2535.55
37	2	60	62	344.40	1.73	56.40	49		1768	2.75	3058.64
37	4	120	122	348.00	1.72	53.30	45		2020	2.75	3474.40
38	2	59	61	354.20	1.63	65.00	66		1542	2.62	2513.46
38	3	1	3	355.10	1.61	64.60	66		1632		2627.52
39	2	74	76	364.05	1.51	73.20	92		1522		2298.22
39	3	23	25	365.10	1.54	66.00	74		1532	2.54	2359.28
40	1	20	22	373.10	1.66	57.80	53		2081		3454.46
44	1	59	60	410.59	1.57	66.30	73			2.37	
44	4	59	61	415.10	1.83	65.10	55		1725	2.10	3156.75
44	6	59	61	418.10	1.77	59.50	51		1552	2.16	2747.04
45	2	59	61	421.80	1.82	56.70	45		1808	2.97	3290.56
45	4	59	61	424.80	1.83	62.50	52		1429	2.86	2615.07
45	6	59	61	427.50	1.83	58.10	47			2.97	
46	2	59	61	431.50	1.77	59.10	51		1702	2.64	3012.54
46	4	59	61	434.50	1.75	60.60	53		2205	2.65	3858.75
46	6	59	61	437.40	1.99	53.80	37		3224	2.77	6415.76
47	2	59	61	441.20	1.80	57.40	47		1702	2.77	3063.60
47	4	59	61	444.20	1.79	57.10	47		1700	3.03	3043.00
47	6	59	61	447.20	1.80	59.00	49		1670	2.81	3006.00
48	2	59	61	450.80	1.85	56.70	44		1553	2.26	2873.05
48	4	59	61	453.80	2.33	40.90	22		1725	2.08	4019.25
48	6	59	61	456.80	1.85	56.50	44		1674	2.78	3096.90
49	2	59	61	460.50	1.85	56.50	44		1643	2.94	3039.55
49	4	59	61	463.50	1.88	54.40	41		1663	3.10	3126.44
49	6	59	61	466.50	1.89	56.70	43		1686	2.76	3186.54
51	2	59	61	479.80	1.83	58.10	47		2014	2.87	3685.62
51	4	59	61	482.80	2.03	49.50	33		1675	3.15	3400.25
51	6	59	61	485.80	1.98	59.30	37		1695	2.84	3356.10
52	2	59	61	489.40	1.94	55.40	40		4101	2.93	7955.94
52	4	59	61	492.40	1.83	55.20	43		4561	2.81	8346.63
52	6	59	61	495.40	1.96	54.00	38		3722	2.61	7295.12
53	2	59	61	499.10	1.67	65.80	65		2340	2.56	3907.80
53	4	59	61	502.10	1.75	61.00	53		1663	3.05	2910.25
53	6	59	61	505.10	1.92	53.20	39		1705	2.63	3273.60
54	2	59	61	508.79	1.84	63.40	52		2229	2.79	4101.36
54	4	59	61	511.79	1.79	61.50	52		1703	3.16	3048.37
54	6	59	61	512.14	1.88	56.00	42			2.66	
55	2	59	61	518.50	1.65	65.60	66			2.61	
55	4	59	61	521.50	1.73	66.50	62			1.89	
55	6	59	61	524.00	1.80	61.60	52			2.72	
56	2	59	61	528.10	1.84	60.60	49			2.62	
56	4	59	61	531.10	1.71	65.10	61			3.16	
56	6	59	61	534.10	1.80	61.00	51			2.78	
57	2	63	65	537.75	1.75	42.80	33			2.80	
57	4	57	59	540.75	1.80	41.70	30			3.08	
57	6	54	56	543.75	1.74	46.20	36				
59	1	40	42	545.60	1.82	61.30	51			2.74	
60	2	59	61	557.00	2.00	38.60	24				
60	CC	22	24	560.95	2.37	17.40	8				
61	1	69	71	561.90	1.81	52.90	41				
61	CC	19	21	563.40	2.37	23.00	11				

[a] Vane = undrained shear strength.

[b] Velocity = compressional-wave velocity.

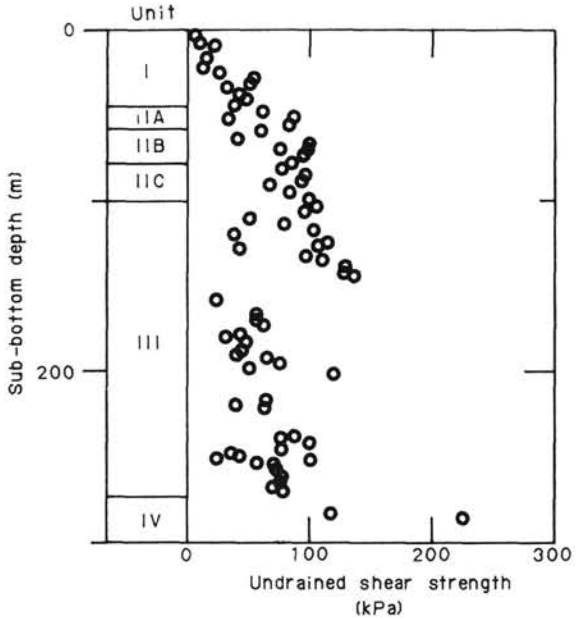

Figure 24. Undrained shear-strength profile for Site 643.

(Fig. 27). (See Chapter 3, this volume.) When the vessel slowed to 5 kt, about 8 mi from the site location, the record quality imprcved considerably, and both basement and two intra-sedimentary reflectors became easily discernible (Fig. 28). An apparent mismatch between the ship's navigation and that of profile NH-1 caused us to arrive at the preferred geological location earlier than anticipated. The beacon was dropped soon thereafter at about sp. 9435 over a somewhat thinner, but stratigraphically similar, sedimentary section (Fig. 29).

The seismic section consists of two distinct sedimentary sequences resting on a strongly reflecting, irregular basement horizon. The basement can be correlated with typical oceanic basement of the seafloor-spreading type farther west in profile NH-1 (Skogseid, 1983). The two main sedimentary units are separated by a prominent unconformable reflector that is the continuation of the base-Miocene, or near base-Miocene, marker at Site 642, earlier identified as reflector A (Fig. 29). The upper unit exhibits poor seismic continuity, except for an irregular interface just below the seafloor. The lack of structuring may indicate local mass movements. The lower unit shows some layering and reflectors at 4.3 and 4.45 s (denoted *A′* and *X* in Fig. 29). This layering appears to be the continuation of horizons that are better developed in the basement depression to the east of Site 643.

There is a particularly good correlation between the seismic record (note that the seismic polarity is negative) and some of

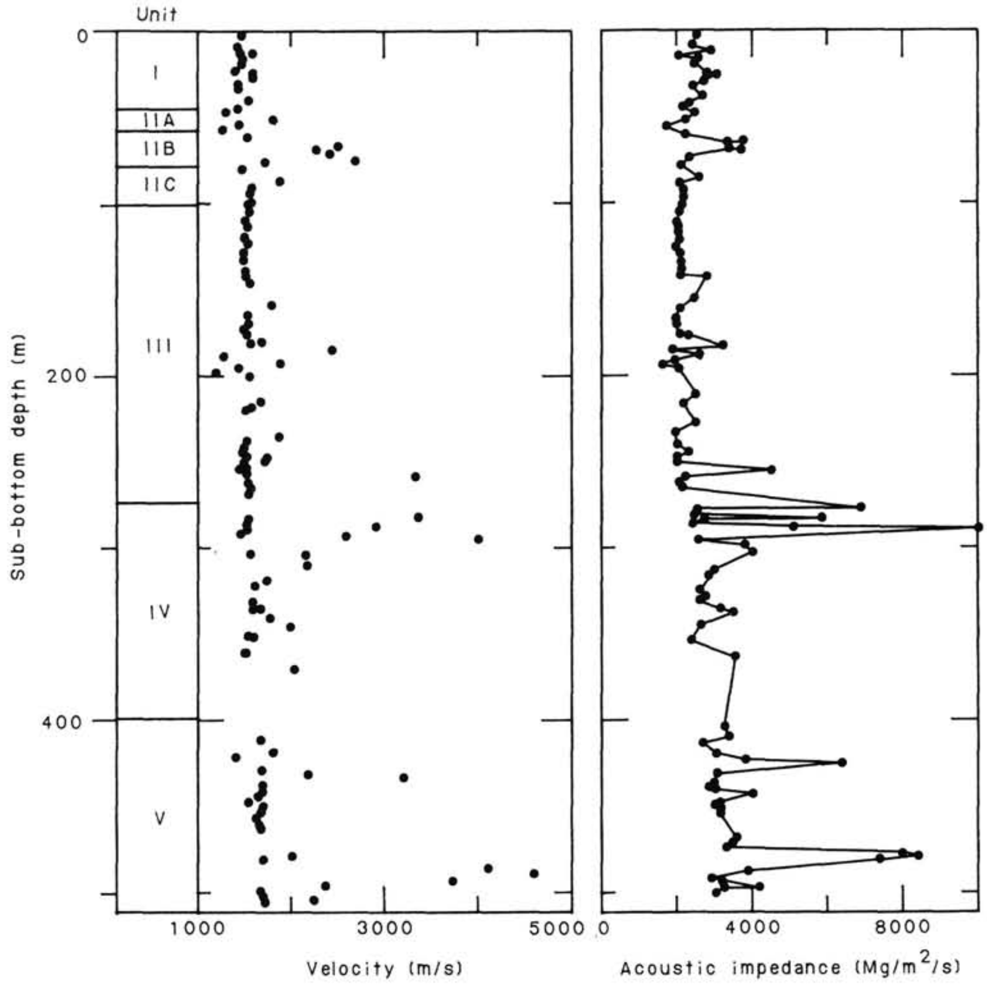

Figure 25. Profiles of compressional-wave velocity and acoustic impedance at Site 643.

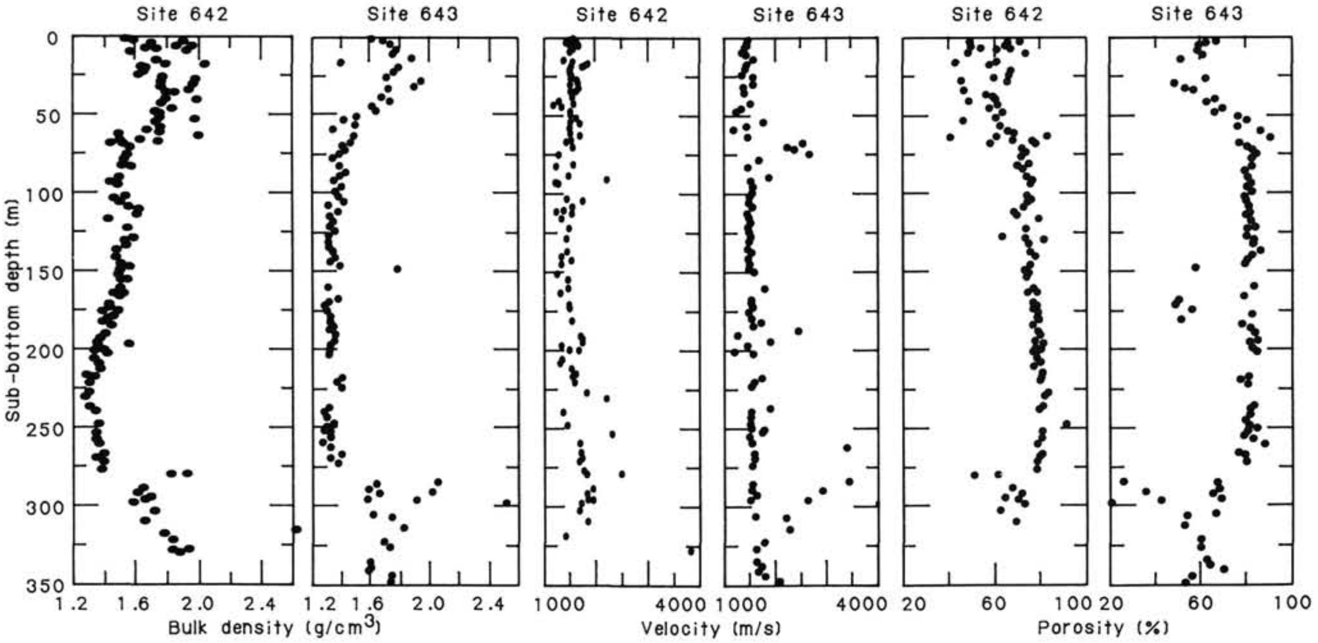

Figure 26. Correlation of physical properties (bulk density, compressional-wave velocity, and porosity) between Sites 642 and 643.

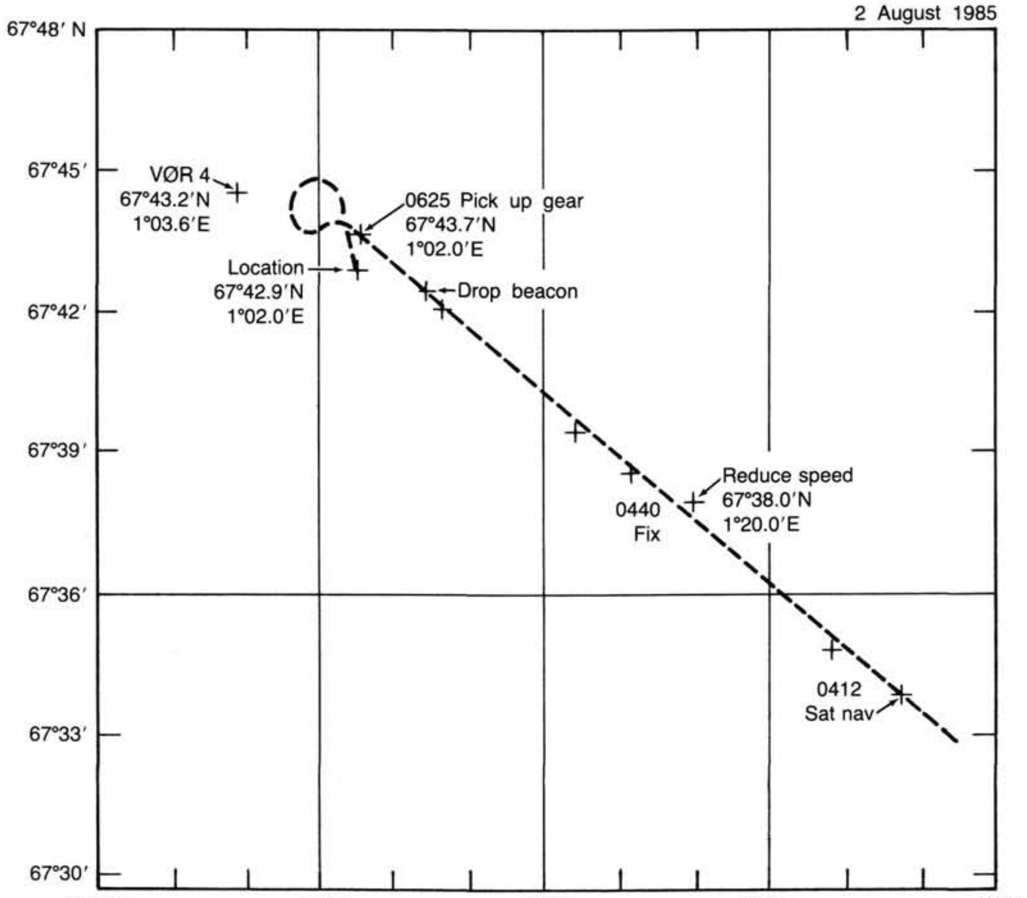

Figure 27. Track chart showing Site 643 and the approach to that site.

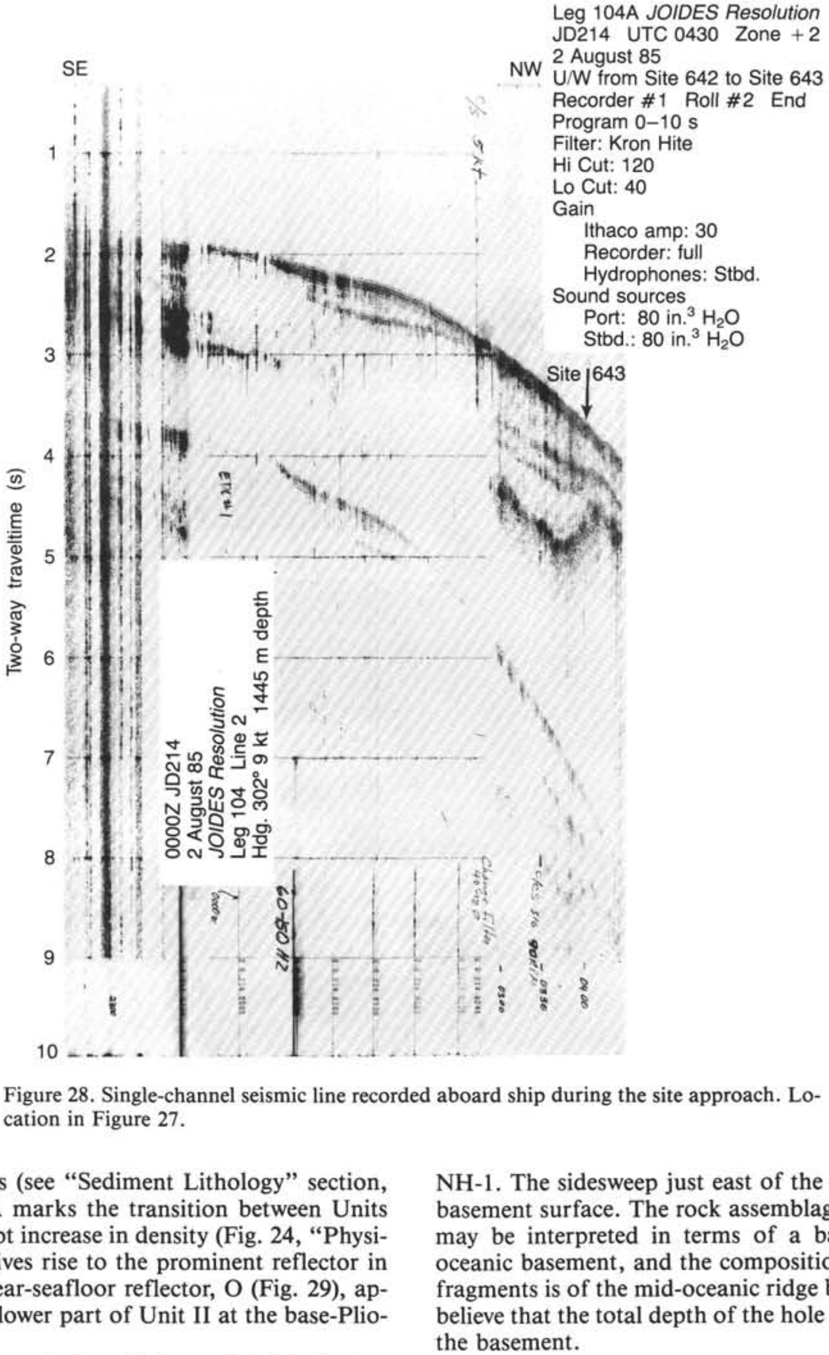

Figure 28. Single-channel seismic line recorded aboard ship during the site approach. Location in Figure 27.

the main lithological units (see "Sediment Lithology" section, this chapter). Reflector A marks the transition between Units III and IV, where an abrupt increase in density (Fig. 24, "Physical Properties" section) gives rise to the prominent reflector in the seismic record. The near-seafloor reflector, O (Fig. 29), appears to be located in the lower part of Unit II at the base-Pliocene.

Reflectors A′ and X (described earlier) are related to the top and base of the extensively laminated and compacted mudstones and zeolitic claystones belonging to Unit V. Again, we observed an increase in the density with respect to the overlying sediments at 410 mbsf. We believe that the base reflector originates from the increasing amount of ashes, reworked pyroclastics, and compacted pumicestones observed at the very base of Unit V ("Sediment Lithology" section, this chapter).

The reflector levels give interval velocities of 1.57 and 1.67 km/s above and below A, respectively. These values correspond well with those measured in the cored material (Fig. 25).

Biostratigraphically ("Biostratigraphy" section, this chapter), the seismic unit below A is dated as earliest Miocene to middle Eocene age (Fig. 29). The profile suggests that reflector A′ (mid-Oligocene) is truncated by reflector A just seaward of Site 643.

According to Figure 29, Hole 643A did not reach the basement reflector; however, the site is located somewhat off profile NH-1. The sidesweep just east of the site indicates an irregular basement surface. The rock assemblages at the base of the hole may be interpreted in terms of a basal sequence resting on oceanic basement, and the composition of the recovered basalt fragments is of the mid-oceanic ridge basalt type. Therefore, we believe that the total depth of the hole is located at or just above the basement.

PETROLOGY

Igneous rocks were recovered at the base of Hole 643A beginning in Section 104-643A-60X, CC. Much of the material recovered in the tops of the last two cores (104-643A-61X and 104-643A-62X) was drilling rubble (Section 104-643A-61X-1, to 80 cm; Section 104-643A-62X-1, to 135 cm). We, therefore, interpret the volcaniclastic rocks in the interval 104-643A-60X, CC (560 mbsf) to total depth (565 mbsf) as being a more or less continuous section (Fig. 30). The problems with the hole that caused the large amount of fill, however, also resulted in poor recovery of the interval.

Description

In Section 104-643A-60X, CC three pieces of rock with chilled margins and preserved contacts with baked sediments were recovered. Macroscopically, the rocks are moderately plagioclase-

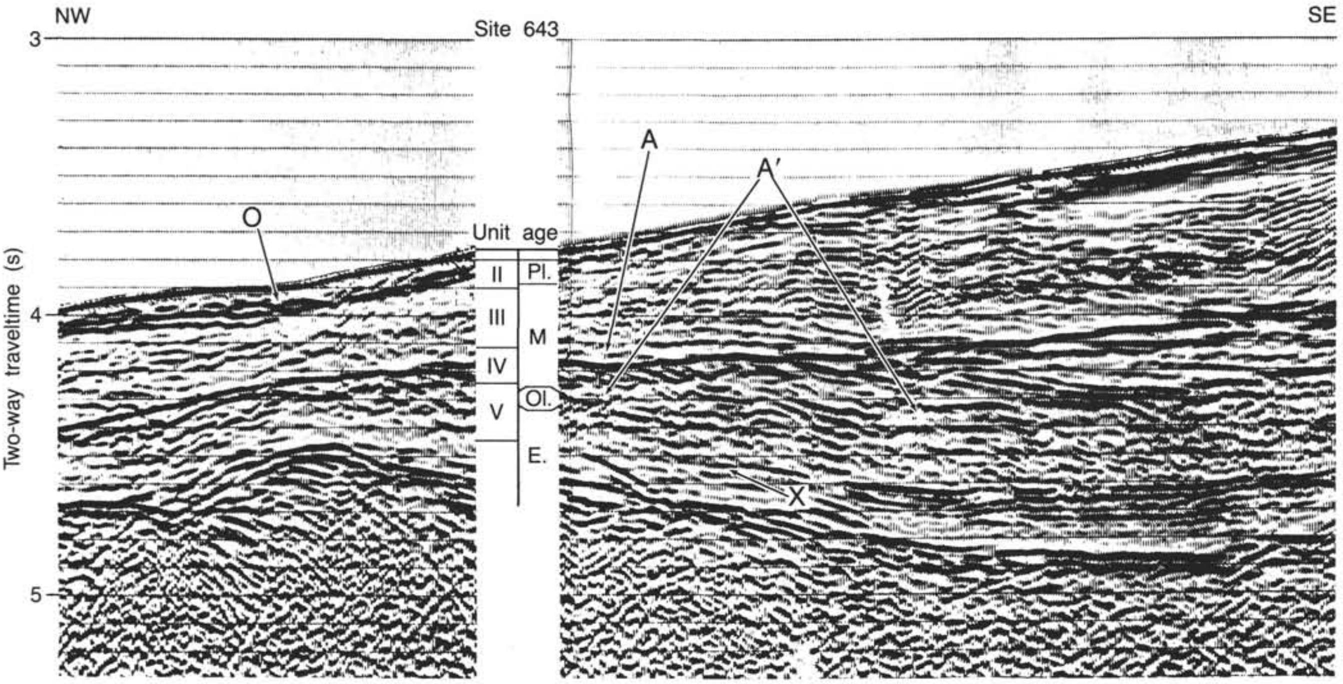

Figure 29. Seismic line NH-1 in the vicinity of Site 643. Lithology and ages from "Sedimentary Lithology" and "Biostratigraphy" sections, respectively, this chapter.

pyroxene phyric and apparently aphanitic. In thin section, however, the groundmass is seen to be virtually completely altered, with suggestions of spherulitic devitrification textures preserved in the alteration mineral fabric. Partially preserved plagioclase needles have the swallowtail morphology typical of quenched magmas. The elongated plagioclase needles, which have length-to-breadth ratios of 50 or more, are locally weakly to strongly subhorizontally oriented.

The next approximately *in-situ* recovery begins at Sample 643A-61X-1, 80 cm, with rubble and unoriented pieces of an altered glassy pillow rind and a glassy flow base. The altered glass has a well-developed, spherulitic devitrification texture. The contact of the glass with the underlying quenched flow is sharp, and small pieces of the underlying flow are entrained in the glass. Below these flows, a conglomerate containing rounded clasts of oxidized basalt was recovered. The conglomerate continues in the next Section (104-643A-61X, CC) where we found a few pieces of nonvesicular, plagioclase-pyroxene phyric rock with chilled margins and baked sediments at their rims. These pieces, which are macroscopically similar to the pieces described earlier from Section 104-643A-60X, CC may be either angular clasts within the conglomerate or have intruded the conglomerate. The sediment itself contains rounded to angular, pebble- to boulder(?)-sized clasts, mostly of volcanic rock in a very dark-green to black smectite matrix. The altered groundmass is veined by calcite that locally forms dogtooth spar several millimeters long.

Section 104-643A-62X-1 is entirely filled with drilling rubble. The sequence continues in Section 104-643A-62X-2 with a sandstone containing clasts of volcanic debris that overlies yet another conglomeratic unit. The conglomerate contains rounded to angular clasts of volcanic and sedimentary rocks, including a zeolitic mudstone similar to lithologies found higher in the section at Site 643. Basaltic pebbles in this conglomerate are coarse-grained, nonvesicular, plagioclase-pyroxene phyric rocks with subophitic texture and containing phenocrysts of plagioclase >1.0 mm and of pyroxene up to 3.5 mm.

Discussion

Because of the poor condition of the recovered interval, relationships among lithologies are uncertain. We cannot with certainty determine whether the quenched dikes of Sections 104-643A-60X, CC and 104-643A-61X, CC are clasts within the immature conglomerate or intruded the sediment. The pillow lava and underlying quenched flow in Section 104-643A-61X-1, however, probably represent *in-situ* flows. Shore-based major- and trace-element analyses (Table 15) of the two flows indicate N-MORB compositions. Compared with Site 642 Upper Series basalts, these are depleted in high field-strength elements.

The conglomeratic sediments below the flows contain pieces that are either pebbles and cobbles of dikes or other intrusions. The lowermost recovery of conglomerate, however, contains coarse-grained mafic rocks that are unambiguously pebbles. Drilling recovered a similar immature conglomerate containing volcanic and minor nonvolcanic clasts at DSDP Site 343. A correlation with the Site 343 conglomerate, which occurs just above basement, suggests that the basaltic conglomerate at Site 643 represents the transition to the volcanic sequence.

REFERENCES

Baldauf, J. G., 1984. Cenozoic diatom biostratigraphy and paleoceanography of the Rockall Plateau Region, North Atlantic, Deep Sea Drilling Project Leg 81. *In* Roberts, D. G., Schnitker, D., et al., *Init. Repts. DSDP*, 81: Washington (U.S. Govt. Printing Office), 439–478.

Barron, J. A., 1985. Miocene to Holocene planktic diatom biostratigraphy. *In* Bolli, H. M., Saunders, J. B., and Perch-Nielsen, K. (Eds.), *Plankton Stratigraphy*: Cambridge (Cambridge University Press), 763–809.

Bennett, R. H., and Nelsen, T. A., 1983. Seafloor characteristics and dynamics affecting geotechnical properties at shelf break. *SEPM Spec. Publ.*, 33:333–355.

Berggren, W. A., 1972. Cenozoic biostratigraphy and paleobiogeography of the North Atlantic. *In* Laughton, A. S., Berggren, W. A., et al., *Init. Repts. DSDP*, 12: Washington (U.S. Govt. Printing Office), 965-1001.

________, 1977. North Atlantic Cenozoic Foraminifera. *In* Swain, F. M. (Ed.), *Stratigraphic Micropaleontology of Atlantic Basins and Borderlands*: Amsterdam (Elsevier), 389-410.

Berggren, W. A., Kent, D. V., and Flynn, J. J., 1985. Paleogene geochronology and chronostratigraphy. *In* Snelling, N. J. (Ed.), *Geochronology and the Geological Record*: Geol. Soc. London, Spec. Paper, 141-195.

Bjørklund, K. R., 1976. Radiolaria from the Norwegian Sea, Leg 38 of the Deep Sea Drilling Project. *In* Talwani, M., Udintsev, G., et al., *Init. Repts. DSDP*, 38: Washington (U.S. Govt. Printing Office), 1101-1168.

Blow, W. H., 1969. Late middle Eocene to Recent planktonic foraminiferal biostratigraphy. *In* Brönnimann, P., and Renz, H. H. (Eds.), *Proc. First Int. Conf. Plankt. Microf.* (Geneva, 1967), 1:199-421.

________, 1979. *The Cainozoic Foraminiferida*, Vols. I and II: Leiden (E. J. Brill).

Caston, V. N. D., 1976. Tertiary sediments of the Vøring Plateau, Norwegian Sea, recovered by Leg 38 of the Deep Sea Drilling Project. *In* Talwani, M., Udintsev, G., et al., *Init. Repts. DSDP*, 38: Washington (U.S. Govt. Printing Office), 761-782.

Edwards, L. E., 1984. Miocene dinocysts from Deep Sea Drilling Project Leg 81, Rockall Plateau, eastern North Atlantic Ocean. *In* Roberts, D. G., Schnitker, D., et al., *Init. Repts. DSDP*, 81: Washington (U.S. Govt. Printing Office), 581-594.

Gieskes, J., Lawrence, J., and Galleisky, G,., 1978. Interstitial water studies, Leg 38. *In* Talwani, M., Udintsev, G., et al., *Init. Repts. DSDP*, Suppl. to Vols. 38, 39, 40, and 41: Washington (U.S. Govt. Printing Office), 121-133.

Hagevang, T., Eldholm, O., and Aalstad, I., 1983. Pre-23 magnetic anomalies between Jan Mayen and Greenland-Senja fracture zones in the Norwegian Sea. *Mar. Geophys. Res.*, 5: 345-363.

Hamilton, E. L., 1974. Prediction of deep sea sediment properties: state of the art. *In* Inderbitzen, A. L. (Ed.), *Deep Sea Sediments, Physical and Mechanical Properties*: New York (Plenum Press), 1-42.

Harland, W. B., Cox, A. V., Llewellyn, P. G., Pickton, C. A. G., Smith, A. G., and Walters, R., 1982. *A Geologic Time Scale*: Cambridge (Cambridge University Press).

King, C., 1983. Cainozoic micropaleontological biostratigraphy of the North Sea. *Rept. Inst. Geol. Sci. London.*, 82(7):1-40.

Manum, S. B., 1976. Dinocysts in Tertiary Norwegian-Greenland Sea sediments (Deep Sea Drilling Project Leg 38), with observations on palynomorphs and palynodebris in relation to environment. *In* Talwani, M., Udintsev, G., et al., *Init. Repts. DSDP*, 38: Washington (U.S. Govt. Printing Office), 897-919.

Martini, E., 1971a. Silicoflagellate zones in the late Oligocene and early Miocene of Europe. *Senckenbergiana Lethaea*, 53:119-122.

________, 1971b. Standard Tertiary and Quaternary calcareous nannoplankton zonation: *Proc. Second Plankt. Conf.*, Rome, 1970, 2: 739-785.

________, 1979. Calcareous nannoplankton and silicoflagellate biostratigraphy at Reykjanes Ridge, northeastern North Atlantic (DSDP Leg 49, Sites 407 and 409). *In* Luyendyk, B. P., Cann, J. R., et al., *Init. Repts. DSDP*, 49: Washington (U.S. Govt. Printing Office), 533-549.

Martini, E., and Müller, C., 1976. Eocene to Pleistocene silicoflagellates from the Norwegian-Greenland Sea (DSDP Leg 38). *In* Talwani, M., Udintsev, G., et al., *Init. Repts. DSDP*, 38: Washington (U.S. Govt. Printing Office), 857-895.

Mudie, P. J., 1987. Palynology and dinoflagellate biostratigraphy of Deep Sea Drilling Project Leg 94, Sites 607 and 611, North Atlantic Ocean. *In* Ruddiman, W. F., Kidd, R. B., Thomas, E., et al., *Init. Repts. DSDP*, 94: Washington (U.S. Govt. Printing Office), 785-812.

Müller, C., 1976. Tertiary and Quaternary calcareous nannoplankton in the Norwegian-Greenland Sea, DSDP Leg 38. *In* Talwani, M., Udintsev, G., et al., *Init. Repts. DSDP*, 38: Washington (U.S. Govt. Printing Office), 823-841.

Murray, J. W., 1979. Cenozoic biostratigraphy and paleoecology of Sites 403 to 406 based on the foraminifers. *In* Montadert, L., Roberts, D. G., et al., *Init. Repts. DSDP*, 48: Washington (U.S. Govt. Printing Office), 415-430.

Schnitker, D., 1979. Cenozoic deep water benthic foraminifers, Bay of Biscay. *In* Montadert, L., Roberts, D. G., et al., *Init. Repts. DSDP*, 48: Washington (U.S. Govt. Printing Office), 377-414.

Schrader, H. J., and Fenner, J., 1976. Norwegian Sea Cenozoic diatom biostratigraphy and taxonomy. *In* Talwani, M., Udintsev, G., et al., *Init. Repts. DSDP*, 38: Washington (U.S. Govt. Printing Office), 921-1099.

Skogseid, J., 1983. A marine geophysical study of profiles between the Vøring Plateau Margin and the Jan Mayen Ridge [Cand. Sci. thesis]. University of Oslo, Oslo.

Stainforth, R. M., Lamb, J. L., Luterbacher, H., Beard, J. H., and Jeffords, R. M., 1975. *Cenozoic Planktonic Foraminiferal Zonation and Characteristics of Index Forms.* Univ. Kansas Paleontol. Contrib. Art., 62.

Streeter, S. S., Belanger, P. E., Kellogg, T. B., and Duplessy, J. C., 1982. Late Pleistocene oceanography of the Norwegian-Greenland Sea: benthic foraminiferal evidence. *Quat. Res.*, 18:72-90.

Talwani, M., and Eldholm, O., 1977. Evolution of the Norwegian-Greenland Sea. *Geol. Soc. Am. Bull.*, 88:969-999.

Talwani, M., Udintsev, G., et al., 1976a. *Init. Repts. DSDP*, 38: Washington (U.S. Govt. Printing Office).

________, 1976b. Sites 338-343. *In* Talwani, M., Udintsev, G., et al., *Init. Repts. DSDP*, 38: Washington (U.S. Govt. Printing Office), 151-388.

Tauxe, L., Tucker, P., Petersen, N. P., and LaBrecque, J. L., 1984. Magnetostratigraphy of Leg 73 sediments. *In* Hsü,, K. J., LaBrecque, J. L., et al., *Init. Repts. DSDP*, 73: Washington (U.S. Govt. Printing Office), 609-622.

Thiede, J., 1980. Palaeo-oceanography, margin stratigraphy and palaeophysiography of the Tertiary North Atlantic and Norwegian-Greenland Seas. *Phil. Trans. Royal Soc. London*, (A) 294:177-185.

Tissot, B. P., and Welte, D. H., 1984. *Petroleum Formation and Occurrence* (2nd ed.): Berlin (Springer-Verlag).

Williams, G. L., and Bujak, J. P., 1977. Cenozoic palynostratigraphy of offshore eastern Canada. *Am. Assoc. Stratigraphic Palynologists, Contrib. Ser.* 5A, 14-47.

Table 15. Major- and minor-element analyses of two Site 643 basalt samples.

Element	Range (ppm)	Mean (ppm)
SiO_2	48.40-49.04	48.72
TiO_2	1.18-1.23	1.21
N_2O_3	17.65-18.10	17.88
*FeO	9.54-10.58	10.06
MnO	0.19-0.21	0.20
MgO	7.76-8.13	7.95
CaO	7.50-7.90	7.70
Na_2O	3.07-3.09	3.08
K_2O	0.30-0.38	0.34
P_2O_5	0.16-0.21	0.19
Element	**Range (ppm)**	**Mean (ppm)**
V	422-450	436
Cr	275-317	296
Co	44-65	55
Ni	62-93	78
Cu	148-149	149
Zn	117-135	126
Rb	3-6	5
Sr	124-129	127
Y	29-34	32
Zr	59-65	62
Nb	3-4	4
Sc	59-60	60

*All Fe calculated as FeO. Data from University of Newcastle upon Tyne, United Kingdom, and Midland Earth Science Associates, United Kingdom.

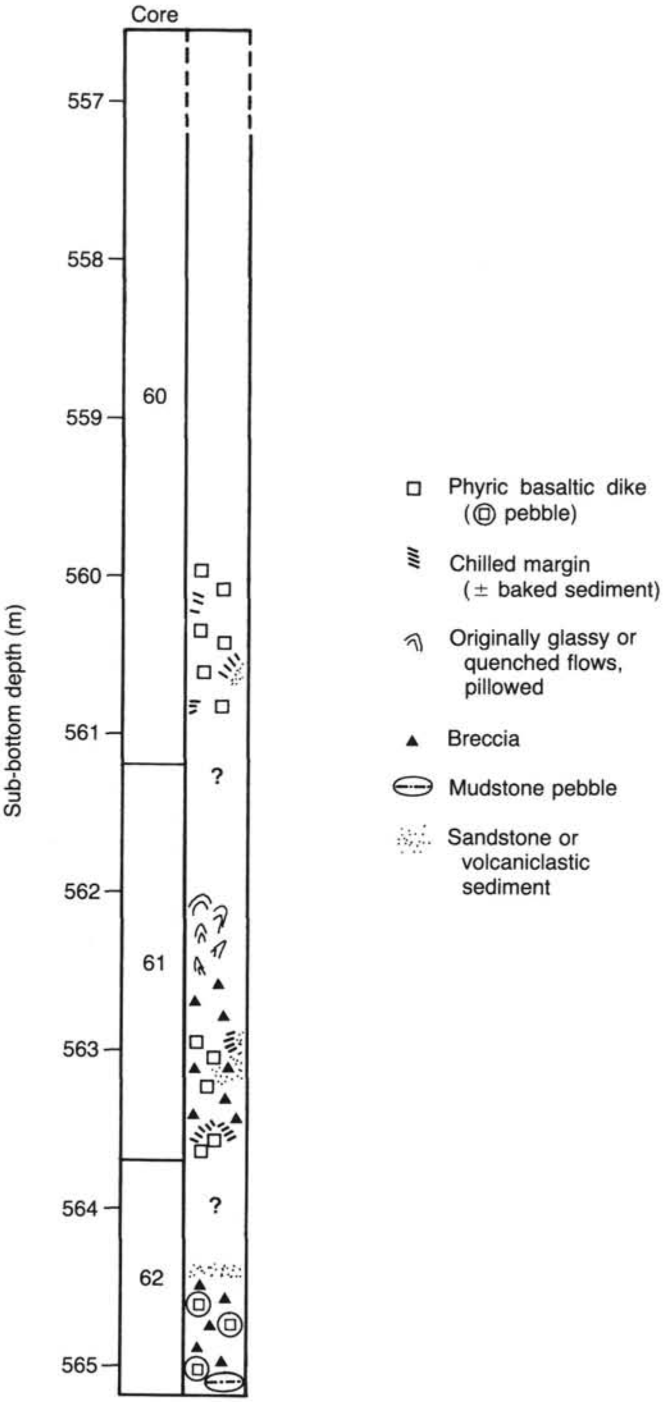

Figure 30. Diagrammatic representation of the lithologies at the base of Hole 643A. Lithologies are placed at their recovered intervals.

SITE 643 HOLE A CORE 1H CORED INTERVAL 2779.8-2785.1 mbsl; 0.0-5.3 mbsf

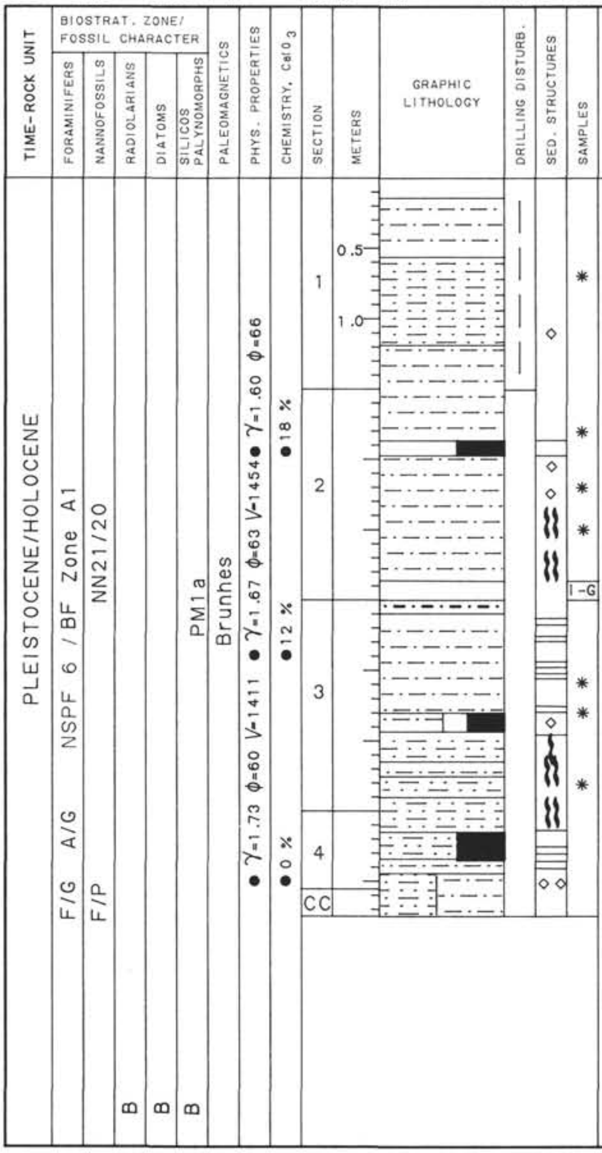

LITHOLOGIC DESCRIPTION

GLACIAL AND INTERGLACIAL FORAMINIFERAL MUDS AND SANDY MUDS

Entire core is undeformed.

Major lithologies:
a. Mud, brown to dark grayish brown (10YR 4/2). Section 1, 14–136 and 139–150 cm; Section 2, 0–14 cm. [IG]
b. Foraminiferal sandy mud, dark grayish brown (10YR 4/2), moderately bioturbated (tubes of 2 mm diameter) with scattered dropstones. Section 2, 44–150 cm; Section 3, 93–114, 123–131, and 138–150 cm; Section 4, 0–14 and 33–46 cm; CC, 0–3 and 5–12 cm. [G]

Minor lithologies:
a. Mud and sandy mud, grading from basal, laminated, very dark gray (5Y 3/1) mud upward into dark olive gray (5Y 3/2) bioturbated sandy mud with abundant dropstones. Section 2, 14–44 cm; Section 3, 70–93 cm; Section 4, 14–33 cm; CC, 12–18 cm. [G]
b. Foraminiferal sandy mud, dark olive gray (5Y 3/2), mottled and extensively bioturbated, with numerous dropstones. Section 3, 114–123 and 131–138 cm; CC, 3–5 cm. [G]
c. Foraminiferal sand, brown to dark grayish brown (10YR 4/2), with numerous large benthic foraminifers (*Pyrgo*). Section 1, 0–14 and 136–139 cm. [IG]
d. Foraminiferal sand (*Pyrgo*), dark grayish brown (10YR 4/2), with numerous, several mm sized granitic and basaltic pebbles. Section 3, 8–11 cm. [IG]

Large dropstones at Section 2, 65 and 75 cm; Section 3, 85 cm; Section 4, 44 cm.

SMEAR SLIDE SUMMARY (%):

	1, 67 D	2, 31 M	2, 71 D	2, 99 D	3, 54 D	3, 78 M	3, 128 D
TEXTURE:							
Sand	5	15	50	50	10	30	5
Silt	40	20	20	10	30	30	25
Clay	55	65	30	40	60	40	70
COMPOSITION:							
Quartz	15	10	40	20	25	30	10
Feldspar	5	2	5	5	5	—	2
Clay	58	60	25	35	44	40	69
Volcanic glass	1	—	—	—	—	—	—
Calcite/dolomite	20	2	—	5	20	—	10
Accessory minerals	1	1	—	—	1	—	1
Glauconite	—	Tr	—	—	—	—	Tr
Goethite	—	—	—	—	—	30	—
Foraminifers	—	—	20	30	—	—	5
Nannofossils	—	—	10	5	5	—	3

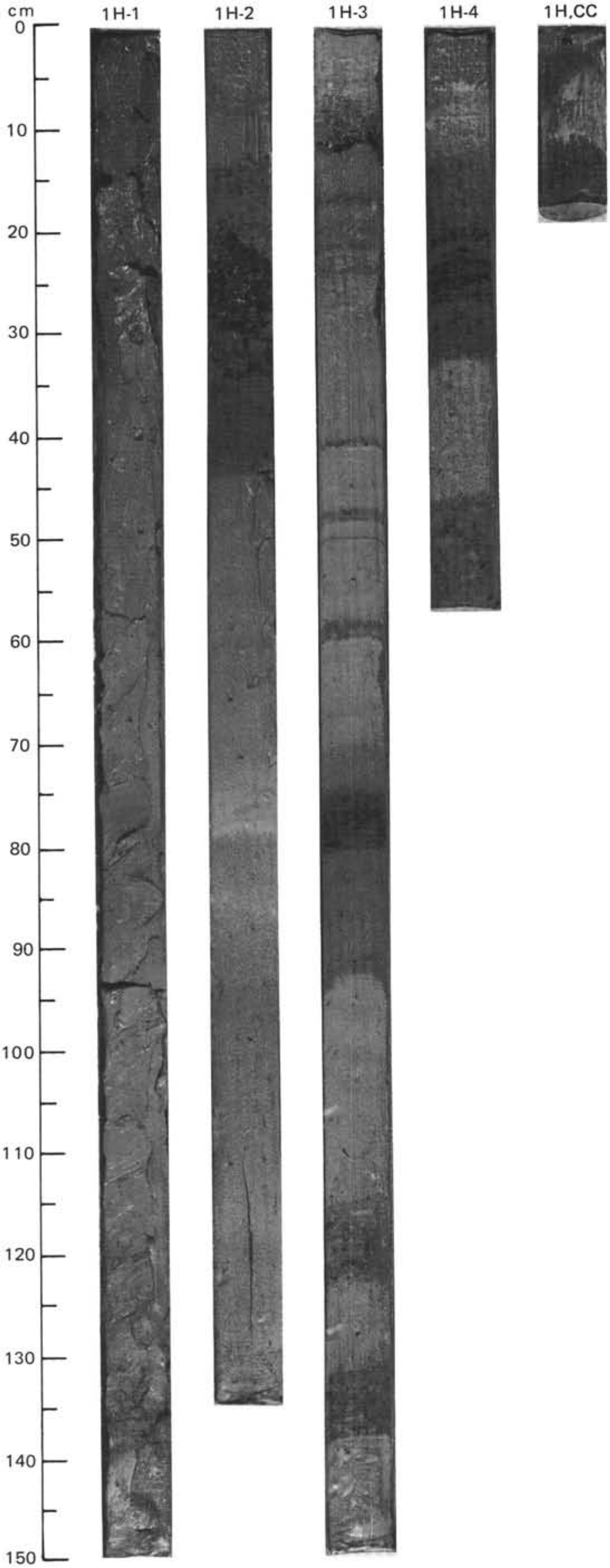
cm
0
10
20
30
40
50
60
70
80
90
100
110
120
130
140
150
1H-1
1H-2
1H-3
1H-4
1H,CC

SITE 643 HOLE A CORE 2H CORED INTERVAL 2785.1-2794.6 mbsl; 5.3-14.8 mbsf

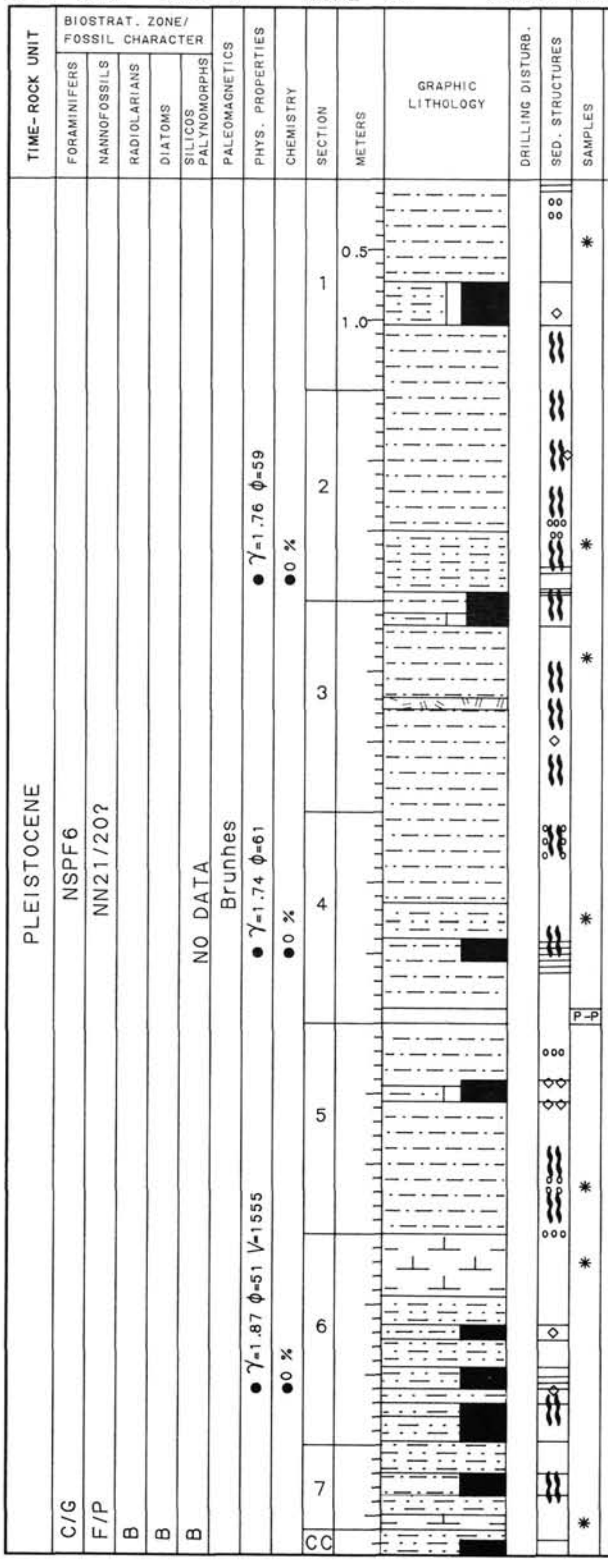

LITHOLOGIC DESCRIPTION

GLACIAL AND INTERGLACIAL FORAMINIFERAL MUDS AND SANDY MUDS

CC moderately disturbed. Remainder of the core undisturbed.

Major lithologies:

a. Foraminiferal sandy mud, olive gray (5Y 4/2), dark gray (5Y 4/1), and dark grayish brown (2.5Y 4/2), extensively bioturbated (tubes of 2 mm diameter). Some layers especially rich in foraminifers. Section 1, 5–71 and 104–150 cm; Section 2, 0–101 cm; Section 3, 14–150 cm; Section 4, 0–63 cm; Section 5, 0–26, 28–38, 55–62, 68–100, 102–113, and 118–139 cm; Section 6, 44–66 and 72–95 cm. [G]

b. Mud and sandy mud, dark gray (5Y 4/1), with a few scattered dropstones. Section 6, 110–112 and 147–150 cm; Section 7, 0–19 and 33–50 cm. [G]

c. Mud, dark brown (10YR 3/3), extensively bioturbated. Section 2, 101–144 cm, with dark olive gray (5Y 3/2) color bands at 120 and 135 cm. [IG]

Minor lithologies:

a. Mud and sandy mud, grading from a basal, laminated, very dark gray (5Y 3/1) mud upward into bioturbated, dark olive gray (5Y 3/2) sandy mud. Dropstones abundant throughout. Section 1, 71–104 cm; Section 2, 143 cm, to Section 3, 14 cm; Section 4, 88–104 cm; Section 5, 26–28 and 38–55 cm; Section 6, 95–110 and 120–147 cm; Section 7, 19–33 cm; CC, 10–22 cm. [G]

b. Foraminiferal sandy mud, dark olive gray (5Y 3/2), mottled and extensively bioturbated with scattered dropstones. Section 5, 62–68 cm; Section 6, 66–72 cm. [G]

c. Foraminiferal nannofossil ooze, olive gray (5Y 5/2) with a minor color banding. Section 6, 0–66 cm; Section 7, 50–57 cm.

d. Volcanic ash, very dark gray (5Y 3/1). Section 3, 72–74.5 cm.

SMEAR SLIDE SUMMARY (%):

	1, 48	2, 118	3, 38	4, 75	5, 114	6, 19	7, 52
	D	D	D	D	M	M	M
TEXTURE:							
Sand	15	5	15	5	25	—	5
Silt	35	25	15	20	15	20	15
Clay	50	70	70	75	60	80	80
COMPOSITION:							
Quartz	20	15	5	20	3	5	2
Feldspar	5	3	1	1	—	—	—
Clay	46	70	72	76	62	10	17
Volcanic glass	—	1	—	—	—	—	—
Calcite/dolomite	15	5	2	2	—	—	—
Accessory minerals	1	1	—	1	—	—	1
Glauconite	—	—	Tr	—	—	—	—
Foraminifers	—	—	15	—	30	15	10
Nannofossils	—	—	5	—	5	70	70

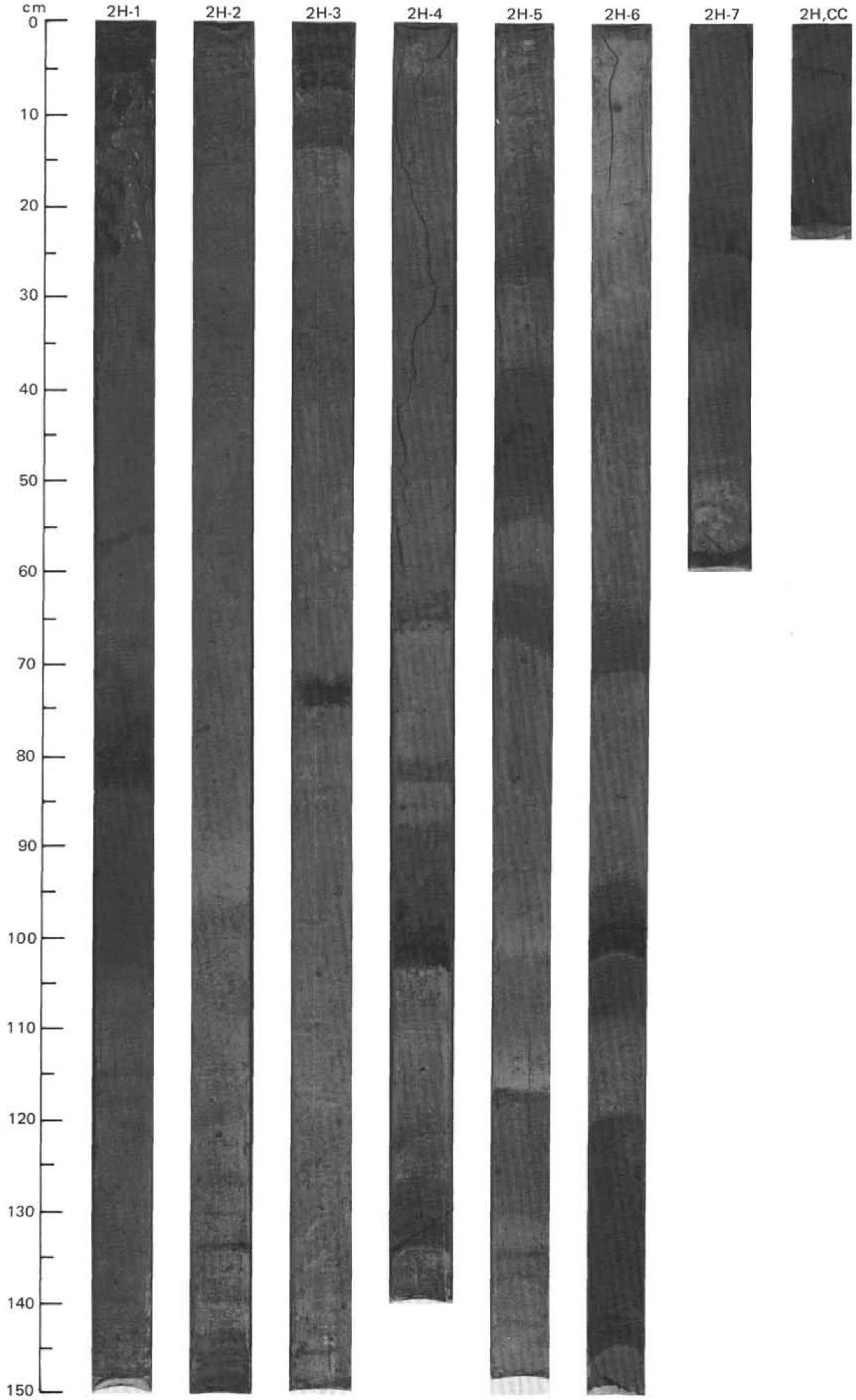
cm
0
10
20
30
40
50
60
70
80
90
100
110
120
130
140
150
2H-1
2H-2
2H-3
2H-4
2H-5
2H-6
2H-7
2H,CC

SITE 643 HOLE A CORE 3H CORED INTERVAL 2794.6-2804.1 mbsl; 14.8-24.3 mbsf

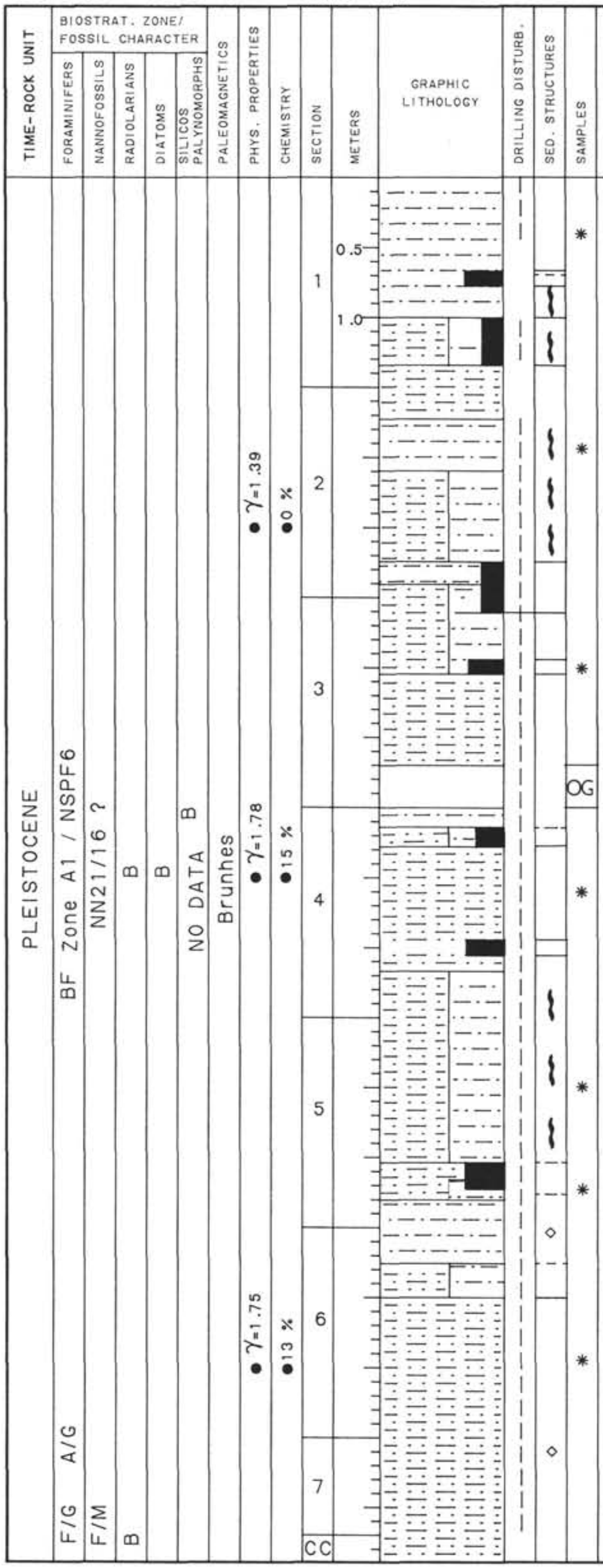

LITHOLOGIC DESCRIPTION

GLACIAL AND INTERGLACIAL FORAMINIFERAL MUDS AND SANDY MUDS

Moderate disturbance in Sections 2 and 3. Slight disturbance in Section 1, 0–23 and 130–140 cm, and in the remainder of the core.

Major lithologies:
a. Foraminiferal mud and sandy mud, olive gray (5Y 4/2), gray (5Y 5/1), and dark gray (5Y 4/1). Slightly to moderately bioturbated and mottled, with scattered dropstones. Section 2, 23–126 cm; Section 4, 111 cm, to Section 5, 101 cm; Section 6, 25–45 cm.
b. Mud, grayish brown (2.5Y 5/2) to dark grayish brown (2.5Y 4/2), moderately to intensely bioturbated and mottled, with dropstones common. Section 4, 0–14, 28–99, and 103–111 cm; Section 5, 125–150 cm; Section 6, 51 cm, to CC.

Minor lithologies:
a. Mud and sandy mud, grading upward from very dark gray (5Y 3/1) at the base to dark olive gray (5Y 3/2) at the top. Generally contain well-defined base, bioturbated, gradational top, and abundant dropstones. Section 1, 69–84 and 101–135 cm; Section 2, 126 cm, to Section 3, 18 cm; Section 3, 45–56 cm; Section 4, 14–28 and 99–103 cm; Section 5, 101–125 cm.
b. Mud and sandy mud, gray (5Y 5/1), olive gray (5Y 4/2), and dark gray (5Y 4/1), slightly to moderately mottled, with rare to common dropstones. Section 1, 0–69, 84–101, and 135–150 cm; Section 2, 0–23 cm; Section 3, 18–45 and 56–150 cm; Section 6, 0–25 and 45–51 cm.

Large dropstones: Section 2, 115 cm; Section 6, 8 and 13 cm; Section 7, 6 cm.

SMEAR SLIDE SUMMARY (%):

	1, 45 D	2, 40 D	3, 49 D	4, 60 D	5, 51 D	5, 122 D	6, 94 D
TEXTURE:							
Sand	40	30	30	5	30	20	5
Silt	30	40	40	55	40	50	50
Clay	30	30	30	40	30	30	45
COMPOSITION:							
Quartz	45	40	60	20	30	60	20
Feldspar	1	—	—	—	—	—	—
Mica	1	—	—	—	—	1	—
Clay	30	30	30	40	30	30	30
Calcite	20	10	5	30	30	5	35
Accessory minerals	3	—	2	—	—	3	—
Pyrite	—	—	3	—	—	1	—
Foraminifers	—	20	—	—	—	—	—
Nannofossils	—	—	—	—	—	—	15

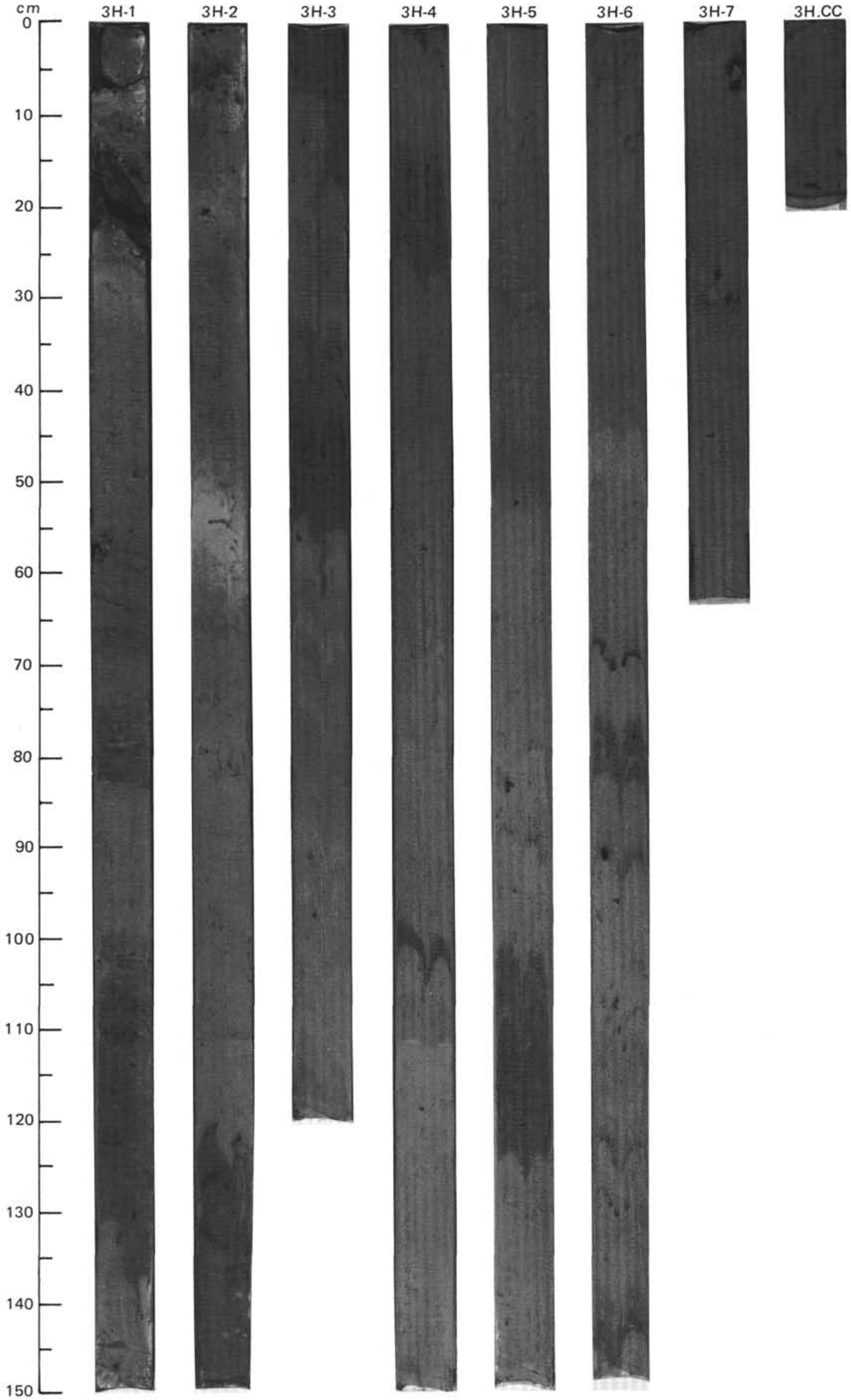
cm
0
10
20
30
40
50
60
70
80
90
100
110
120
130
140
150
3H-1
3H-2
3H-3
3H-4
3H-5
3H-6
3H-7
3H.CC

SITE 643 HOLE A CORE 4H CORED INTERVAL 2804.1-2813.6 mbsl; 24.3-33.8 mbsf

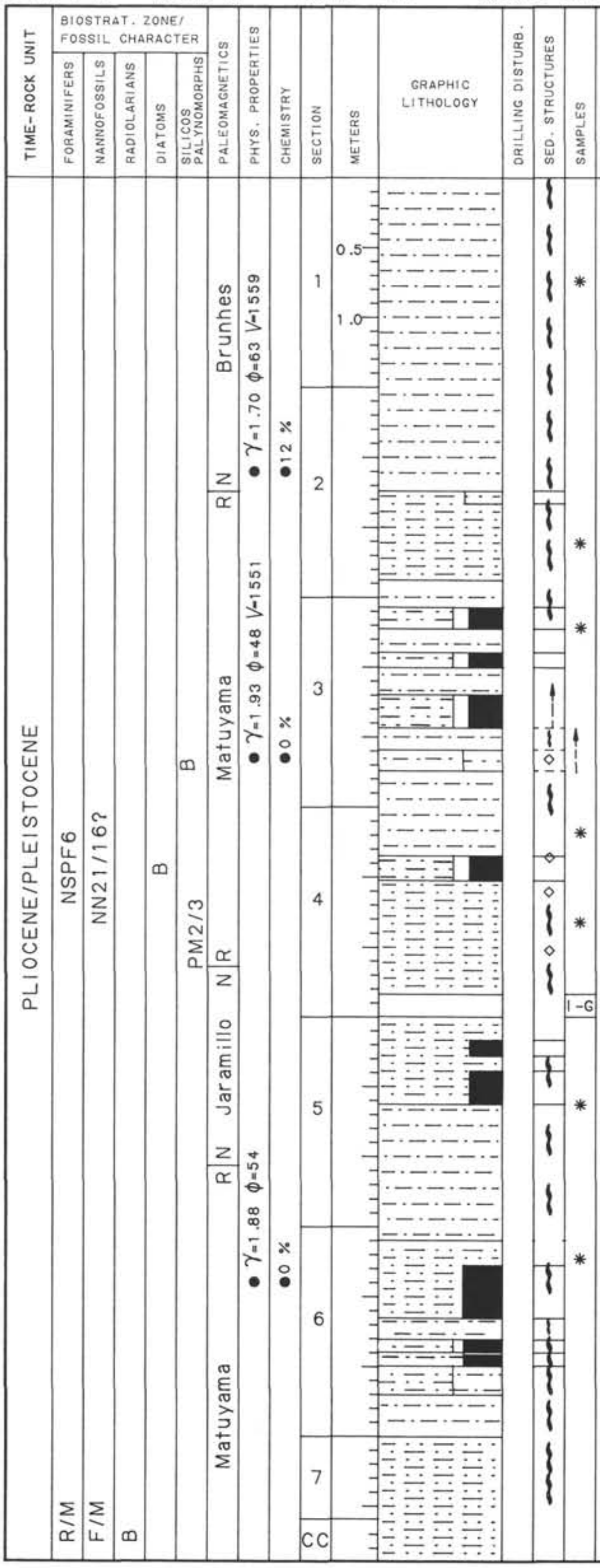

LITHOLOGIC DESCRIPTION

GLACIAL AND INTERGLACIAL MUDS, SANDY MUDS, AND CALCAREOUS MUDS AND SANDY MUDS

Entire core is undisturbed.

Major lithology: Calcareous muds and sandy muds, olive gray (5Y 3/2), olive brown (5Y 4/4), and dark grayish brown (2.5Y 4/2), mildly to moderately bioturbated and mottled, with dropstones rare to common. Section 1 to Section 2, 75 cm; Section 3, 94–108 cm and 126 cm, to Section 4, 15 cm; Section 5, 62 cm, to Section 6, 10 cm; Section 6, 130–150 cm.

Minor lithologies:
a. Muds and sandy muds, grading upward from very dark gray (5Y 3/1), generally at a well-defined base, to dark gray (5Y 4/1) at a bioturbated top. Contain abundant dropstones. Section 2, 75–79 cm; Section 3, 8–20, 46–49, 69–94, and 108–126 cm; Section 4, 35–50 cm; Section 5, 23–30 and 42–62 cm; Section 6, 30–67 cm, 83–85, and 90–93.
b. Mud and sandy mud, very dark gray (5Y 3/1) with scattered dropstones. CC, 0–5, 12–15, and 27–30 cm.

Large dropstones: Section 3, 119, 121, and 126 cm; Section 4, 24, 42, 49, 55, and 95 cm.

SMEAR SLIDE SUMMARY (%):

	1, 75 D	2, 110 D	3, 222 D	4, 15 M	4, 85 D	5, 60 M	6, 23 D
TEXTURE:							
Sand	15	20	40	40	10	30	5
Silt	20	30	30	50	40	50	35
Clay	65	50	30	10	50	20	60
COMPOSITION:							
Quartz	25	30	50	30	50	65	45
Feldspar	—	—	5	—	—	3	—
Mica	—	—	—	—	—	1	—
Clay	10	30	30	10	30	—	40
Volcanic glass	—	—	—	—	—	20	—
Calcite	30	20	5	—	20	—	15
Accessory minerals	—	—	10	2	—	10	—
Foraminifers	—	15	—	55	—	1	—
Nannofossils	—	5	—	3	—	—	—

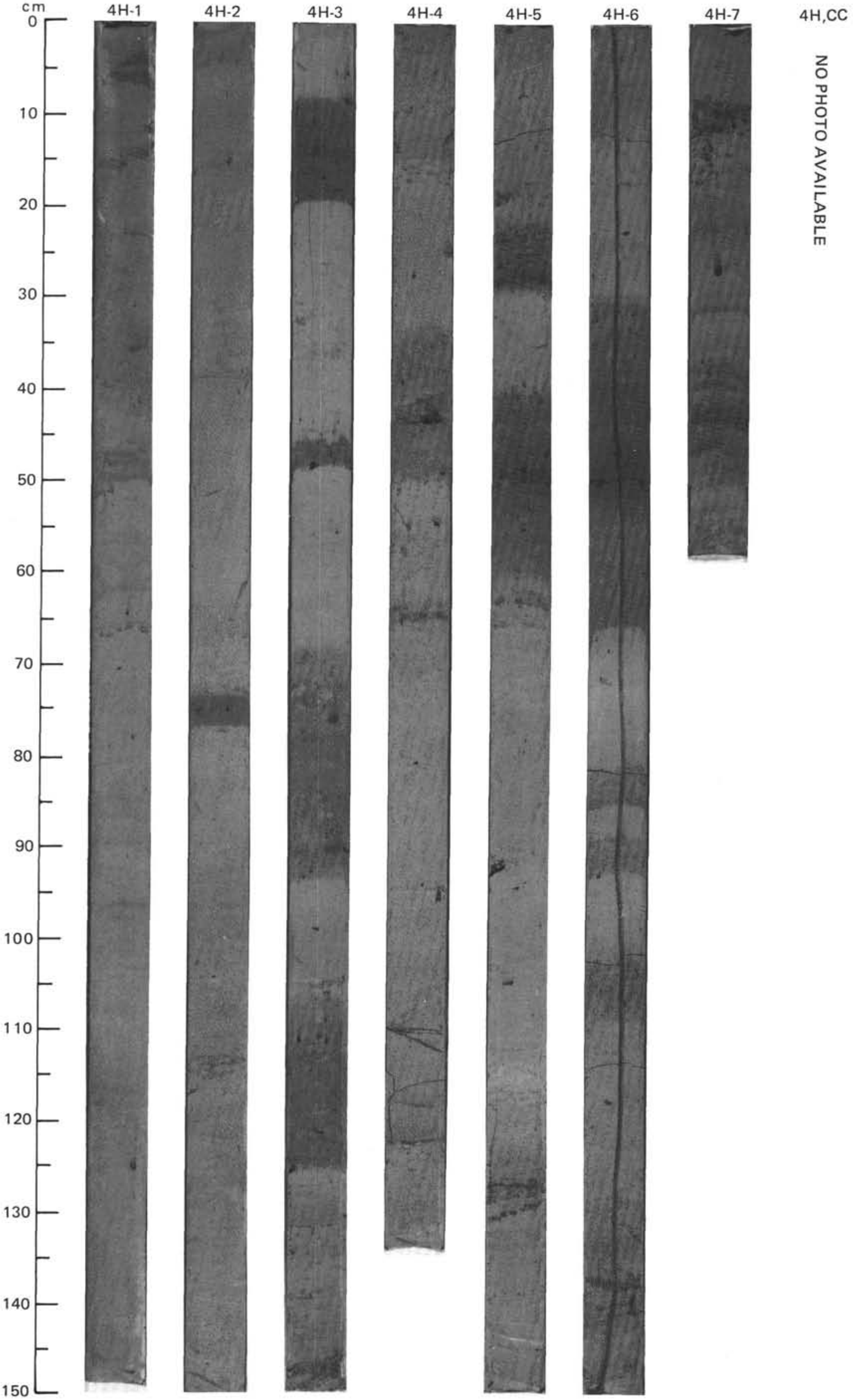
cm
0
10
20
30
40
50
60
70
80
90
100
110
120
130
140
150
4H-1
4H-2
4H-3
4H-4
4H-5
4H-6
4H-7
4H,CC
NO PHOTO AVAILABLE

SITE 643 HOLE A CORE 5H CORED INTERVAL 2813.6-2823.1 mbsl; 33.8-43.3 mbsf

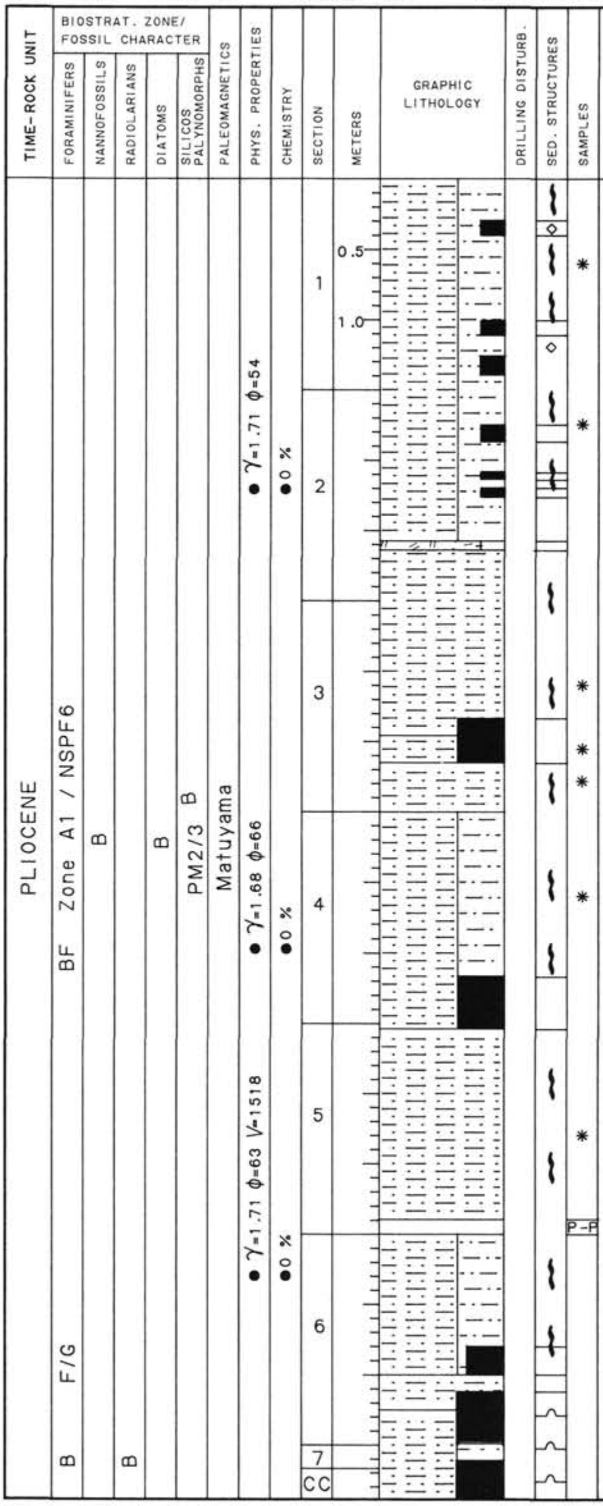

LITHOLOGIC DESCRIPTION

GLACIAL AND INTERGLACIAL MUDS AND SANDY MUDS

Entire core is undisturbed.

Major lithologies:
a. Muds and sandy muds, dark gray (5Y 4/1) and olive gray (5Y 4/2), with abundant dropstones and minor to moderate bioturbation. Section 1, 0–33, 39–100, and 115–127 cm; Section 1, 143 cm, to Section 2, 29 cm; Section 2, 42–107 cm; Section 4, 0–120 cm; Section 6, 0–83 and 137–143 cm; Section 7, 0–14 cm.
b. Muds, dark grayish brown (2.5Y 4/2) to greenish gray (5GY 5/1), with moderate bioturbation and rare to common dropstones. Section 2, 107 cm, to Section 3, 95 cm; Section 3, 115–150 cm; Section 5, 2–150 cm; Section 6, 100–127 cm.

Minor lithologies:
a. Mud and sandy mud, very dark gray (5Y 3/1) with scattered dropstones. Section 1, 33–39 cm; Section 6, 127–137 and 143–150 cm; Section 7, 14 cm, to CC.
b. Sandy mud, dark olive gray (5Y 3/1) with abundant dropstones. Section 1, 100–115 cm; Section 2, 29–42 cm; Section 6, 83–100 cm.
c. Mud and sandy mud, very dark gray (5Y 3/1) and laminated at base, grading to dark olive gray (5Y 3/2) and bioturbated at the top. Section 1, 127–143 cm; Section 3, 85–113 cm; Section 4, 120 cm, to Section 5, 2 cm.
d. Volcanic ash, disseminated. Section 2, 107–114 cm.

Section 6, 135 cm, to CC is a slumped sequence.
Large dropstones: Section 1, 35, 39, and 120 cm.

SMEAR SLIDE SUMMARY (%):

	1, 58 D	2, 23 D	3, 60 D	3, 101 D	3, 135 D	4, 60 D	5, 75 D
TEXTURE:							
Sand	10	30	20	20	10	10	30
Silt	40	40	40	40	50	40	40
Clay	50	30	40	40	40	50	30
COMPOSITION:							
Quartz	40	60	60	50	50	50	60
Clay	50	30	40	40	40	50	30
Calcite/dolomite	—	—	—	—	5	—	—
Accessory minerals	10	10	—	10	5	—	10

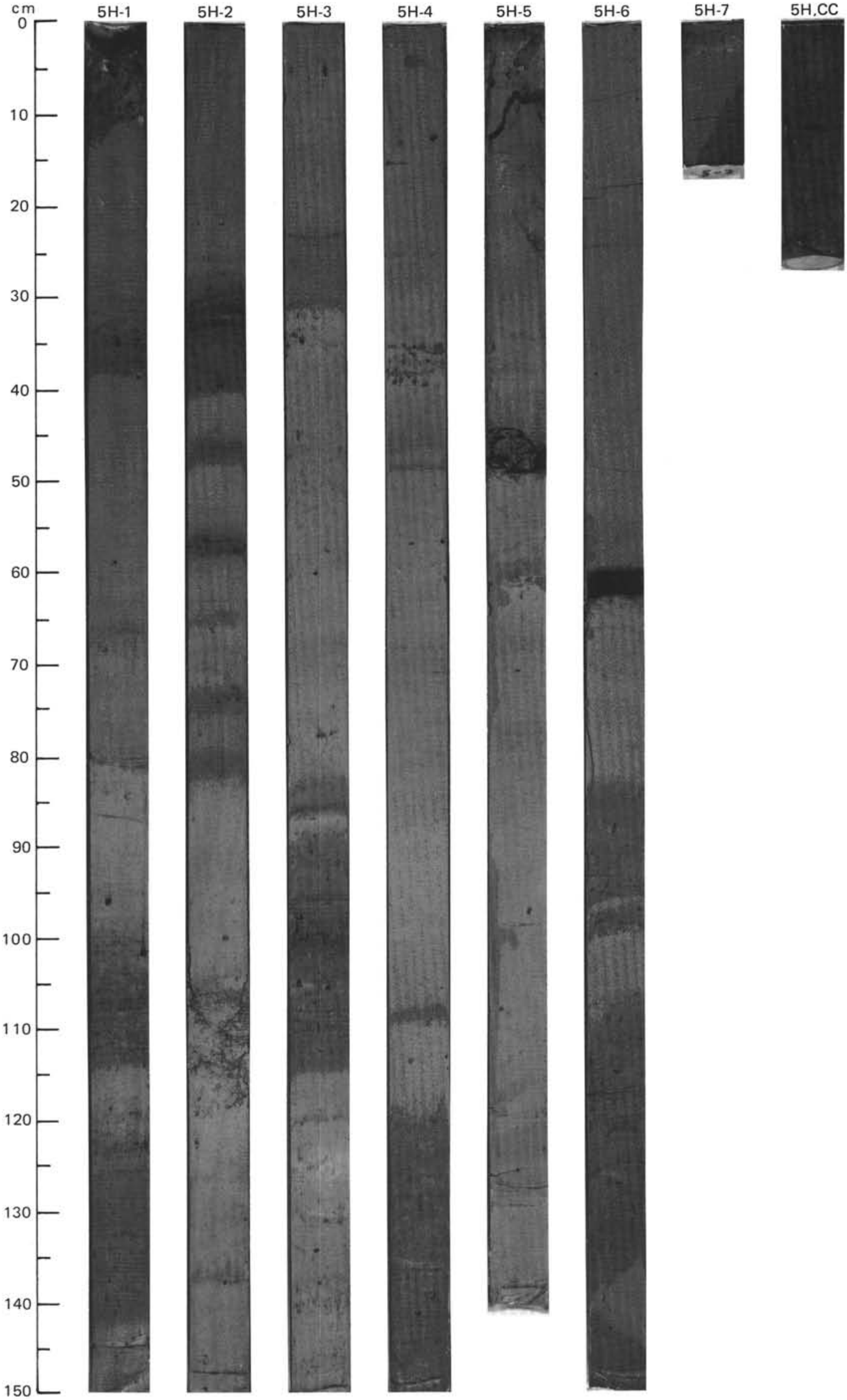
cm
0
10
20
30
40
50
60
70
80
90
100
110
120
130
140
150
5H-1
5H-2
5H-3
5H-4
5H-5
5H-6
5H-7
5H,CC

SITE 643 HOLE A CORE 6H CORED INTERVAL 2823.1-2832.6 mbsl; 43.3-52.8 mbsf

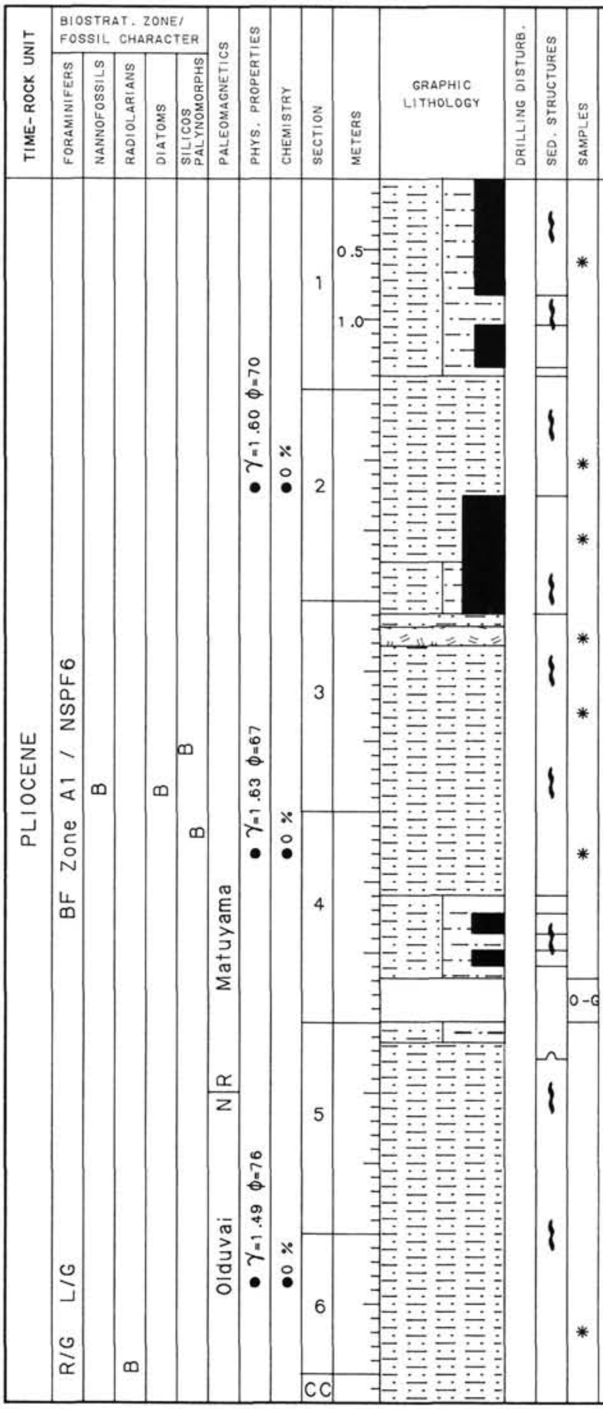

LITHOLOGIC DESCRIPTION

GLACIAL AND INTERGLACIAL MUDS AND SANDY MUDS

Entire core is undisturbed.

Major lithologies:
Muds, greenish gray (5GY 5/1) to dark greenish gray (5GY 4/1), with minor bioturbation and mottling and minor dropstones. Section 1, 140 cm, to Section 2, 123 cm; Section 3, 4 cm, to Section 4, 47 cm; and Section 5, 12 cm, to CC.

Minor lithologies:
a. Mud and sandy mud, dark gray (5Y 4/1) to very dark gray (5Y 3/1), with minor to moderate bioturbation and common to abundant dropstones. Section 1, 83–140 and 115–133 cm; Section 2, 85 cm, to Section 3, 4 cm; Section 4, 76–83 and 100–110 cm; and Section 5, 4–12 cm.
b. Mud and sandy mud, very dark gray (5Y 3/1) and laminated at the base, grading upward to olive gray (5Y 4/2) and bioturbated, with scattered dropstones Section 4, 100–111 cm.
c. Volcanic ash, partially to completely disseminated. Section 3, 22–27 cm.
d. Overconsolidated olive gray mudstone (base of a slump at Section 5, 5–20 cm).

SMEAR SLIDE SUMMARY (%):

	1, 60 D	2, 52 D	2, 103 D	3, 25 M	3, 80 D	4, 35 D	6, 68 M
TEXTURE:							
Sand	10	5	40	80	10	—	20
Silt	60	35	30	—	50	40	—
Clay	30	60	30	20	40	60	80
COMPOSITION:							
Quartz	65	40	70	—	60	50	20
Clay	30	60	30	20	40	50	80
Volcanic glass	—	—	—	80	—	—	—
Accessory minerals	5	—	—	—	—	—	—

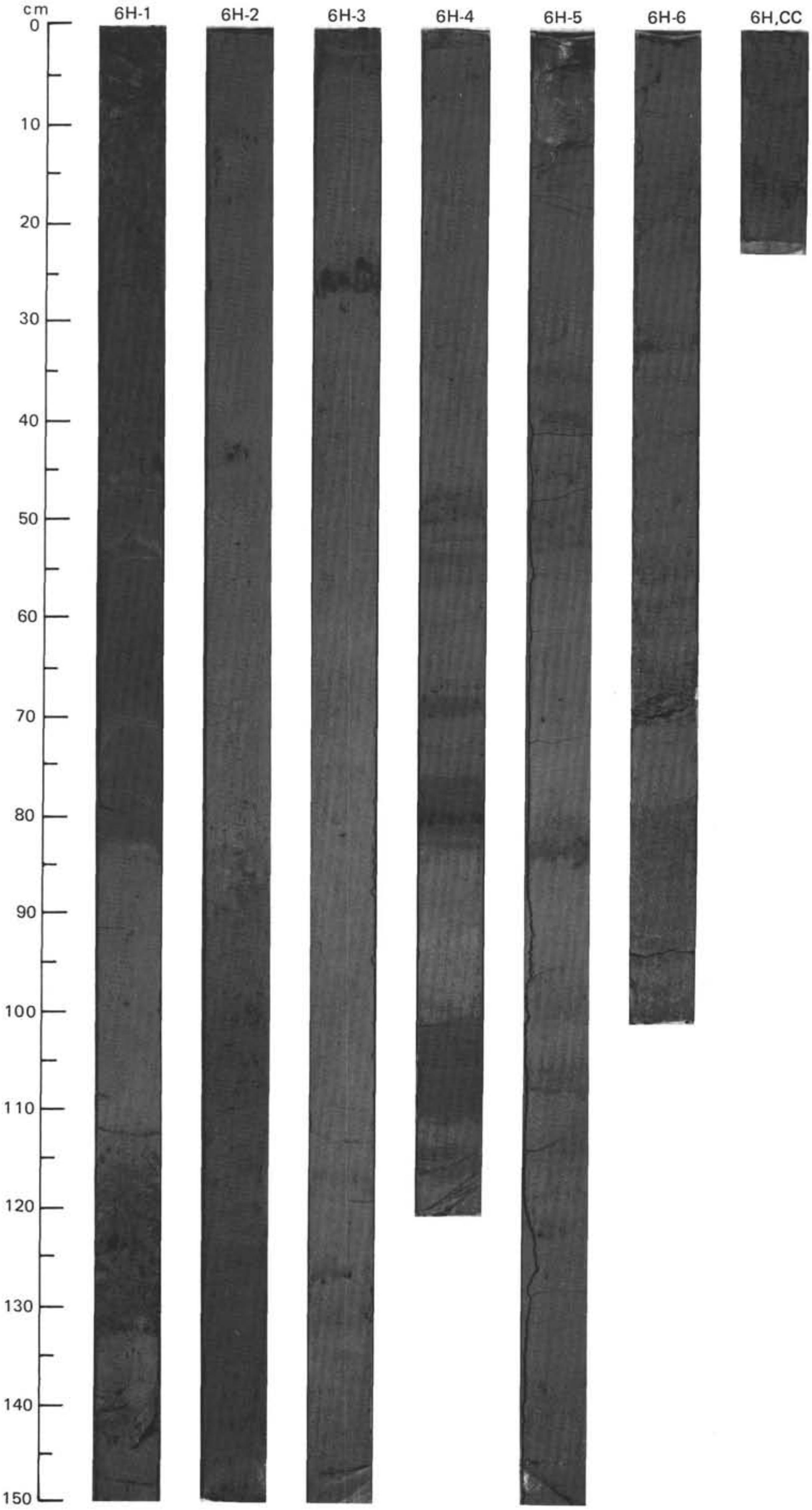
cm
0
10
20
30
40
50
60
70
80
90
100
110
120
130
140
150
6H-1
6H-2
6H-3
6H-4
6H-5
6H-6
6H,CC

SITE 643 HOLE A CORE 7H CORED INTERVAL 2832.6-2842.1 mbsl; 52.8-62.3 mbsf

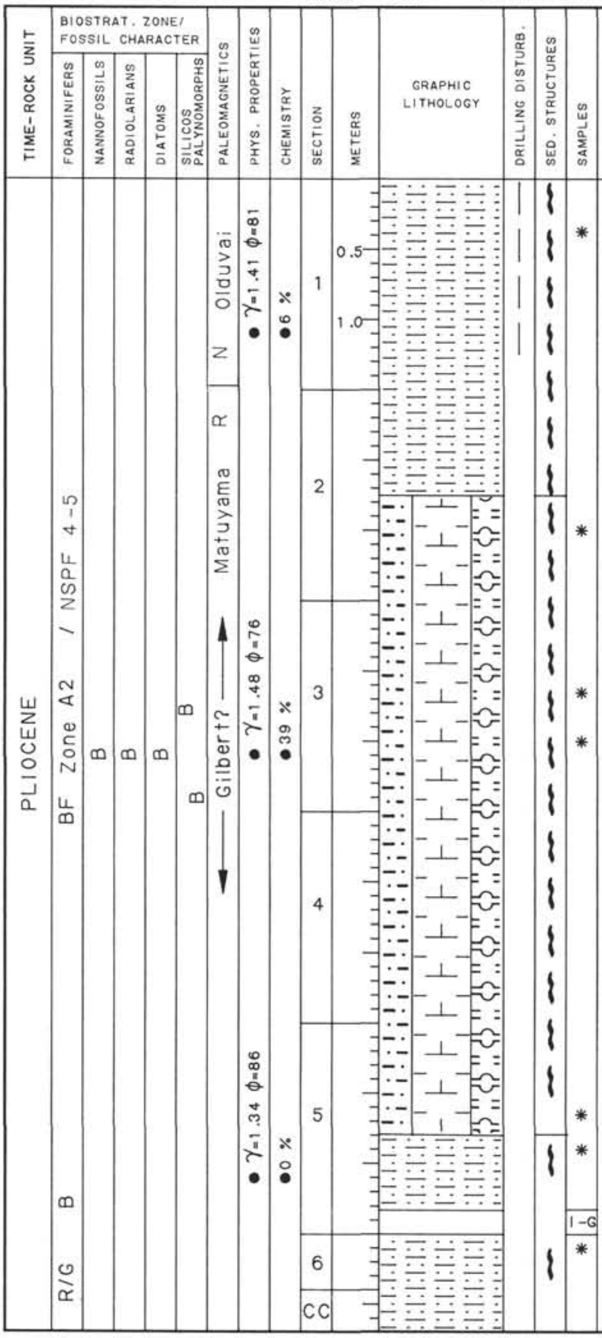

LITHOLOGIC DESCRIPTION

MUD, NANNOFOSSIL OOZE, AND SILICEOUS NANNOFOSSIL OOZE

Section 1 moderately disturbed. Remainder of core is undisturbed.

Major lithologies:
a. Muds, greenish gray (5GY 5/1), lightly mottled and bioturbated. Section 1 to Section 2, 72 cm; Section 5, 80 cm, to CC.
b. Nannofossil ooze and siliceous nannofossil ooze, gray (5Y 5/1) to olive gray (5Y 4/2), bioturbated and mottled. Section 2, 72 cm, to Section 5, 80 cm.

Minor lithology: Volcanic ash, black sandy lens. Section 3, 65–67 cm.

SMEAR SLIDE SUMMARY (%):

	1, 38 D	2, 102 D	3, 66 M	3, 103 D	5, 65 D	5, 92 D	6, 15 D
TEXTURE:							
Sand	—	—	60	—	—	—	—
Silt	10	20	—	25	30	40	20
Clay	90	80	40	75	70	60	80
COMPOSITION:							
Quartz	10	4	10	3	5	30	10
Clay	90	15	35	10	20	55	85
Volcanic glass	—	—	50	—	—	—	—
Accessory minerals	—	—	—	—	—	4	—
Nannofossils	—	70	5	65	50	—	—
Diatoms	—	1	—	1	—	—	—
Radiolarians	—	—	—	1	—	1	—
Sponge spicules	—	5	—	20	25	10	5

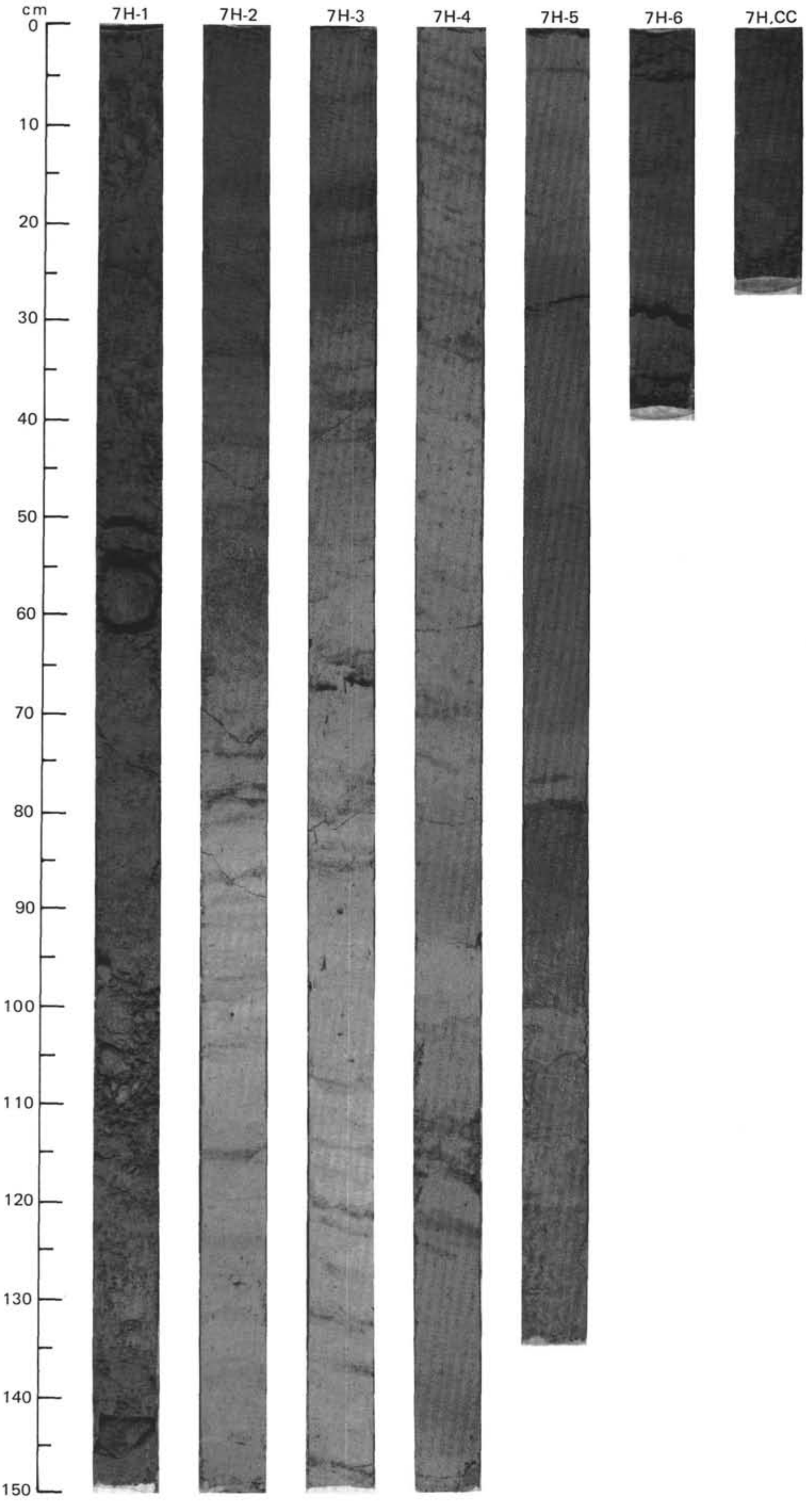
cm
0
10
20
30
40
50
60
70
80
90
100
110
120
130
140
150
7H-1
7H-2
7H-3
7H-4
7H-5
7H-6
7H,CC

SITE 643 HOLE A CORE 8H CORED INTERVAL 2842.1-28516 mbsl; 62.3-71.8 mbsf

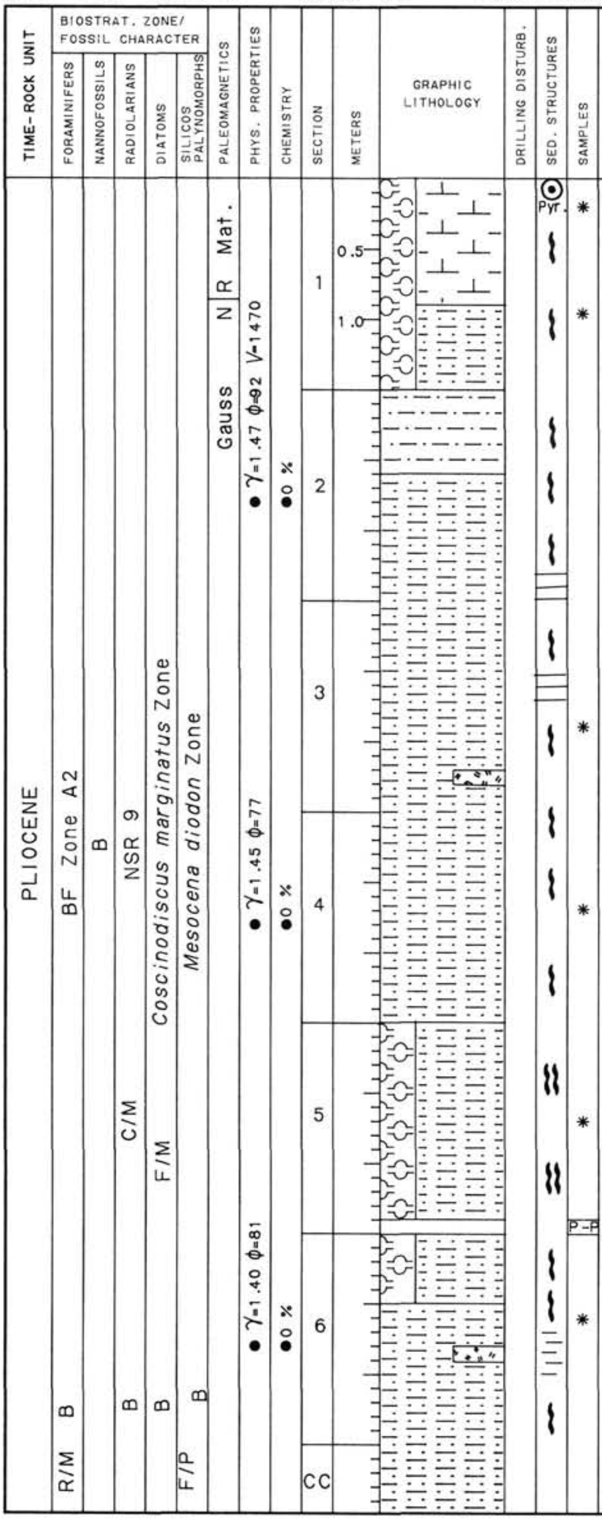

LITHOLOGIC DESCRIPTION

MUD/SANDY MUD, SILICEOUS NANNOFOSSIL OOZE, AND SILICEOUS MUD

Entire core is undisturbed.

Major lithologies:

a. Mud and sandy mud, dusky yellow green (5GY 5/2) to olive gray (5Y 5/2), mottled, and contains abundant faint pyritized burrow tubes. Scattered faint green color lamination. Section 2 to Section 4; Section 6, 48–150 cm; CC.

b. Siliceous mud, dark olive gray (5Y 3/2) to dark greenish gray (10GY 5/2), extensively mottled and slumped. Section 5 to Section 6, 48 cm.

c. Siliceous mud, dusky yellow green (5GY 5/2), moderately mottled. Section 1, 96–150 cm.

d. Siliceous nannofossil ooze, dusky yellow green (5GY 5/2), moderately mottled. Section 1, 0–96 cm.

SMEAR SLIDE SUMMARY (%):

	1, 22 D	1, 96 D	2, 47 D	3, 91 D	4, 70 D	5, 70 D	6, 63 D
TEXTURE:							
Sand	—	5	10	2	5	5	5
Silt	20	20	20	18	25	35	15
Clay	80	75	70	80	70	60	80
COMPOSITION:							
Quartz	5	15	25	10	15	15	15
Feldspar	—	2	5	2	1	2	—
Clay	15	70	65	80	70	60	75
Volcanic glass	1	2	2	1	1	2	2
Accessory minerals	1	1	1	1	1	1	1
Foraminifers	1	—	—	—	—	—	—
Nannofossils	62	—	—	—	—	—	—
Diatoms	10	—	—	2	2	10	2
Sponge spicules	5	10	2	4	10	10	5

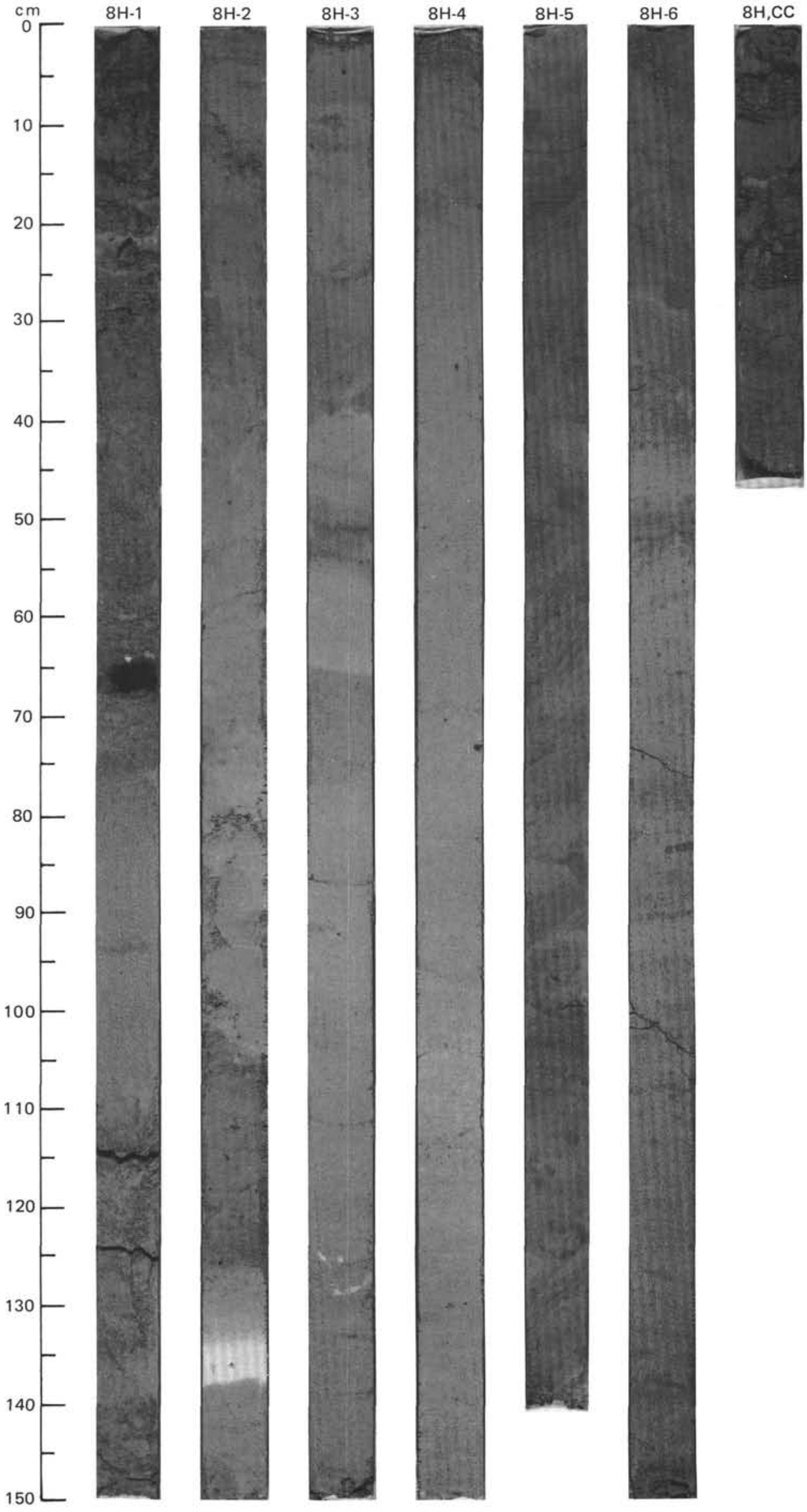
cm
0
10
20
30
40
50
60
70
80
90
100
110
120
130
140
150
8H-1
8H-2
8H-3
8H-4
8H-5
8H-6
8H,CC

SITE 643 HOLE A CORE 9H CORED INTERVAL 2851.6-2861.1 mbsl; 71.8-81.3 mbsf

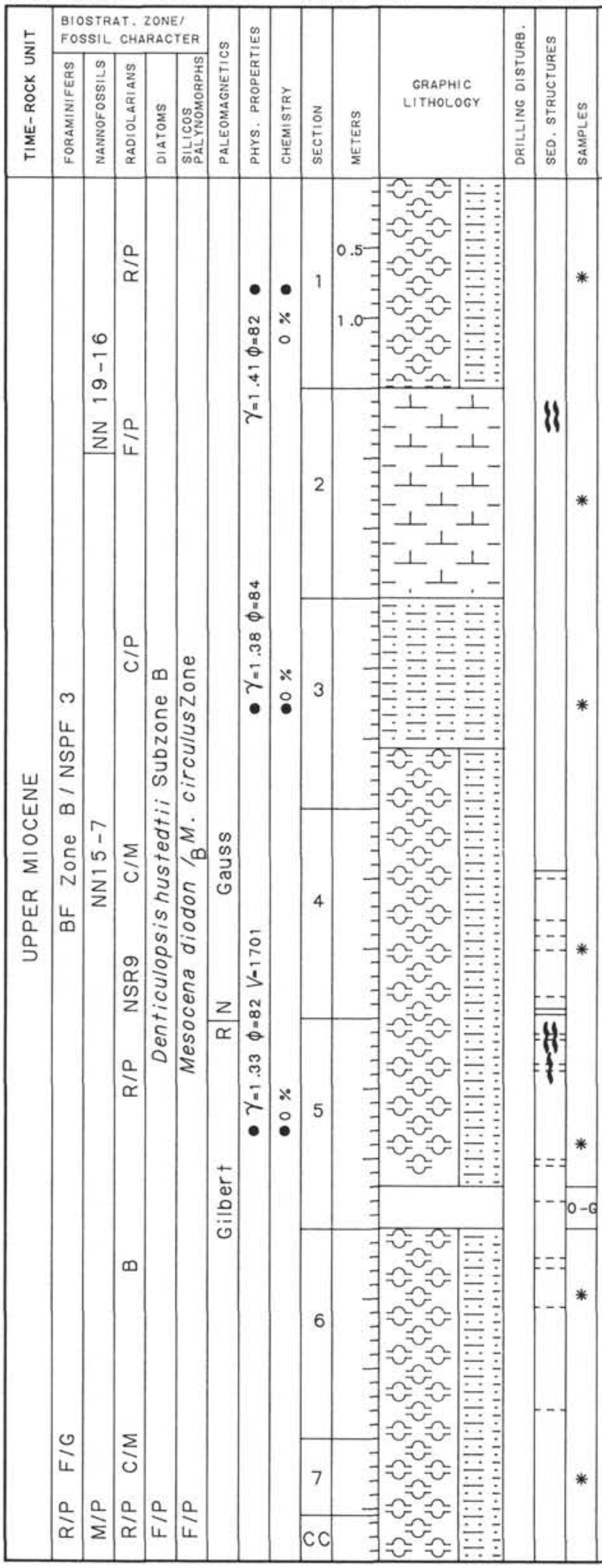

LITHOLOGIC DESCRIPTION

SILICEOUS MUD AND NANNOFOSSIL OOZE

Major lithologies:
a. Siliceous mud and mud, olive gray (5Y 5/2) to greenish gray (10GY 5/2). Extensively mottled with abundant, faint pyrite-impregnated burrow tubes. Color banding common. Section 1; Section 3 to Section 6, 55 cm; Section 7, 0–54 cm; CC.
b. Siliceous mud, olive gray (5Y 4/2) to dark gray (5Y 4/1), extremely mottled and slumped. Section 6, 55–127 cm.
c. Nannofossil ooze, olive gray (5Y 5/2), extensively mottled. Section 2.

Minor lithology: Volcanic ash. Dark gray (5Y 4/1) ash layer, heavily bioturbated, at Section 2, 23–25 cm. Dark gray (5Y 4/1) disseminated ash lenses at Section 4, 11, 12, and 46–48 cm.

SMEAR SLIDE SUMMARY (%):

	1, 70 D	2, 91 D	3, 75 D	4, 102 D	5, 86 D	6, 50 D	7, 29 D
TEXTURE:							
Sand	2	—	2	2	1	1	1
Silt	18	20	28	10	19	37	29
Clay	80	80	70	78	80	62	70
COMPOSITION:							
Quartz	7	5	10	10	5	15	5
Feldspar	—	—	1	1	—	—	—
Clay	80	37	73	78	82	62	72
Volcanic glass	2	—	1	3	1	2	2
Calcite/dolomite	1	—	—	—	—	—	—
Accessory minerals	1	—	—	—	—	1	—
Pyrite	2	—	—	—	—	—	—
Glauconite	—	—	—	1	—	—	—
Foraminifers	—	1	—	—	—	—	—
Nannofossils	—	50	—	—	2	—	
Diatoms	2	2	5	2	5	10	10
Radiolarians	—	—	—	—	—	—	1
Sponge spicules	5	5	10	5	5	10	10

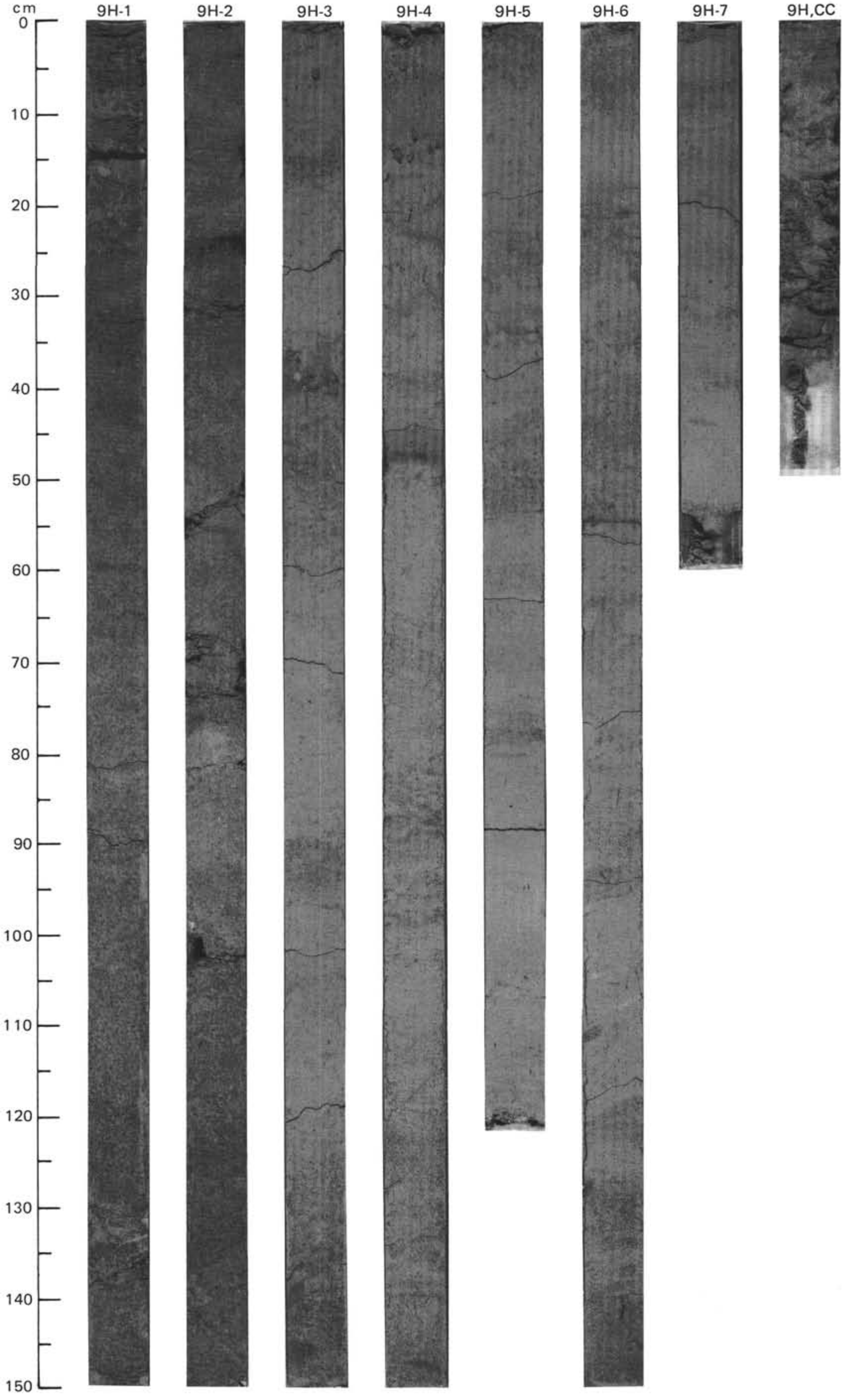
cm
0
10
20
30
40
50
60
70
80
90
100
110
120
130
140
150
9H-1
9H-2
9H-3
9H-4
9H-5
9H-6
9H-7
9H,CC

SITE 643 HOLE A CORE 10H CORED INTERVAL 2861.1-2870.6 mbsl; 81.3-90.8 mbsf

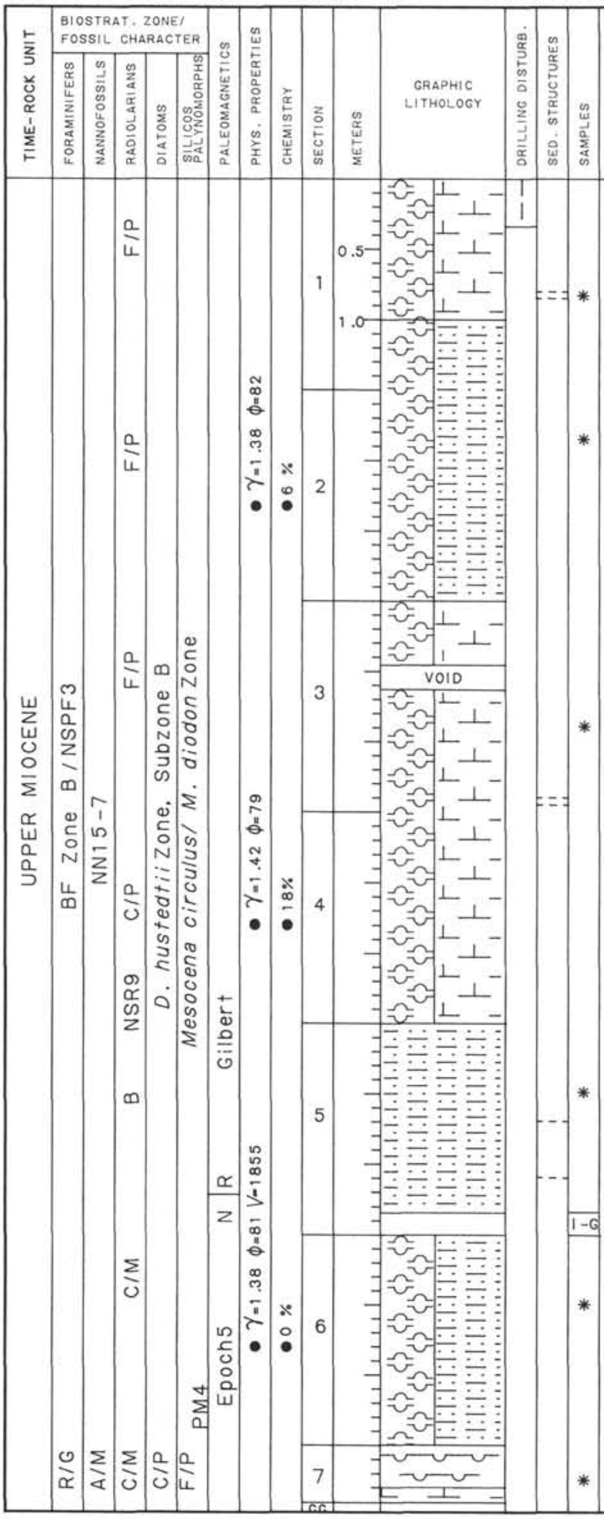

LITHOLOGIC DESCRIPTION

SILICEOUS MUD AND DIATOMACEOUS NANNOFOSSIL OOZE

Section 1, 0–36 cm, is moderately disturbed. Remainder of the core is undisturbed.

Major lithologies:
a. Siliceous mud, gray (5Y 5/1) to olive gray (5Y 5/2), moderately mottled. Section 1, 100–150 cm; Section 2.
b. Siliceous mud to mud, dark olive gray (5Y 3/2). Section 5, 0–70 and 110–150 cm; Section 6. Section 5, 70–110 cm, heavily slumped.
c. Diatomaceous nannofossil ooze, gray (5Y 4/1) to olive gray (5Y 5/2), moderately mottled. Section 1, 0–100 cm; Section 3; Section 4, 0–36 and 107–150 cm. Section 4, 0–36 and 107–150 cm. Section 4, 36–107 cm, is a dark gray (5Y 4/1), slumped, diatomaceous nannofossil ooze.
d. Diatom ooze, olive gray (5Y 5/2) and moderately mottled. Section 7, 0–36 and 40–41 cm.

Minor lithologies:
a. Nannofossil ooze, dark olive gray (5Y 3/2). Section 7, 36–38 cm.
b. Volcanic ash. Dark gray (5Y 4/1) ash pocket at Section 5, 20–23 cm.

Pyritized ash lens at Section 7, 1–3 cm.

SMEAR SLIDE SUMMARY (%):

	1, 83 D	2, 31 D	3, 90 D	4, 130 D	5, 50 D	6, 50 D	7, 220 D
TEXTURE:							
Sand	—	—	—	—	1	3	2
Silt	30	20	20	25	24	17	60
Clay	70	80	80	75	75	80	38
COMPOSITION:							
Quartz	1	5	2	5	15	10	10
Clay	17	80	14	14	74	79	34
Volcanic glass	—	1	—	—	1	1	1
Calcite/dolomite	—	1	—	—	—	—	—
Accessory minerals	—	1	—	—	—	—	—
Foraminifers	—	—	1	—	—	—	—
Nannofossils	50	—	65	60	—	—	—
Diatoms	25	2	15	15	5	5	40
Radiolarians	2	—	—	1	—	—	5
Sponge spicules	5	10	3	5	5	5	10

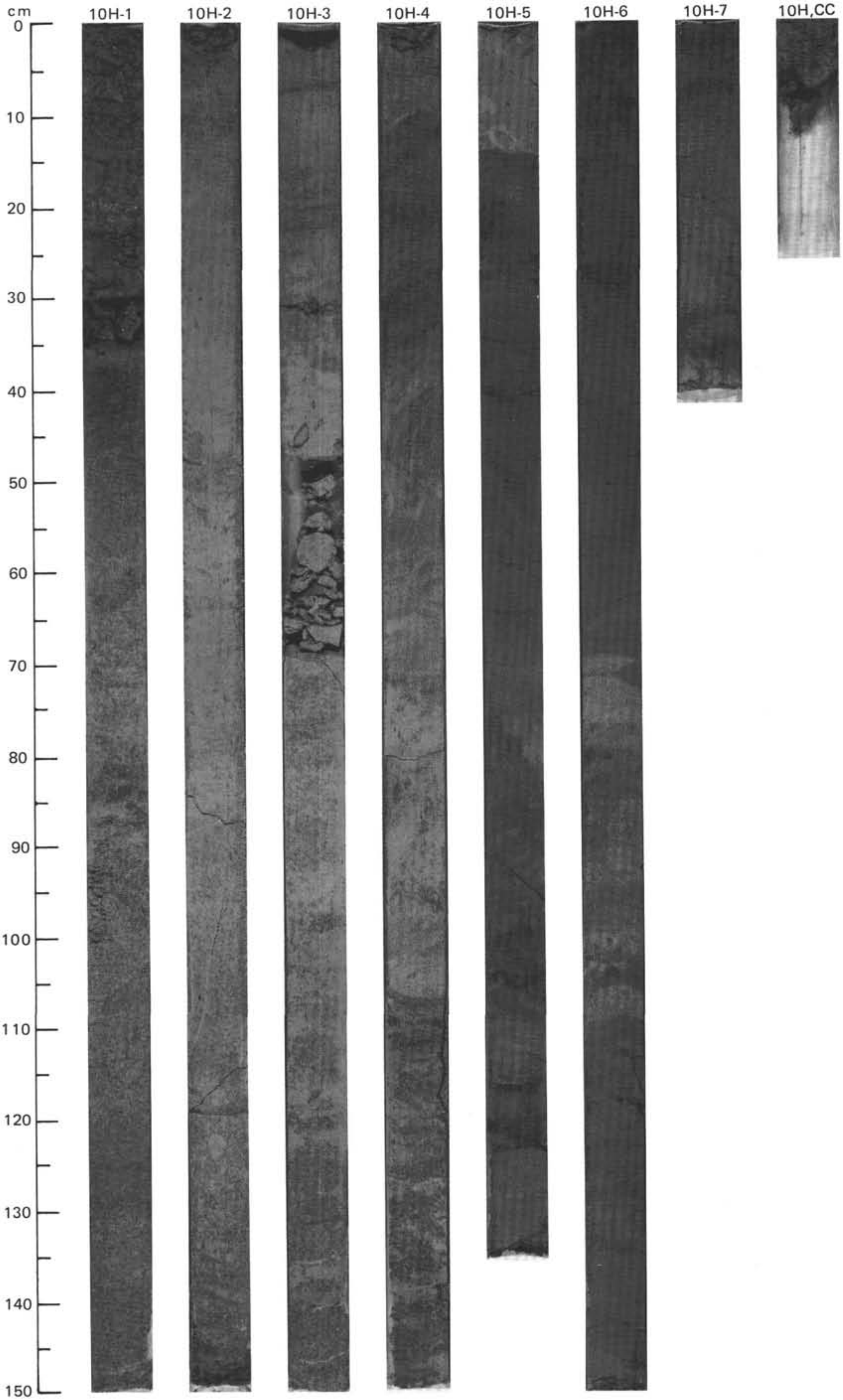
cm
0
10
20
30
40
50
60
70
80
90
100
110
120
130
140
150
10H-1
10H-2
10H-3
10H-4
10H-5
10H-6
10H-7
10H,CC

SITE 643 HOLE A CORE 11H CORED INTERVAL 2870.6-2880.1 mbsl; 90.8-100.3 mbsf

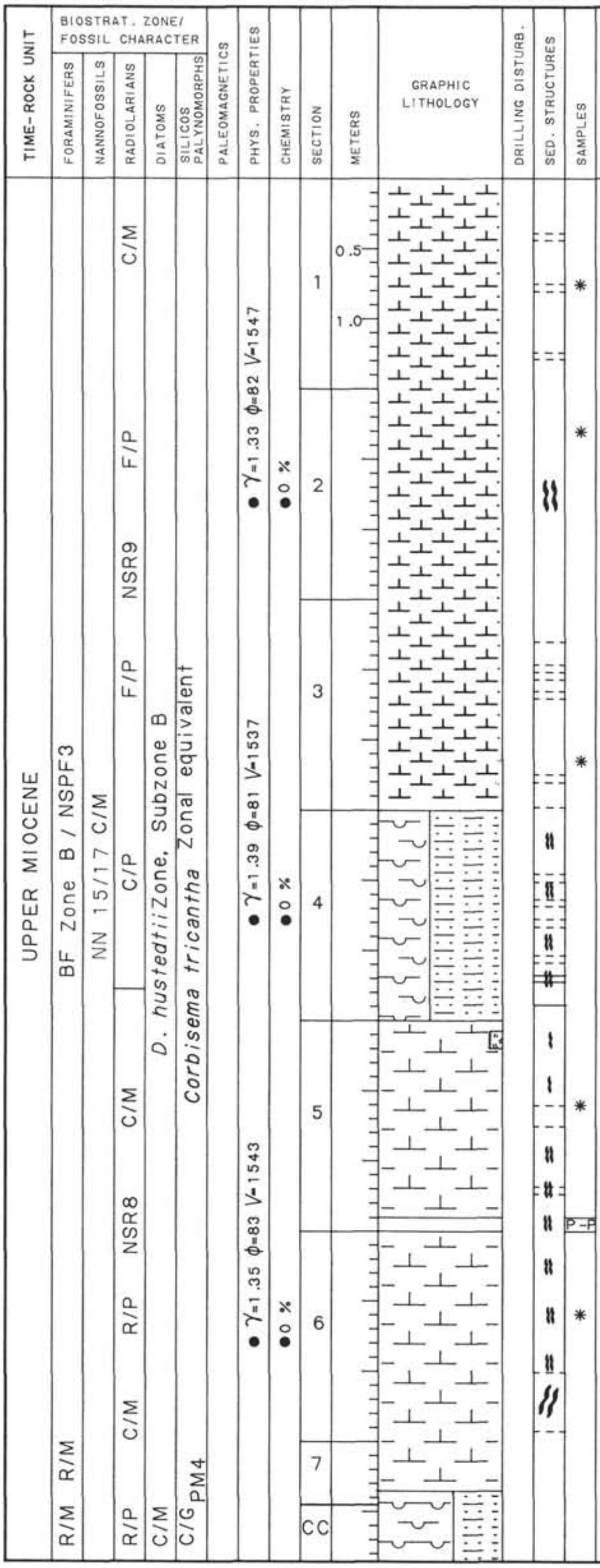

LITHOLOGIC DESCRIPTION

DIATOMACEOUS NANNOFOSSIL OOZE AND DIATOMACEOUS MUD

Entire core is undisturbed.

Major lithologies:
a. Diatomaceous nannofossil ooze, gray (5Y 5/1) to greenish gray (5GY 5/2), mottled and extensively bioturbated. Section 1 to Section 3; Section 5 (weakly slumped); Section 6, 0–100 cm and 100–150 cm (weakly slumped); Section 7, 0–35 cm.
b. Diatomaceous mud, light gray (5Y 6/1) and extensively bioturbated, with abundant banding in green. Section 4; CC.

Minor lithology: Volcanic ash: dark gray ash lens, Section 1, 10 cm; discrete layer, Section 1, 103–106 cm; thin layer, Section 2, 27 cm; bioturbated ashes, Section 2, 70–74 and 140–142 cm, Section 4, 80–86 and 107–115 cm; light gray discrete layers, Section 5, 6–10 cm, and Section 7, 8–10 cm.

SMEAR SLIDE SUMMARY (%):

	1, 76 D	2, 30 D	3, 115 D	4, 90 D	5, 59 D	6, 59 D	CC, 10 D
TEXTURE:							
Sand	—	—	—	5	—	—	5
Silt	25	25	40	45	40	45	35
Clay	75	75	60	50	60	55	60
COMPOSITION:							
Quartz	2	2	—	10	—	—	10
Feldspar	—	—	—	—	—	—	1
Clay	24	15	9	50	8	11	57
Volcanic glass	1	—	—	—	—	—	1
Calcite/dolomite	2	2	—	—	—	1	—
Foraminifers	—	—	1	—	—	1	—
Nannofossils	50	60	55	—	50	45	—
Diatoms	15	15	25	30	30	30	20
Radiolarians	1	1	—	—	2	2	1
Sponge spicules	5	5	10	10	10	10	10

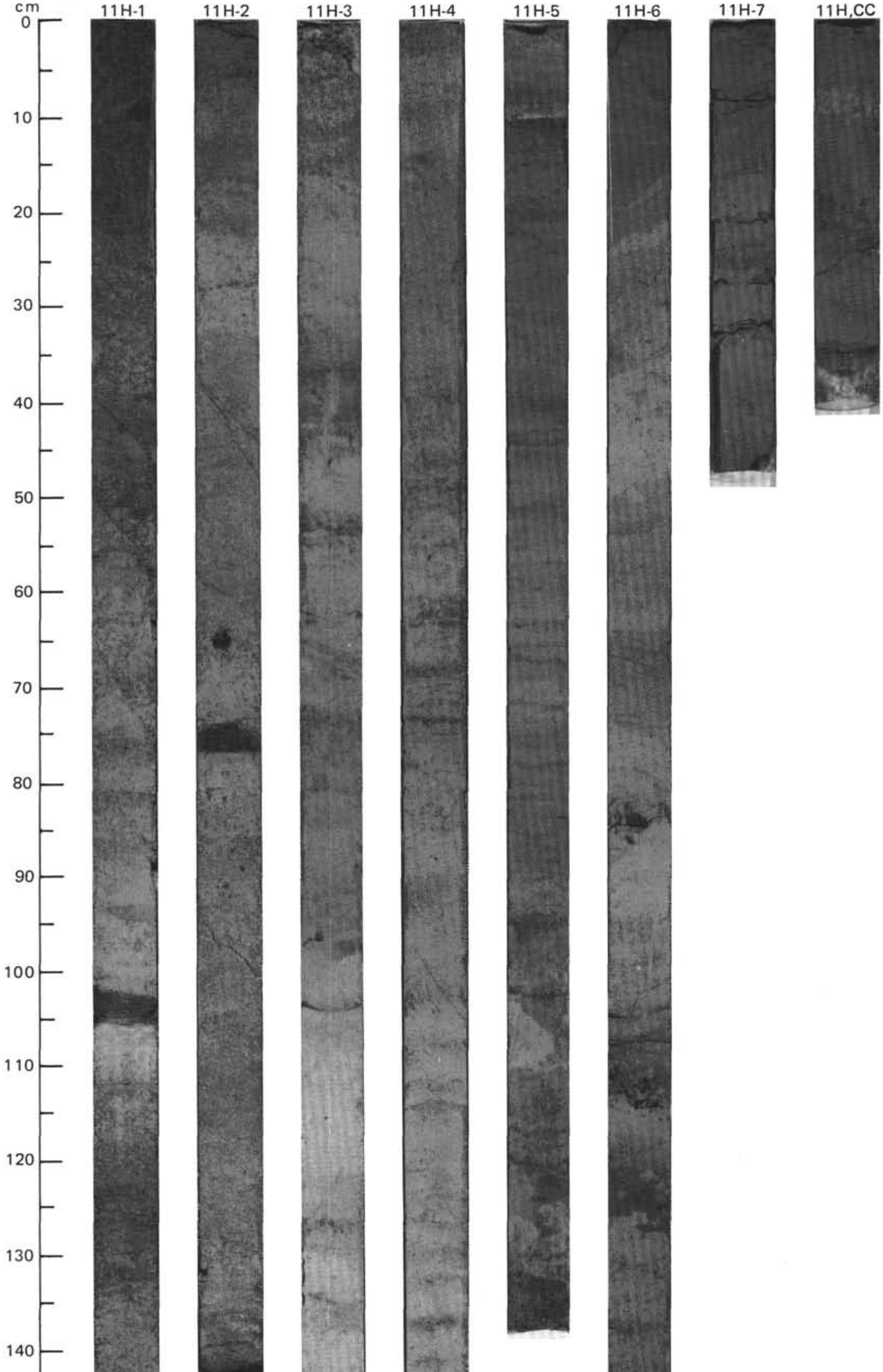
cm
0
10
20
30
40
50
60
70
80
90
100
110
120
130
140
150
11H-1
11H-2
11H-3
11H-4
11H-5
11H-6
11H-7
11H,CC

SITE 643 HOLE A CORE 12H CORED INTERVAL 2880.1-2889.6 mbsl; 100.3-109.8 mbsf

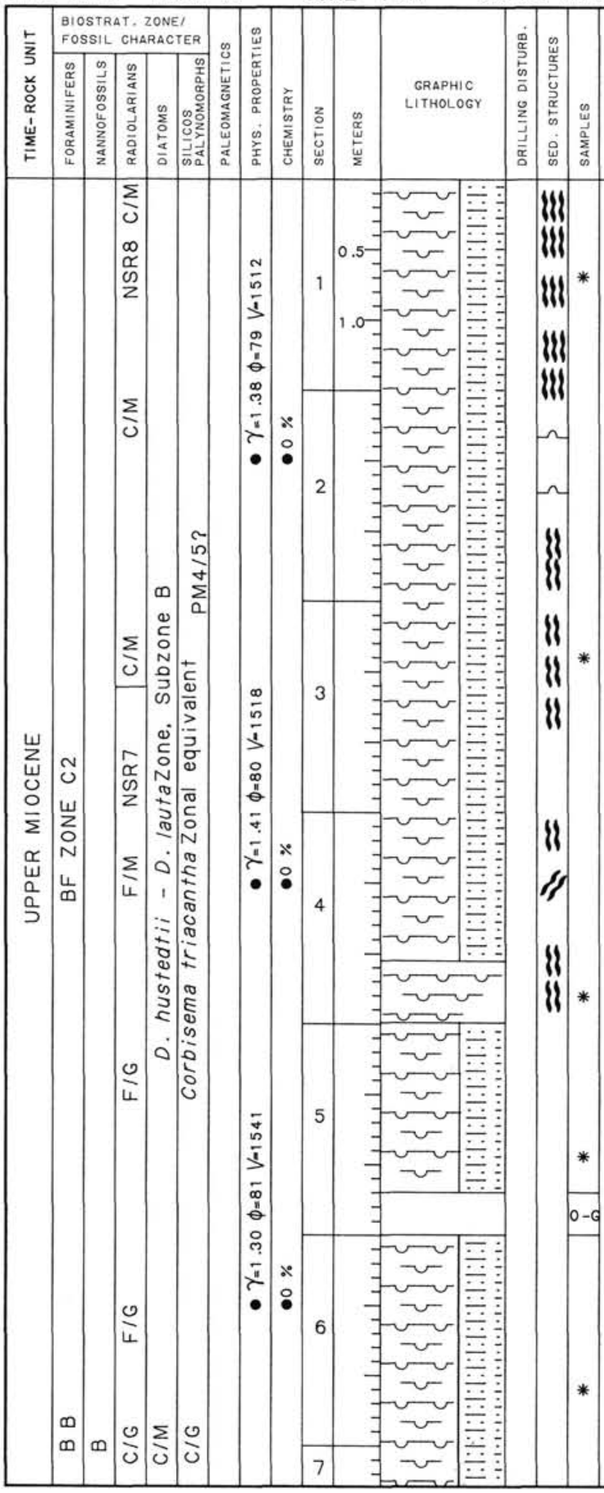

LITHOLOGIC DESCRIPTION

DIATOMACEOUS MUD AND DIATOM OOZE

Entire core is undisturbed.

Major lithologies:
a. Diatomaceous mud, greenish gray (5GY 5/2) to dark olive gray (5Y 3/2), extensively mottled and bioturbated, with abundant dark olive gray (5Y 3/2) color banding and burrow fillings. Burrow types include: faint, pyrite-impregnated tubes, irregular tubes 122 mm in diameter (*Chondrides*?), and cm-scale irregular burrows. Section 1; Section 2 (entire section is a portion of a slump, with the interval from 45 to 90 cm identified as a debris flow); Section 3; Section 4, 0–105 cm (15–105 cm is slumped); Section 5 to Section 7.
b. Diatom ooze, greenish gray (5GY 5/2), extensively mottled and bioturbated. Section 4, 105–150 cm.

Minor lithology: Volcanic ash. Dark gray (5Y 4/1) disseminated, bioturbated ash, Section 3, 112–114 cm; pyritized ash lens, Section 4, 98 cm; sandy ash lenses, Section 5, 47 and 59–61 cm.

SMEAR SLIDE SUMMARY (%):

	1, 70 D	3, 40 D	4, 130 D	5, 93 D	6, 108 D
TEXTURE:					
Sand	5	—	10	15	10
Silt	40	50	60	45	50
Clay	55	50	30	40	40
COMPOSITION:					
Quartz	15	5	5	2	5
Clay	51	48	28	36	51
Volcanic glass	1	1	1	—	1
Diatoms	20	30	50	40	30
Radiolarians	2	5	5	5	2
Sponge spicules	10	10	10	15	10
Silicoflagellates	1	1	1	2	1

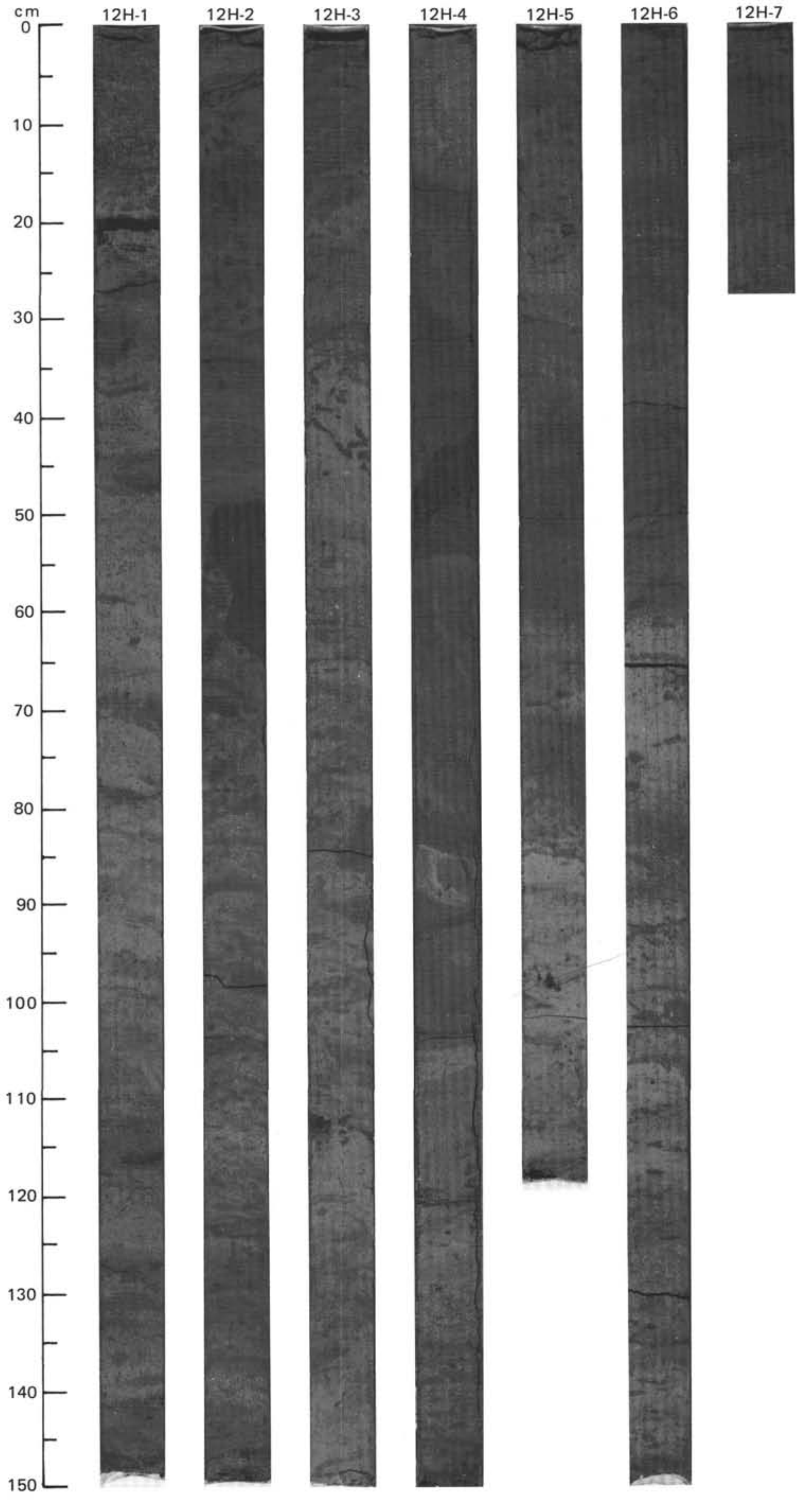
cm
0
10
20
30
40
50
60
70
80
90
100
110
120
130
140
150
12H-1
12H-2
12H-3
12H-4
12H-5
12H-6
12H-7

SITE 643 HOLE A CORE 13H CORED INTERVAL 2889.6-2899.1 mbsl; 109.8-119.3 mbsf

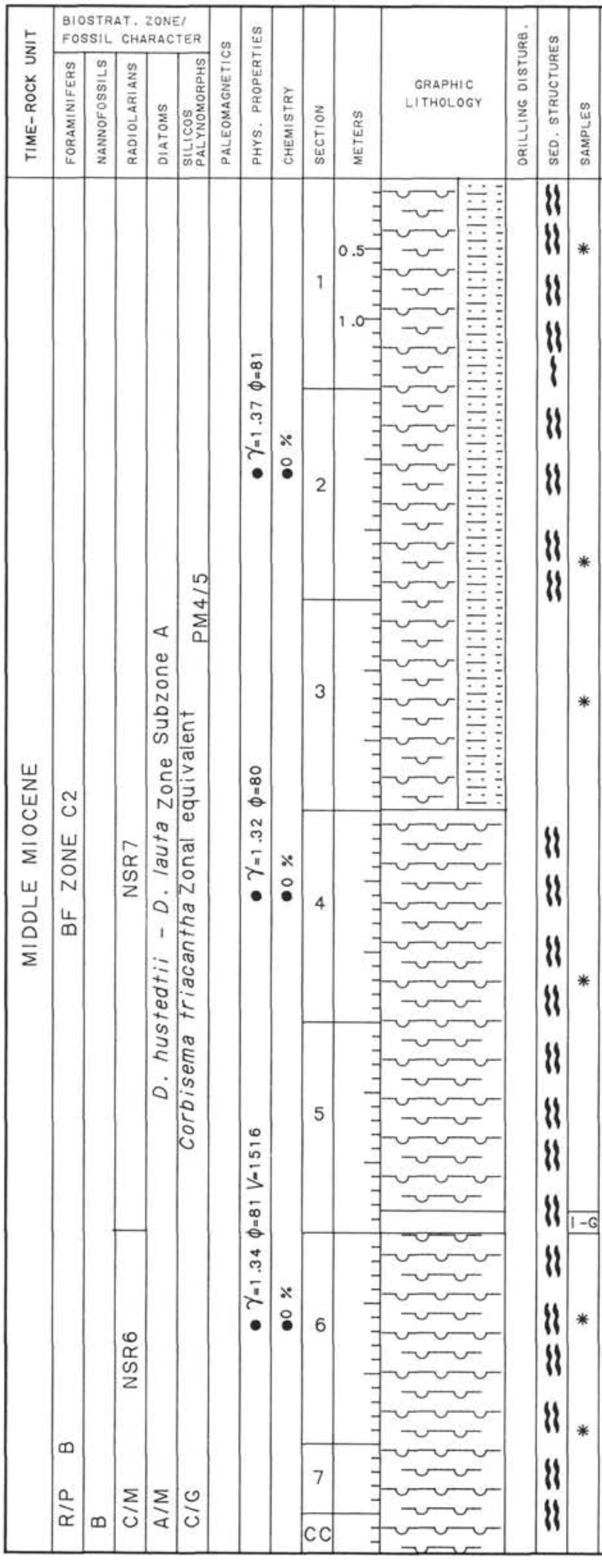

LITHOLOGIC DESCRIPTION

DIATOM OOZE AND DIATOMACEOUS MUD

Entire core is undisturbed.

Major lithologies:
a. Diatom ooze to diatomaceous mud, grayish green (10GY 5/2) to dark olive gray (5Y 3/2), extensively bioturbated and mottled. Large indistinct burrows are common. Section 1 to Section 3.
b. Diatom ooze, grayish green (10GY 5/2), extensively bioturbated and mottled, with abundant color banding. Section 4 to CC.

Minor lithology: Volcanic ash, light gray (5Y 5/1) and disseminated. CC, 13–14 cm.

SMEAR SLIDE SUMMARY (%):

	1, 51 D	1, 120 D	3, 70 D	4, 115 D	6, 57 D	6, 134 D
TEXTURE:						
Sand	25	30	20	15	20	30
Silt	45	50	60	55	60	40
Clay	30	20	20	30	20	30
COMPOSITION:						
Quartz	5	10	5	10	7	10
Clay	30	20	20	23	16	20
Volcanic glass	—	—	—	1	—	—
Accessory minerals	—	—	—	—	1	—
Diatoms	40	50	55	50	60	50
Radiolarians	5	10	5	5	5	10
Sponge spicules	20	10	15	10	10	10
Silicoflagellates	—	—	—	1	1	—

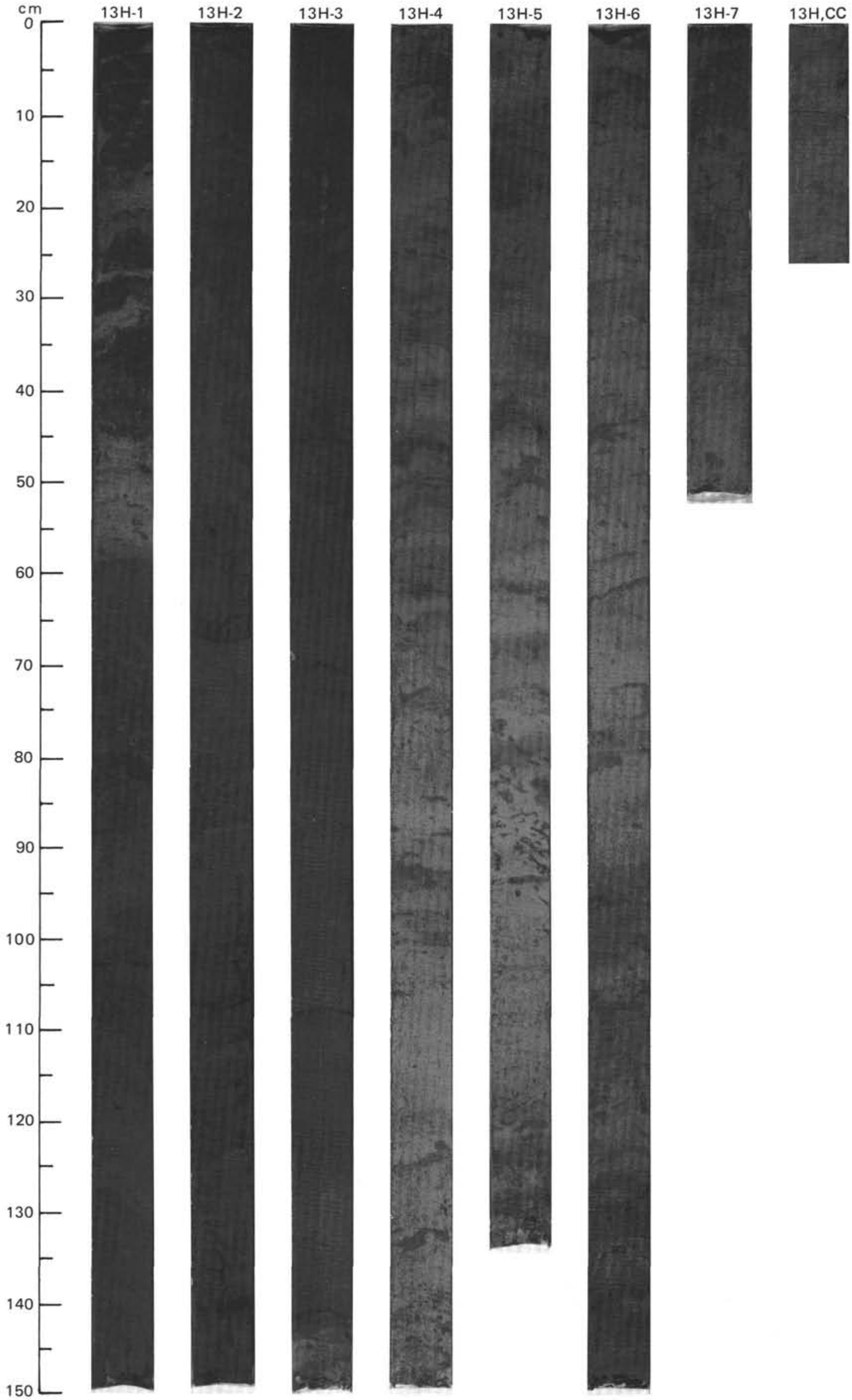
cm
0
10
20
30
40
50
60
70
80
90
100
110
120
130
140
150
13H-1
13H-2
13H-3
13H-4
13H-5
13H-6
13H-7
13H,CC

SITE 643 HOLE A CORE 14H CORED INTERVAL 2899.1-2908.6 mbsl; 119.3-128.8 mbsf

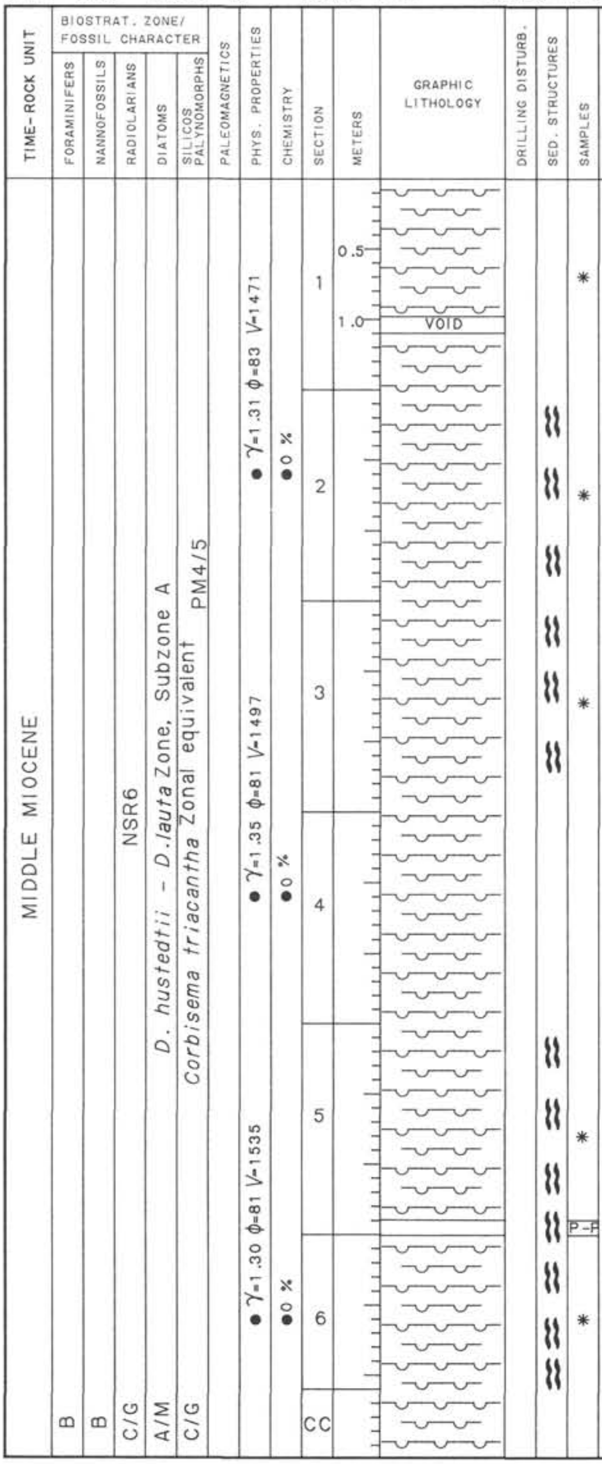

LITHOLOGIC DESCRIPTION

DIATOM OOZE

Entire core is undisturbed.

Major lithology: Diatom ooze, grayish green (10GY 5/2), extensively bioturbated and mottled, with abundant dark olive gray (5Y 3/2) color banding.

Minor lithology: Volcanic ash. Light gray ash, Section 1, 90–91 cm; dark gray ash, Section 4, 128–130 cm.

SMEAR SLIDE SUMMARY (%):

	1, 70 D	2, 73 D	3, 82 D	4, 26 D	5, 80 D	6, 60 D
TEXTURE:						
Sand	15	30	15	15	20	20
Silt	60	50	55	65	60	60
Clay	25	20	30	20	20	20
COMPOSITION:						
Quartz	5	5	5	5	5	3
Clay	25	8	20	18	18	16
Volcanic glass	—	—	—	1	1	—
Accessory minerals:						
Pyrite	—	5	—	—	—	—
Diatoms	50	60	55	50	60	55
Radiolarians	5	5	5	5	5	5
Sponge spicules	15	15	20	20	10	20
Silicoflagellates	—	2	—	1	1	1

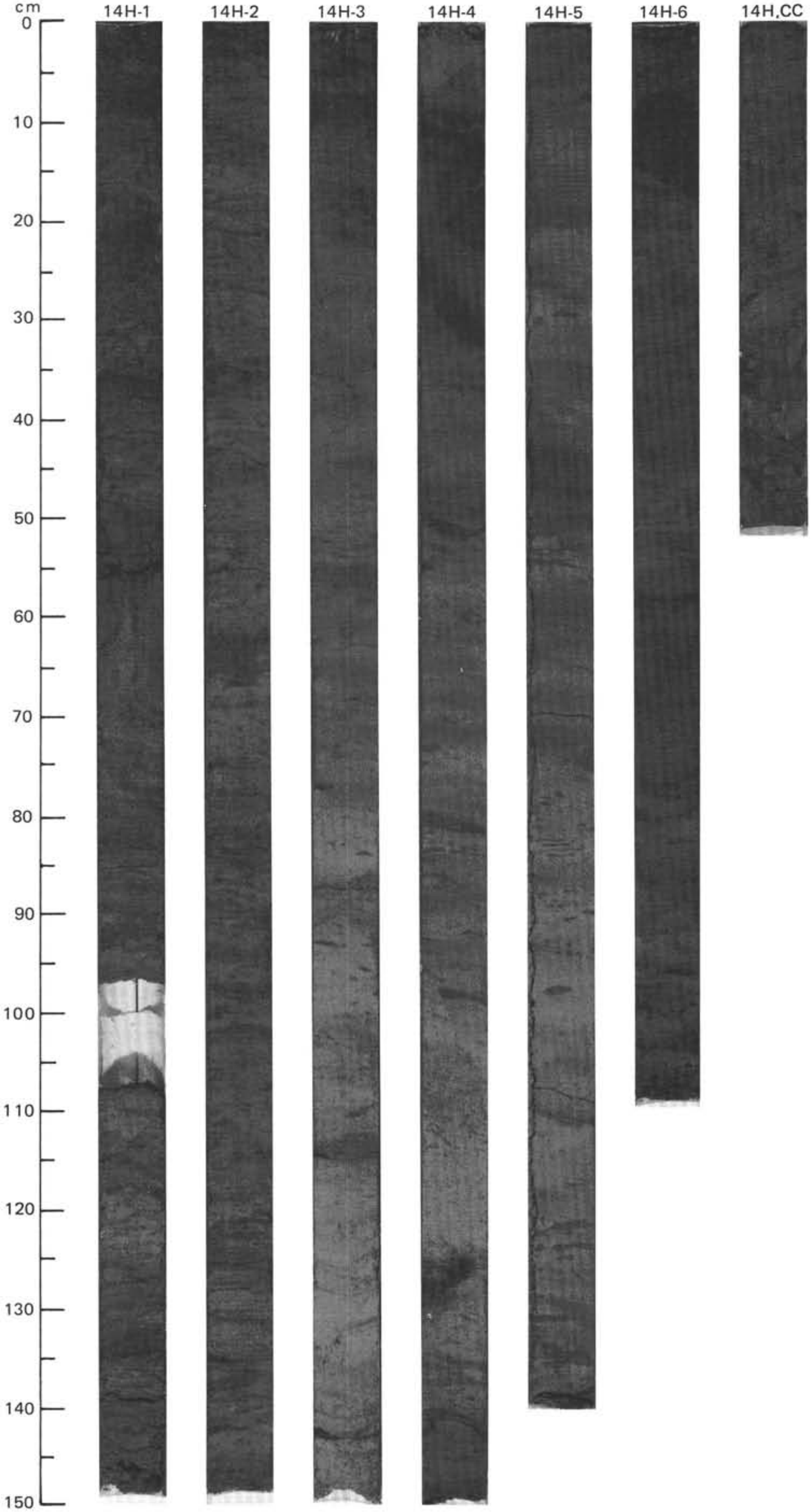
cm
0
10
20
30
40
50
60
70
80
90
100
110
120
130
140
150
14H-1
14H-2
14H-3
14H-4
14H-5
14H-6
14H,CC

SITE 642 HOLE A CORE 15H CORED INTERVAL 2908.6-2918.1 mbsl; 128.8-138.3 mbsf

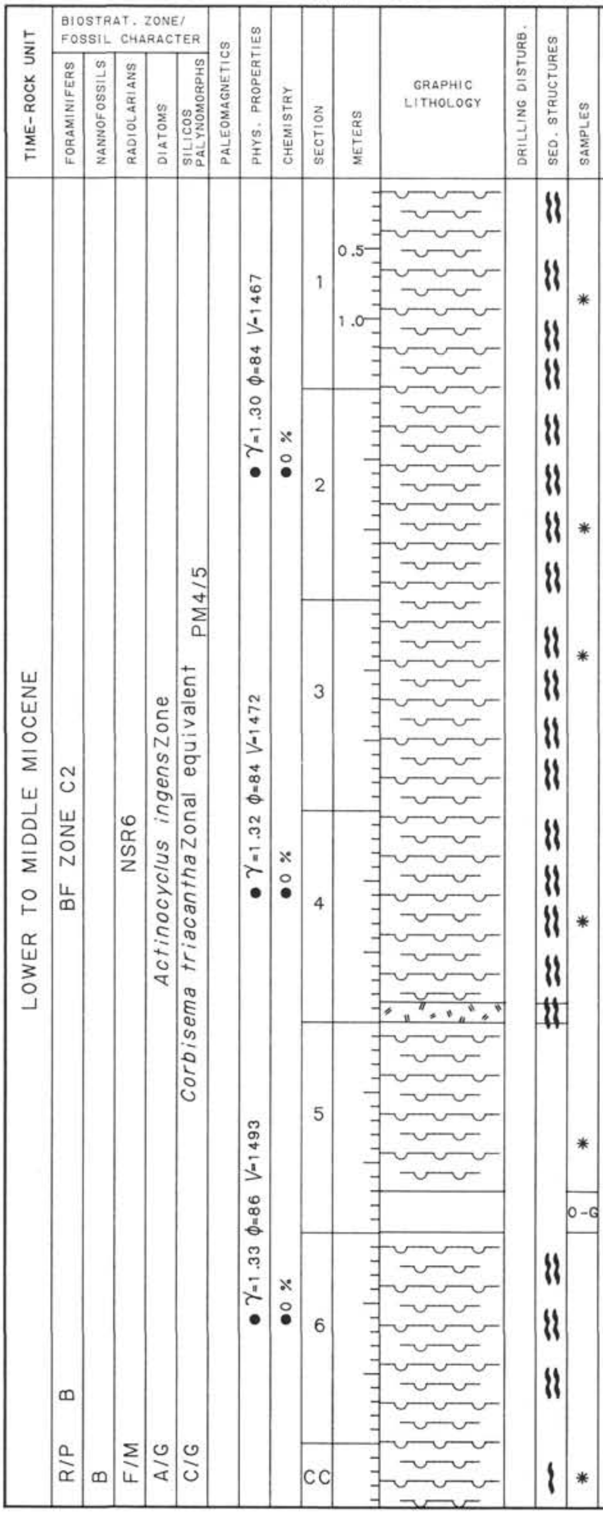

LITHOLOGIC DESCRIPTION

DIATOM OOZE

Entire core is undisturbed.

Major lithology: Diatom ooze, grayish green (10GY 5/2), extensively bioturbated and mottled, with common dark olive gray (5Y 3/2) color banding and burrow fillings. Section 5, 23–42 cm, is a dark olive gray diatom ooze with large, well-developed *Zoophycos* trace fossils and several younger generations of burrows.

Minor lithology: Volcanic ash, very dark gray (5Y 3/1), Section 4, 138–150 cm.

SMEAR SLIDE SUMMARY (%):

	1, 84 D	2, 95 D	3, 40 D	4, 73 D	5, 91 D	CC, 30 D
TEXTURE:						
Sand	15	20	20	20	20	15
Silt	65	60	60	60	60	55
Clay	20	20	20	20	20	30
COMPOSITION:						
Quartz	5	5	5	5	7	10
Clay	13	21	13	13	16	23
Volcanic glass	—	1	—	—	—	—
Accessory minerals	—	1	—	—	—	—
Diatoms	60	50	55	55	50	50
Radiolarians	5	5	5	5	5	5
Sponge spicules	15	15	20	20	20	10
Silicoflagellates	2	2	2	2	2	2

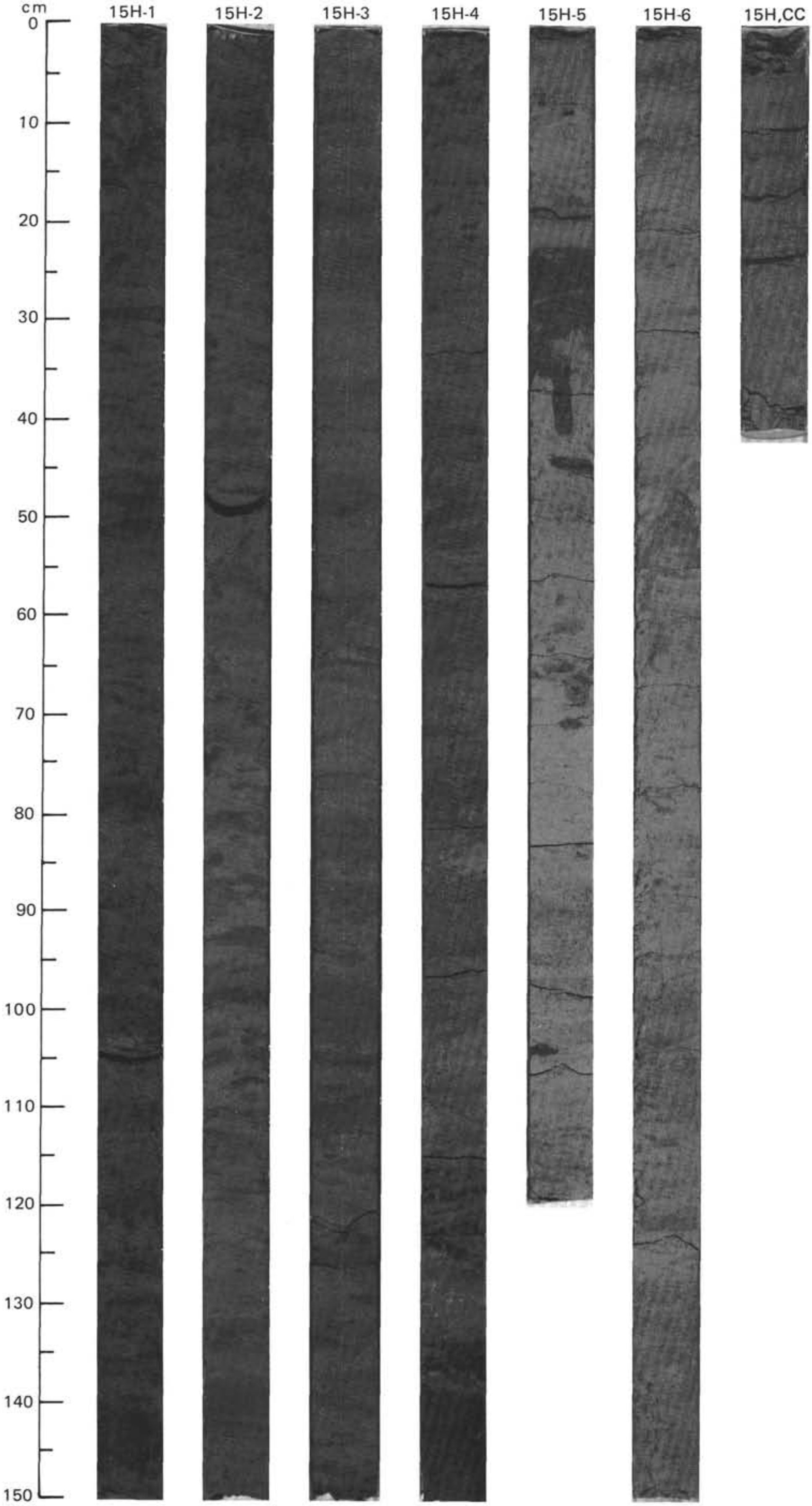
cm
0
10
20
30
40
50
60
70
80
90
100
110
120
130
140
150
15H-1
15H-2
15H-3
15H-4
15H-5
15H-6
15H,CC

SITE 643 HOLE A CORE 16H CORED INTERVAL 2918.1-2927.6 mbsl; 138.3-147.8 mbsf

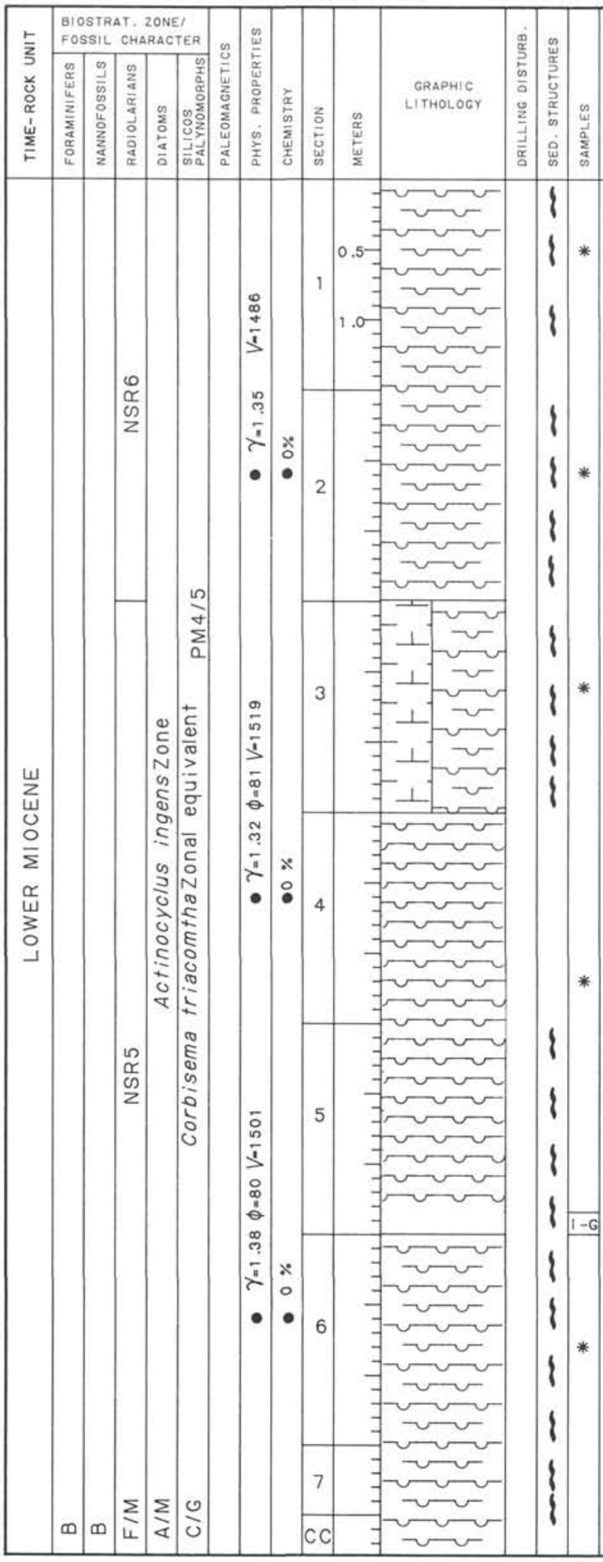

LITHOLOGIC DESCRIPTION

DIATOM OOZE

Entire core is undisturbed.

Major lithology: Diatom ooze, grayish green (10GY 5/2), moderately bioturbated and mottled, with common olive gray (5Y 4/2) color banding. Section 1 to Section 2; Section 4 to CC. Section 3 is a nannofossil-diatom ooze.

Minor lithology: Volcanic ash, in discrete layers of varying thickness: Section 1, 134 cm; Section 2, 21–22 cm (light gray ash); Section 6, 43–48 cm (gray ash).

SMEAR SLIDE SUMMARY (%):

	1, 50 D	2, 55 D	3, 60 D	4, 120 D	6, 80 D
TEXTURE:					
Sand	15	15	10	20	15
Silt	55	60	45	60	55
Clay	30	25	45	20	30
COMPOSITION:					
Quartz	10	5	1	5	20
Clay	23	14	24	19	24
Nannofossils	—	—	20	—	—
Diatoms	50	60	40	55	40
Radiolarians	5	5	2	5	5
Sponge spicules	10	15	10	15	10
Silicoflagellates	2	1	1	1	1

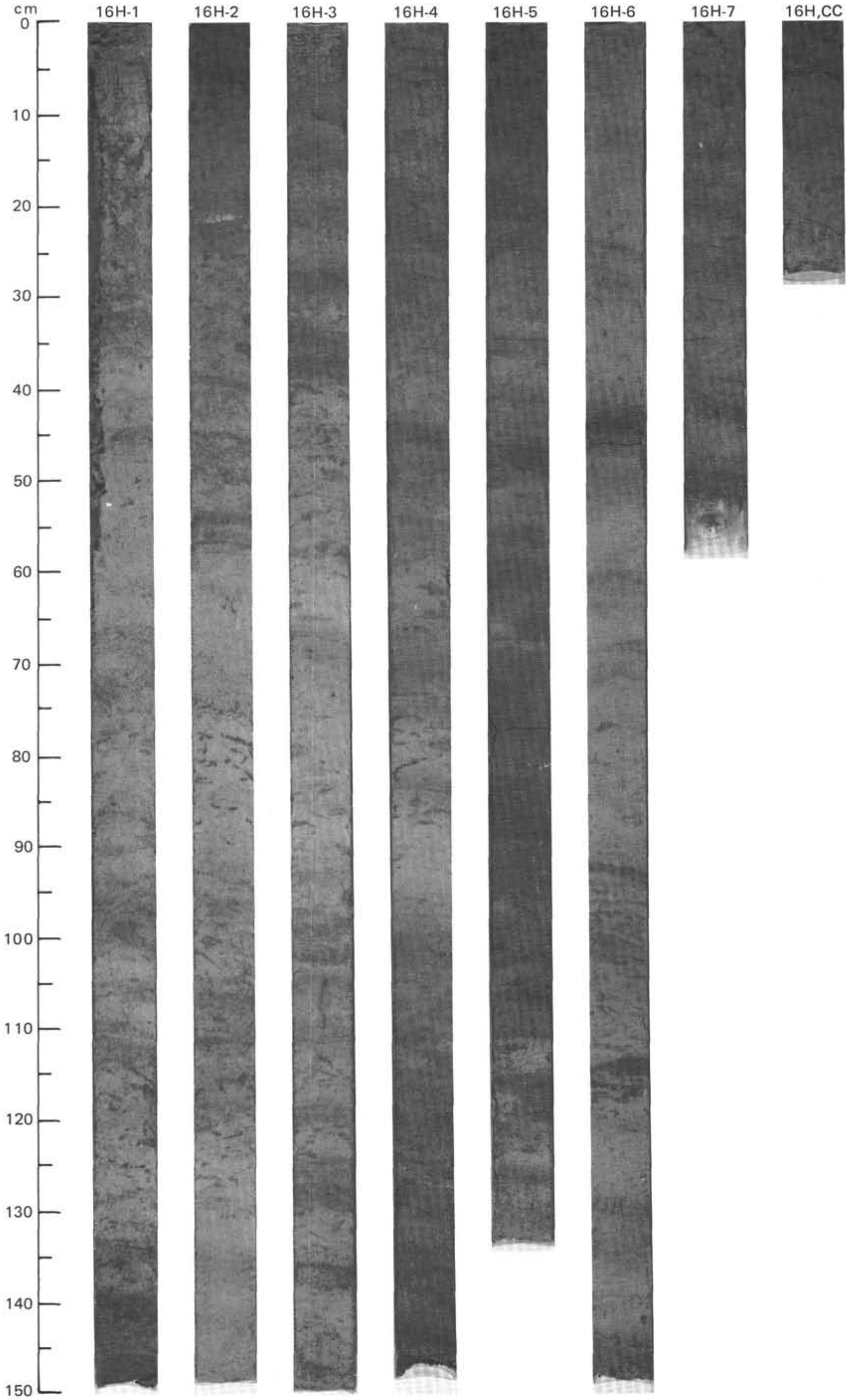
cm
0
10
20
30
40
50
60
70
80
90
100
110
120
130
140
150
16H-1
16H-2
16H-3
16H-4
16H-5
16H-6
16H-7
16H,CC

SITE 643 HOLE A CORE 17X CORED INTERVAL 2927.6-2937.1 mbsl; 147.8-157.3 mbsf

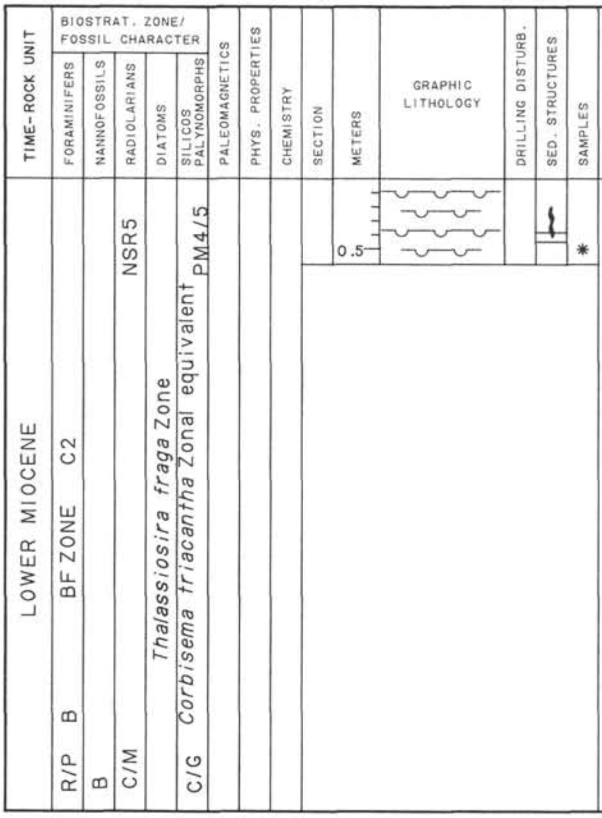

LITHOLOGIC DESCRIPTION

DIATOM OOZE

Entire core is undisturbed.

Major lithology: Diatom ooze, grayish green (5G 5/2) to olive gray (5Y 4/2), moderately bioturbated and mottled.

Minor lithology: Volcanic ash, dark gray discrete layer. Section 1, 40–43 cm.

SMEAR SLIDE SUMMARY (%):

	1, 50 D
TEXTURE:	
Sand	15
Silt	55
Clay	30
COMPOSITION:	
Quartz	10
Clay	24
Diatoms	50
Radiolarians	5
Sponge spicules	10
Silicoflagellates	1

SITE 643 HOLE A CORE 18X CORED INTERVAL 2937.1-2946.6 mbsl; 157.3-166.8 mbsf

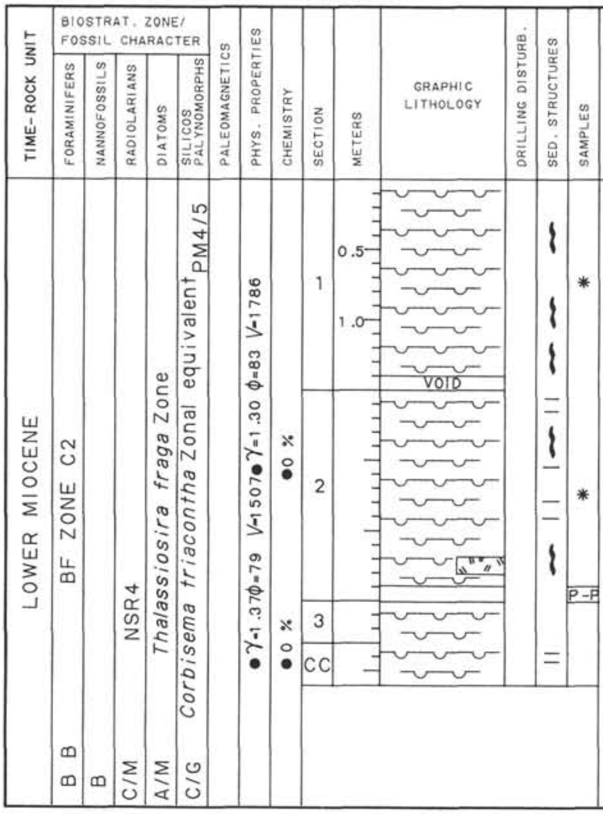

LITHOLOGIC DESCRIPTION

DIATOM OOZE

Entire core is undisturbed.

Major lithology: Diatom ooze, grayish green (5GY 5/2), moderately bioturbated and mottled. Olive gray (5Y 4/2) color banding common.

Minor lithology: Volcanic ash, dark gray (5Y 4/1) and disseminated. Section 2, 125–126 and 128–130 cm.

SMEAR SLIDE SUMMARY (%):

	1, 86 D	2, 79 D
TEXTURE:		
Sand	20	20
Silt	60	50
Clay	29	30
COMPOSITION:		
Quartz	5	5
Clay	19	25
Diatoms	55	50
Radiolarians	5	5
Sponge spicules	15	15
Silicoflagellates	1	1

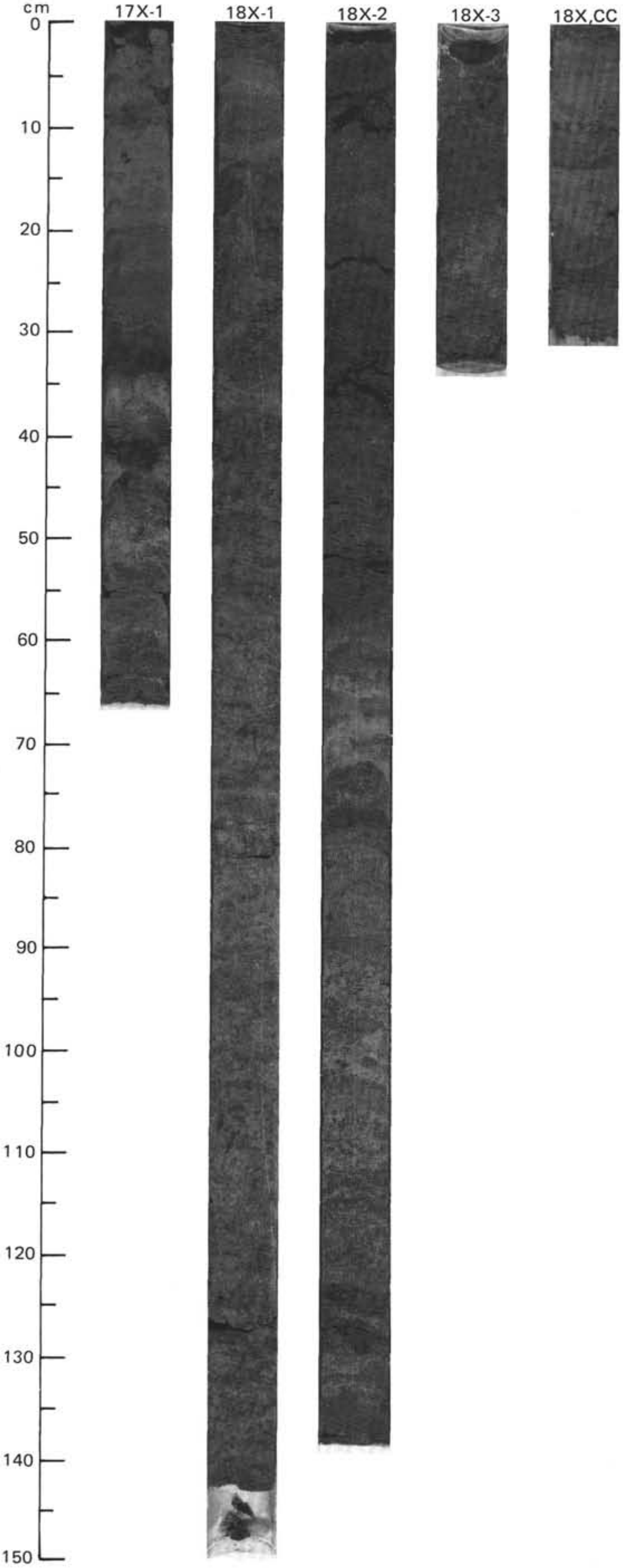
cm
0
10
20
30
40
50
60
70
80
90
100
110
120
130
140
150
17X-1
18X-1
18X-2
18X-3
18X,CC

SITE 643 HOLE A CORE 19X CORED INTERVAL 2946.6-2956.1 mbsl; 166.8-176.3 mbsf

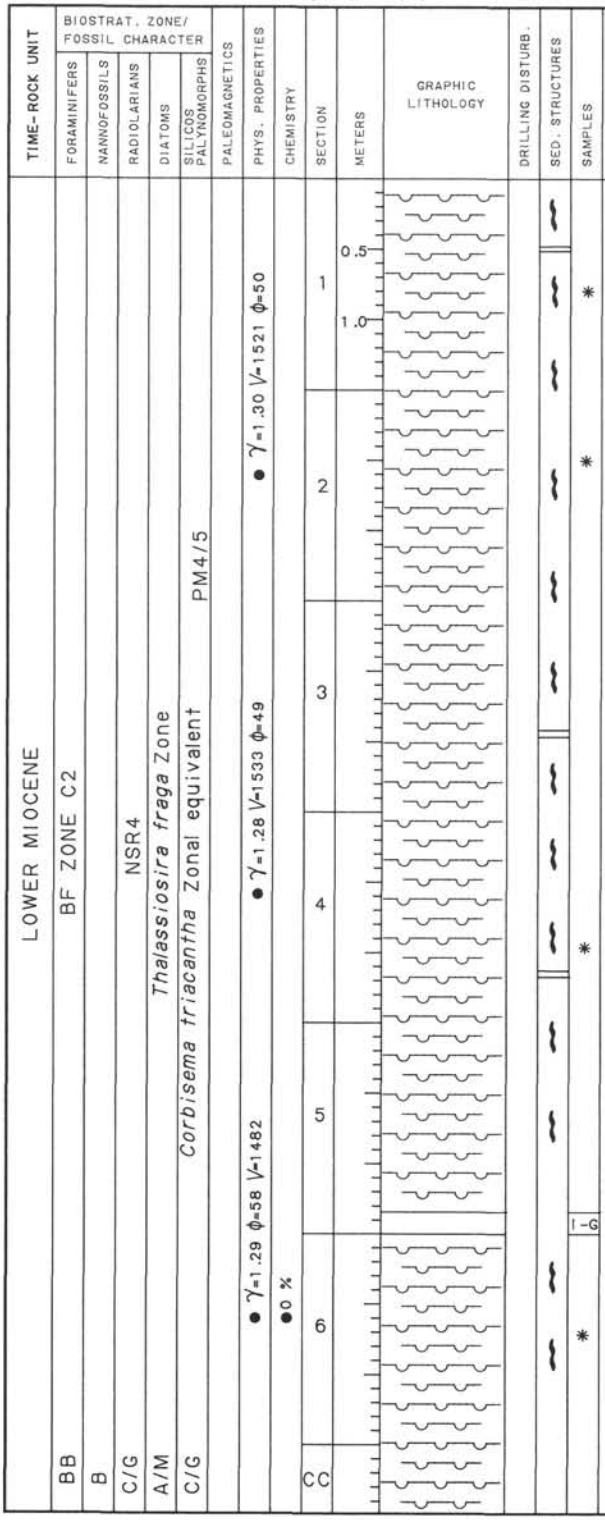

LITHOLOGIC DESCRIPTION

DIATOM OOZE

Section 1, 0–30 cm is slightly disturbed. The remainder of the core is undisturbed.

Major lithology: Diatom ooze, grayish green (5G 5/2), moderatley bioturbated and mottled. Rare to common diffuse color banding in olive gray (5Y 4/2) and greenish gray (5GY 5/1).

Minor lithology: Volcanic ash. Very dark gray (5Y 3/1) discrete ash, Section 1, 48–51 cm; dark gray (5Y 4/1) discrete ash, Section 3, 92–97 cm; light gray (5Y 6/1) discrete ash, Section 4, 117 cm.

SMEAR SLIDE SUMMARY (%):

	1, 81 D	2, 47 D	4, 92 D	6, 72 D
TEXTURE:				
Sand	15	15	15	20
Silt	65	55	50	60
Clay	20	30	35	20
COMPOSITION:				
Quartz	5	5	5	5
Feldspar	—	—	1	—
Clay	12	23	21	18
Volcanic glass	1	1	1	—
Accessory minerals	—	1	—	—
Diatoms	60	55	50	55
Radiolarians	5	5	5	5
Sponge spicules	15	10	15	15
Silicoflagellates	1	1	2	2

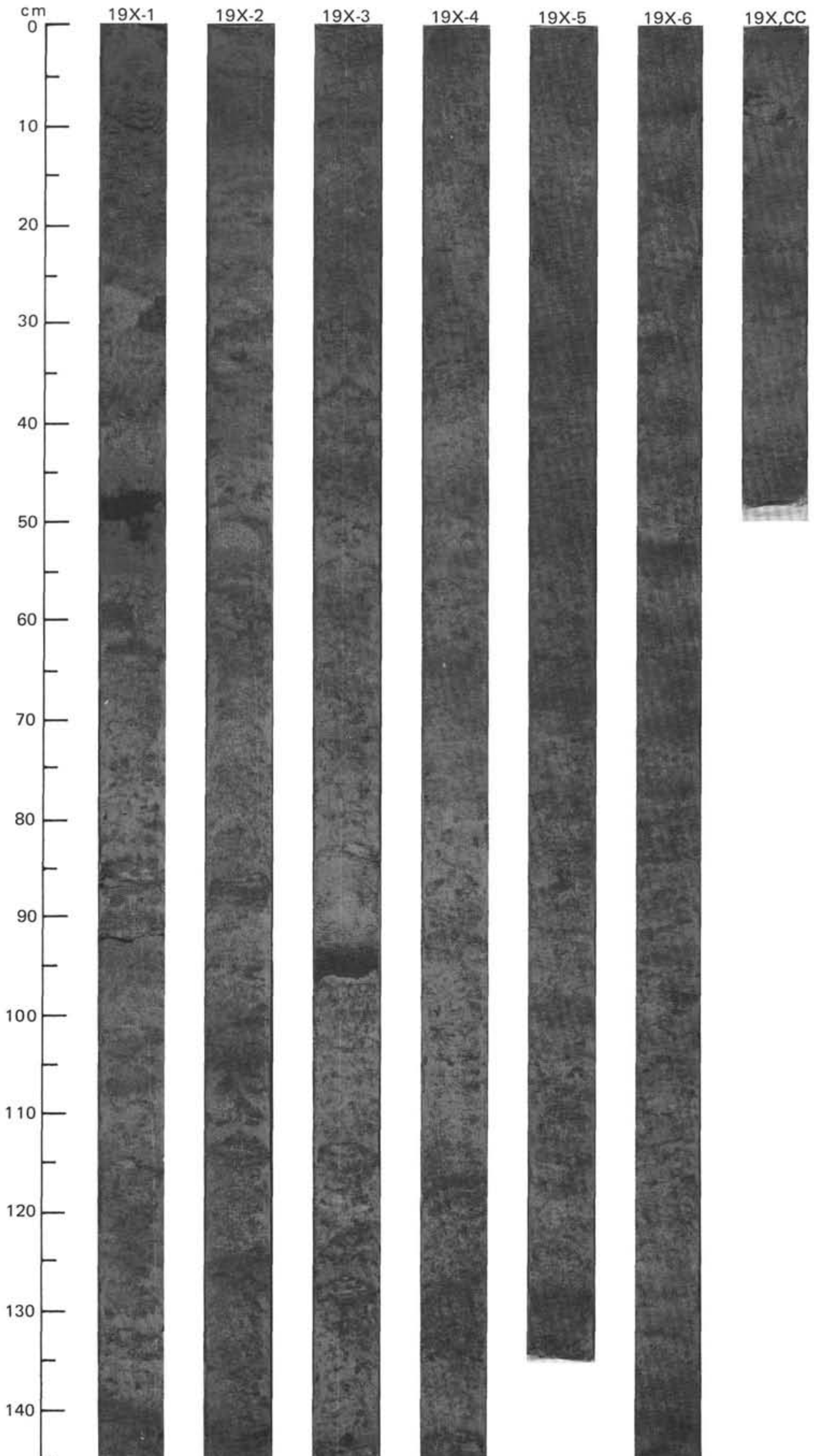
cm
0
10
20
30
40
50
60
70
80
90
100
110
120
130
140
150
19X-1
19X-2
19X-3
19X-4
19X-5
19X-6
19X,CC

SITE 643 HOLE A CORE 20X CORED INTERVAL 2956.1-2965.6 mbsl; 176.3-185.8 mbsf

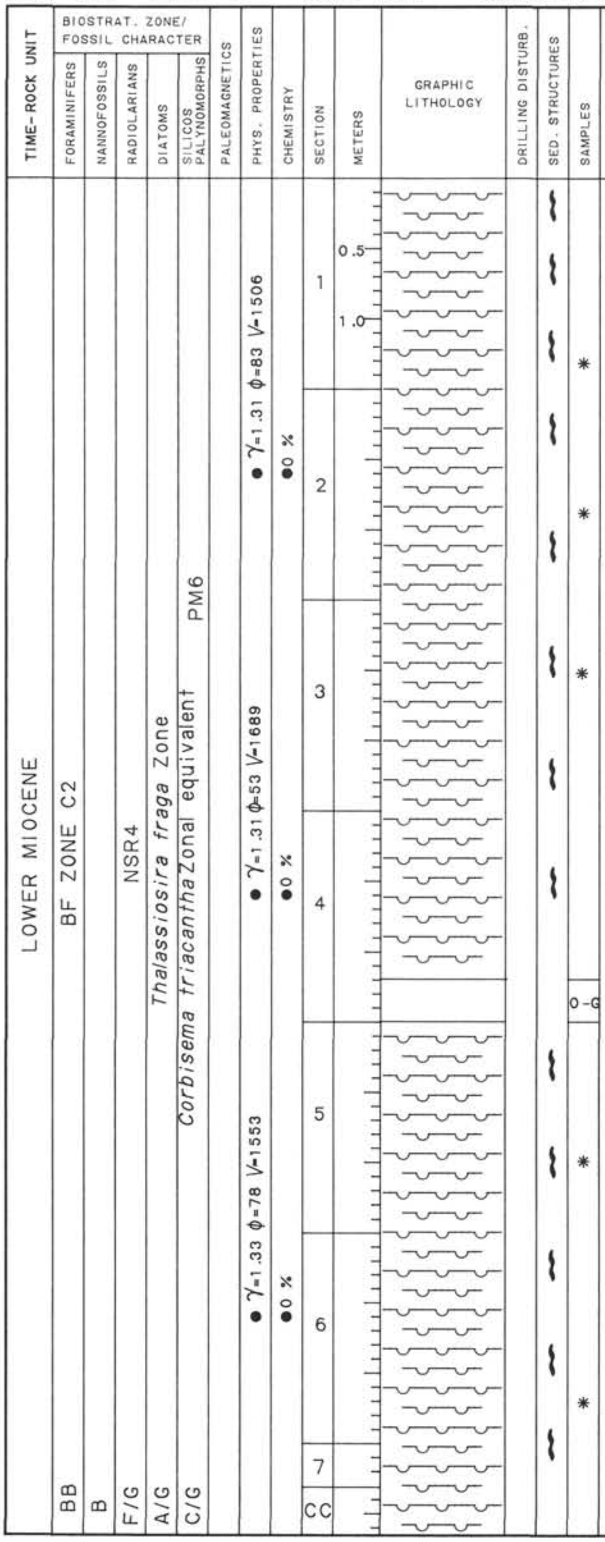

LITHOLOGIC DESCRIPTION

DIATOM OOZE

Entire core is undeformed.

Major lithology: Diatom ooze, grayish green (5G 5/2) to olive gray (5Y 4/2), moderately bioturbated and mottled with olive gray (5Y 4/2) and minor dark greenish gray (5GY 4/1). Rare diffuse color banding in same colors.

SMEAR SLIDE SUMMARY (%):

	1, 130 D	2, 93 D	3, 50 D	5, 100 D	6, 111 D
TEXTURE:					
Sand	20	20	5	5	10
Silt	65	60	80	75	80
Clay	15	20	15	20	10
COMPOSITION:					
Quartz	5	5	1	1	5
Feldspar	1	—	—	—	—
Clay	12	18	20	10	10
Volcanic glass	1	—	—	1	—
Diatoms	60	50	65	70	50
Radiolarians	5	5	1	1	2
Sponge spicules	15	20	10	15	30
Silicoflagellates	1	2	3	3	3

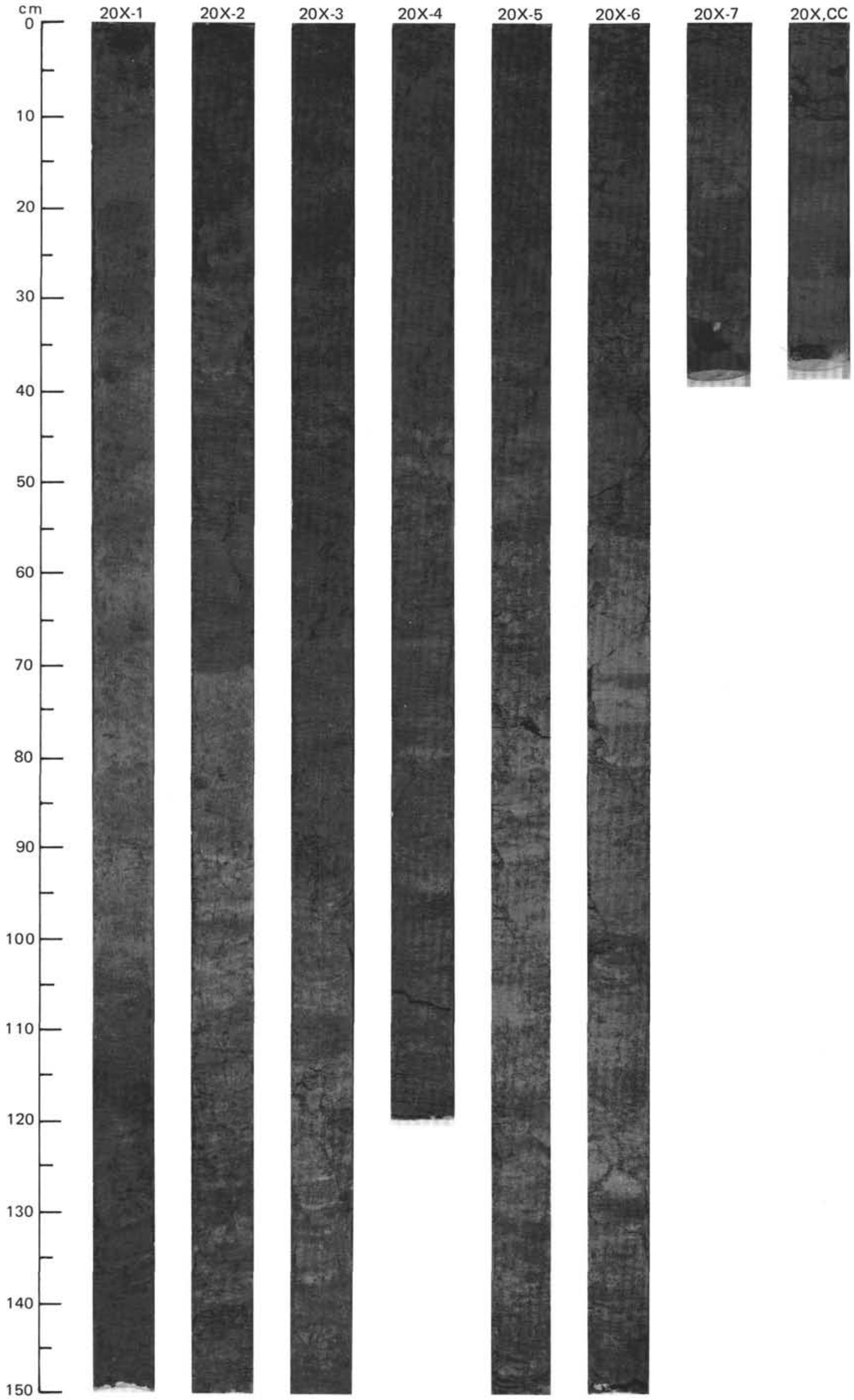
cm
0
10
20
30
40
50
60
70
80
90
100
110
120
130
140
150
20X-1
20X-2
20X-3
20X-4
20X-5
20X-6
20X-7
20X,CC

SITE 643 HOLE A CORE 21X CORED INTERVAL 2965.6-2975.1 mbsl; 185.8-195.3 mbsf

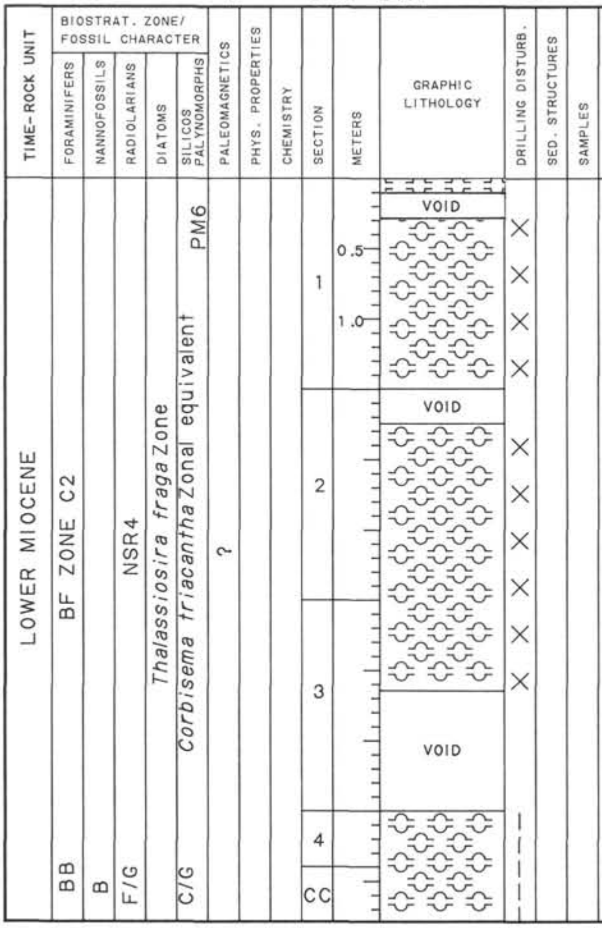

LITHOLOGIC DESCRIPTION

SILICEOUS OOZE

Sections 1, 2, and 3 are completely deformed by drilling, with orientation unknown. Section 4 and the CC are moderately deformed.

Major lithology: Siliceous ooze, greenish gray (5GY 5/1), with minor bioturbation and mottling, and minor diffuse color banding.

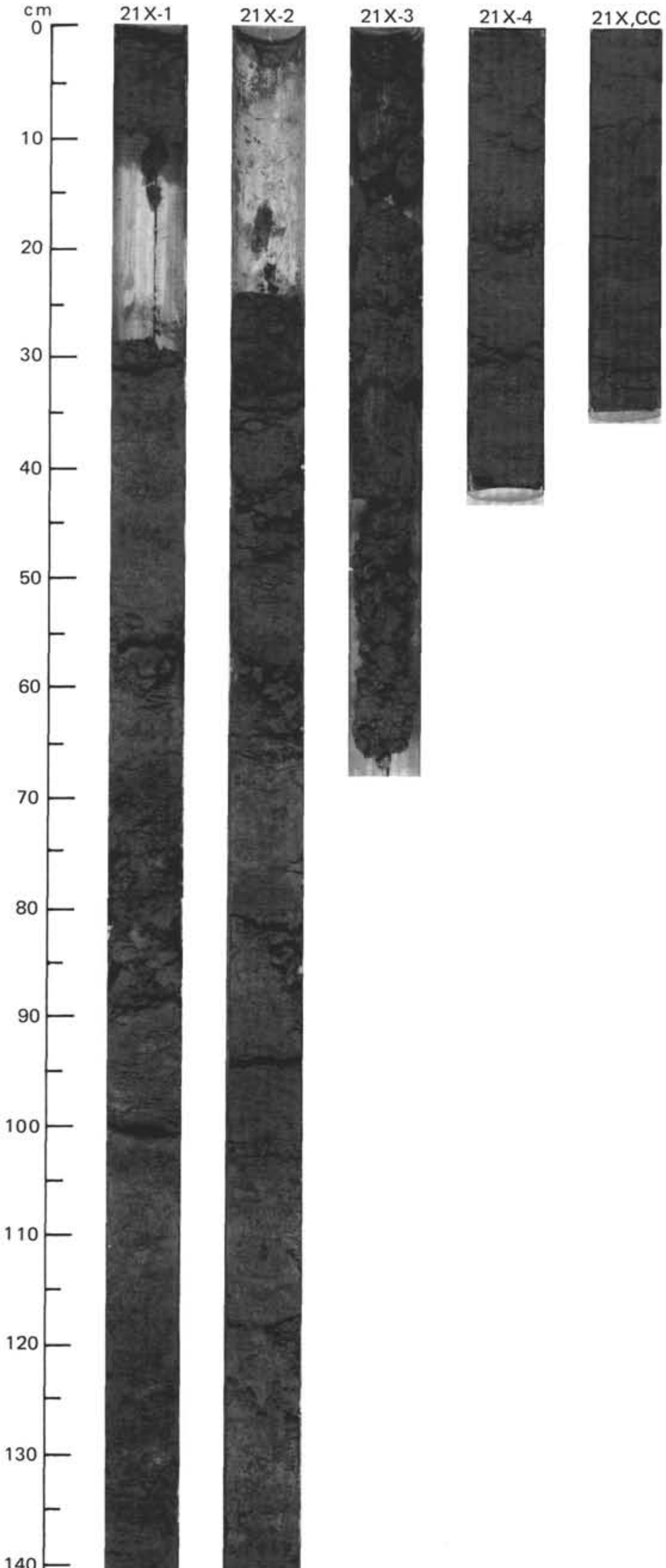
cm
0
10
20
30
40
50
60
70
80
90
100
110
120
130
140
150
21X-1
21X-2
21X-3
21X-4
21X,CC

SITE 643 HOLE A CORE 22X CORED INTERVAL 2975.1-2984.9 mbsl; 195.3-205.1 mbsf

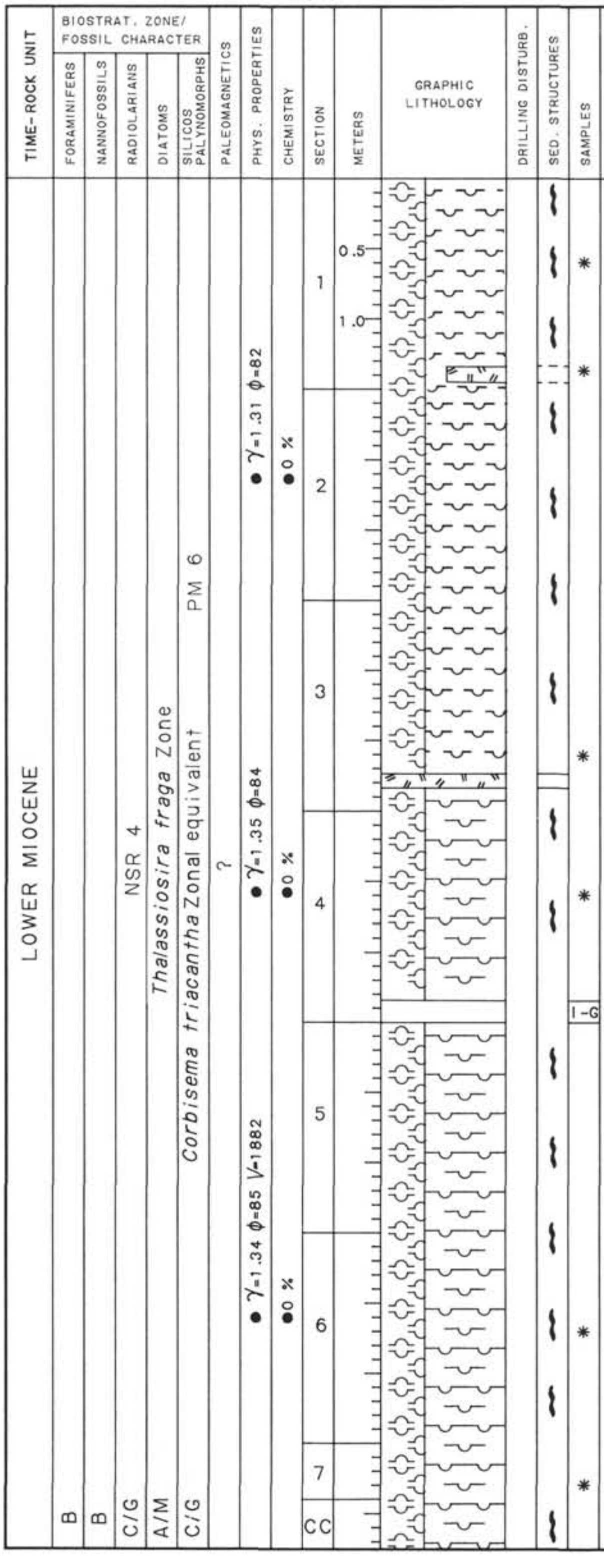

LITHOLOGIC DESCRIPTION

DIATOM OOZE AND SILICEOUS OOZE

Entire core is undisturbed.

Major lithology: Diatom ooze and siliceous ooze, olive gray (5Y 4/2) and greenish gray (5GY 5/1), moderately bioturbated and mottled.

Minor lithology: Volcanic ash. Black sandy ash, partially to completely disseminated, Section 1, 134–144 cm; black sandy ash in discrete layer, Section 3, 126–129 cm.

SMEAR SLIDE SUMMARY (%):

	1, 56 D	1, 135 M	3, 110 M	4, 64 D	6, 63 D	7, 18 M
TEXTURE:						
Sand	15	90	5	5	10	—
Silt	70	—	70	70	65	80
Clay	15	10	25	25	25	20
COMPOSITION:						
Quartz	4	10	—	3	5	—
Clay	15	—	20	25	20	10
Volcanic glass	1	90	1	—	—	—
Diatoms	45	—	40	40	50	45
Radiolarians	2	—	1	5	1	1
Sponge spicules	30	—	35	25	20	40
Silicoflagellates	3	—	2	2	3	4

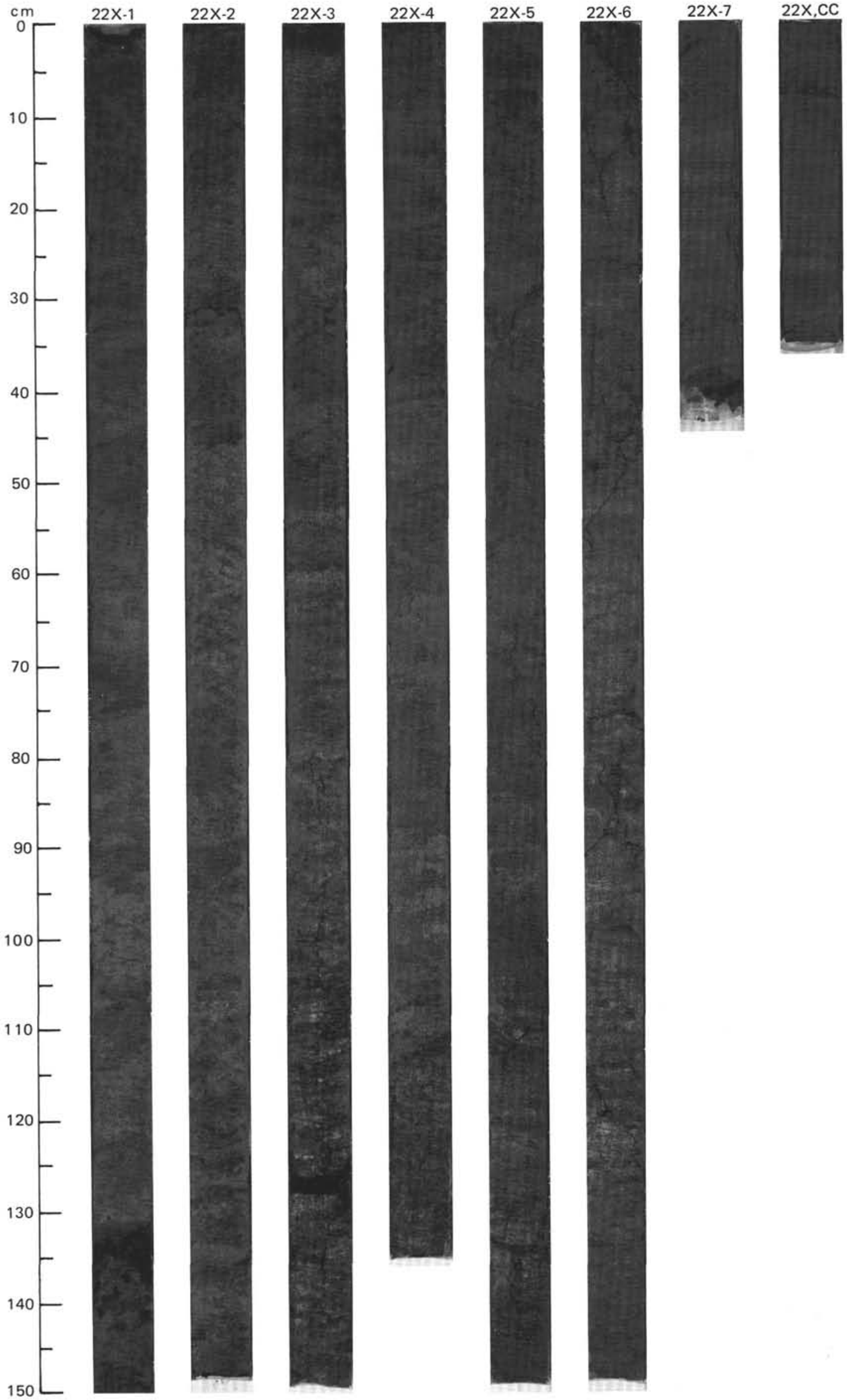
cm
0
10
20
30
40
50
60
70
80
90
100
110
120
130
140
150
22X-1
22X-2
22X-3
22X-4
22X-5
22X-6
22X-7
22X,CC

SITE 643 HOLE A CORE 23X CORED INTERVAL 2984.9-2994.7 mbsl; 205.1-214.9 mbsf

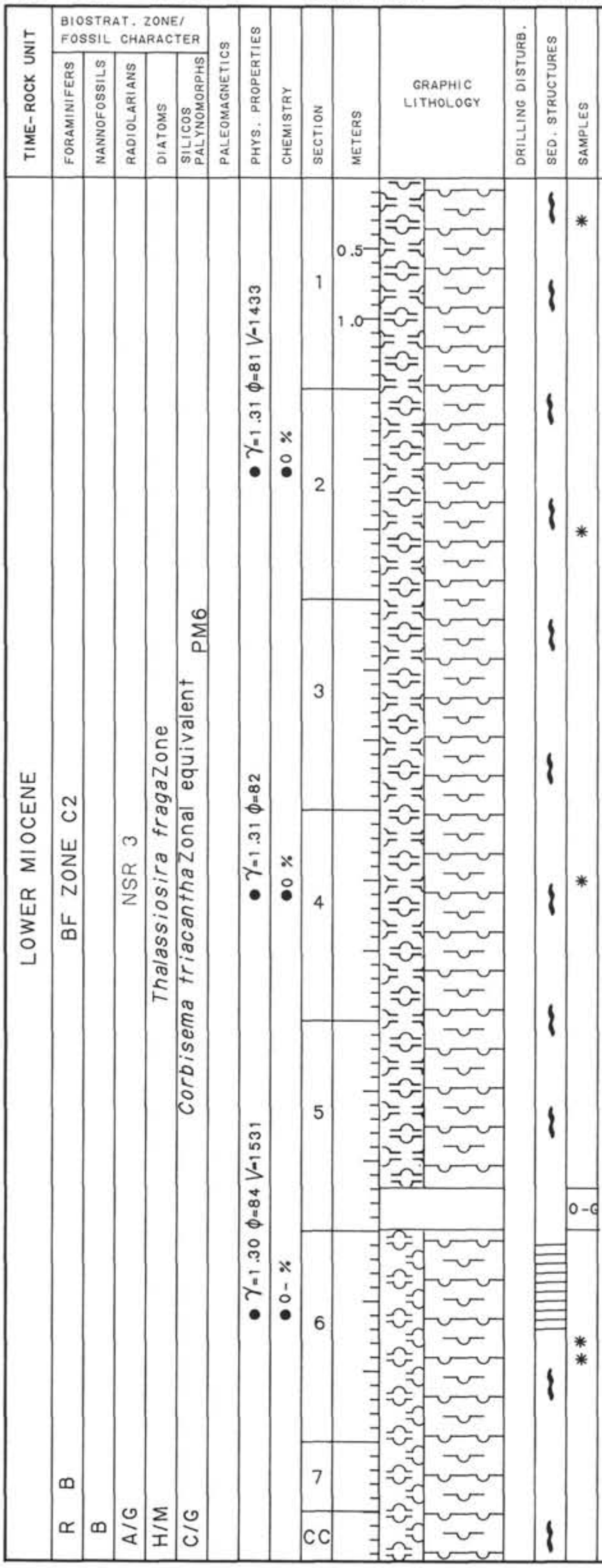

LITHOLOGIC DESCRIPTION

DIATOM OOZE AND SILICEOUS OOZE

Entire core is undisturbed.

Major lithology: Diatom ooze and siliceous ooze, olive gray (5Y 4/2), greenish gray (5GY 5/1), and minor dark grayish brown (2.5Y 4/2), moderately bioturbated and mottled. Faint color banding in Section 6, 0–70 cm.

SMEAR SLIDE SUMMARY (%):

	1, 30 M	2, 100 D	4, 52 D	6, 78 D	6, 88 M
TEXTURE:					
Sand	5	—	—	—	—
Silt	75	80	70	80	80
Clay	20	20	30	20	20
COMPOSITION:					
Quartz	3	—	—	—	—
Clay	15	10	20	10	20
Accessory minerals:					
Pyrite	20	—	—	—	—
Diatoms	35	50	40	50	30
Radiolarians	1	8	5	5	2
Sponge spicules	25	30	30	30	40
Silicoflagellates	1	2	5	5	8

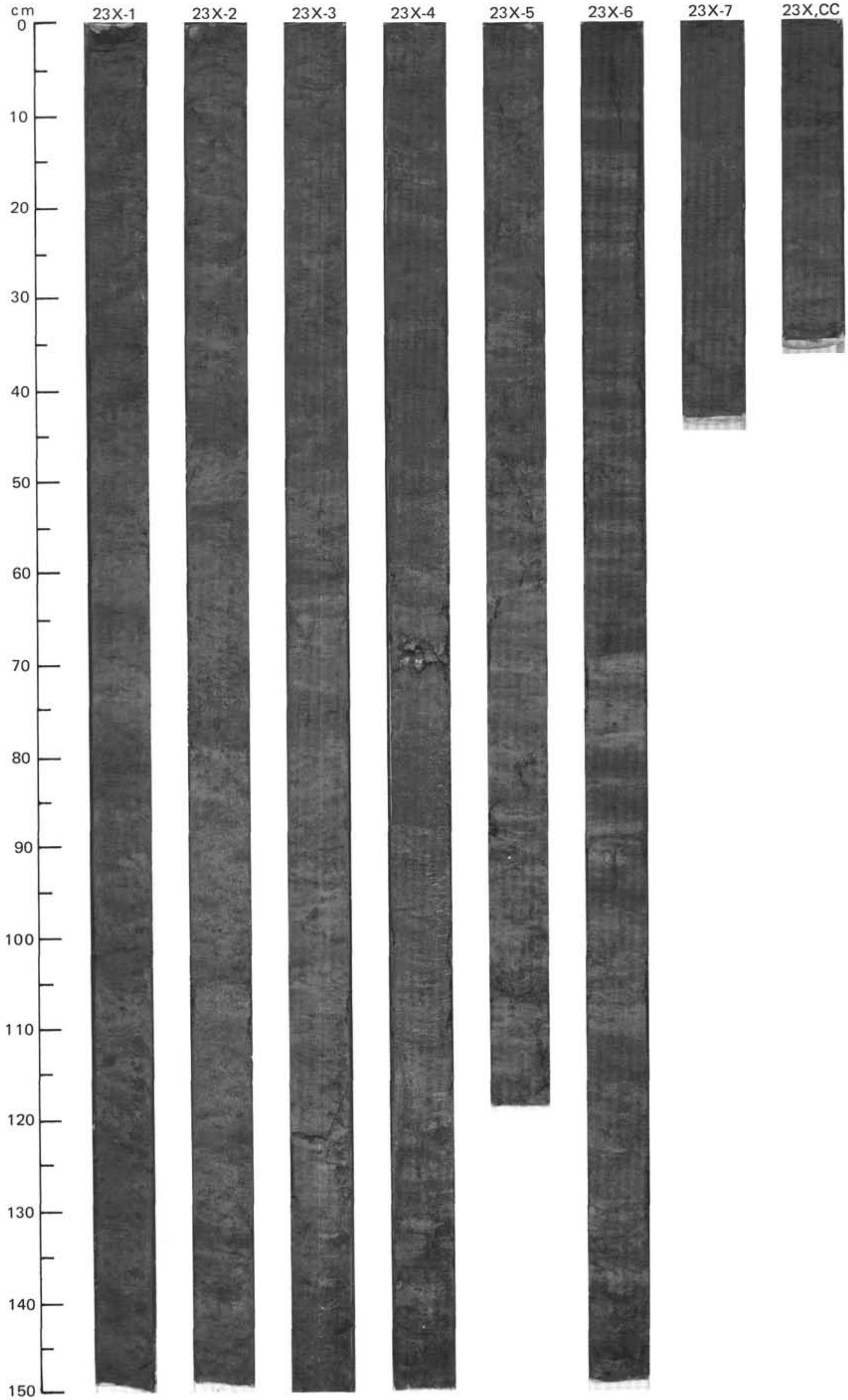
cm
0
10
20
30
40
50
60
70
80
90
100
110
120
130
140
150
23X-1
23X-2
23X-3
23X-4
23X-5
23X-6
23X-7
23X,CC

SITE 643 HOLE A CORE 24X CORED INTERVAL 2994.7-3004.5 mbsl; 214.9-224.7 mbsf

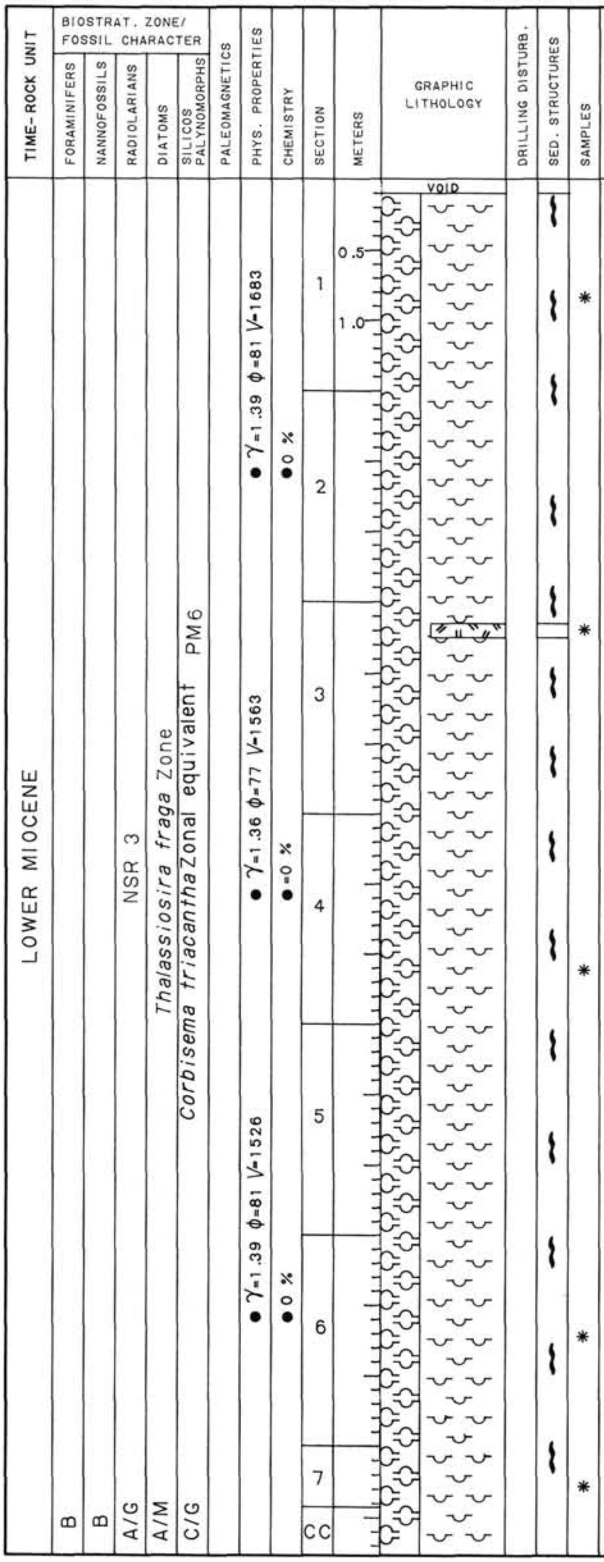

LITHOLOGIC DESCRIPTION

DIATOM OOZE AND SILICEOUS OOZE

Section 1, 0–70 cm, highly disturbed to displaced. Remainder of the core is undisturbed.

Major lithology: Diatom ooze and siliceous ooze, olive gray (5Y 4/2) to greenish gray (5GY 5/1), lightly to moderately bioturbated and mottled.

Minor lithology: Volcanic ash, gray and sandy, in a discrete layer with irregular surfaces; Section 3, 19–25 cm.

SMEAR SLIDE SUMMARY (%):

	1, 80 D	3, 18 M	4, 110 D	6, 73 D	7, 38 D
TEXTURE:					
Sand	5	30	—	10	—
Silt	80	60	70	80	75
Clay	15	10	30	10	25
COMPOSITION:					
Clay	10	5	20	10	20
Volcanic glass	—	60	5	1	1
Diatoms	50	20	40	50	35
Radiolarians	3	—	3	2	1
Sponge spicules	35	15	30	25	40
Silicoflagellates	2	—	2	2	3

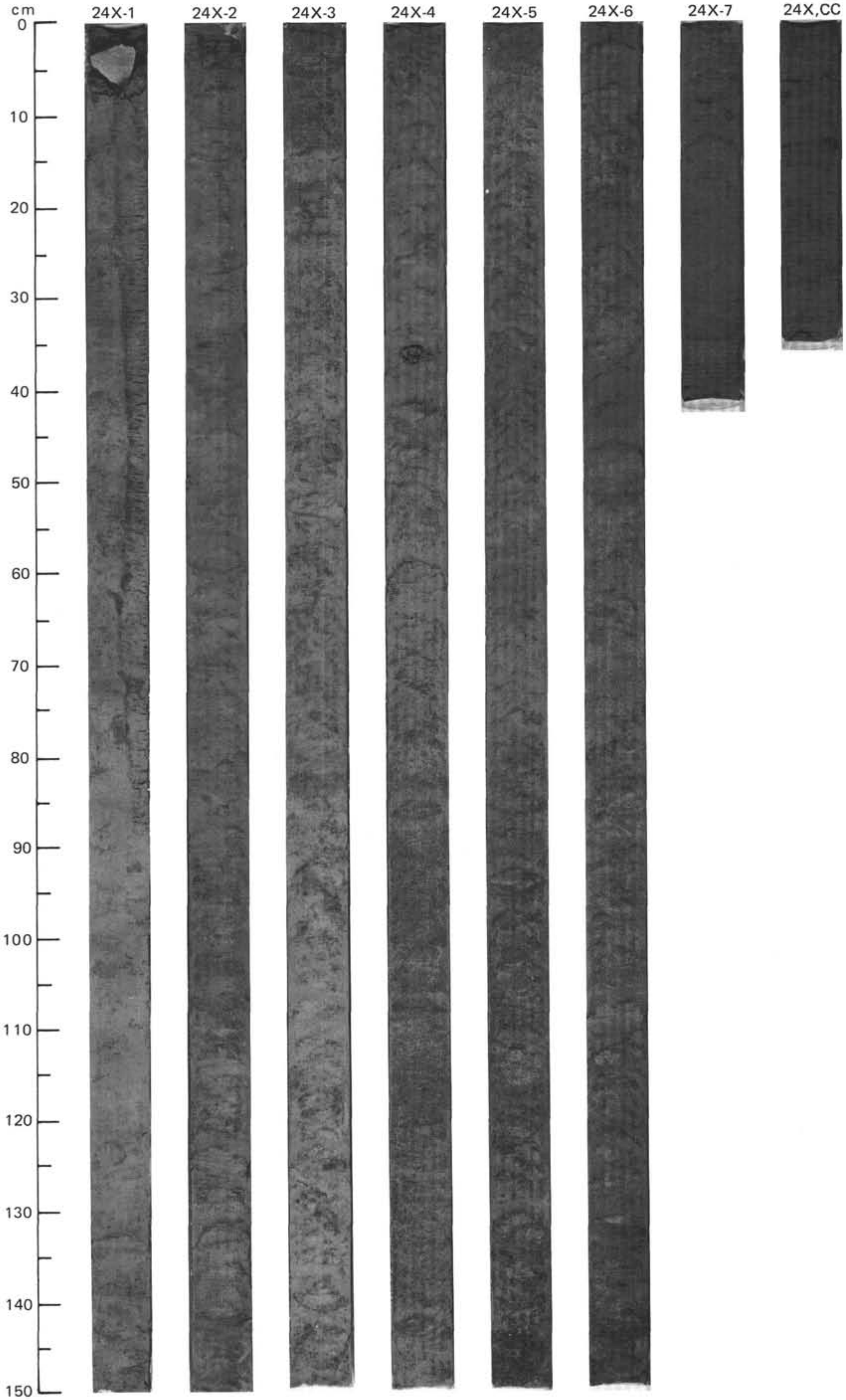
cm
0
10
20
30
40
50
60
70
80
90
100
110
120
130
140
150
24X-1
24X-2
24X-3
24X-4
24X-5
24X-6
24X-7
24X,CC

SITE 643 HOLE A CORE 25X CORED INTERVAL 3004.5-3014.3 mbsl; 224.7-234.5 mbsf

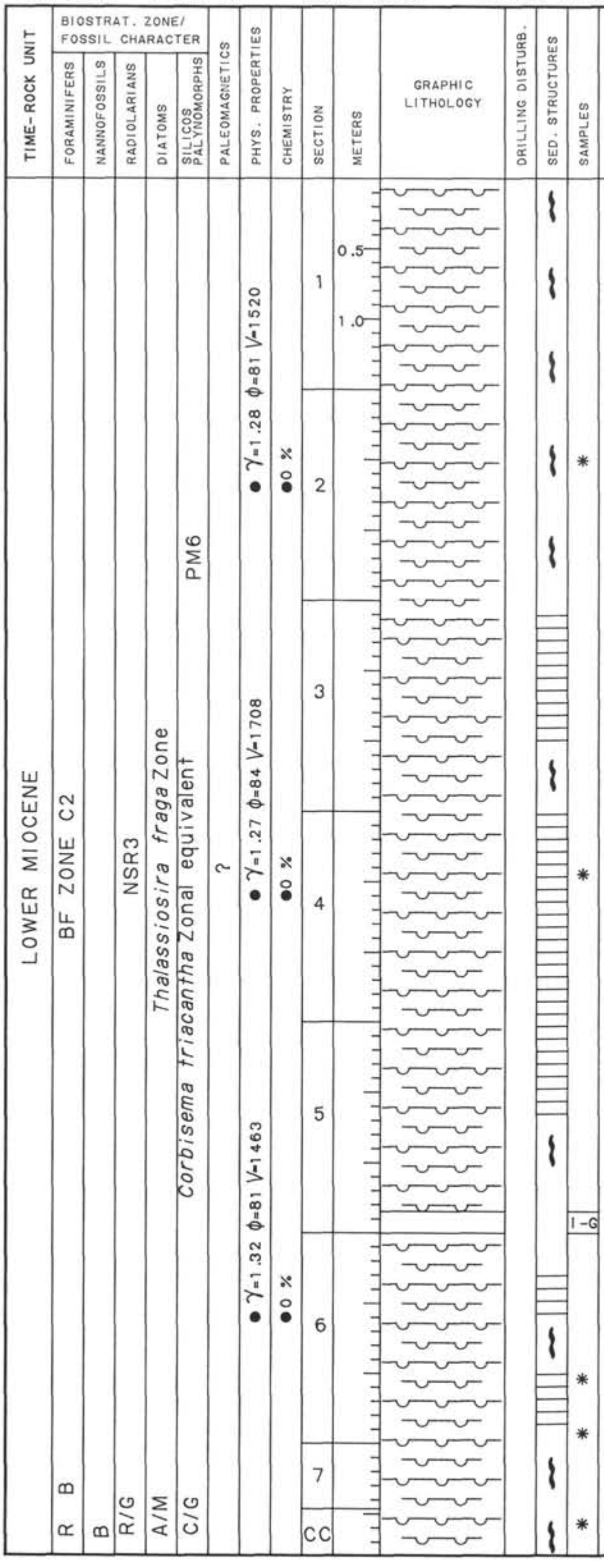

LITHOLOGIC DESCRIPTION

DIATOM OOZE

Entire core is undisturbed.

Major lithology: Diatom ooze, olive gray (5Y 5/2 to 5Y 4/2), with minor to moderate bioturbation and mottling. Indistinct color banding with greenish gray (5GY 5/1) and minor very dark gray (5Y 3/1) in Section 3, 0–100 cm; Section 4; Section 5, 2–15 and 27–64 cm; Section 6, 25–60 and 100–135 cm.

Minor lithology: Volcanic ash, black, pyritized, and sandy, in a thin, discrete lamination; CC, 11 cm.

SMEAR SLIDE SUMMARY (%):

	2, 50 D	4, 45 M	6, 100 D	6, 140 D	CC, 12 M
TEXTURE:					
Sand	15	5	20	15	60
Silt	65	65	65	65	30
Clay	20	30	15	20	10
COMPOSITION:					
Clay	15	25	10	15	5
Volcanic glass	2	—	—	1	50
Accessory minerals:					
Pyrite	—	5	—	—	—
Diatoms	50	40	60	50	25
Radiolarians	5	1	2	2	—
Sponge spicules	25	25	25	30	20
Silicoflagellates	3	4	3	2	—

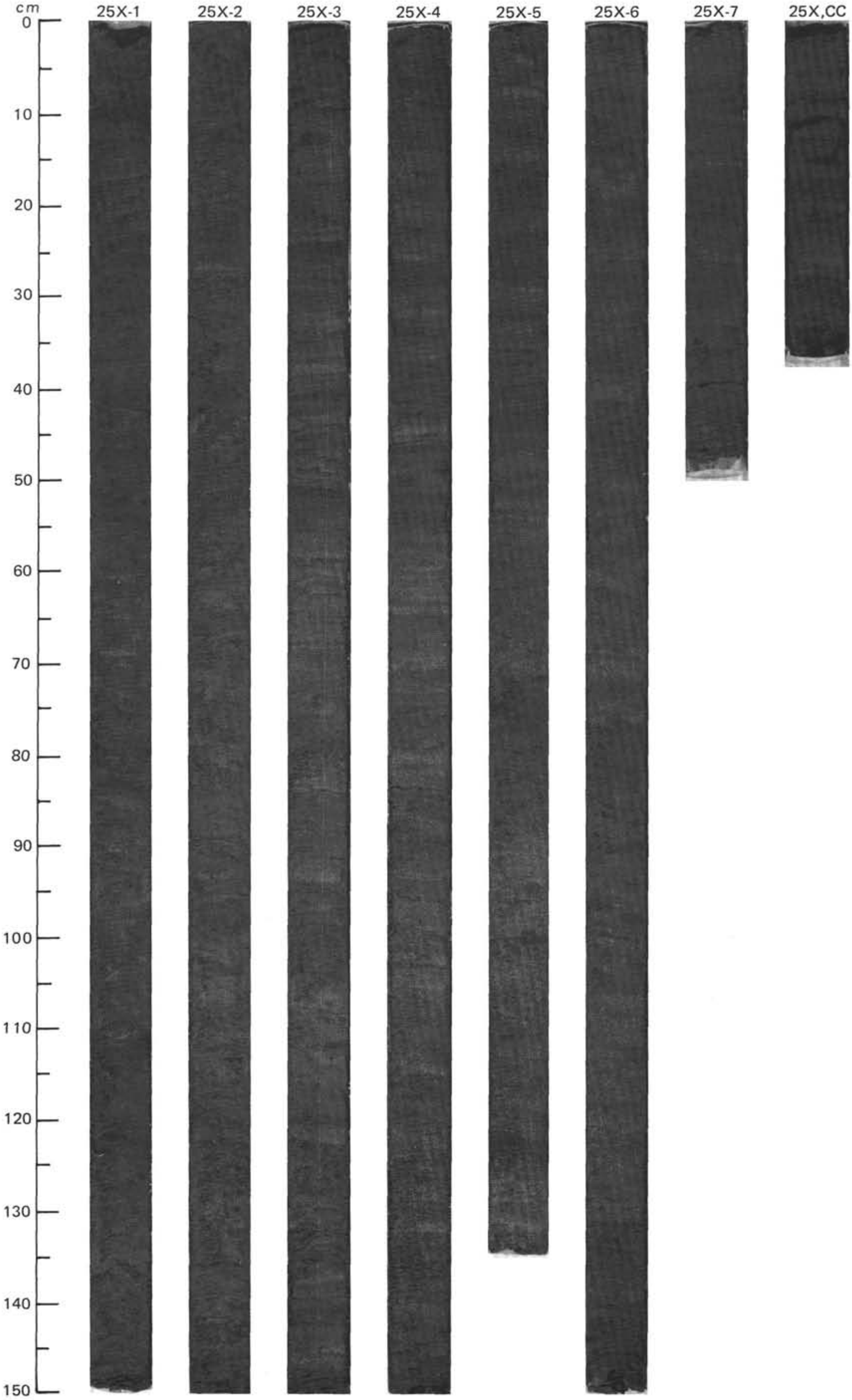
cm
0
10
20
30
40
50
60
70
80
90
100
110
120
130
140
150
25X-1
25X-2
25X-3
25X-4
25X-5
25X-6
25X-7
25X,CC

SITE 643 HOLE A CORE 26X CORED INTERVAL 3014.3-3024.1 mbsl; 234.5-244.3 mbsf

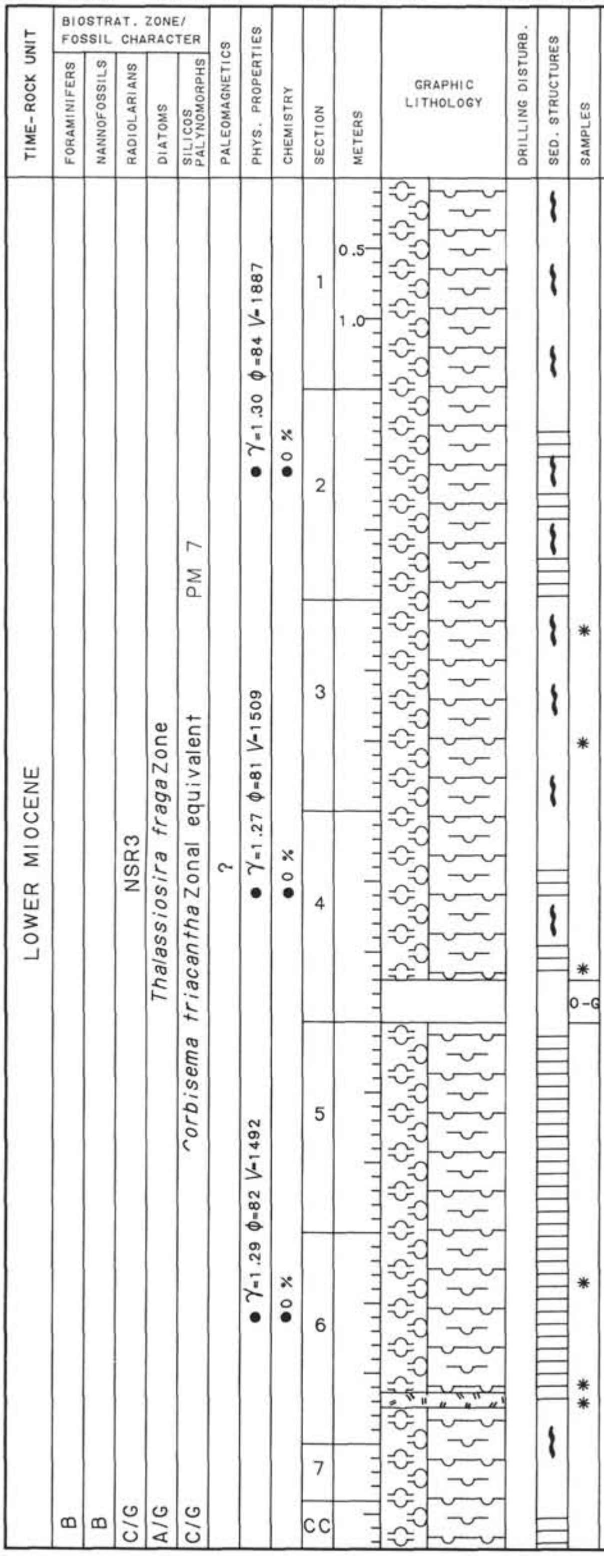

LITHOLOGIC DESCRIPTION

DIATOM OOZE AND SILICEOUS OOZE

Entire core is undisturbed.

Major lithology: Diatom ooze, greenish gray (5GY 5/1), and siliceous ooze, olive gray (5Y 5/2 to 5Y 4/2), either bioturbated and mottled together or indistinctly interbedded. Faint color banding best developed at Section 2, 25–40, 75–95, and 115–140 cm; Section 4, 40–55 and 85–102 cm; Section 5 to Section 6, 102 cm; CC, 12–32 cm.

Minor lithology: Volcanic ash: black, sandy, partially disseminated ash, Section 4, 117–119 cm; gray, sandy, discrete ash layer, Section 6, 116–119 cm.

SMEAR SLIDE SUMMARY (%):

	3, 18 M	3, 99 D	4, 119 M	6, 35 D	6, 105 D	6, 117 M
TEXTURE:						
Sand	95	20	50	5	10	60
Silt	—	60	25	85	75	35
Clay	5	20	25	10	15	5
COMPOSITION:						
Clay	—	20	25	10	10	5
Volcanic glass	—	—	40	—	3	90
Accessory minerals:						
Pyrite	—	—	—	—	—	5
Diatoms	5	45	20	40	40	—
Radiolarians	—	1	—	—	2	—
Sponge spicules	95	30	15	45	30	—
Silicoflagellates	—	4	—	5	5	—

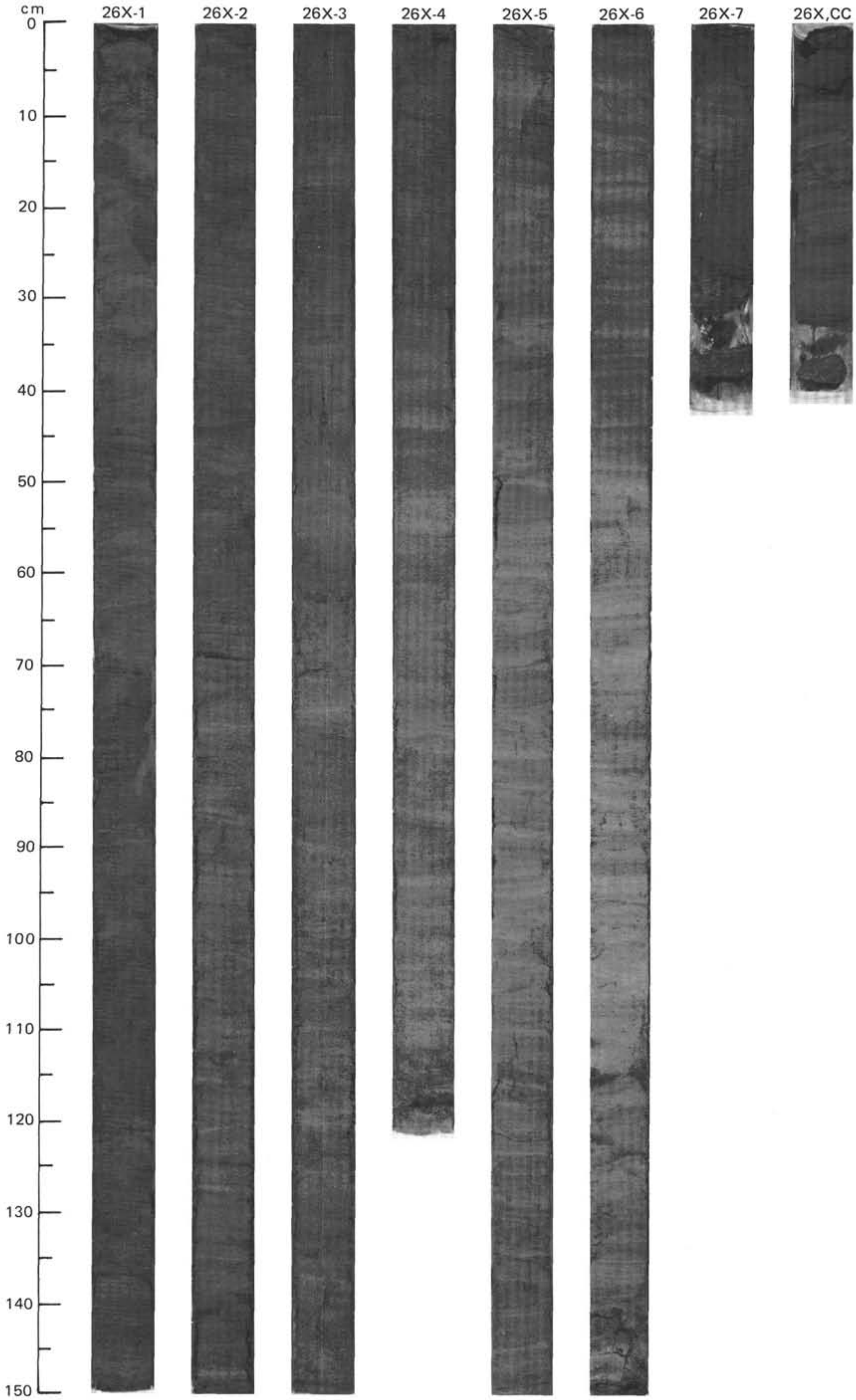
cm
0
10
20
30
40
50
60
70
80
90
100
110
120
130
140
150
26X-1
26X-2
26X-3
26X-4
26X-5
26X-6
26X-7
26X,CC

SITE 643 HOLE A CORE 27X CORED INTERVAL 3024.1-3033.9 mbsl; 244.3-254.1 mbsf

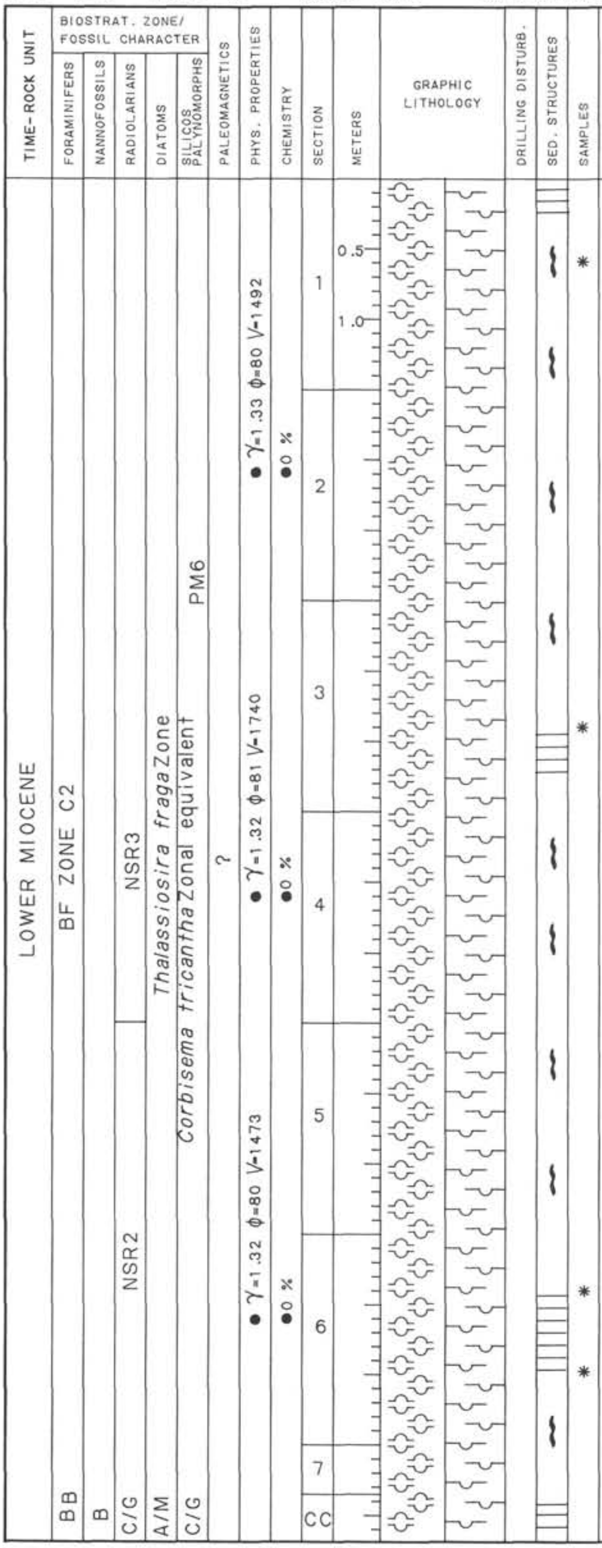

LITHOLOGIC DESCRIPTION

DIATOM OOZE AND SILICEOUS OOZE

Sections 4 and 5 are slightly disturbed. Remainder of the core is undisturbed.

Major lithology: Diatom ooze and siliceous ooze, olive gray (5Y 4/2), greenish gray (5GY 5/1), to very dark grayish brown (2.5YR 3/2). Bioturbation and mottling minor to common, with faint color banding at Section 1, 7–25 cm; Section 3, 100–130 cm; Section 6, 45–100 cm; CC, 12–20 and 26–33 cm.

SMEAR SLIDE SUMMARY (%):

	1, 59 D	3, 86 D	6, 40 D	6, 98 M
TEXTURE:				
Sand	10	—	—	—
Silt	80	70	70	80
Clay	10	30	30	20
COMPOSITION:				
Clay	10	25	—	—
Volcanic glass	Tr	1	—	—
Diatoms	55	30	30	40
Radiolarians	2	1	3	5
Sponge spicules	30	40	40	30
Silicoflagellates	3	3	2	5

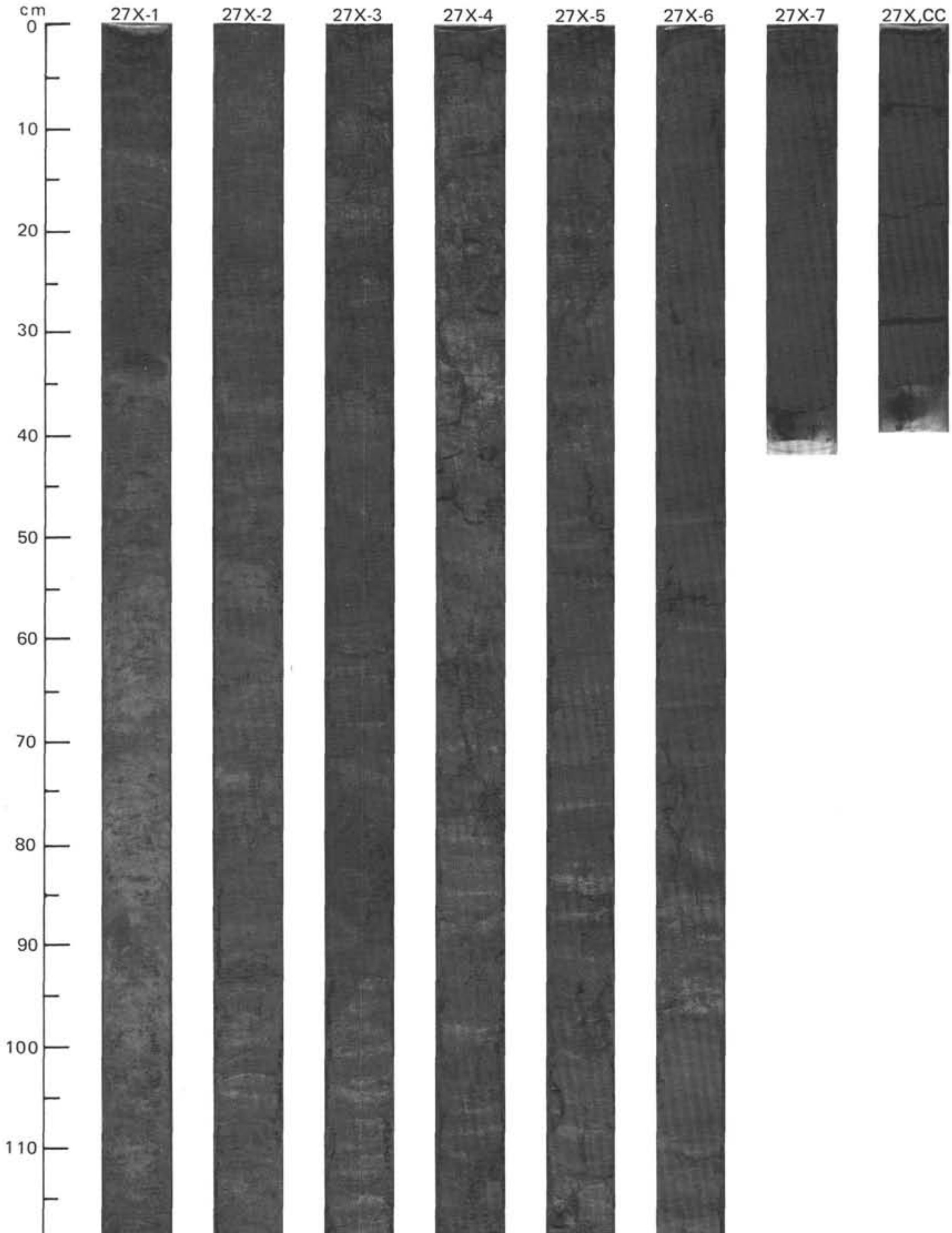
cm
0
10
20
30
40
50
60
70
80
90
100
110
120
130
140
150
27X-1
27X-2
27X-3
27X-4
27X-5
27X-6
27X-7
27X,CC

SITE 643 HOLE A CORE 28X CORED INTERVAL 3033.9-3043.7 mbsl; 254.1-263.9 mbsf

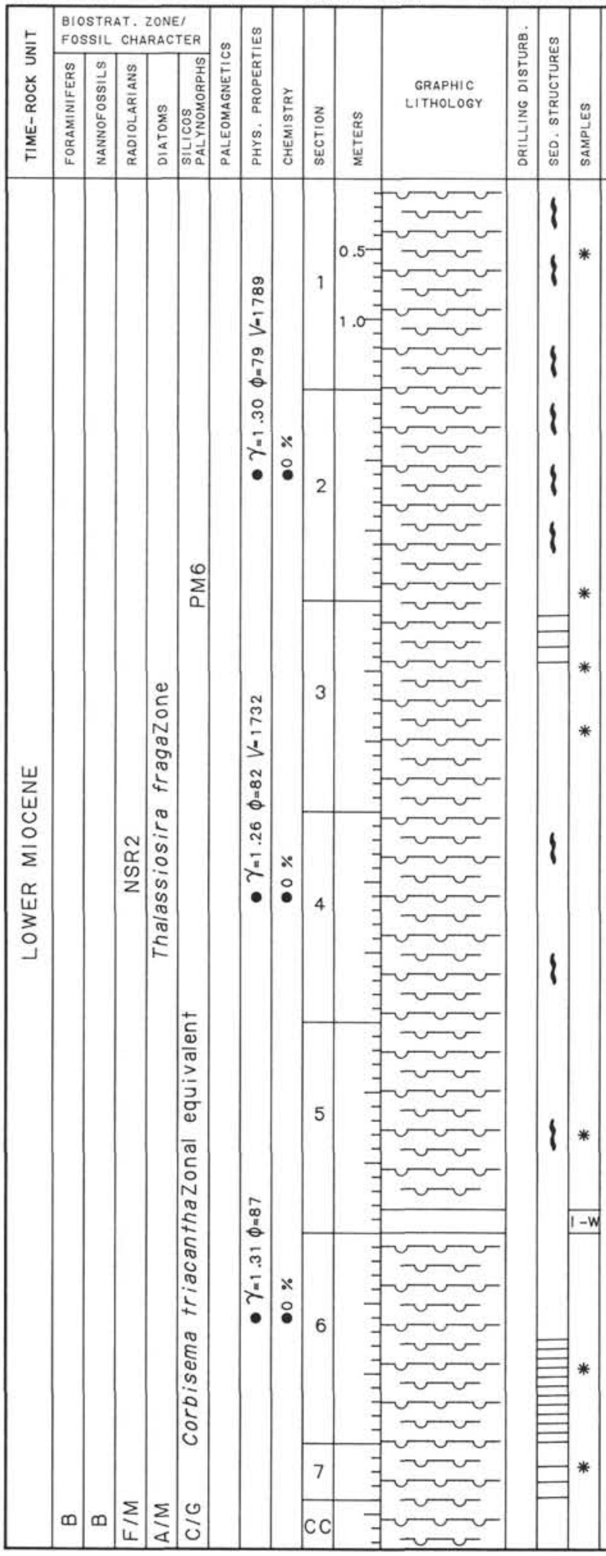

LITHOLOGIC DESCRIPTION

DIATOM OOZE

Entire core is undisturbed.

Major lithologies:
a. Diatom ooze, dark grayish brown (2.5YR 4/2), with minor mottling in dark gray (5Y 4/1) and greenish gray (5GY 5/1). Section 1, 0–41 and 131–150 cm; Section 2, 0–10, 50–72, and 107–149 cm; Section 3, 2–72 and 115–150 cm.
b. Diatom ooze, greenish gray (5GY 5/1), bioturbated and mottled with olive gray (5Y 4/2) and grayish brown (2.5YR 4/2). Section 1, 41–131 cm; Section 2, 10–50 and 72–107 cm; Section 3, 0–2 and 72–115 cm.
c. Diatom ooze, olive gray (5Y 4/2), with faint color banding in olive gray (5Y 4/2) and dark gray (5Y 4/1). Minor bioturbation and mottling. Section 4 to CC.

Minor lithology: Volcanic ash: pyritized ash, two small pockets, Section 1, 67–69 cm; disseminated pyritized ash, Section 2, 149–150 cm.

SMEAR SLIDE SUMMARY (%):

	1, 55 D	2, 148 M	3, 50 D	3, 96 D	5, 78 D	6, 98 D	7, 19 D
TEXTURE:							
Sand	15	—	15	20	5	10	15
Silt	65	—	55	70	70	60	55
Clay	20	—	30	10	25	30	30
COMPOSITION:							
Quartz	2	—	3	10	3	5	7
Clay	15	20	25	10	20	25	21
Volcanic glass	3	50	—	15	—	—	—
Diatoms	60	10	50	50	40	50	55
Radiolarians	—	—	—	—	2	5	10
Sponge spicules	20	20	20	25	35	10	5
Silicoflagellates	—	—	2	—	—	5	2

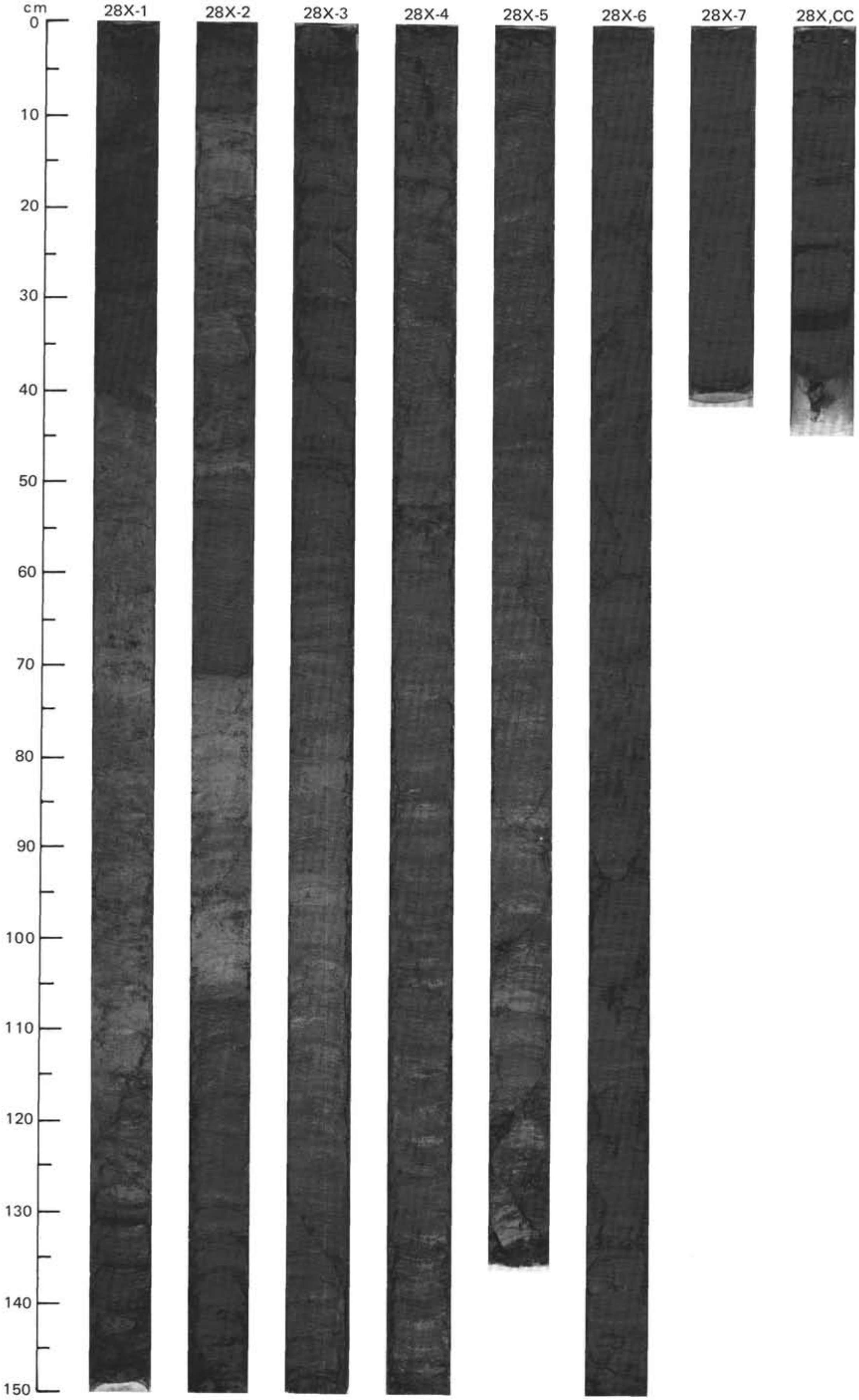
cm
0
10
20
30
40
50
60
70
80
90
100
110
120
130
140
150
28X-1
28X-2
28X-3
28X-4
28X-5
28X-6
28X-7
28X,CC

SITE 643 HOLE A CORE 29X CORED INTERVAL 3043.7-3053.5 mbsl; 263.9-273.7 mbsf

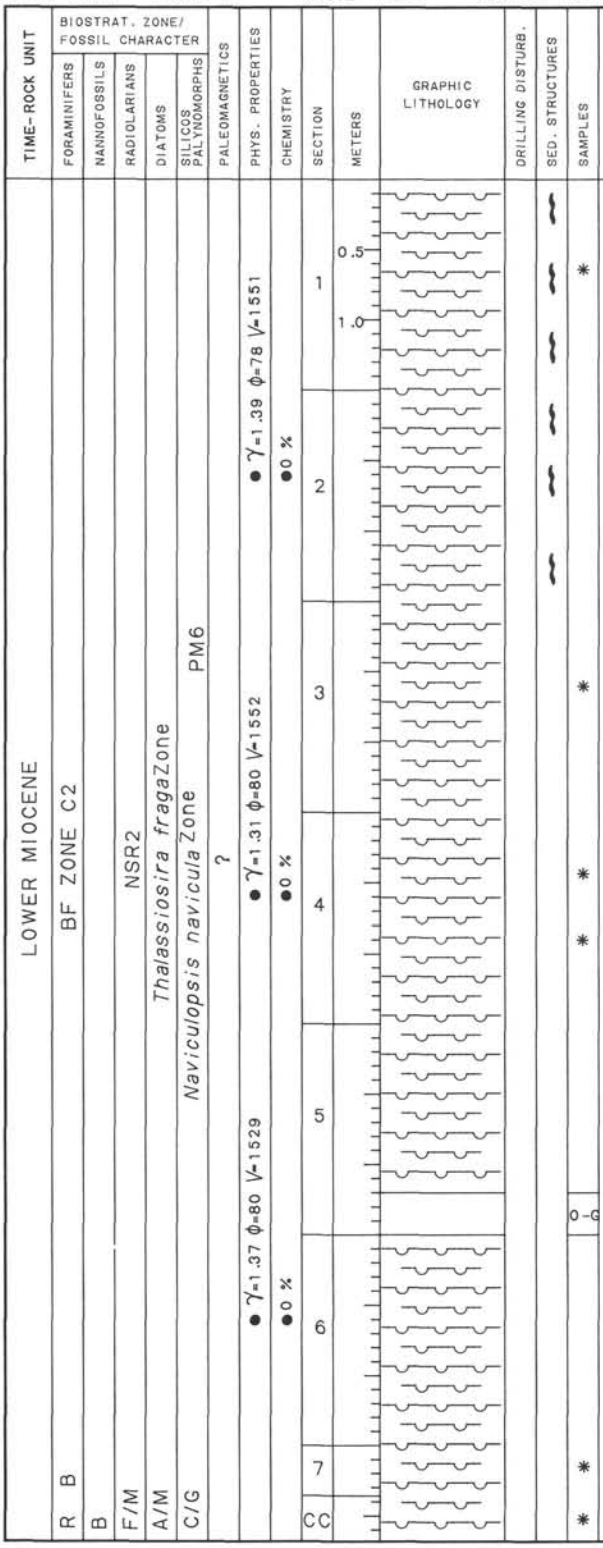

LITHOLOGIC DESCRIPTION

DIATOM OOZE

Entire core is undisturbed.

Major lithologies:
a. Diatom ooze, olive gray (5Y 4/2), moderately bioturbated and mottled. Section 1 to Section 3; Section 5 to Section 6.
b. Diatom ooze, olive gray (5Y 4/2) to grayish green (5G 5/2), slightly mottled. Section 4, 0–41 and 48–150 cm; Section 7, 0–10 and 12–33 cm; CC.

Minor lithology: Mud, light brownish gray (2.5Y 6/2), homogeneous. Section 4, 41–48 cm; Section 7, 10–12 cm.

SMEAR SLIDE SUMMARY (%):

	1, 70 D	3, 64 D	4, 45 M	4, 82 D	2, 12 M	CC, 18 D
TEXTURE:						
Sand	15	20	—	15	—	15
Silt	60	60	3	55	10	55
Clay	25	20	97	30	90	30
COMPOSITION:						
Quartz	5	10	—	10	—	10
Clay	23	17	97	29	90	24
Volcanic glass	1	—	—	—	—	—
Accessory minerals	—	1	—	—	—	—
Diatoms	60	55	2	50	5	50
Radiolarians	5	5	—	1	—	5
Sponge spicules	5	10	1	10	5	10
Silicoflagellates	2	1	—	—	—	1

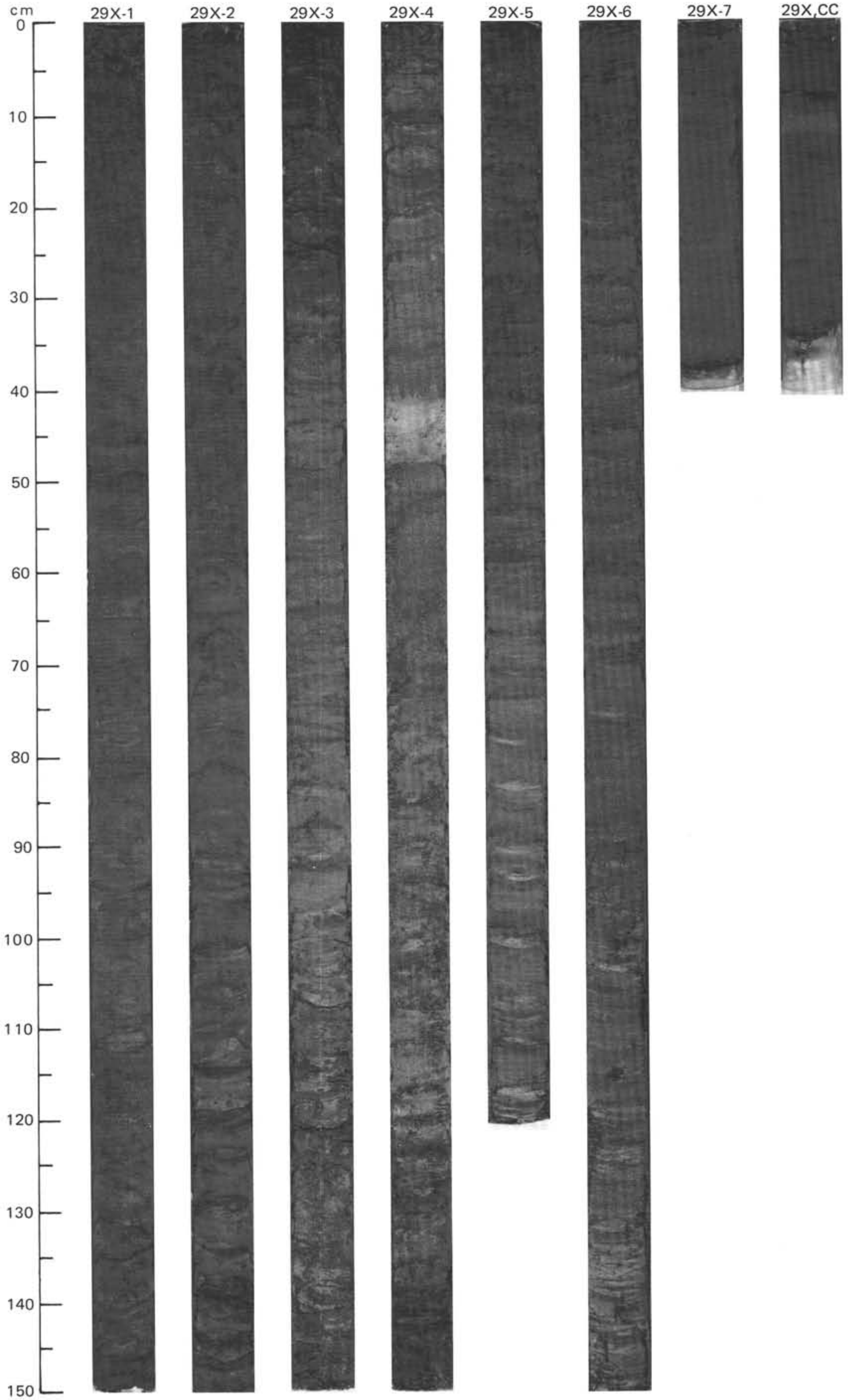
cm
0
10
20
30
40
50
60
70
80
90
100
110
120
130
140
150
29X-1
29X-2
29X-3
29X-4
29X-5
29X-6
29X-7
29X,CC

SITE 643 HOLE A CORE 30X CORED INTERVAL 3053.5-3063.3 mbsl; 273.7-283.5 mbsf

	BIOSTRAT. ZONE/ FOSSIL CHARACTER													
TIME-ROCK UNIT	FORAMINIFERS	NANNOFOSSILS	RADIOLARIANS	DIATOMS	SILICOS PALYNOMORPHS	PALEOMAGNETICS	PHYS. PROPERTIES	CHEMISTRY	SECTION	METERS	GRAPHIC LITHOLOGY	DRILLING DISTURB.	SED. STRUCTURES	SAMPLES
LOWER MIOCENE	BB R/P BF ZONE C2	B	F/M NSR2	A/M *Thalassiosira fraga* Zone	CG *Naviculopsis navicula* Zone PM6	?	γ=2.03 ϕ=26 V-3367●	11 %●	CC		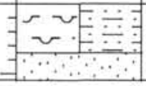	×		*

LITHOLOGIC DESCRIPTION

DIATOMACEOUS MUD AND SILTSTONE

CC, 44–55 cm, is a drilling breccia. Remainder of the core is undisturbed.

Major lithologies:
a. Diatomaceous mud, dark olive gray (5Y 3/2), with faint color banding. CC, 0–35 cm.

Major unconformity at 35 cm in the CC.

b. Siltstone, light brownish gray (2.5Y 6/2), with abundant to predominant compaction laminations, abundant compacted dark burrow fillings, and abundant pyrite impregnations. CC, 35–44 cm.

SMEAR SLIDE SUMMARY (%):

	CC, 18 D
TEXTURE:	
Silt	20
Clay	80
COMPOSITION:	
Quartz	5
Clay	79
Diatoms	5
Radiolarians	1
Sponge spicules	10

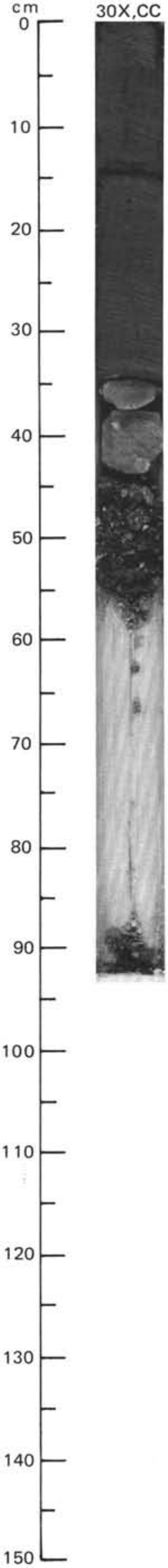
cm
30X,CC
0
10
20
30
40
50
60
70
80
90
100
110
120
130
140
150

SITE 643 HOLE A CORE 31X CORED INTERVAL 3063.3-3073.1 mbsl; 283.5-293.3 mbsf

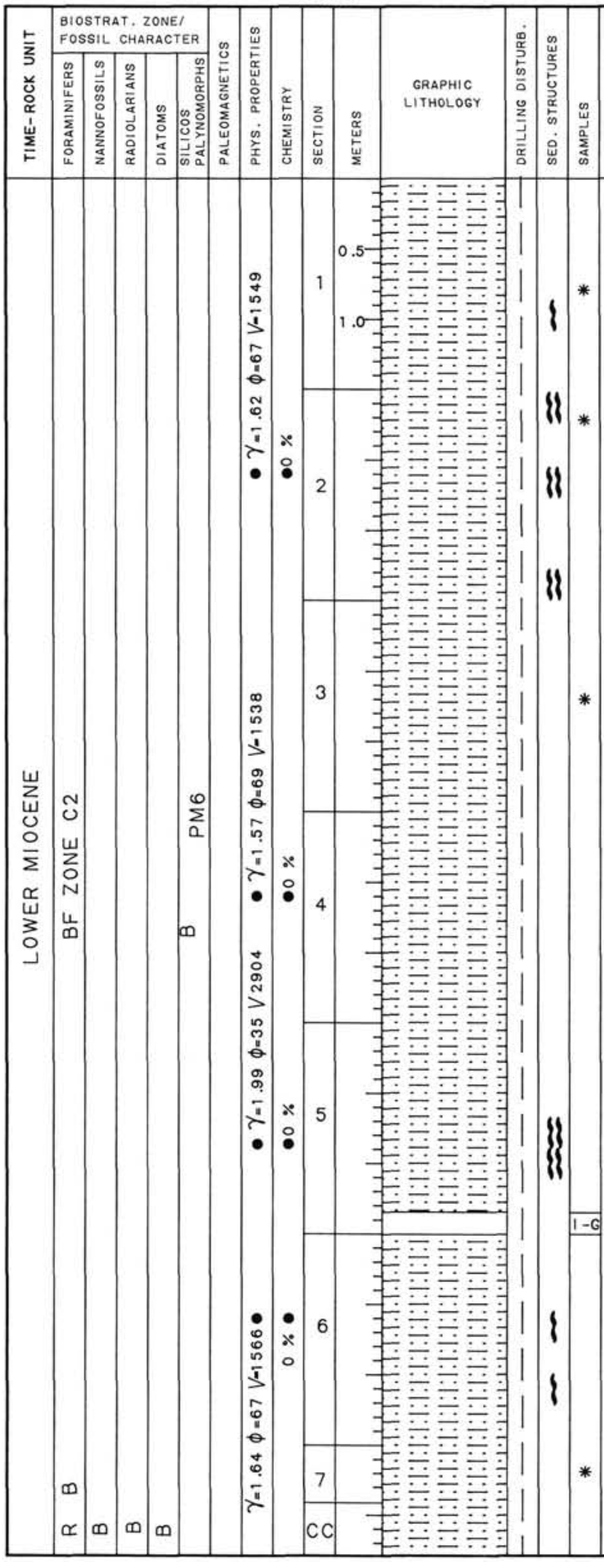

LITHOLOGIC DESCRIPTION

MUD AND MUDSTONE

Entire core is moderately disturbed, with coherent blocks in drilling breccia.

Major lithologies:
a. Mud, dark olive gray (5Y 3/1), extensively bioturbated and mottled, with faint color laminations. Section 1, 40 cm, to Section 2.
b. Mud to mudstone, olive gray (5Y 4/2) to grayish green (5GY 5/2), semiconsolidated and containing abundant compaction laminations. Commonly disrupted into "drilling biscuits." Section 3 to Section 5, 70 cm; Section 5, 103 cm, to CC.
c. Mudstone, grayish green (5GY 5/2) to olive gray (5Y 4/2), completely lithified. Contains abundant compaction laminations and abundant compacted *Zoophycos* burrows. Section 1, 0–40 cm; Section 5, 70–103 cm.

SMEAR SLIDE SUMMARY (%):

	1, 80 D	2, 21 D	3, 73 D	7, 20 D
TEXTURE:				
Sand	5	5	5	5
Silt	15	20	15	10
Clay	80	75	80	85
COMPOSITION:				
Quartz	10	10	10	10
Clay	78	73	79	86
Volcanic glass	1	1	1	1
Accessory minerals	—	—	—	1
Glauconite	1	1	Tr	—
Pyrite	5	5	5	—
Diatoms	—	—	Tr	—
Sponge spicules	5	10	5	2

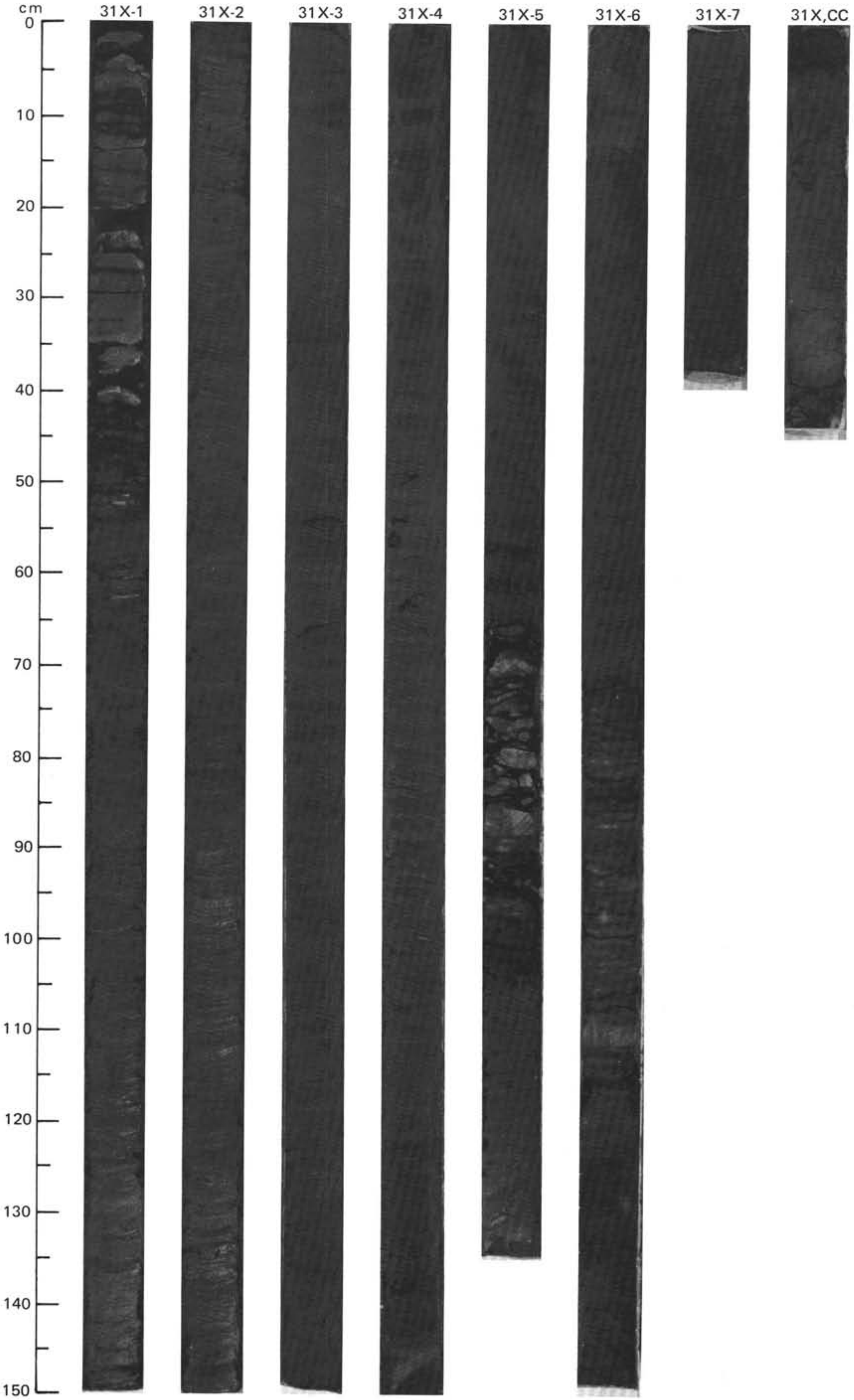
cm
0
10
20
30
40
50
60
70
80
90
100
110
120
130
140
150
31X-1
31X-2
31X-3
31X-4
31X-5
31X-6
31X-7
31X,CC

SITE 643 HOLE A CORE 32X CORED INTERVAL 3073.1-3082.9 mbsl; 293.3-303.1 mbsf

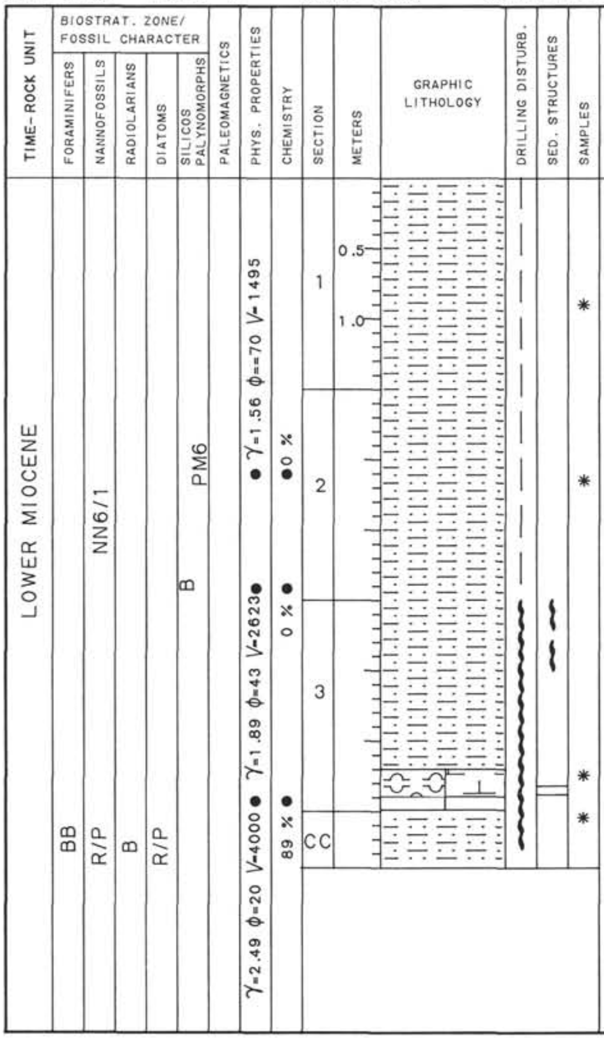

LITHOLOGIC DESCRIPTION

MUD, MUDSTONE, AND NANNOFOSSIL OOZE

Section 1 and Section 2 are moderately disturbed. Section 3 and the CC are moderately to highly disturbed, often to coherent fragments within drilling breccia ("drilling biscuits").

Major lithologies:

a. Mud and mudstone, dark olive gray (5Y 3/1), mottled with minor dark color bands. Section 1 to Section 2, 135 cm.

b. Mudstone, olive gray (5Y 4/2) to grayish green (5GY 5/2), completely lithified. Compacted burrows and compaction lamination common. Section 3, 6–57 cm.

c. Mud to mudstone, dark olive gray (5Y 3/2) to grayish green (5GY 5/2), with compaction lamination. Commonly disrupted to "drilling biscuits" and drilling breccia. Section 3, 66–120 and 130–150 cm; CC, 5–11 and 13–37 cm.

d. Siliceous nannofossil ooze, light brownish gray (2.5Y 6/2) to grayish brown (2.5Y 5/2), with compaction lamination. Section 3, 120–130 and 140–150 cm; CC, 0–5 and 11–13 cm.

Minor lithology: Mudstone, dark grayish brown (2.5Y 4/2), with pelloidal concretions. Section 3, 57–66 cm.

SMEAR SLIDE SUMMARY (%):

	1, 89 D	2, 72 D	3, 126 M	CC, 4 M
TEXTURE:				
Sand	2	1	5	—
Silt	17	6	15	3
Clay	81	93	80	97
COMPOSITION:				
Quartz	5	5	1	2
Clay	81	93	81	97
Volcanic glass	1	1	2	—
Accessory minerals	—	Tr	—	—
Pyrite	10	—	—	—
Diatoms	—	—	10	—
Sponge spicules	—	—	5	1
Silicoflagellates	—	—	2	—

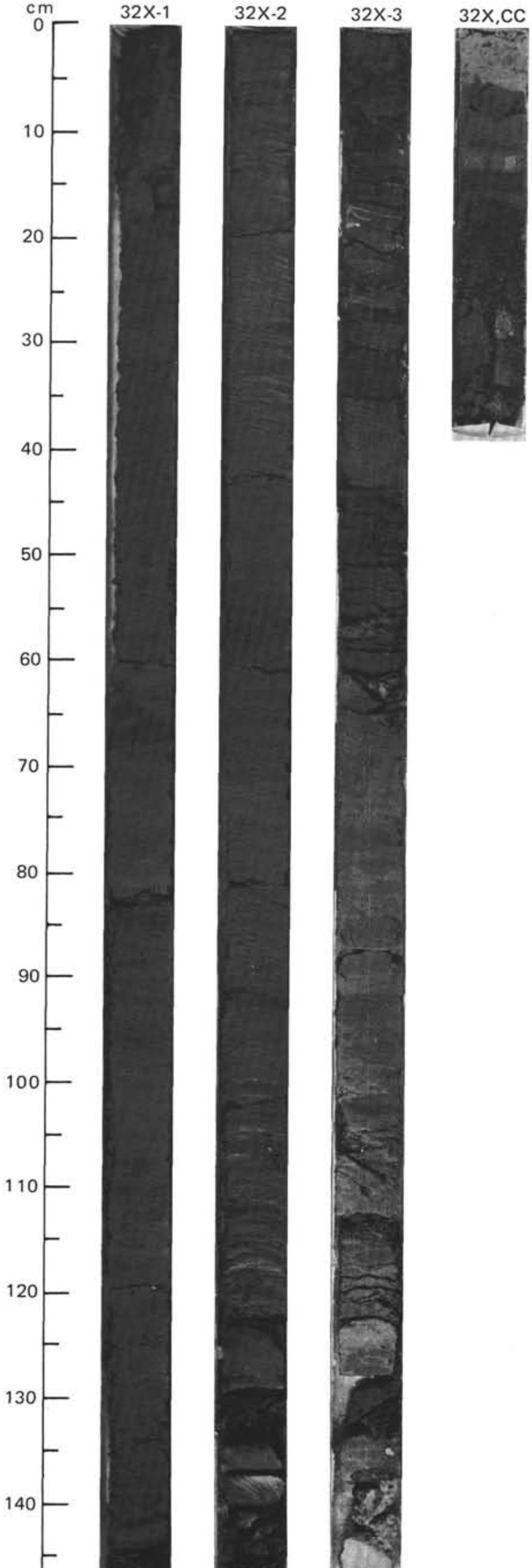
cm
0
10
20
30
40
50
60
70
80
90
100
110
120
130
140
150
32X-1
32X-2
32X-3
32X,CC

SITE 643 HOLE A CORE 33X CORED INTERVAL 3082.9-3092.7 mbsl; 303.1-312.9 mbsf

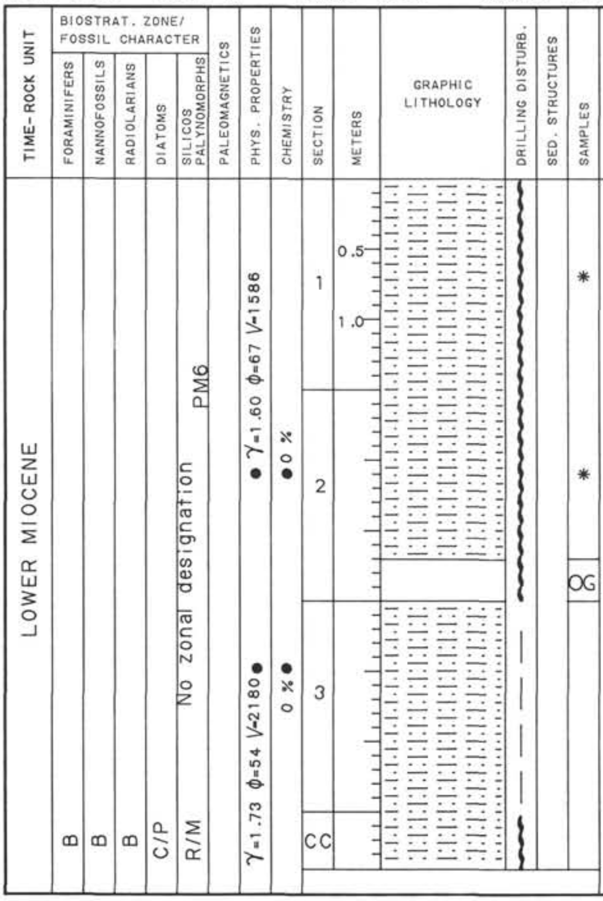

LITHOLOGIC DESCRIPTION

MUD

Sections 1 and 2 and the CC are highly disturbed. Section 3 is moderately disturbed.

Major lithology: Mud to mudstone, olive gray (5Y 4/2) to grayish green (5GY 5/2), with abundant compaction laminations. Often fragmented into "drilling biscuits" and drilling breccia.

SMEAR SLIDE SUMMARY (%):

	1, 70 D	2, 63 D
TEXTURE:		
Sand	5	1
Silt	15	14
Clay	80	85
COMPOSITION:		
Quartz	10	5
Clay	77	84
Volcanic glass	1	1
Accessory minerals:		
Glauconite	1	—
Pyrite	10	10

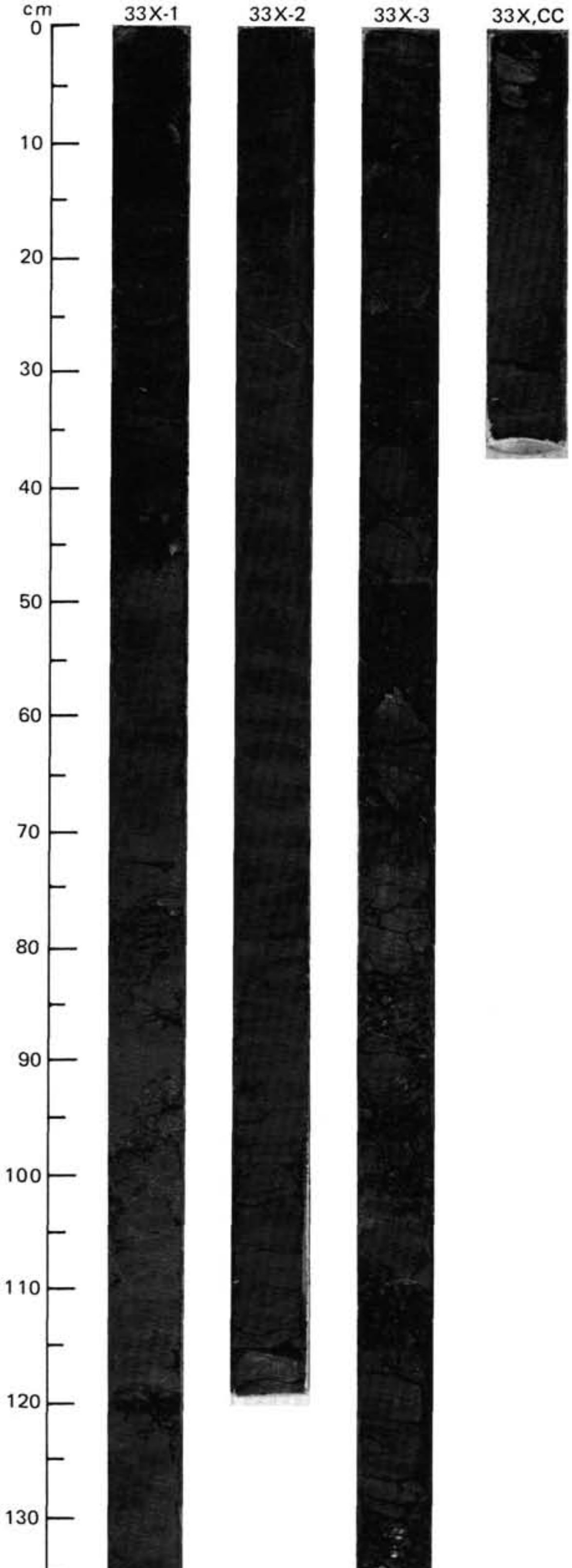
cm
0
10
20
30
40
50
60
70
80
90
100
110
120
130
140
150
33X-1
33X-2
33X-3
33X,CC

SITE 643 HOLE A CORE 34X CORED INTERVAL 3092.7-3102.5 mbsl; 312.9-322.7 mbsf

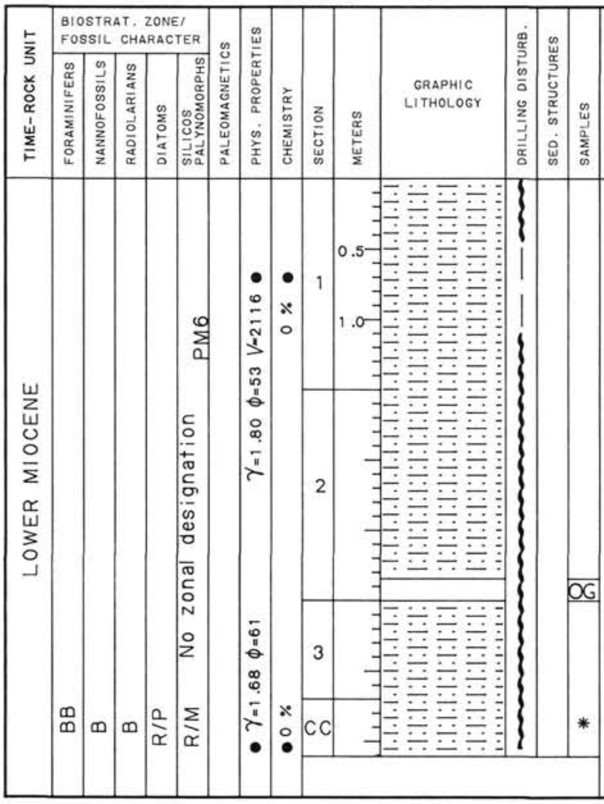

LITHOLOGIC DESCRIPTION

MUD AND MUDSTONE

Section 1, 60–104 cm, is moderately disturbed. Remainder of core is highly disturbed.

Major lithologies:
a. Mudstone, dark olive gray (5Y 3/2) to grayish green (5GY 5/2), with abundant compaction lamination. Often disrupted into "drilling biscuits" and drilling breccia. Section 1, 0–60 and 140–150 cm; Secton 2 to CC.
b. Mudstone, completely lithified, with abundant compaction laminations and compacted burrows. Secton 1, 60–104 cm.

SMEAR SLIDE SUMMARY (%):

	CC, 19 D
TEXTURE:	
Sand	5
Silt	20
Clay	75
COMPOSITION:	
Quartz	15
Clay	73
Volcanic glass	1
Accessory minerals:	
Pyrite	10
Sponge spicules	1

SITE 643 HOLE A CORE 35X CORED INTERVAL 3102.5-3112.3 mbsl; 322.7-332.5 mbsf

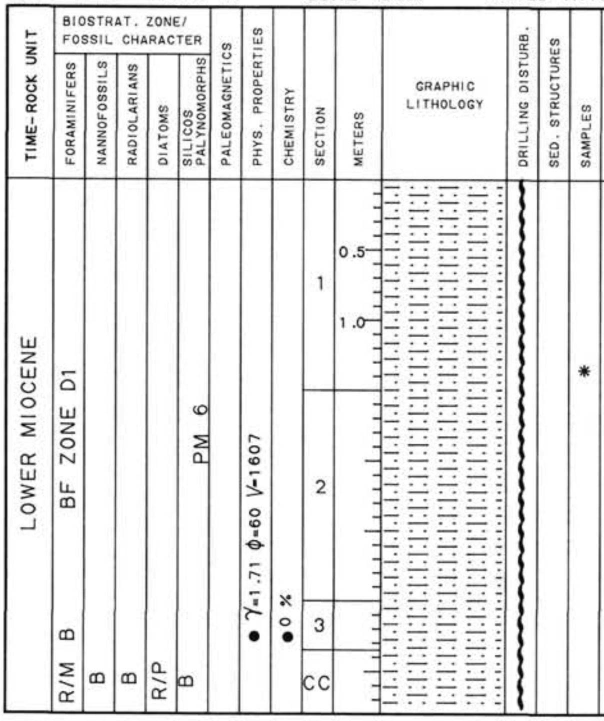

LITHOLOGIC DESCRIPTION

MUD

Entire core is highly disturbed, commonly forming "drilling biscuits."

Major lithology: Mudstone, dark olive gray (5Y 3/2) to grayish green (5GY 5/2), with abundant compaction lamination.

SMEAR SLIDE SUMMARY (%):

	1, 136 D
TEXTURE:	
Sand	2
Silt	24
Clay	74
COMPOSITION:	
Quartz	10
Clay	74
Volcanic glass	1
Accessory minerals:	
Pyrite	15

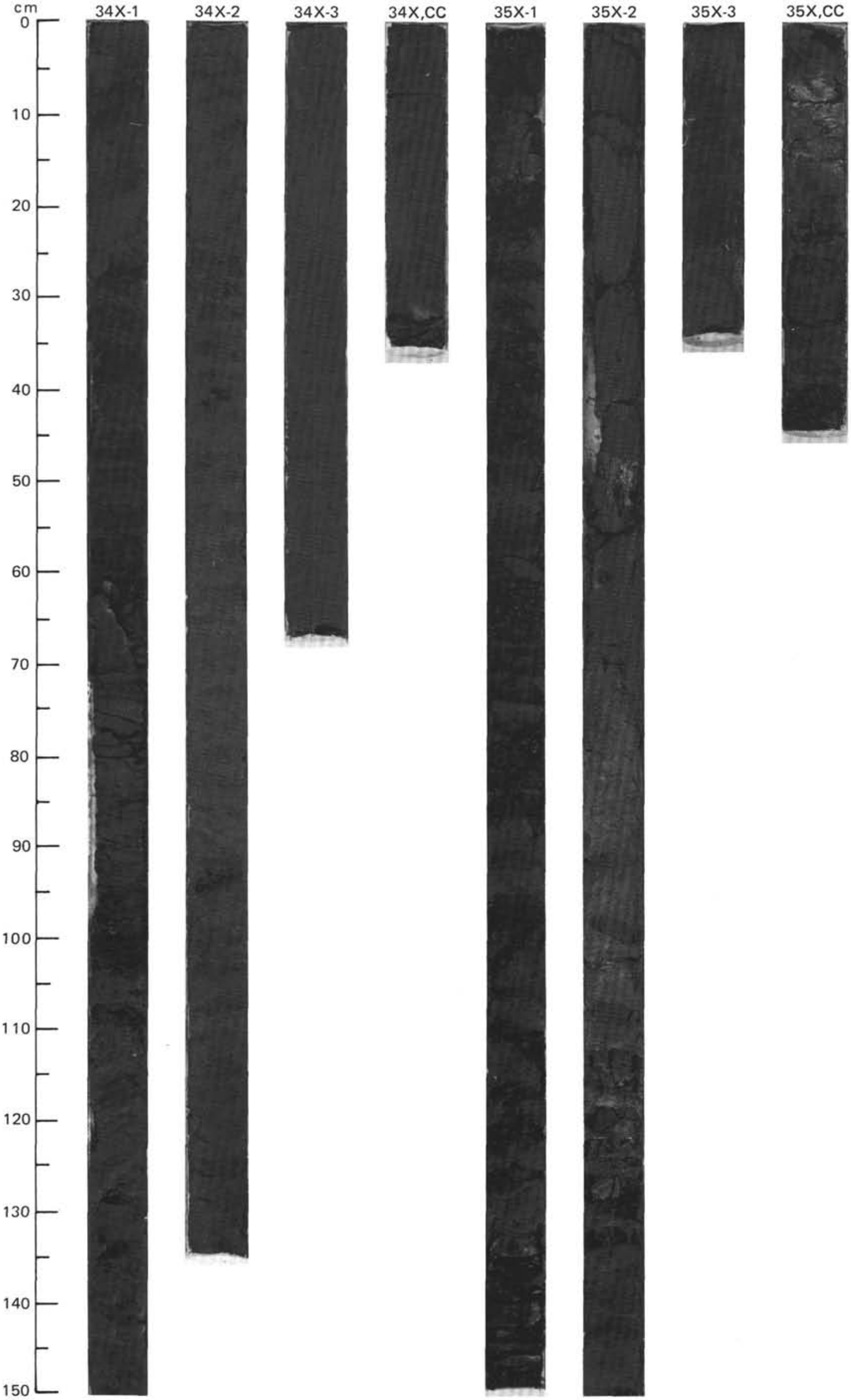
cm
0
10
20
30
40
50
60
70
80
90
100
110
120
130
140
150
34X-1
34X-2
34X-3
34X,CC
35X-1
35X-2
35X-3
35X,CC

SITE 643 HOLE A CORE 36X CORED INTERVAL 3112.3-3122.1 mbsl; 332.5-342.3 mbsf

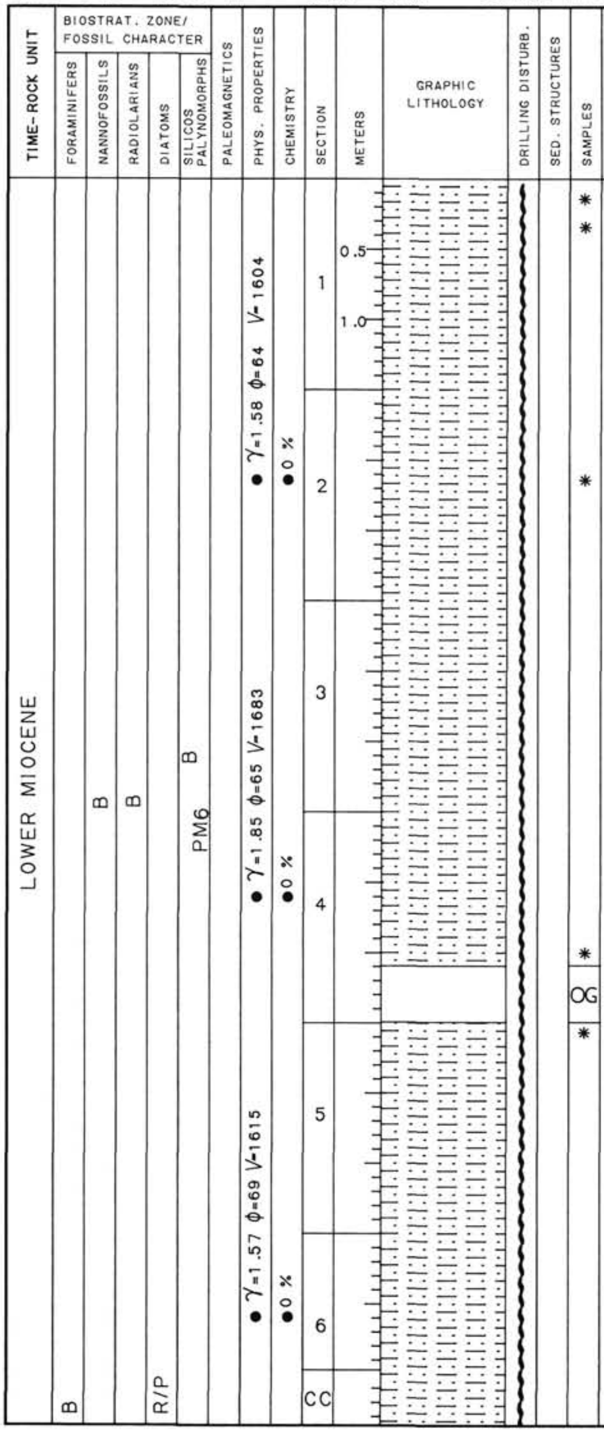

LITHOLOGIC DESCRIPTION

MUD

Entire core is highly disturbed, often forming "drilling biscuits."

Major lithologies:
a. Mud, grayish green (5GY 5/2) to dark olive gray (5Y 3/2), with abundant compaction lamination, commonly forming "drilling biscuits." Section 1, 55–150 cm; Section 2 to CC.
b. Mud, grayish green (5GY 5/2), with abundant compaction lamination. Section 1, 27–55 cm.
b. Mud, black (5Y 2/1), severely disturbed. Section 1, 0–27 cm.

SMEAR SLIDE SUMMARY (%):

	1, 14 D	1, 37 D	2, 66 D	4, 99 D	5, 5 M
TEXTURE:					
Sand	—	1	2	4	4
Silt	30	20	26	26	1
Clay	70	79	72	70	99
COMPOSITION:					
Quartz	5	10	10	15	1
Clay	70	79	72	74	—
Volcanic glass	5	1	2	1	—
Accessory minerals:					
Pyrite	20	10	15	10	—
Nannofossils	—	—	—	—	99
Sponge spicules	—	—	1	—	—

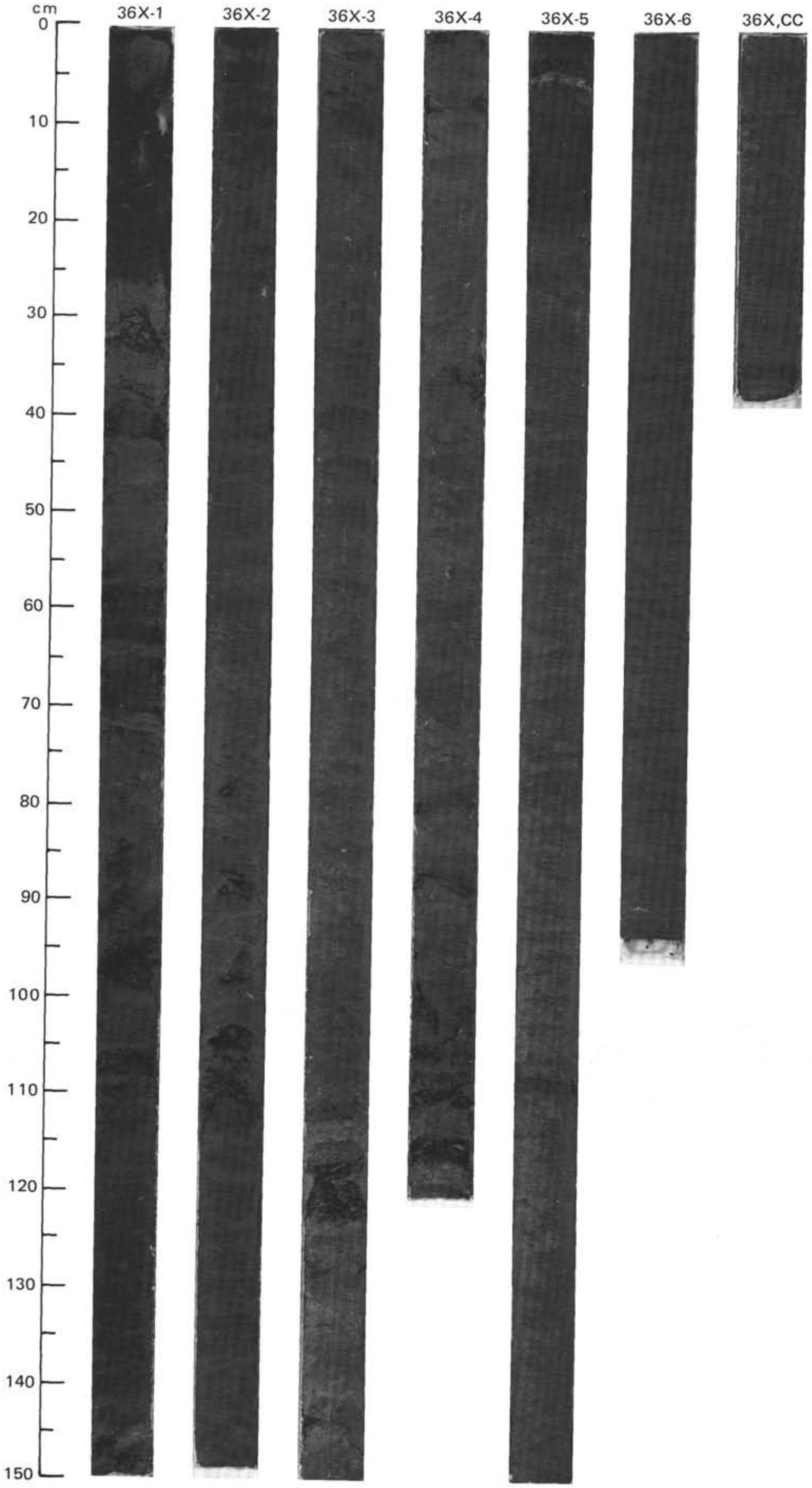
cm
0
10
20
30
40
50
60
70
80
90
100
110
120
130
140
150
36X-1
36X-2
36X-3
36X-4
36X-5
36X-6
36X,CC

SITE 643 HOLE A CORE 37X CORED INTERVAL 3122.1-3131.9 mbsl; 342.3-352.1 mbsf

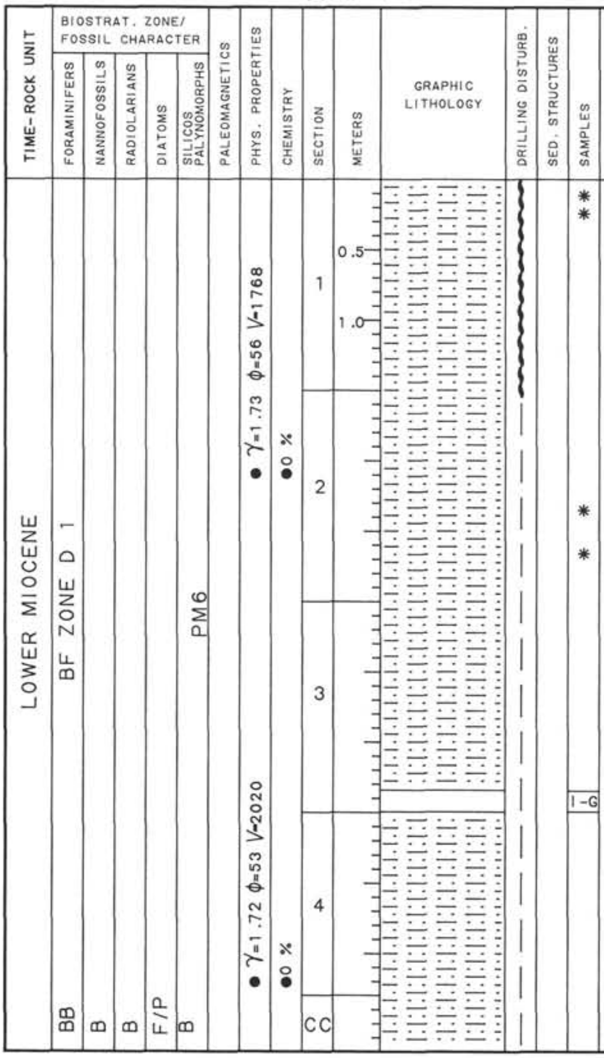

LITHOLOGIC DESCRIPTION

MUD

Sections 2, 3, 4, and the CC are moderately disturbed. Section 1, 25–150 cm, is highly disturbed.

Major lithologies:
a. Mudstone, dark olive gray (5Y 3/2), with abundant compaction lamination. Section 2, CC.
b. Mudstone, grayish green (5GY 5/2), with abundant compaction lamination, and highly disturbed. Section 1, 0–5 and 25–150 cm.

Minor lithology: Calcareous mudstone, light olive brown (2.5Y 5/4), completely lithified. Section 1, 5–20 cm.

SMEAR SLIDE SUMMARY (%):

	1, 12 M	1, 22 D	2, 83 M	2, 114 D
TEXTURE:				
Sand	—	2	5	5
Silt	10	26	33	27
Clay	90	72	62	68
COMPOSITION:				
Quartz	1	10	10	15
Clay	40	72	62	68
Volcanic glass	—	2	2	5
Calcite	56	—	—	—
Accessory minerals:	—	—	1	—
Pyrite	—	15	10	10
Diatoms	1	1	15	—
Sponge spicules	2	—	—	2

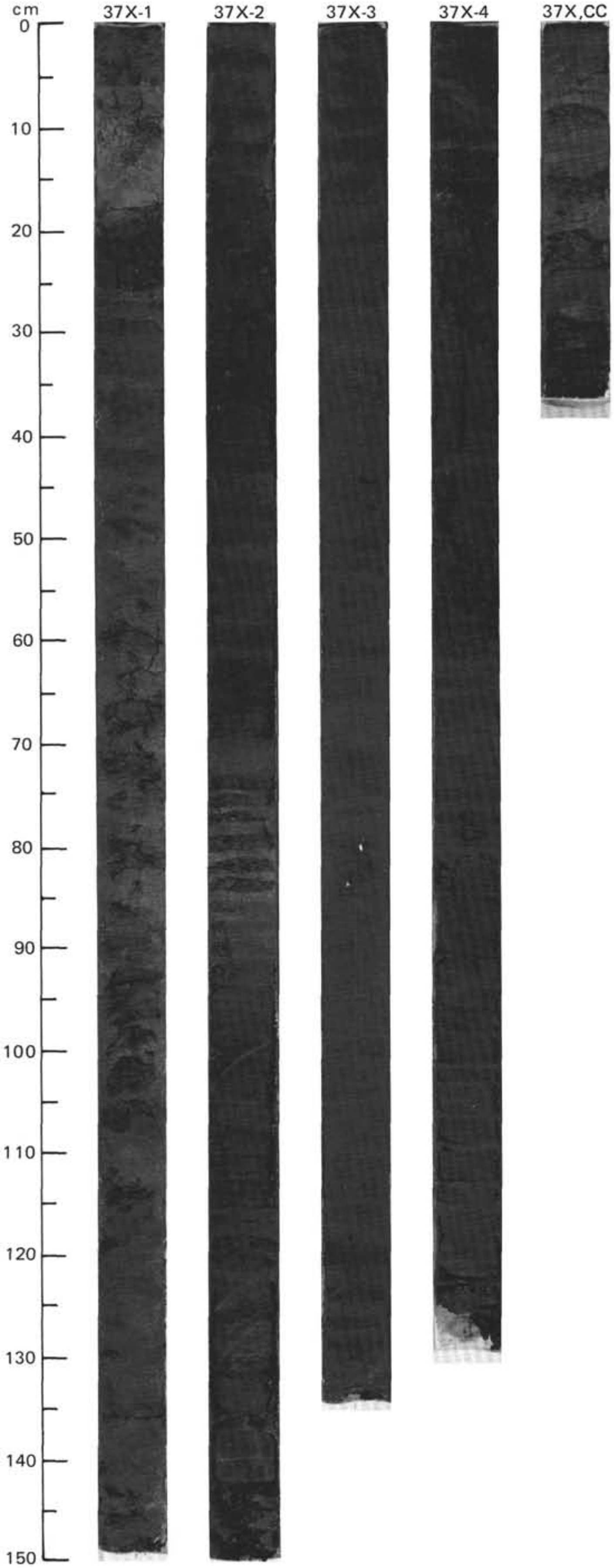
cm
0
10
20
30
40
50
60
70
80
90
100
110
120
130
140
150
37X-1
37X-2
37X-3
37X-4
37X,CC

SITE 643 HOLE A CORE 38X CORED INTERVAL 3131.9-3141.6 mbsl; 352.1-361.8 mbsf

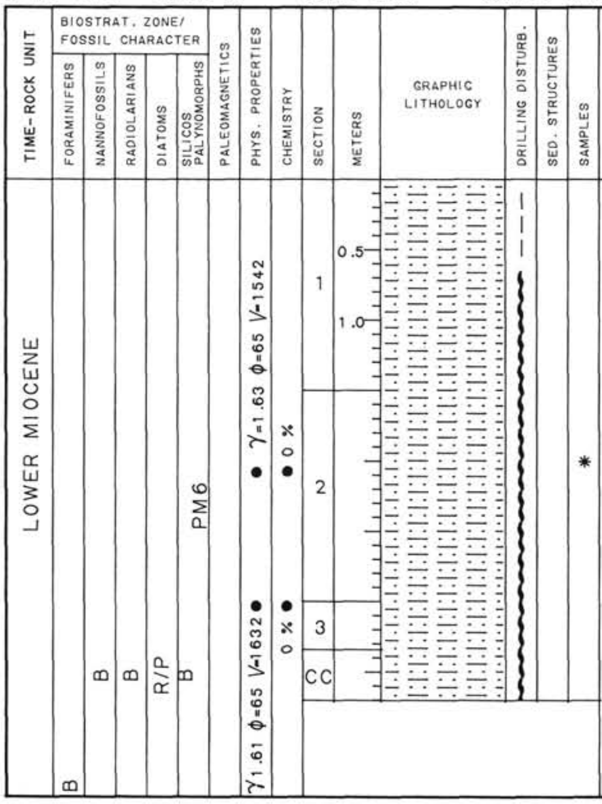

LITHOLOGIC DESCRIPTION

MUD

Section 1, 60–100 cm, is moderately disturbed. Remainder of the core is highly disturbed.

Major lithology: Mudstone, dark olive gray (5Y 3/2), with abundant compaction laminations, commonly disturbed to form "drilling biscuits."

SMEAR SLIDE SUMMARY (%):

	2, 50 D
TEXTURE:	
Sand	5
Silt	20
Clay	75
COMPOSITION:	
Quartz	10
Clay	74
Volcanic glass	5
Accessory minerals:	
Pyrite	10
Glauconite	1

SITE 643 HOLE A CORE 39X CORED INTERVAL 3141.6-3151.2 mbsl; 361.8-371.4 mbsf

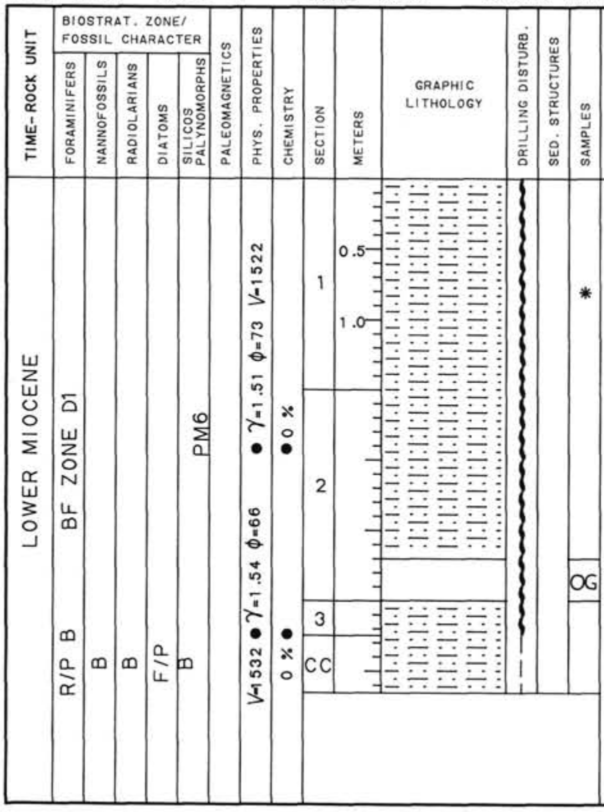

LITHOLOGIC DESCRIPTION

MUD

Section 1 to Section 3 is highly disturbed. The CC is moderately disturbed.

Major lithology: Mudstone, dark olive gray (5Y 3/2), with abundant compaction lamination. Section 1 to Section 3, 26 cm.

Minor lithology: Mudstone, grayish green (5GY 5/2), with common compaction laminations.

SMEAR SLIDE SUMMARY (%):

	1, 77 D
TEXTURE:	
Sand	1
Silt	21
Clay	78
COMPOSITION:	
Quartz	5
Clay	78
Volcanic glass	2
Accessory minerals:	
Pyrite	10
Diatoms	5

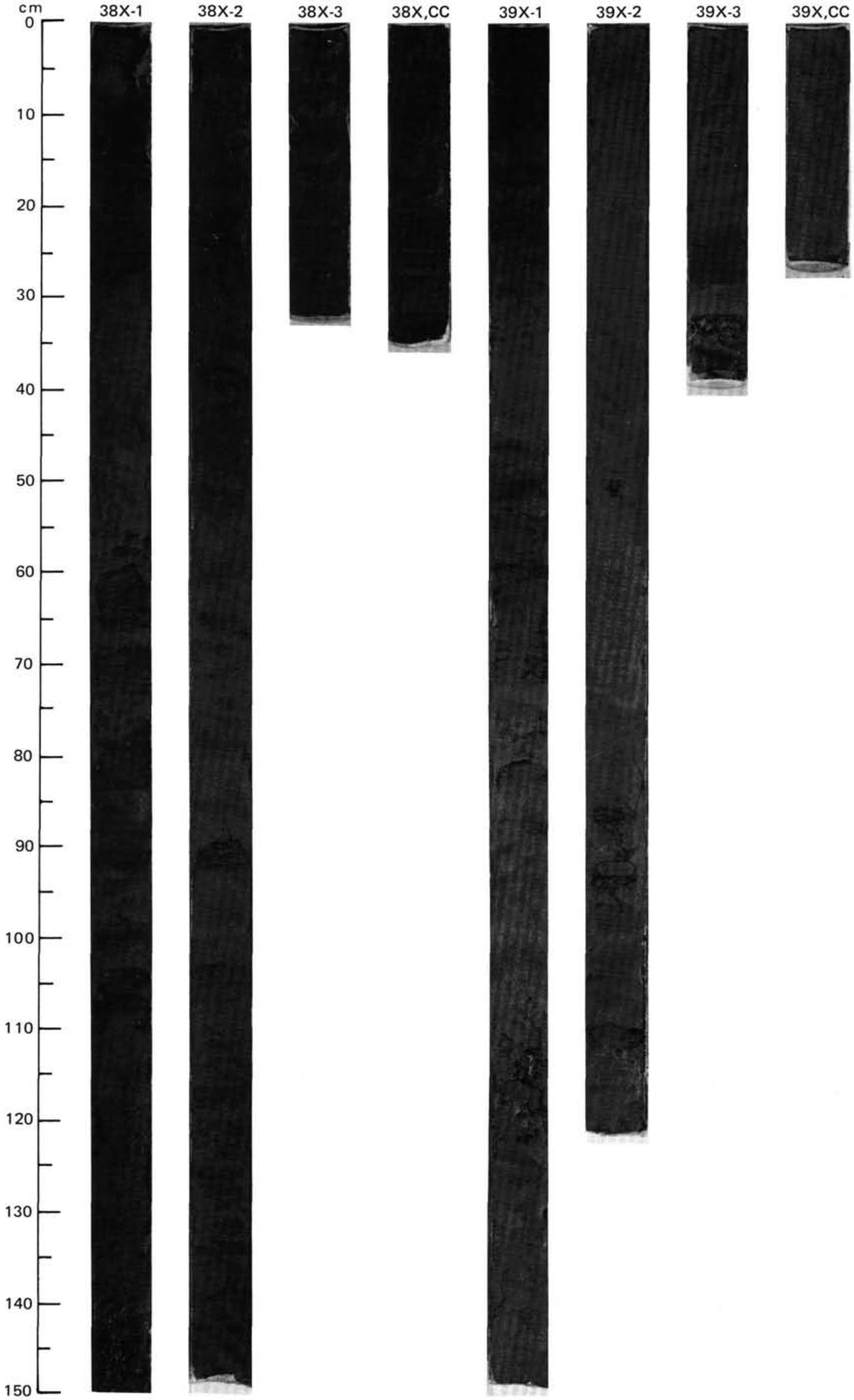
cm
0
10
20
30
40
50
60
70
80
90
100
110
120
130
140
150
38X-1
38X-2
38X-3
38X,CC
39X-1
39X-2
39X-3
39X,CC

SITE 643 HOLE A CORE 40X CORED INTERVAL 3151.2-3160.9 mbsl; 371.4-381.1 mbsf

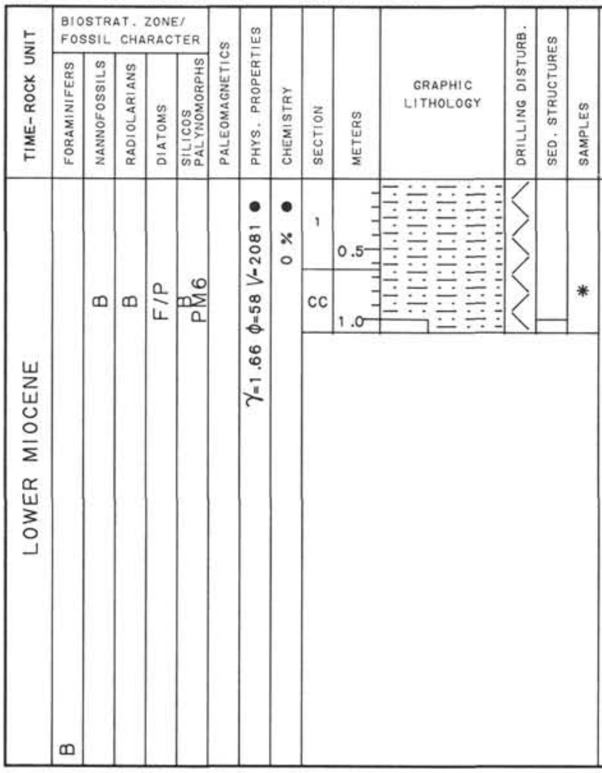

LITHOLOGIC DESCRIPTION

MUD AND MUDSTONE

Entire core is moderately to highly disturbed.

Major lithology: Mud and mudstone, dark olive gray (5Y 3/2) with abundant compaction lamination where moderately fragmented, greenish gray (5GY 5/1) where highly fragmented.

Minor lithology: Calcareous mudstone, brown (10YR 5/3) and homogeneous, with minor pyrite. CC, 39–43 cm.

SMEAR SLIDE SUMMARY (%):

	CC, 19 D
TEXTURE:	
Silt	10
Clay	90
COMPOSITION:	
Quartz	12
Clay	80
Volcanic glass	1
Accessory minerals:	
Pyrite	5
Diatoms	1
Sponge spicules	1

SITE 643 HOLE A CORE 41X CORED INTERVAL 3160.9-3170.5 mbsl; 381.1-390.7 mbsf

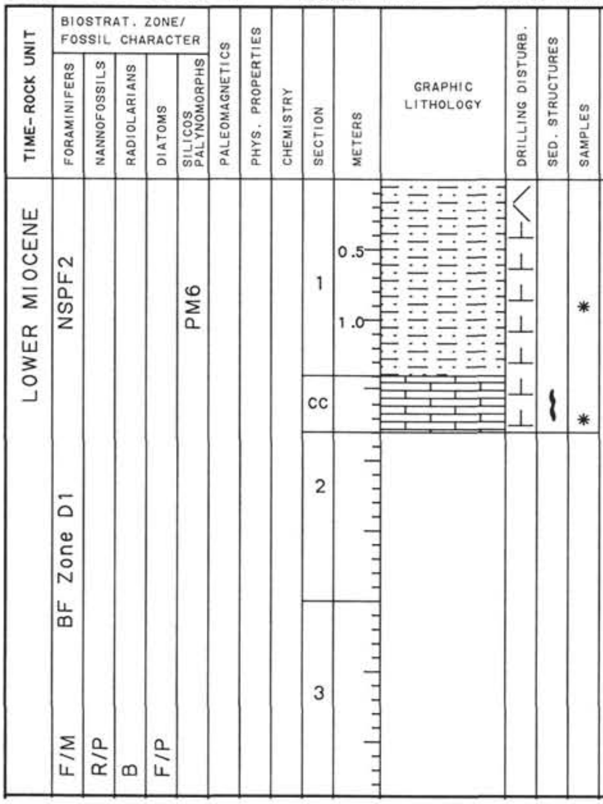

LITHOLOGIC DESCRIPTION

MUD

Entire core is moderately to highly disturbed.

Major lithology: Mud to mudstone, gray (5Y 4/1) to dark greenish gray (5GY 4/1), with abundant compaction laminations. Fragmentation into "drilling biscuits" is common.

Minor lithology: Calcareous mudstone, yellowish brown (10YR 5/4) and completely lithified. CC, 33–40 cm.

SMEAR SLIDE SUMMARY (%):

	1, 96 D	CC, 35 M
TEXTURE:		
Silt	20	5
Clay	80	95
COMPOSITION:		
Quartz	10	—
Clay	80	7
Volcanic glass	3	1
Calcite	—	90
Accessory minerals	1	—
Pyrite/manganese	5	—
Foraminifers	—	1
Diatoms	1	—
Sponge spicules	—	1

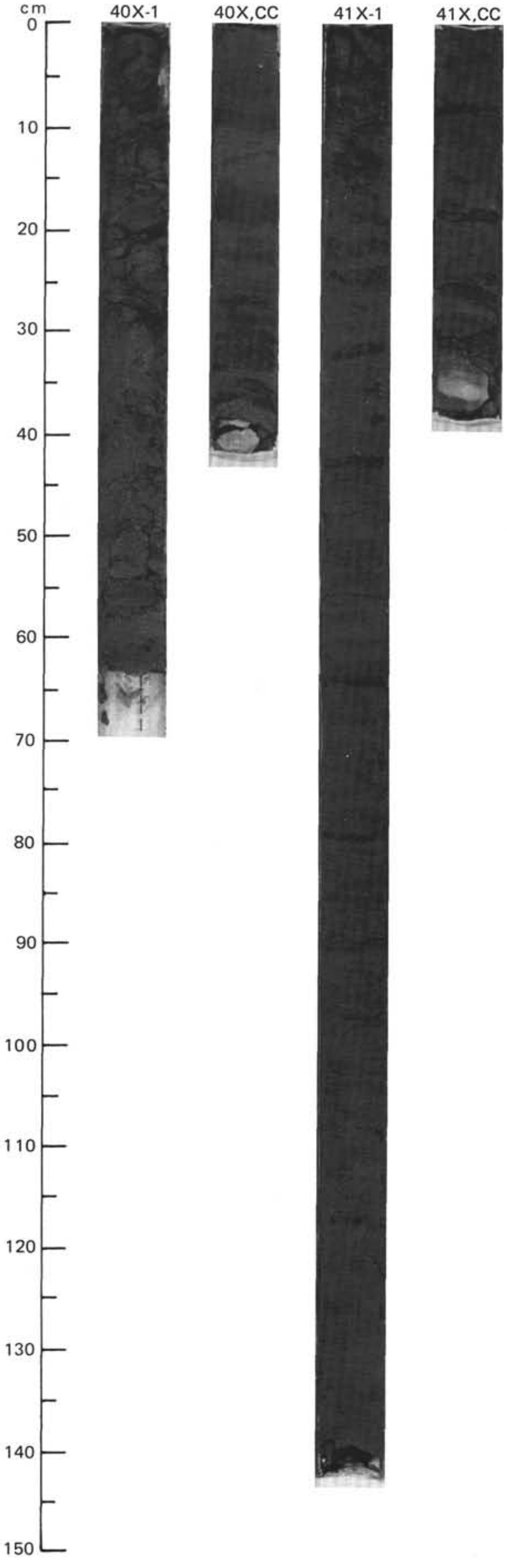
cm
0
10
20
30
40
50
60
70
80
90
100
110
120
130
140
150
40X-1
40X,CC
41X-1
41X,CC

SITE 643 HOLE A CORE 42X CORED INTERVAL 3170.5-3180.2 mbsl; 390.7-400.4 mbsf

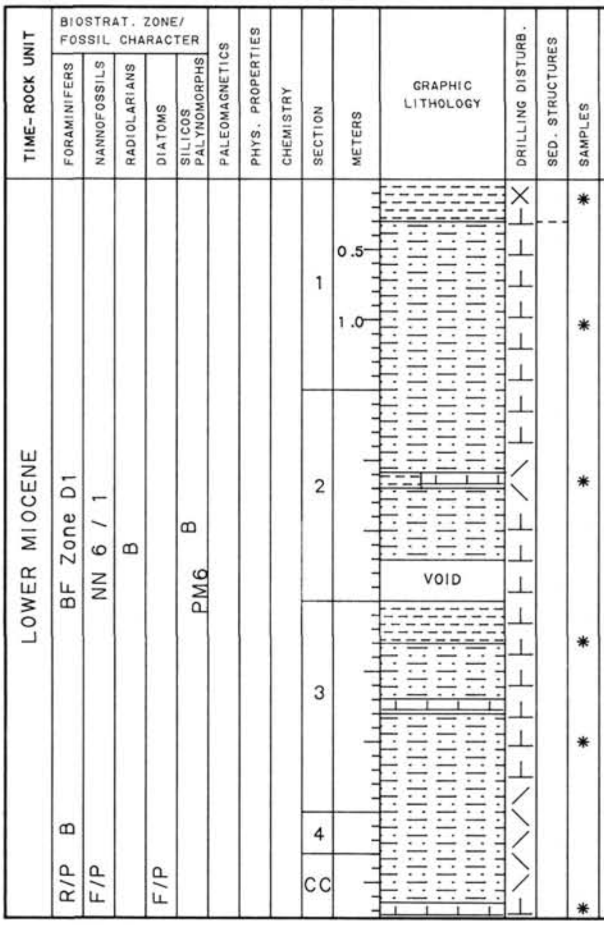

LITHOLOGIC DESCRIPTION

MUDSTONE

Entire core is moderately to highly fragmented.

Major lithology: Mudstone, dark gray (5Y 4/1), very dark gray (5Y 3/1), and dark greenish gray (5GY 4/1). Coherent blocks ("drilling biscuits") and drilling breccia show similar mixed colors. Blocks contain common to abundant compaction laminations and minor compacted burrows.

Minor lithologies:
a. Claystone, dark greenish gray (5GY 4/1). Section 1, 0–30 cm; Section 3, 0–30 cm.
b. Marly nannofossil chalk, light gray (5Y 6/1), and nannofossil chalk, yellowish-brown (10YR 5/4). Section 3, 77–80 cm; CC, 39–45 cm.

SMEAR SLIDE SUMMARY (%):

	1, 18 M	1, 104 D	2, 63 M	3, 29 M	3, 99 D	CC, 42 M
TEXTURE:						
Sand	—	—	—	—	10	—
Silt	10	20	10	10	10	5
Clay	90	80	90	90	80	95
COMPOSITION:						
Quartz	1	3	1	2	15	—
Mica	—	—	—	5	—	—
Clay	90	80	30	90	80	10
Volcanic glass	3	2	2	1	2	—
Accessory minerals:						
Pyrite/manganese	5	15	2	2	3	—
Nannofossils	—	—	65	—	—	90
Diatoms	1	—	—	—	—	—

SITE 643 HOLE A CORE 43X CORED INTERVAL 3180.2-3189.8 mbsl; 400.4-410.0 mbsf

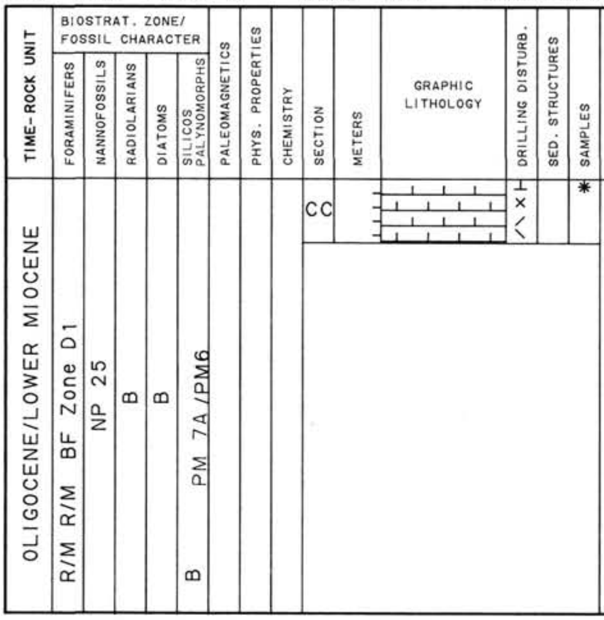

LITHOLOGIC DESCRIPTION

NANNOFOSSIL CHALK

Entire core is moderately to highly fragmented.

Major lithology: Nannofossil chalk, greenish gray (5GY 4/1) and yellowish brown (10YR 5/4). Minor burrowing in dark greenish gray (5GY 4/1) and gray (5Y 5/1).

SMEAR SLIDE SUMMARY (%):

	CC, 8 D
TEXTURE:	
Silt	5
Clay	95
COMPOSITION:	
Clay	20
Nannofossils	80

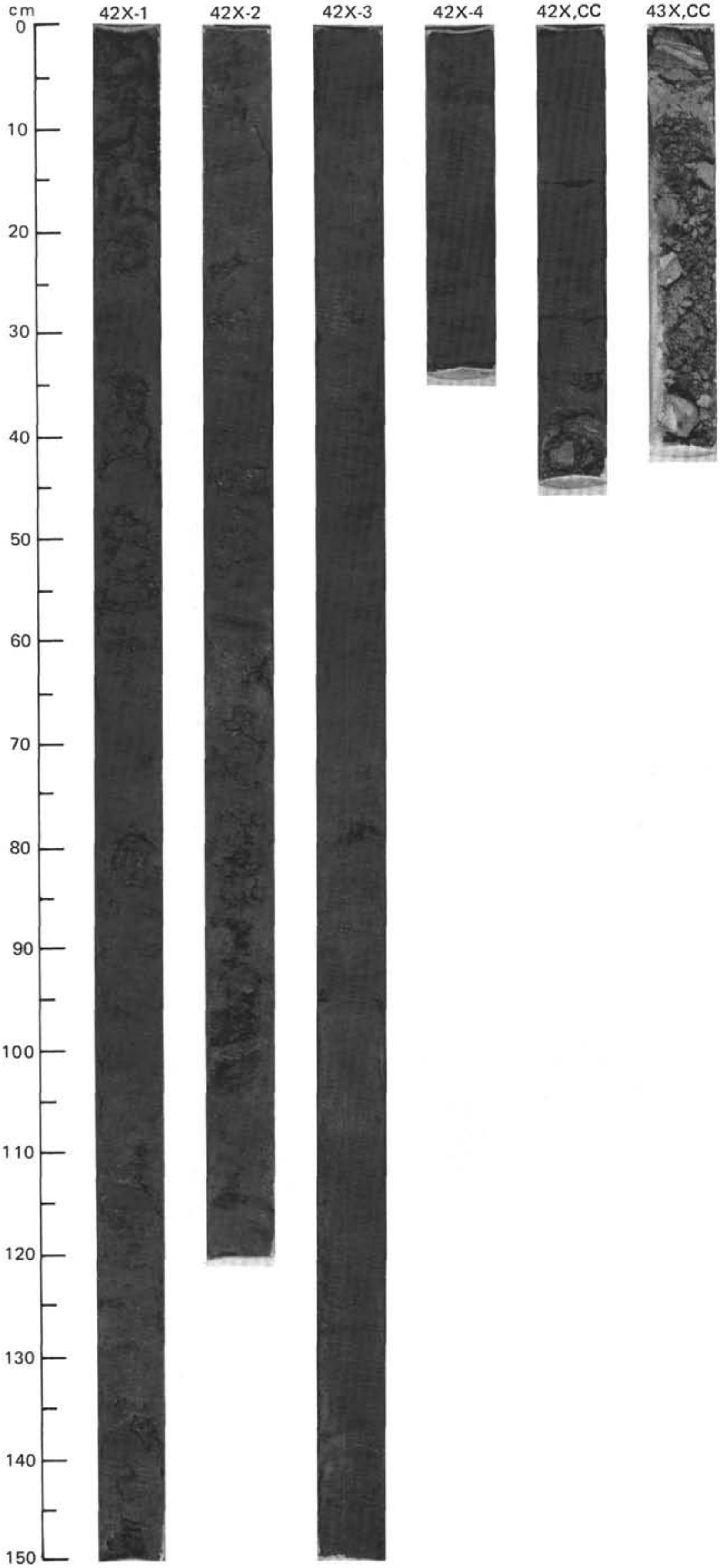
cm
0
10
20
30
40
50
60
70
80
90
100
110
120
130
140
150
42X-1
42X-2
42X-3
42X-4
42X,CC
43X,CC

SITE 643 HOLE A CORE 44X CORED INTERVAL 3189.8-3199.5 mbsl; 410.0-419.7 mbsf

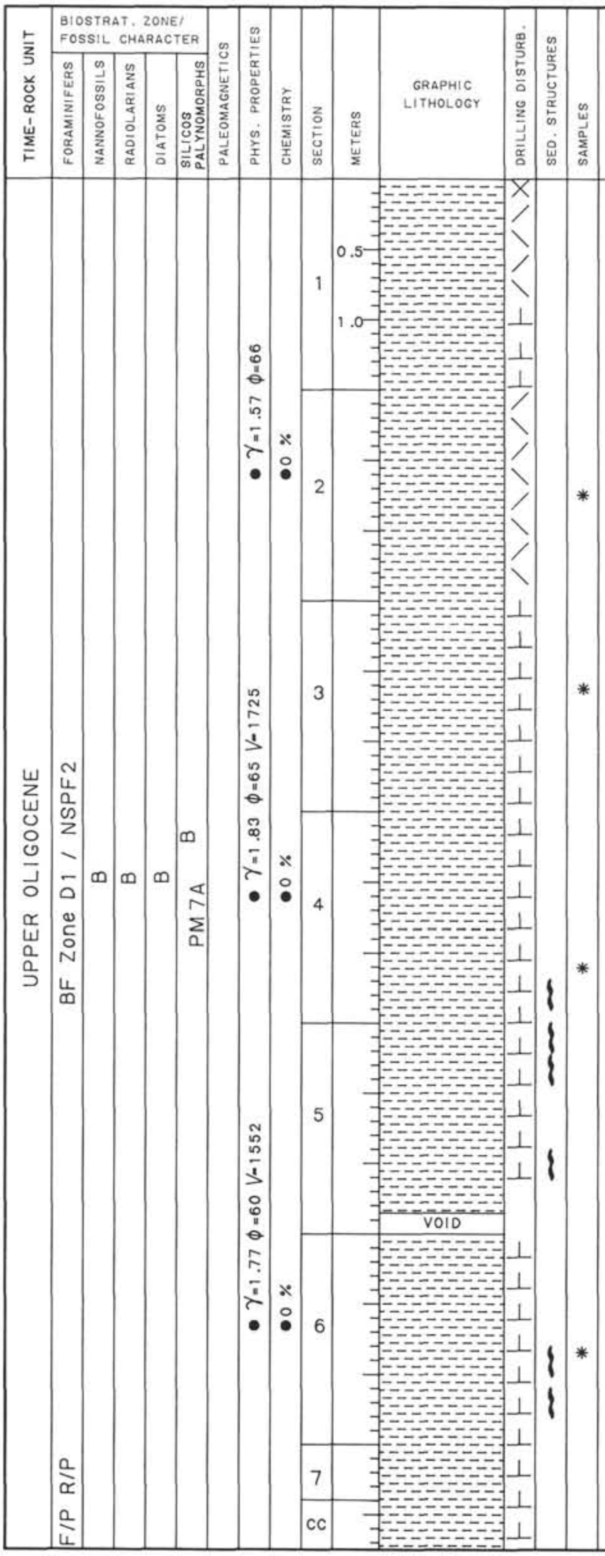

LITHOLOGIC DESCRIPTION

ZEOLITIC CLAYSTONE

Entire core is moderately to highly fragmented.

Major lithology: Zeolitic claystone, greenish gray (5GY 4/1), dark greenish gray (5GY 5/1), dark gray (5Y 4/1), and very dark gray (5Y 3/1). Mottled and gradationally color-banded on a scale of 1–5 cm, with interbedded colors on a scale of 5–10 cm. Commonly fragmented to form "drilling biscuits" with compaction laminations common.

Minor lithology: Dolomite sandstone pebble. Section 4, 124–126 cm.

SMEAR SLIDE SUMMARY (%):

	2, 74 D	3, 64 D	4, 107 D	6, 90 D
TEXTURE:				
Silt	10	10	10	10
Clay	90	90	90	90
COMPOSITION:				
Quartz	2	2	1	2
Clay	80	90	90	80
Volcanic glass	1	1	2	2
Accessory minerals:				
Zeolites	5	5	4	15
Pyrite/manganese	10	2	3	1
Diatoms	1	—	—	—
Radiolarians	1	—	—	—

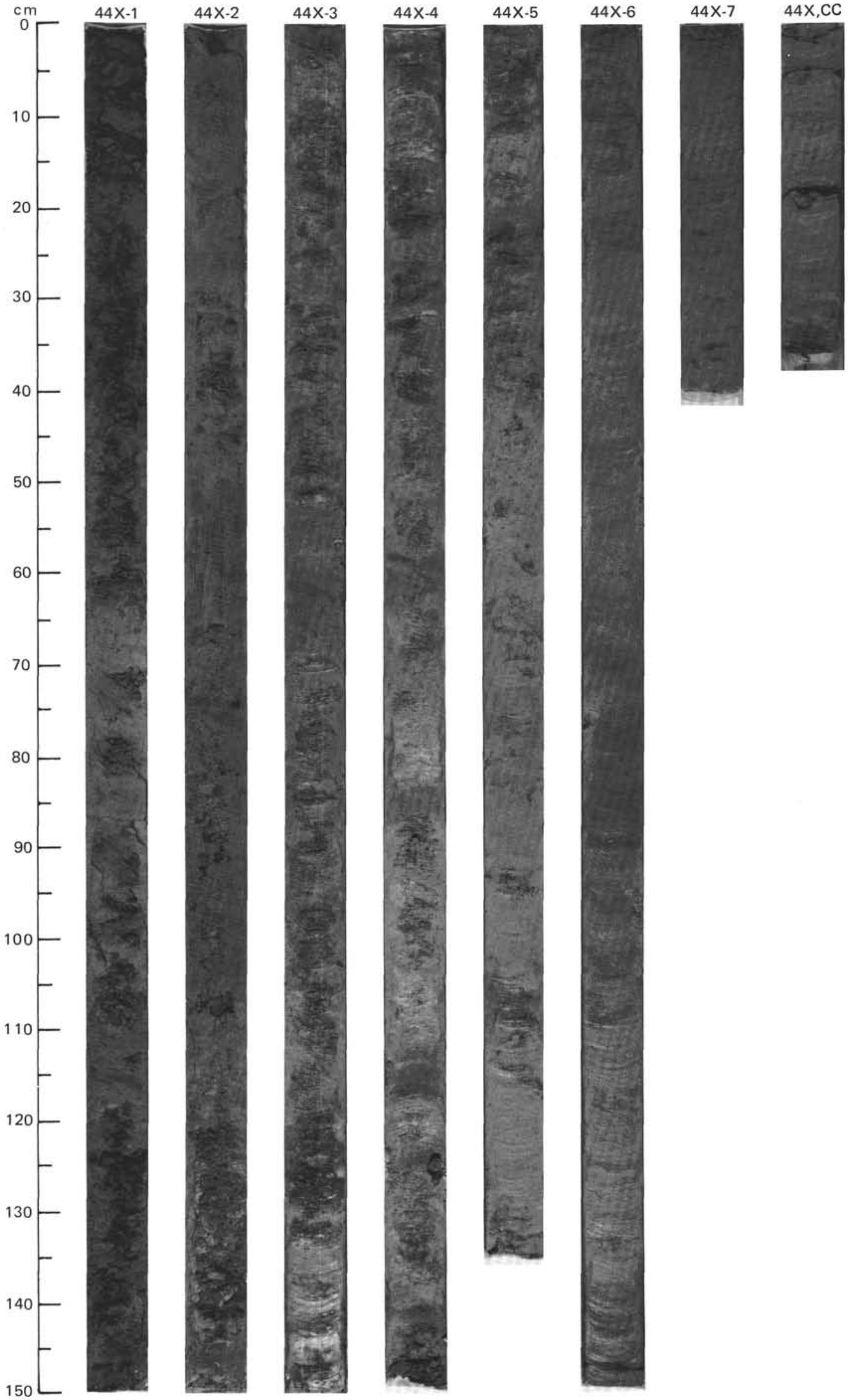
cm
0
10
20
30
40
50
60
70
80
90
100
110
120
130
140
150
44X-1
44X-2
44X-3
44X-4
44X-5
44X-6
44X-7
44X,CC

SITE 643 HOLE A CORE 45X CORED INTERVAL 3199.5-3209.2 mbsl; 419.7-429.4 mbsf

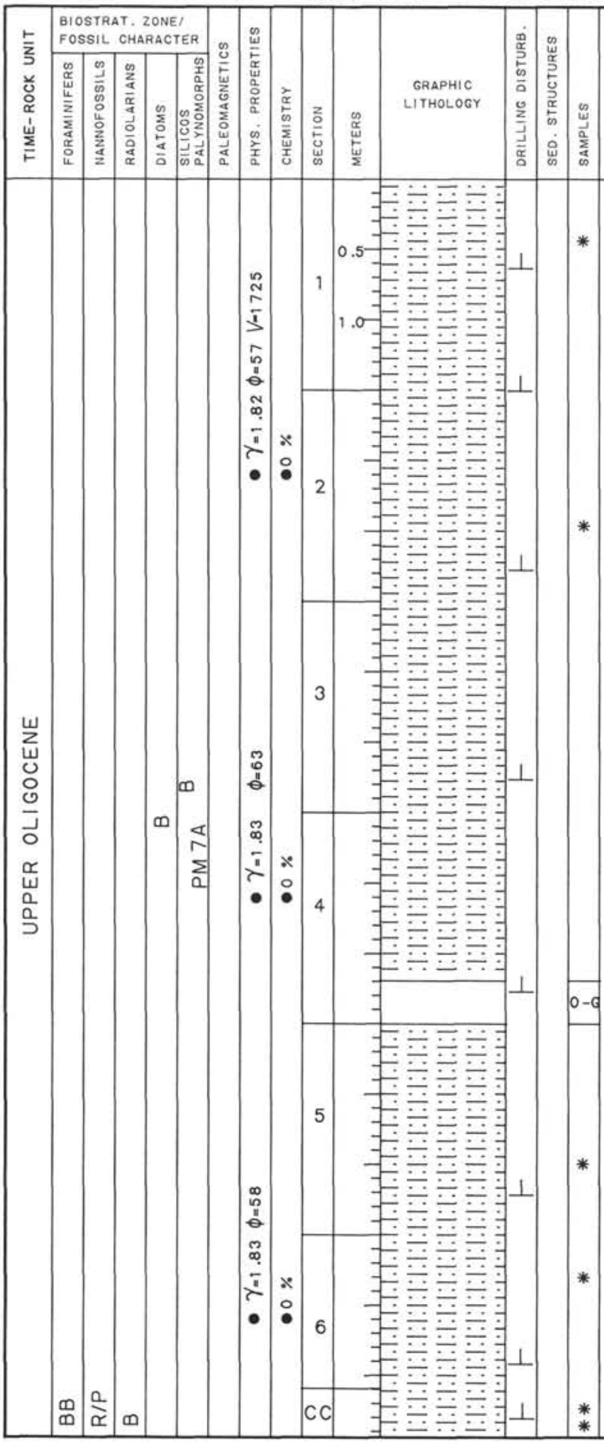

LITHOLOGIC DESCRIPTION

ZEOLITIC MUDSTONE

Entire core is moderately to highly fragmented.

Major lithology: Zeolitic mudstone, grayish green (5GY 5/1), mottled with small white dots of zeolites, with scattered green color banding.

Minor lithology: Calcareous mudstone, light gray (2.5Y 7/2). CC, 35 cm.

SMEAR SLIDE SUMMARY (%):

	1, 49 D	2, 90 D	5, 95 D	6, 30 D	CC, 32 M	CC, 35 M
TEXTURE:						
Sand	—	—	—	—	—	10
Silt	15	20	10	15	20	70
Clay	85	80	90	85	80	20
COMPOSITION:						
Quartz	2	5	—	2	2	—
Clay	78	78	88	83	76	25
Volcanic glass	5	2	1	5	1	—
Calcite/dolomite	—	—	1	—	—	75
Accessory minerals	—	—	—	Tr	1	—
Zeolite	15	15	10	10	5	—
Pyrite	—	—	—	—	15	—

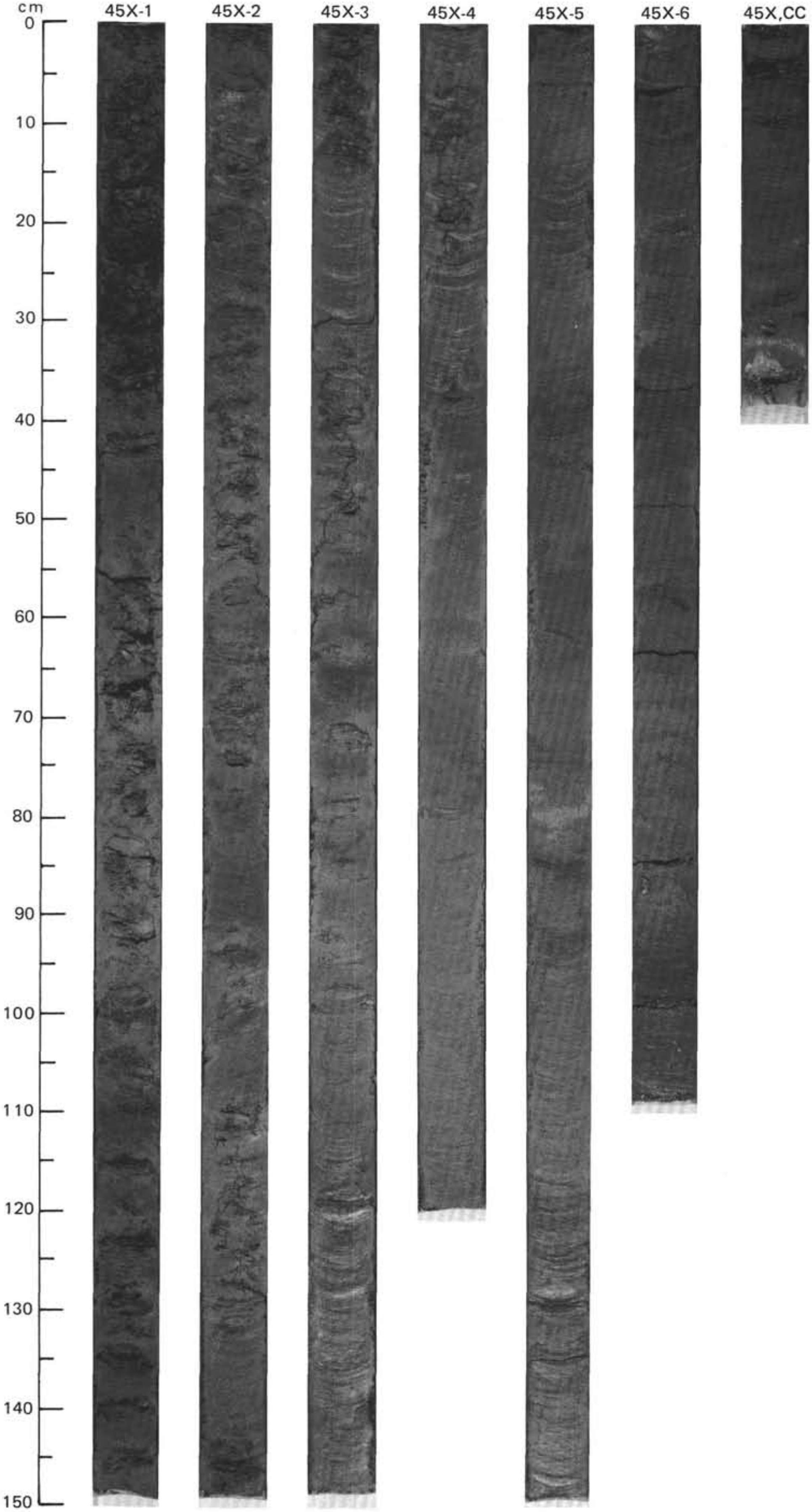
cm
0
10
20
30
40
50
60
70
80
90
100
110
120
130
140
150
45X-1
45X-2
45X-3
45X-4
45X-5
45X-6
45X,CC

SITE 643 HOLE A CORE 46X CORED INTERVAL 3209.2-3218.9 mbsl; 429.4-439.1 mbsf

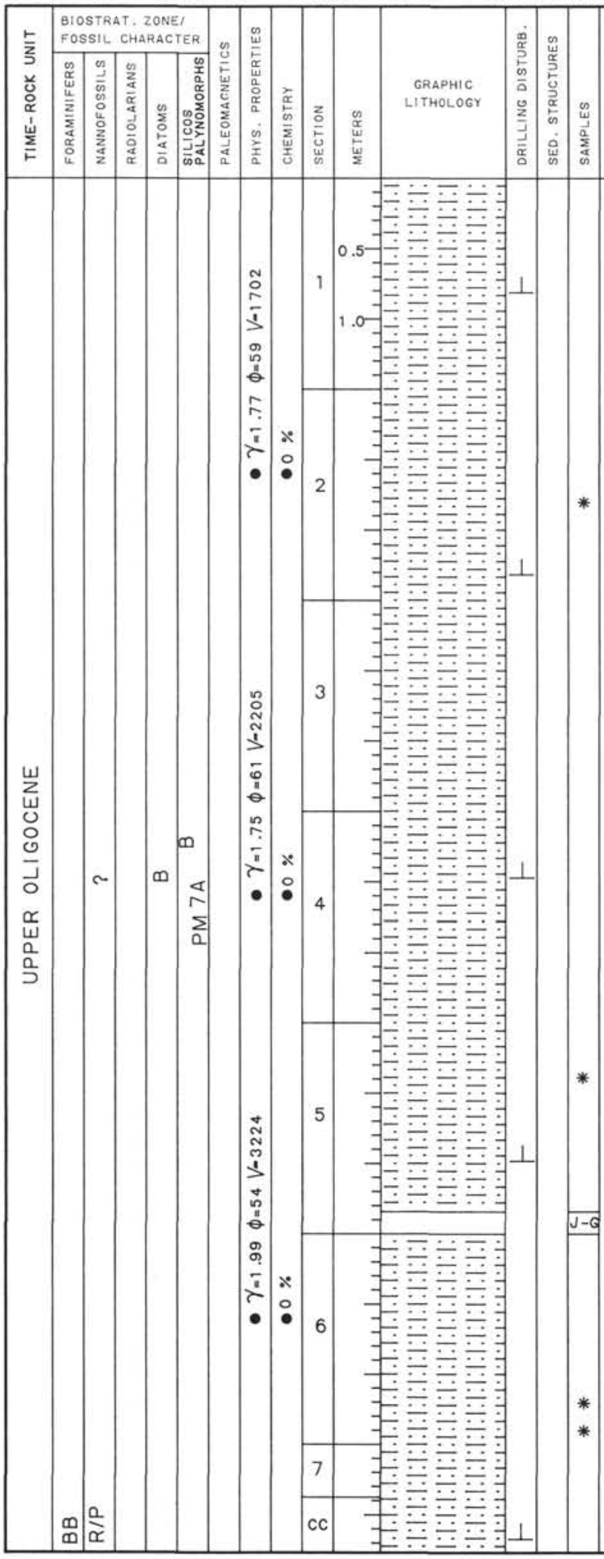

LITHOLOGIC DESCRIPTION

ZEOLITIC MUDSTONE

Entire core is moderately fragmented.

Major lithology: Zeolitic mudstone, grayish green (5GY 5/1), mottled with whitish dots (zeolites), and containing scattered faint green and brown color banding.

Minor lithologies:
a. Mudstone, grayish brown (2.5Y 5/2), rich in altered biogenic(?) opal (cristobalite?). Section 5, 36–40 cm.
b. Pyrite concretions. Section 5, 54 and 89 cm; Section 6, 60 and 78 cm.

SMEAR SLIDE SUMMARY (%):

	2, 80 D	5, 40 M	6, 128 M	6, 140 D
TEXTURE:				
Sand	5	—	—	—
Silt	20	20	5	—
Clay	75	80	95	—
COMPOSITION:				
Quartz	2	—	—	1
Clay	73	40	95	79
Volcanic glass	15	—	—	5
Accessory minerals:				
Zeolite	10	5	5	15
Opal	—	54	—	—

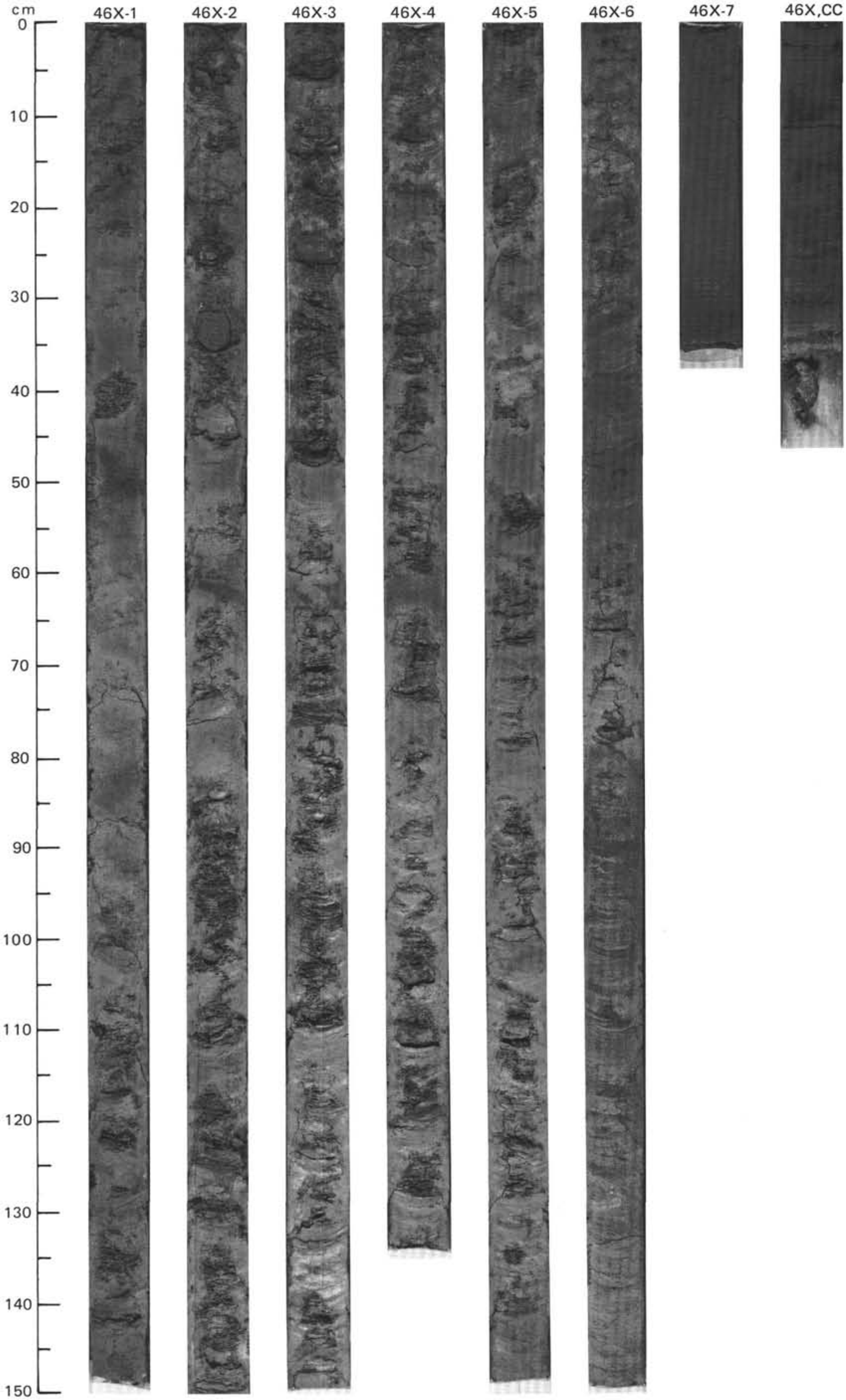
cm
0
10
20
30
40
50
60
70
80
90
100
110
120
130
140
150
46X-1
46X-2
46X-3
46X-4
46X-5
46X-6
46X-7
46X,CC

SITE 643 HOLE A CORE 47X CORED INTERVAL 3218.9-3228.5 mbsl; 439.1-448.7 mbsf

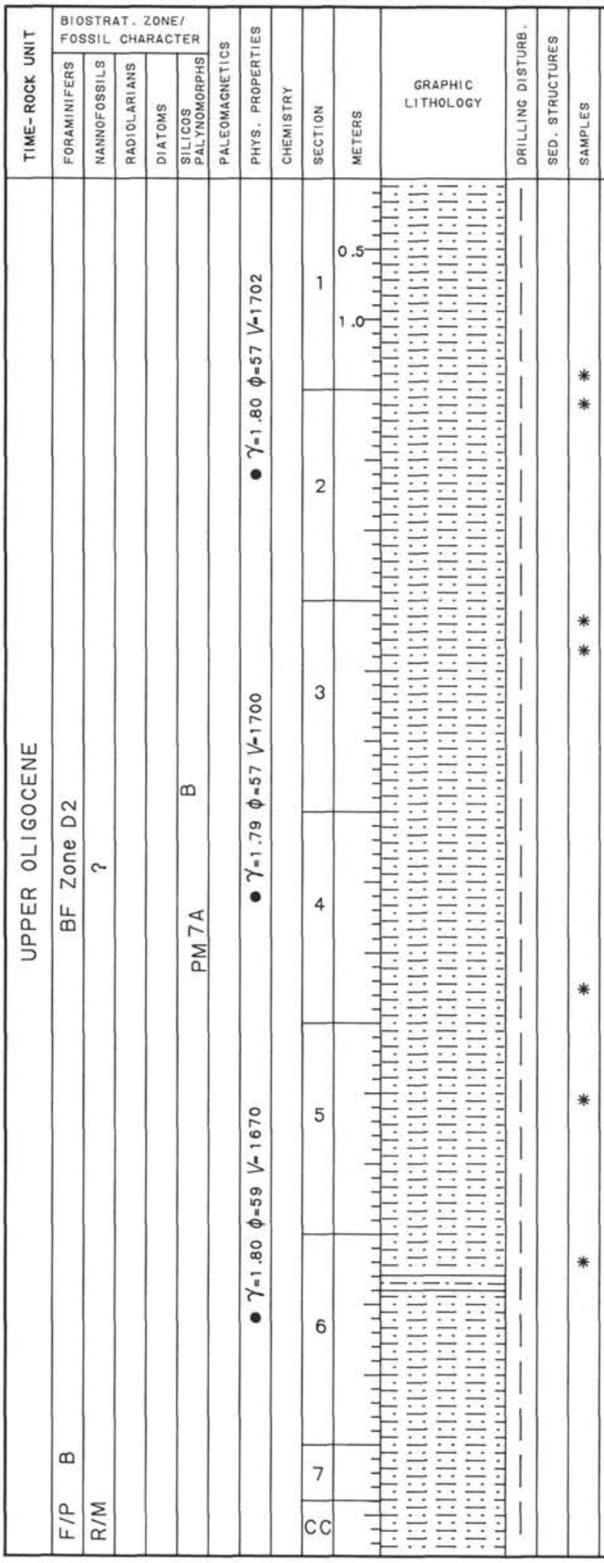

LITHOLOGIC DESCRIPTION

MUDSTONE

Entire core is moderately disturbed.

Major lithology: Mudstone, grayish-green (5GY 5/1), mottled with some whitish dots (zeolites?) and scattered green color banding.

Minor lithologies:
a. Mudstone, white to light gray (5Y 6/1). Section 3, 30–32 cm; Section 4, 119–126 cm; Section 5, 81–82 and 140–150 cm; Section 7, 36–37 cm; CC, 5–6 cm.
b. Sandy calcareous mudstone, grayish green (5Y 5/1). Section 6, 28–34 cm.
c. Mudstone, dark brown (7.5YR 3/2), dark reddish brown (5YR 3/2) to very dark grayish brown (10YR 3/2), extensively bioturbated and mottled. Rich in hematite. Section 1, 131–136 cm; Section 2, 93–102, 110–150 cm; Section 3, 5–23, 44–45, 62–63, and 102–110 cm; Section 4, 7–12, 20–25, and 30–35 cm; Section 6, 79–82 cm.

SMEAR SLIDE SUMMARY (%):

	2, 135 M	2, 5 M	3, 15 M	3, 31 M	4, 123 M	5, 53 D	6, 29 M
TEXTURE:							
Sand	—	—	—	15	—	—	50
Silt	5	2	2	25	20	2	—
Clay	95	98	98	60	80	98	50
COMPOSITION:							
Quartz	—	1	2	30	2	—	—
Mica	—	—	—	5	—	—	—
Clay	90	98	—	58	77	98	50
Volcanic glass	—	1	—	—	1	1	—
Calcite/dolomite	—	—	58	5	—	—	50
Accessory minerals	—	—	—	2	—	1	—
Goethite	10	—	40	—	—	—	—
Pyrite	—	—	—	—	20	—	—

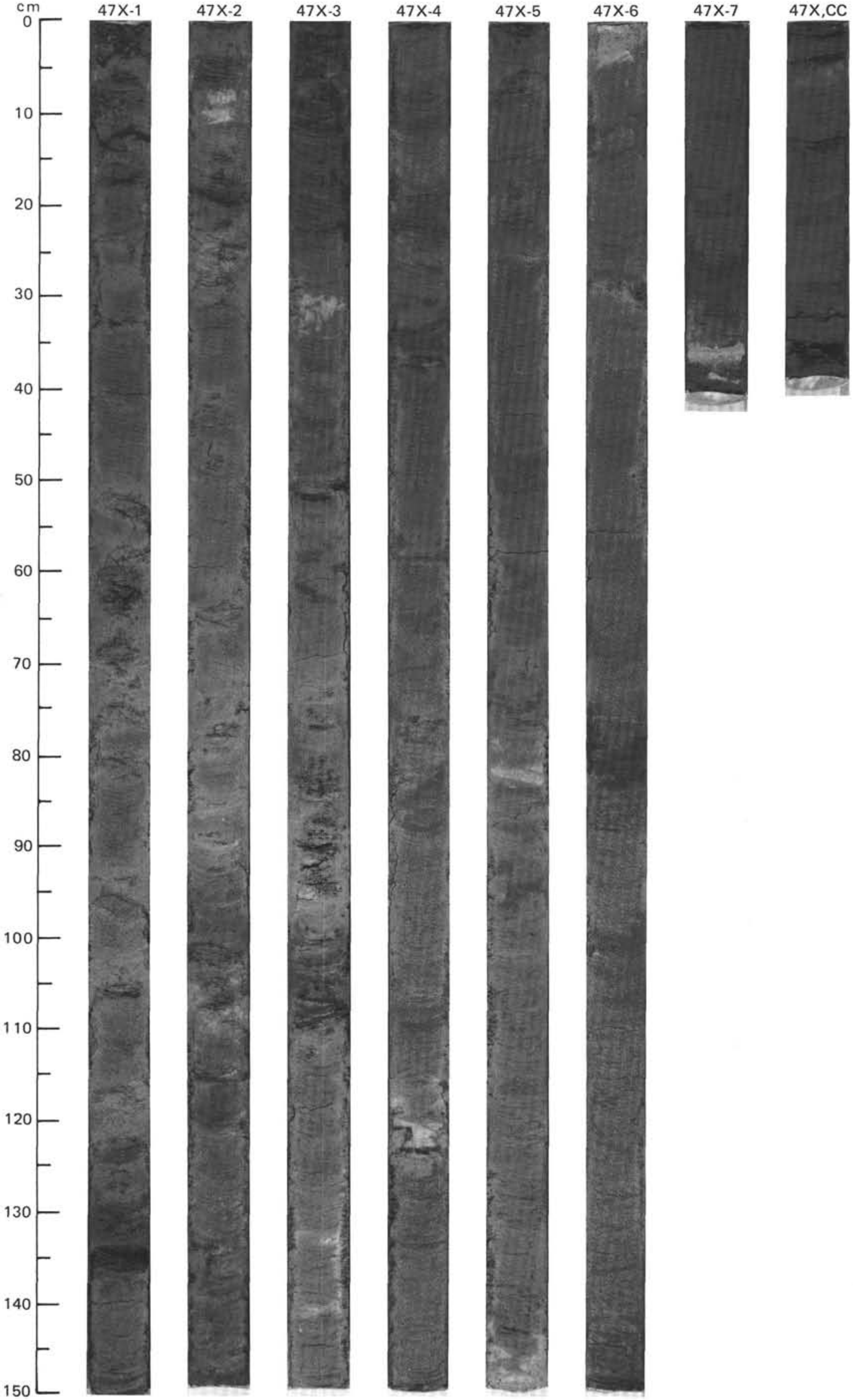
cm
0
10
20
30
40
50
60
70
80
90
100
110
120
130
140
150
47X-1
47X-2
47X-3
47X-4
47X-5
47X-6
47X-7
47X,CC

SITE 643 HOLE A CORE 48X CORED INTERVAL 3228.5-3238.2 mbsl; 448.7-458.4 mbsf

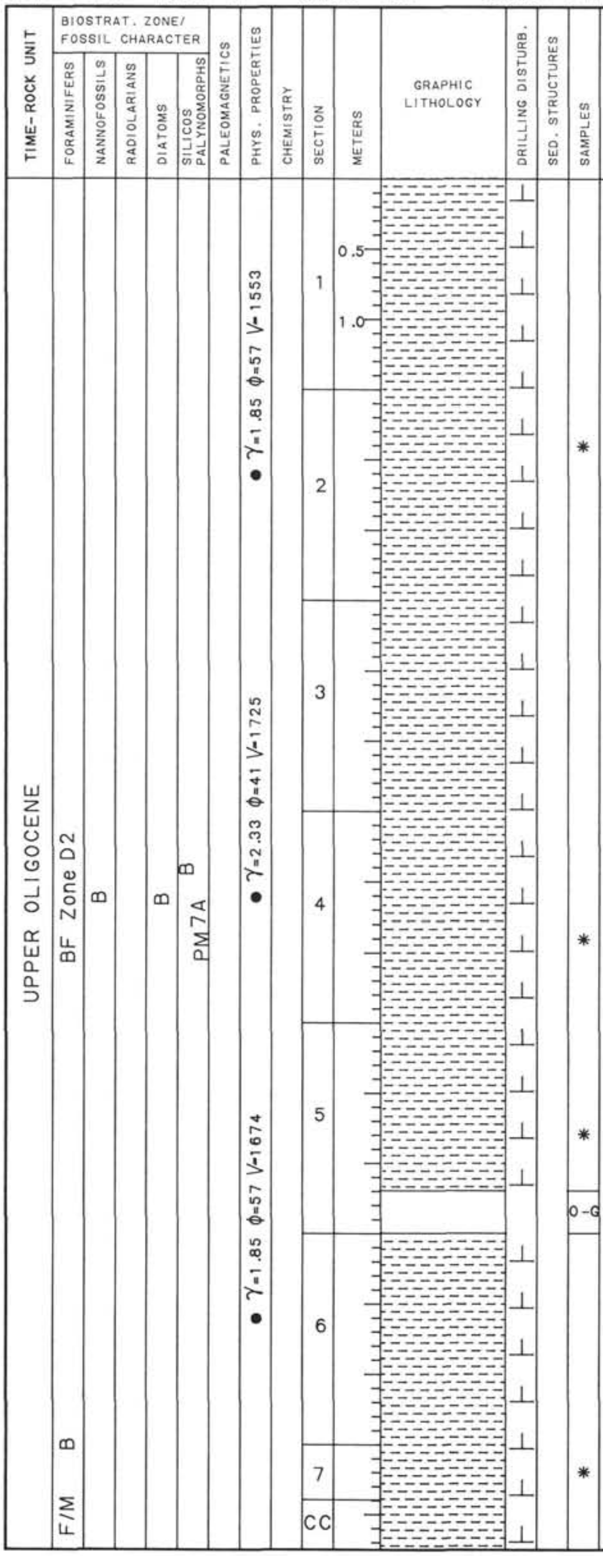

LITHOLOGIC DESCRIPTION

CLAYSTONE

Entire core is moderately fragmented.

Major lithology: Claystone, grayish green (5GY 5/1), mottled with white dots (zeolites?), and showing green to greenish brown color banding.

Minor lithologies:
a. Mudstone, dark gray (5Y 4/1) to dark grayish brown (2.5Y 3/2). Section 1, 57–60 and 128–129 cm; Section 4, 79–86 and 125–133 cm; Section 5, 26–29, 44–45, 57–60, and 69–76 cm; Section 6, 49–53, 66–71, and 116–118 cm; CC, 30–33 cm.
b. Sandy calcareous mud, grayish green (5GY 5/1). Section 4, 88–94 cm.

SMEAR SLIDE SUMMARY (%):

	2, 40 D	4, 89 M	5, 74 M	7, 26 D
TEXTURE:				
Sand	—	40	6	1
Silt	2	2	8	10
Clay	98	58	86	89
COMPOSITION:				
Quartz	2	2	5	1
Feldspar	—	—	2	—
Clay	98	58	86	89
Volcanic glass	—	—	5	—
Calcite/dolomite	—	40	—	—
Accessory minerals	—	—	2	—
Opaque minerals	—	—	—	10

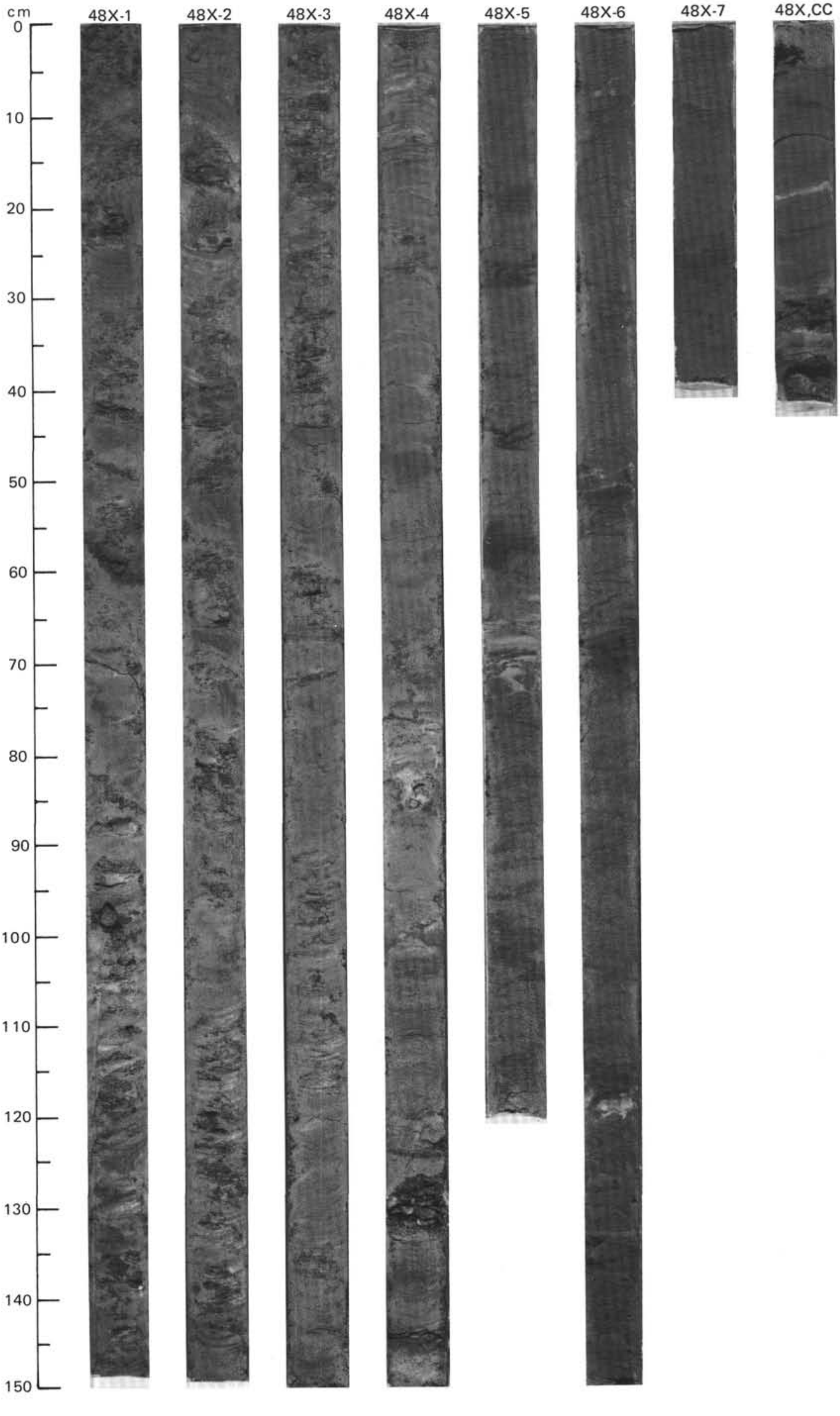
cm
0
10
20
30
40
50
60
70
80
90
100
110
120
130
140
150
48X-1
48X-2
48X-3
48X-4
48X-5
48X-6
48X-7
48X,CC

SITE 643 HOLE A CORE 49X CORED INTERVAL 3238.2-3247.9 mbsl; 458.4-468.1 mbsf

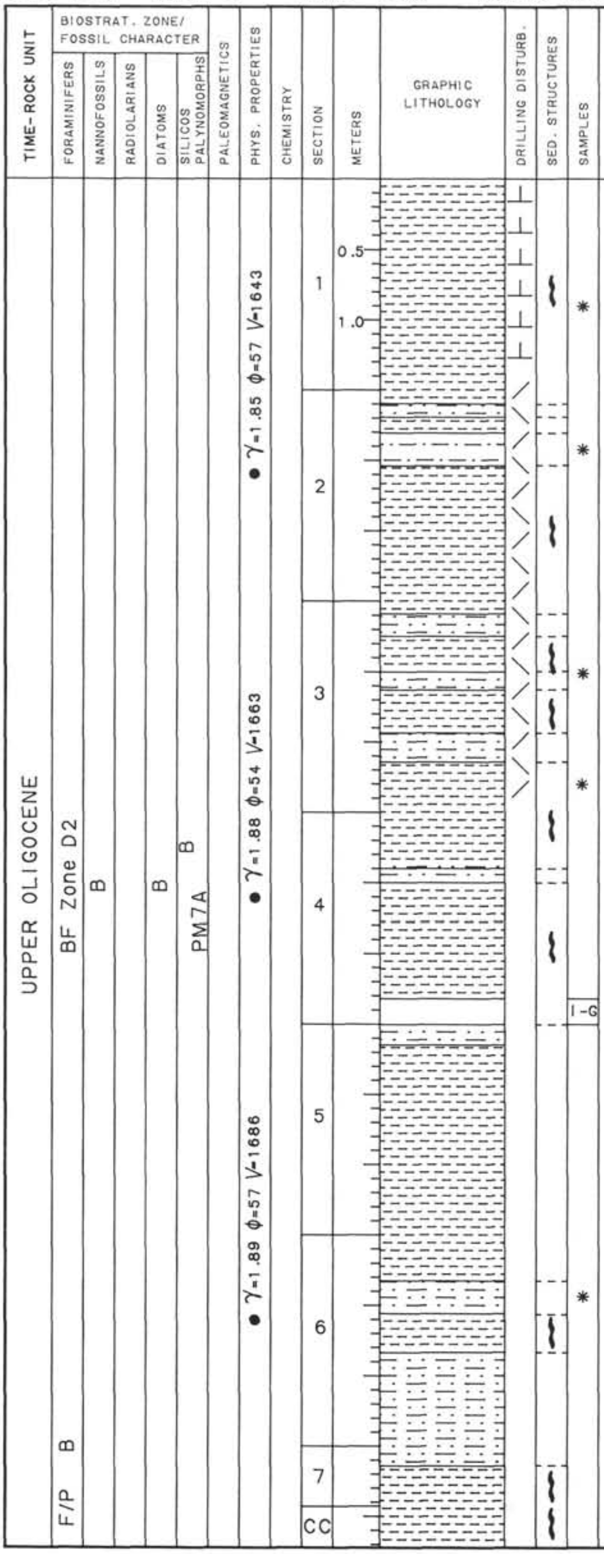

LITHOLOGIC DESCRIPTION

CLAYSTONE AND MUDSTONE

Major lithology: Claystone, dark reddish brown (5YR 3/3) to grayish brown (10YR 5/2), with minor to common mottling and burrows in greenish gray (5GY 5/1). Gradationally interbedded with more homogeneous mudstone, dark greenish gray (5G 4/1) to light greenish gray (5GY 7/1).

Minor lithology: Sandy mud, light greenish gray (5GY 7/1). Section 2, 35–53 cm.

SMEAR SLIDE SUMMARY (%):

	1, 97 D	2, 44 M	3, 55 D	3, 130 D	5, 38 D	6, 42 D
TEXTURE:						
Sand	5	20	—	—	—	—
Silt	2	30	20	5	5	15
Clay	93	50	80	95	95	85
COMPOSITION:						
Quartz	2	20	3	5	3	1
Mica	—	—	7	—	—	4
Clay	93	50	85	95	95	85
Volcanic glass	5	—	1	—	—	1
Calcite/dolomite	—	—	—	—	—	8
Accessory minerals	—	—	1	—	1	—
Opaque minerals	—	30	1	—	1	—
Zeolites	—	—	2	—	—	1

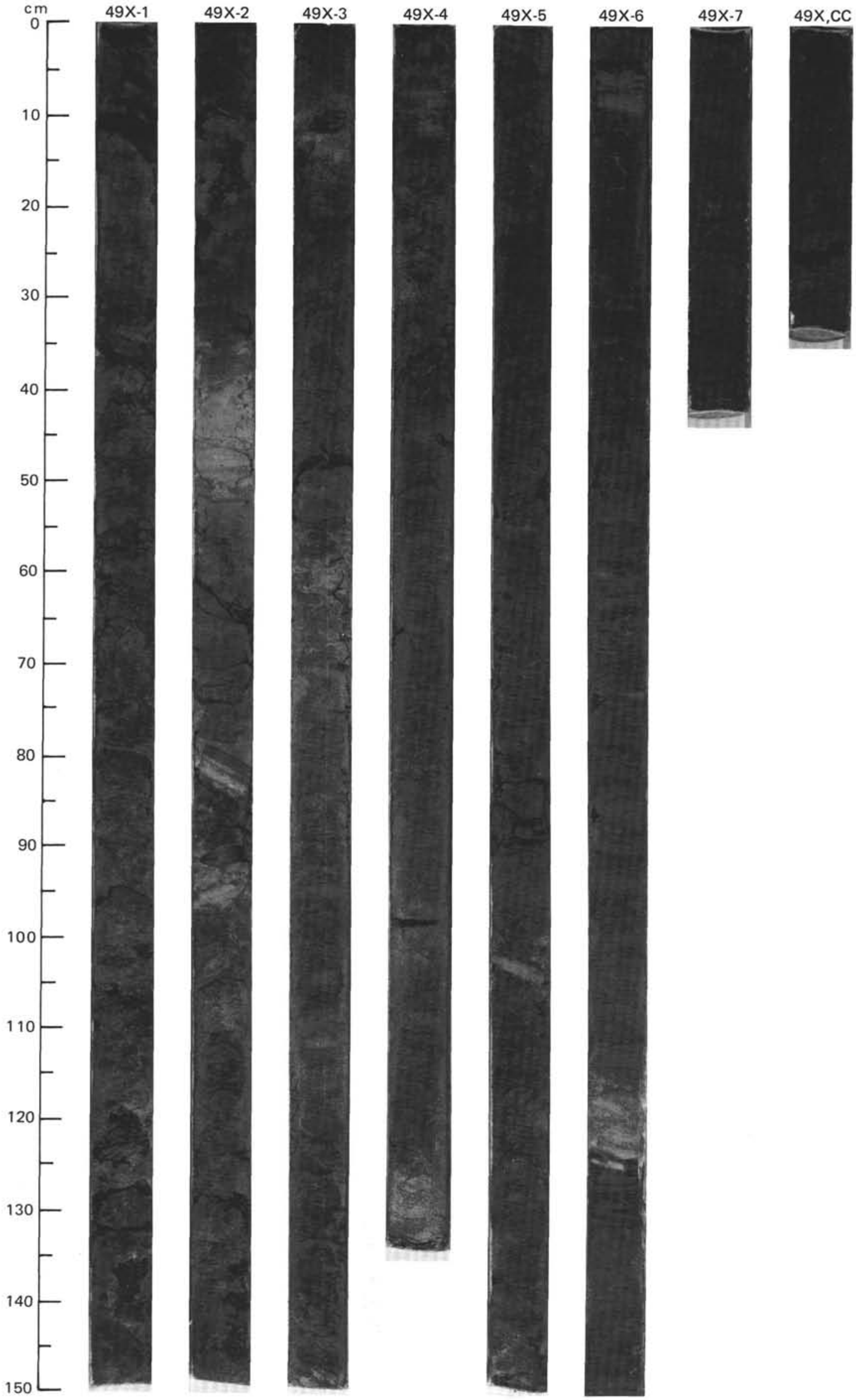
cm
0
10
20
30
40
50
60
70
80
90
100
110
120
130
140
150
49X-1
49X-2
49X-3
49X-4
49X-5
49X-6
49X-7
49X,CC

SITE 643 HOLE A CORE 50X CORED INTERVAL 3247.9-3257.5 mbsl; 468.1-477.7 mbsf

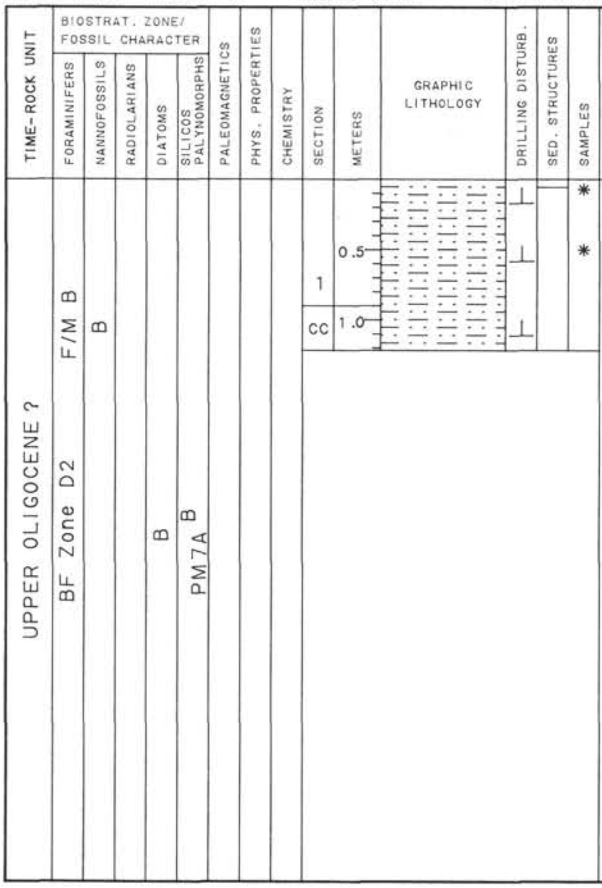

LITHOLOGIC DESCRIPTION

MUD TO MUDSTONE AND DOLOMITE SANDSTONE

Entire core is moderately fragmented.

Major lithologies:
a. Mud (plastic) to mudstone, greenish gray (5GY 5/1, 5G 5/1) to dark greenish gray (5GY 4/1, 5G 4/1), with minor to abundant mottling in these colors. Minor diffuse color banding in dark reddish brown. Section 1, 5–85 cm; Section 2, 2–35 cm.
b. Dolomite sandstone, pale brown (10YR 6/3). Single pebble, consisting of well-rounded, well-sorted, medium sand-sized dolomite grains, with approximately 30 percent fine-grained dolomite matrix. Section 1, 0–5 cm.

Minor lithology: Mud (plastic) to mudstone, dark gray (5YR 4/1) and homogeneous. Section 1, 85 cm, to CC, 2 cm.

SMEAR SLIDE SUMMARY (%):

	1, 3 M	1, 57 D
TEXTURE:		
Sand	100	—
Silt	—	10
Clay	—	90
COMPOSITION:		
Quartz	—	2
Mica	—	5
Clay	—	88
Volcanic glass	—	1
Dolomite	100	—
Accessory minerals	—	1
Zeolites	—	2
Opaque minerals	—	1

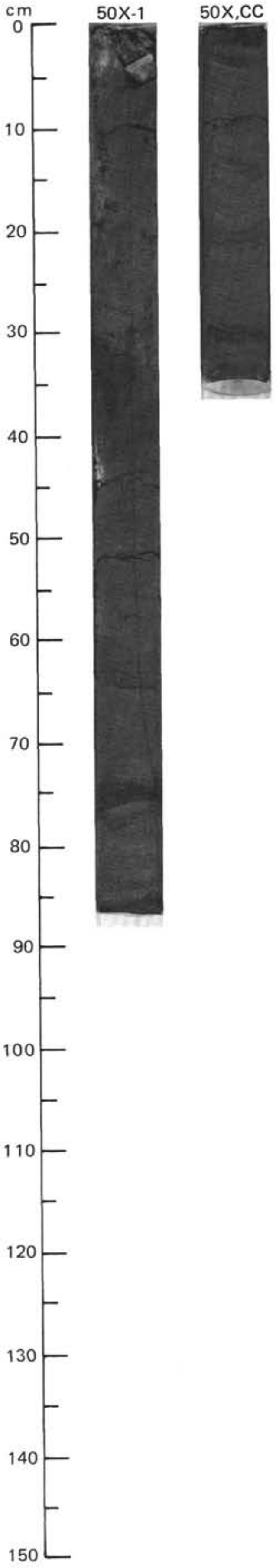
cm
0
10
20
30
40
50
60
70
80
90
100
110
120
130
140
150
50X-1
50X,CC

SITE 643 HOLE A CORE 51X CORED INTERVAL 3257.5-3267.1 mbsl; 477.7-487.3 mbsf

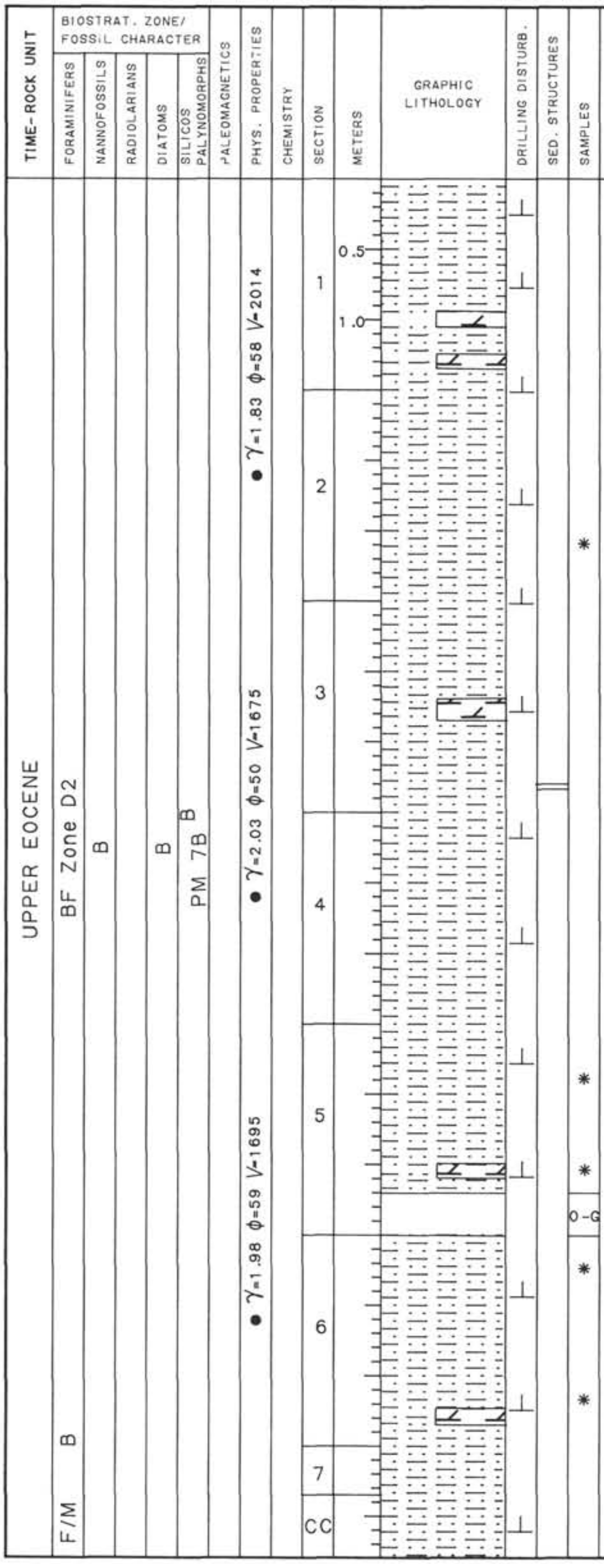

LITHOLOGIC DESCRIPTION

MUD TO MUDSTONE

Entire core is moderately fragmented.

Major lithologies:
a. Muds (plastic) to mudstone, greenish gray (5GY 5/1, 5G 5/1) to dark greenish gray (5GY 4/1, 5G 4/1) and dark gray (5Y 4/1), with common to abundant mottling and diffuse internal color banding. Minor mottling in bluish gray (5B 4/2). Section 1 to Section 4, 71 cm; Section 4, 137 cm, to Section 5, 50 cm; Section 5, 75–103 and 113–150 cm; Section 6, 26–45 cm; Section 6, 65 cm, to Section 7, 28 cm; CC, 0–18 cm.
b. Muds (plastic) to mudstone, dark reddish gray (5YR 4/2), dark reddish brown (5YR 3/3), and dark grayish brown (10YR 4/2), with minor to abundant mottling by Lithology a. Section 4, 71–137 cm; Section 5, 50–75 and 103–113 cm; Section 6, 0–26 and 45–65 cm; Section 7, 28–37 cm; CC, 18–45 cm.

Minor lithology: Sand, calcareous, in concentrated to disseminated zones. Section 1, 97–102 and 123–128 cm; Section 3, 70–86 and 136 cm; Section 5, 107–109 cm; Section 6, 111–113, 116–118, and 122–133 cm.

SMEAR SLIDE SUMMARY (%):

	2, 108 M	5, 46 M	5, 107 M	6, 21 D	6, 122 M
TEXTURE:					
Sand	—	—	98	—	90
Silt	20	10	—	10	5
Clay	80	90	2	90	5
COMPOSITION:					
Quartz	1	2	2	2	20
Mica	6	6	1	5	—
Clay	80	90	2	90	5
Volcanic glass	2	1	—	—	—
Calcite/dolomite	—	1	95	2	70
Accessory minerals	—	—	—	—	5
Zeolites	3	—	—	1	—
Pyrite/manganese	8	—	—	—	—

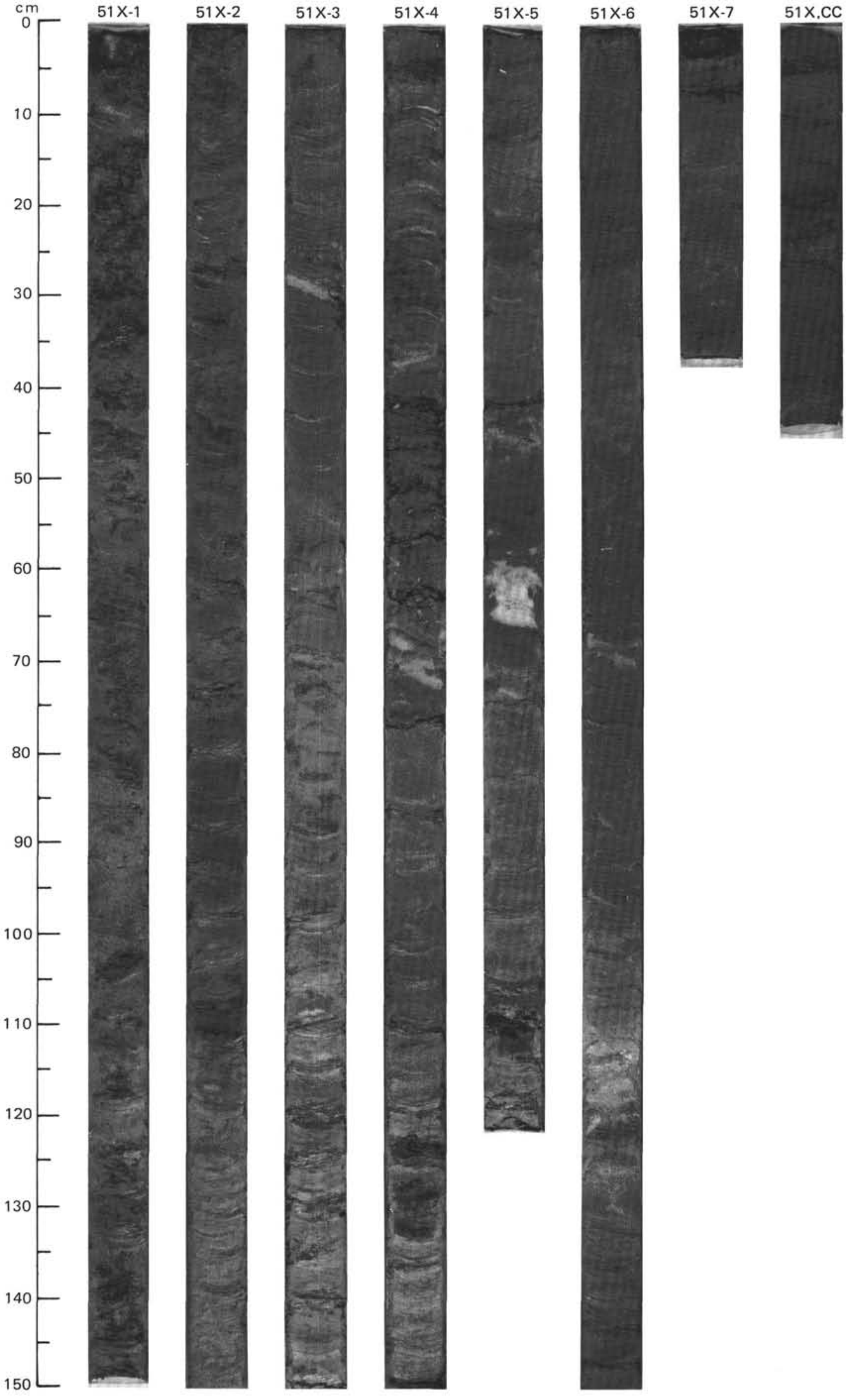
cm
0
10
20
30
40
50
60
70
80
90
100
110
120
130
140
150
51X-1
51X-2
51X-3
51X-4
51X-5
51X-6
51X-7
51X,CC

SITE 643 HOLE A CORE 52X CORED INTERVAL 3267.1-3276.8 mbsl; 487.3-497.0 mbsf

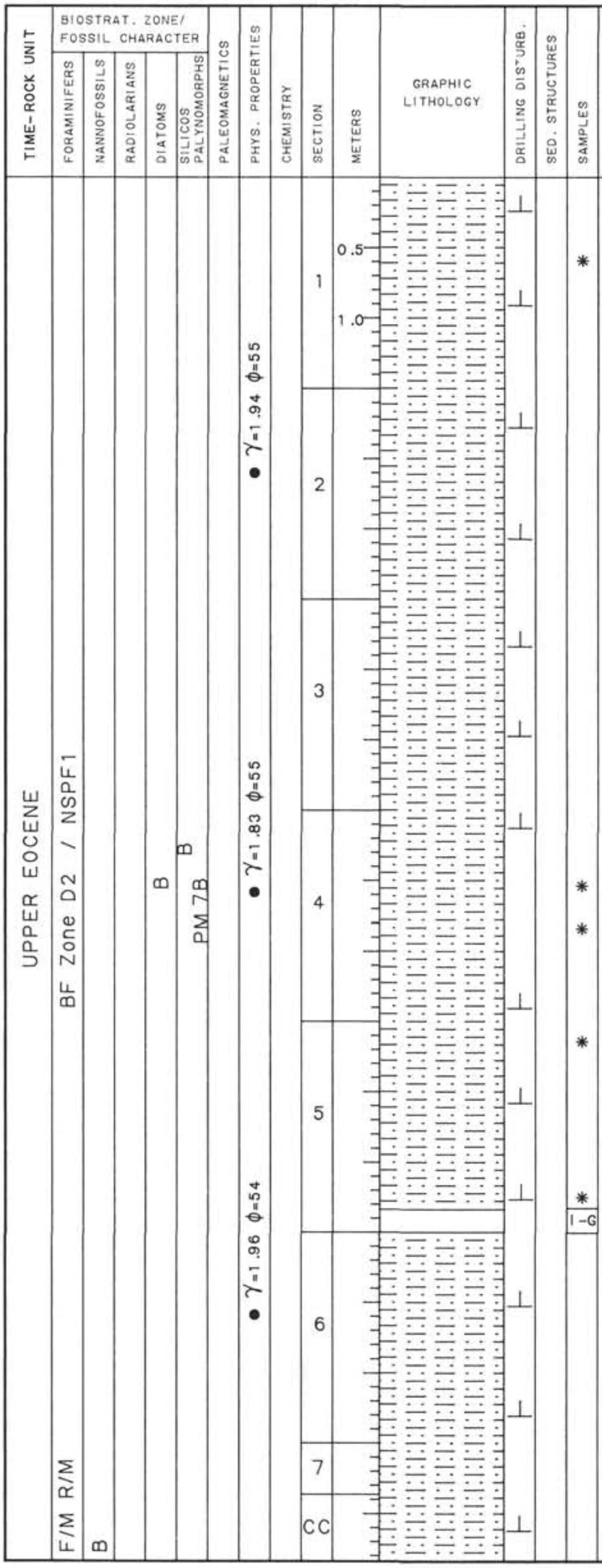

LITHOLOGIC DESCRIPTION

MUD TO MUDSTONE

Entire core is slightly to moderately fractured.

Major lithologies:
a. Mud (plastic) to mudstone, dark gray (5Y 4/1), greenish gray (5G 5/1), and dark greenish gray (5G 4/1), with minor to abundant mottling, diffuse color banding, and gradational contacts between colors. Section 1, 91 cm, to Section 2, 125 cm; Section 3 to Section 5, 12 cm; Section 5, 16 cm, to CC, 24 cm; CC, 31–48 cm.
b. Mud (plastic) to mudstone, dark reddish gray (10YR 4/1) to dark gray (5YR 4/1), with minor mottling and minor diffuse color banding. Section 1, 0–91 cm; Section 2, 125–150 cm; Section 5, 12–16 cm; CC, 24–31 cm.

Minor lithologies:
a. Mud (plastic), bluish gray (5B 4/2), present as diffuse mottles or color bands. Section 4, 39–41 and 53 cm; Section 5, 116–121 cm; Section 6, 109–150 cm (minor); CC.
b. Sand, white, calcite or dolomite. Section 4, 56–57 cm.
c. Sand, white, quartz and feldspar. Section 5, 124–125 cm.

SMEAR SLIDE SUMMARY (%):

	1, 61 D	4, 57 M	4, 86 D	5, 10 D	5, 125 M
TEXTURE:					
Sand	—	100	—	—	80
Silt	5	—	5	5	20
Clay	95	—	95	95	—
COMPOSITION:					
Quartz	2	—	1	2	80
Feldspar	—	—	—	—	15
Mica	3	—	3	3	—
Clay	95	—	95	95	—
Calcite/dolomite	—	100	—	—	5
Accessory minerals:					
Zeolite	—	—	1	—	—

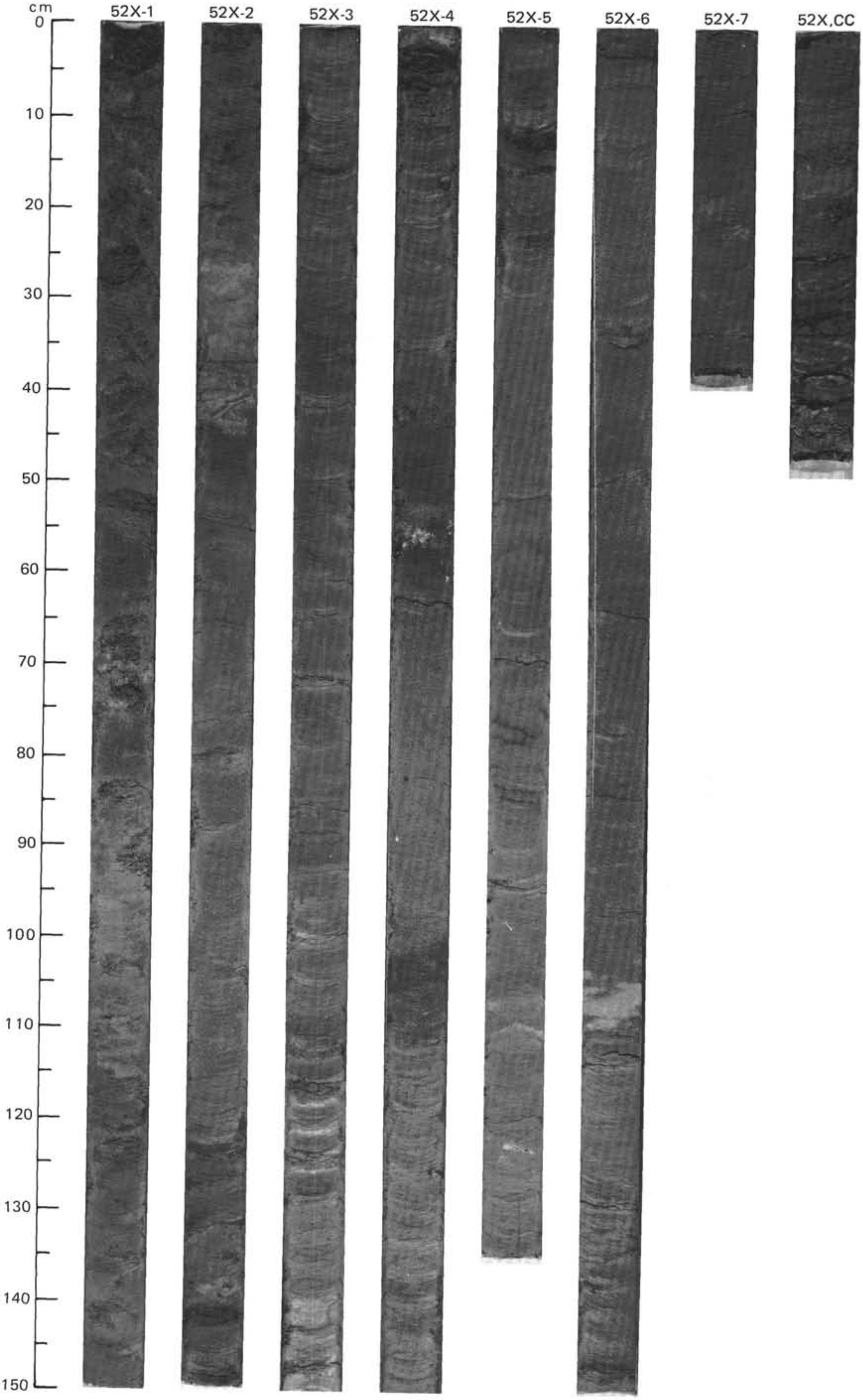
cm
0
10
20
30
40
50
60
70
80
90
100
110
120
130
140
150
52X-1
52X-2
52X-3
52X-4
52X-5
52X-6
52X-7
52X,CC

SITE 643 HOLE A CORE 53X CORED INTERVAL 3276.8-3286.5 mbsl; 497.0-506.7 mbsf

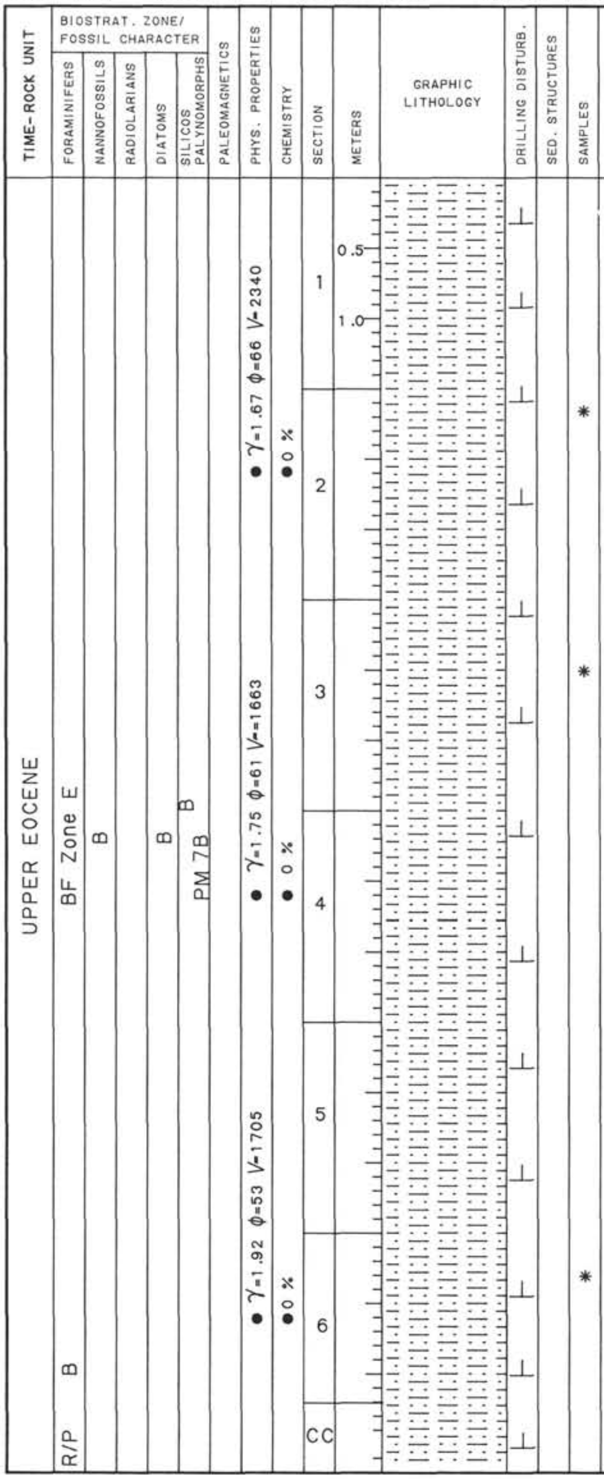

LITHOLOGIC DESCRIPTION

MUD TO MUDSTONE

Entire core is moderately fragmented, consisting of coherent blocks ("drilling biscuits") and drilling breccia.

Major lithologies:
a. Mud (plastic) to mudstone, dark gray (5Y 4/1) to dark greenish gray (5GY 4/1). "Drilling biscuits" have internal features ranging from structureless to abundant compaction laminations, with possible discontinuous, nonparallel depositional laminations. Section 1 to Section 5.
b. Mud (plastic) to mudstone, dark reddish brown (5YR 2.5/2) to dark gray (5YR 4/1), with rare to common mottles and diffuse color bands of lithology a. Section 6 to CC.

SMEAR SLIDE SUMMARY (%):

	2, 15 D	3, 51 M	6, 33 D
TEXTURE:			
Silt	5	2	10
Clay	95	98	90
COMPOSITION:			
Quartz	1	3	1
Mica	3	—	3
Clay	95	—	93
Calcite/dolomite	1	97	2
Accessory minerals:			
Opaque minerals	—	—	1

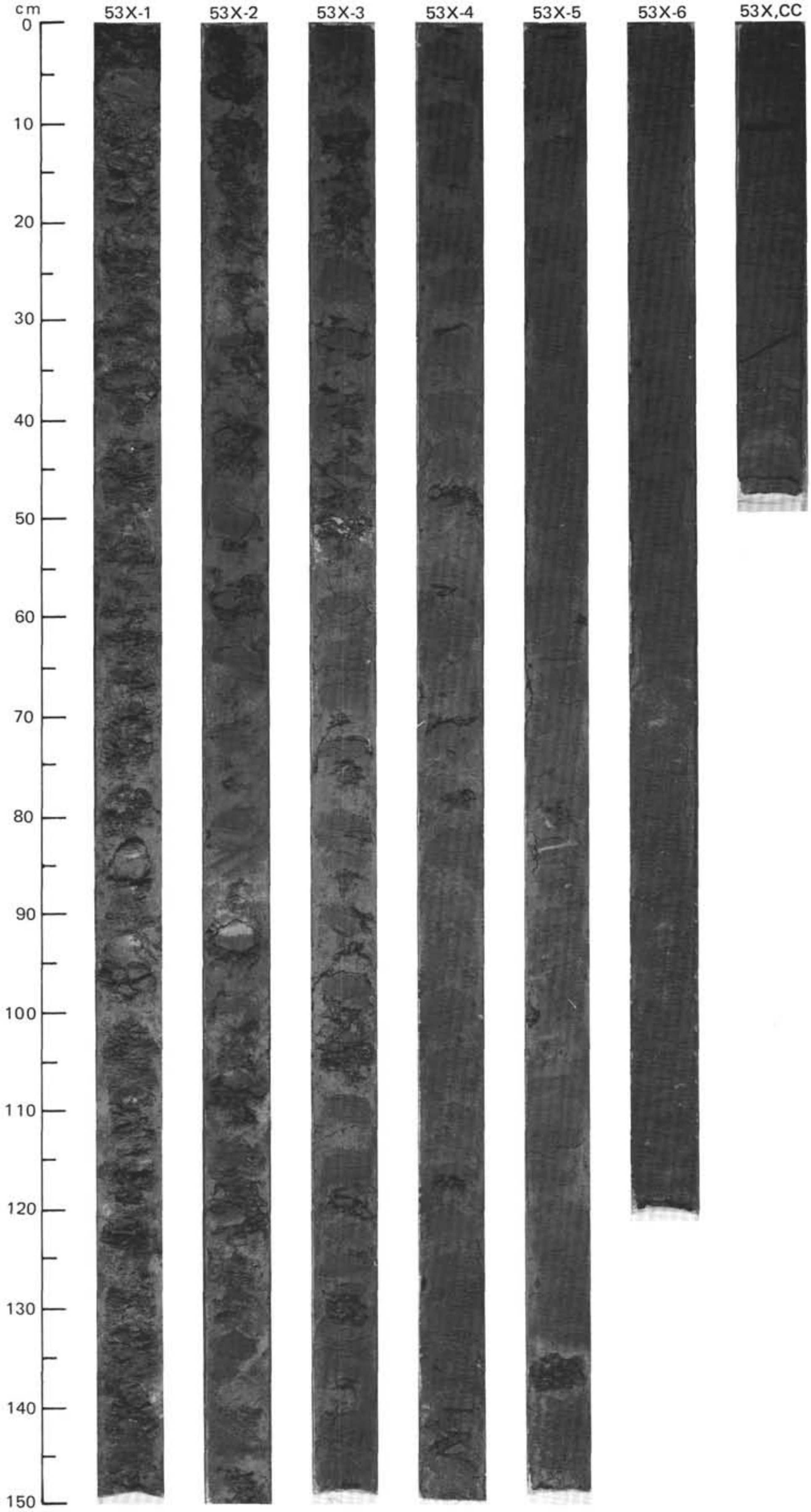
cm
0
10
20
30
40
50
60
70
80
90
100
110
120
130
140
150
53X-1
53X-2
53X-3
53X-4
53X-5
53X-6
53X,CC

SITE 643 HOLE A CORE 54X CORED INTERVAL 3286.5-3296.2 mbsl; 506.7-516.4 mbsf

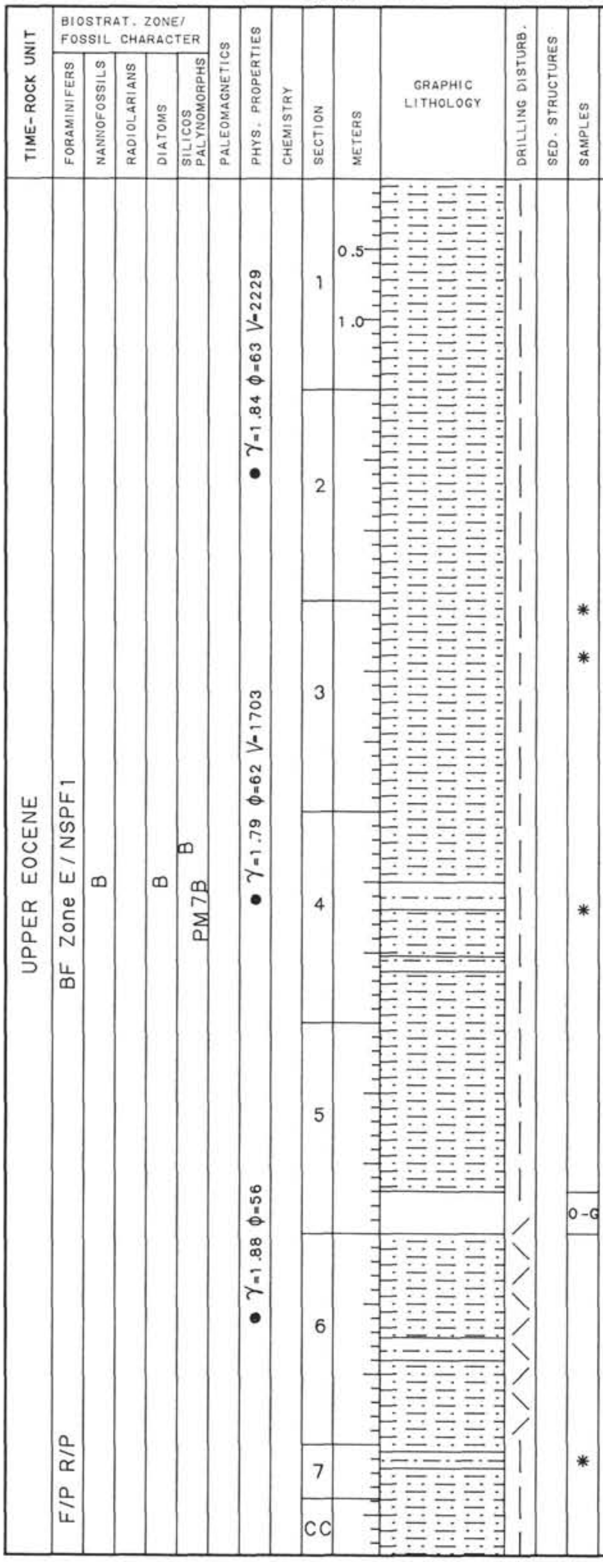

LITHOLOGIC DESCRIPTION

MUDSTONE

Section 1 to Section 5, Section 7, and the CC are moderately fragmented. Section 6 is highly fragmented.

Major lithologies:

a. Mudstone, greenish gray (5GY 5/1), with extensive compaction laminations and color banding. Section 1 to Section 2; Section 3, 0–32 and 81–96 cm; Section 4, 70–103 cm; Section 4, 111 cm, to Section 5, 40 cm; Section 5, 45–70 and 90–106 cm; Section 6, 0–75 cm; Section 6, 86 cm, to Section 7, 5 cm; Section 7, 18–37 cm; CC, 0–40 cm.

b. Mudstone, dark reddish brown (5YR 3/2), with extensive compaction lamination and color banding. Section 3, 61–81 cm; Section 3, 96 cm, to Section 4, 61–81 cm; Section 3, 96 cm, to Section 4, 50 cm; Section 5, 70–90 and 106–122 cm.

Minor lithology: Sandy mudstone, gray (5Y 6/1) to bluish gray (5B 5/1), with compaction laminations and color banding. Section 3, 32–44 cm; Section 4, 50–70 and 103–111 cm; Section 6, 75–86 cm; Section 7, 5–18 cm.

SMEAR SLIDE SUMMARY (%):

	3, 15 D	3, 39 M	4, 72 D	7, 20 M
TEXTURE:				
Sand	10	10	—	40
Silt	10	20	5	10
Clay	80	70	95	50
COMPOSITION:				
Quartz	10	4	10	20
Feldspar	—	2	—	10
Mica	10	—	5	3
Clay	75	20	84	45
Volcanic glass	—	—	—	2
Calcite/dolomite	5	54	—	20
Accessory minerals:				
Pyrite	—	20	—	—
Zeolite	—	—	1	—

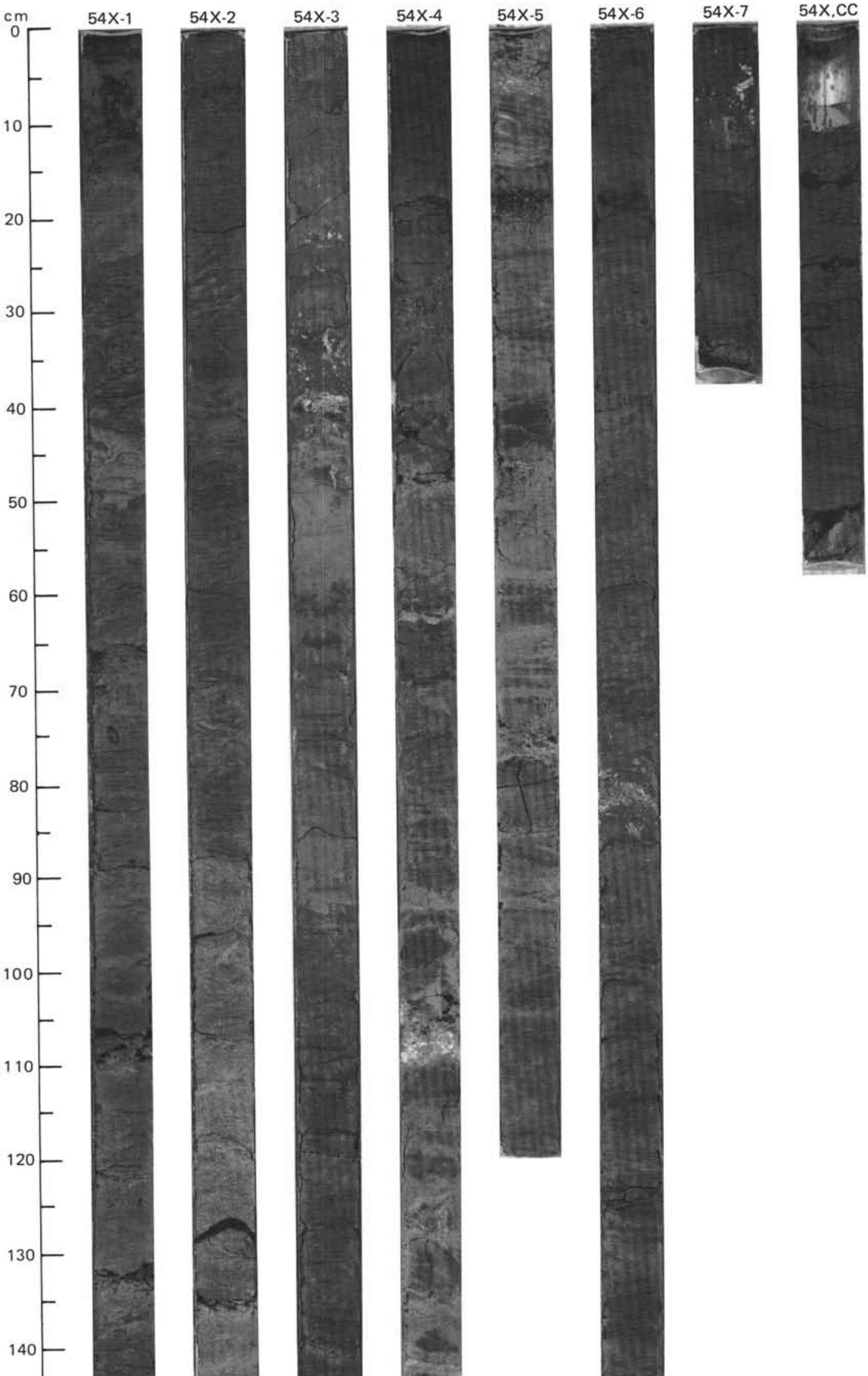
cm
0
10
20
30
40
50
60
70
80
90
100
110
120
130
140
150
54X-1
54X-2
54X-3
54X-4
54X-5
54X-6
54X-7
54X,CC

SITE 643 HOLE A CORE 55X CORED INTERVAL 3296.2-3305.8 mbsl; 516.4-526.0 mbsf

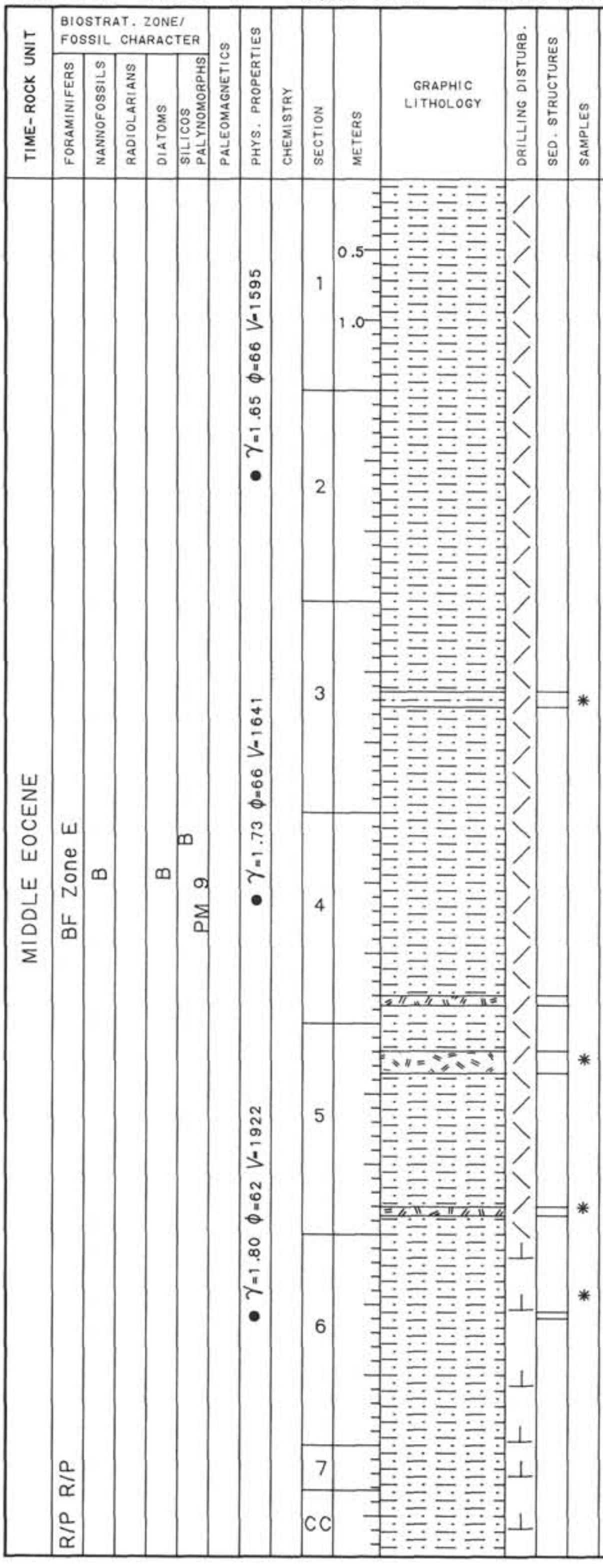

LITHOLOGIC DESCRIPTION

MUDSTONE

Section 1 to Section 5 is highly fragmented. Section 6 to CC is moderately fragmented.

Major lithologies:
a. Mudstone, greenish gray (5GY 5/1), with abundant compaction lamination, and scattered color banding in grayish green (5G 4/2) and dark reddish brown (5YR 3/2). Section 1 to Section 2; Section 6 to CC.
b. Mudstone, with predominant color banding in greenish gray (5GY 5/1) and grayish green (5G 4/2), containing abundant compaction lamination. Section 4.
c. Mudstone, with predominant color banding in greenish gray (5GY 5/1) and dark reddish brown (5YR 4/2), containing abundant compaction lamination. Section 4.
d. Mudstone, reddish gray (5YR 5/2), with abundant compaction lamination. Section 5, 0–20, 35–106, and 138–150 cm.

Minor lithologies:
a. Sandy mudstone, greenish gray (5GY 5/1) to grayish green (5G 4/2), volcanic ash to altered volcanic ash. Section 4, 130–134 cm; Section 5, 20–35 and 130–138 cm; Section 6, 55–60 cm.
b. Sandy mudstone, greenish gray (5GY 5/1) and calcareous. Section 3, 67–76 cm.

SMEAR SLIDE SUMMARY (%):

	3, 72 M	5, 20 M	5, 137 M	6, 48 D
TEXTURE:				
Sand	20	50	50	—
Silt	11	30	40	2
Clay	69	20	10	98
COMPOSITION:				
Quartz	1	2	60	1
Mica	—	1	—	—
Clay	69	10	10	98
Volcanic glass	—	85	30	—
Calcite/dolomite	30	2	—	—

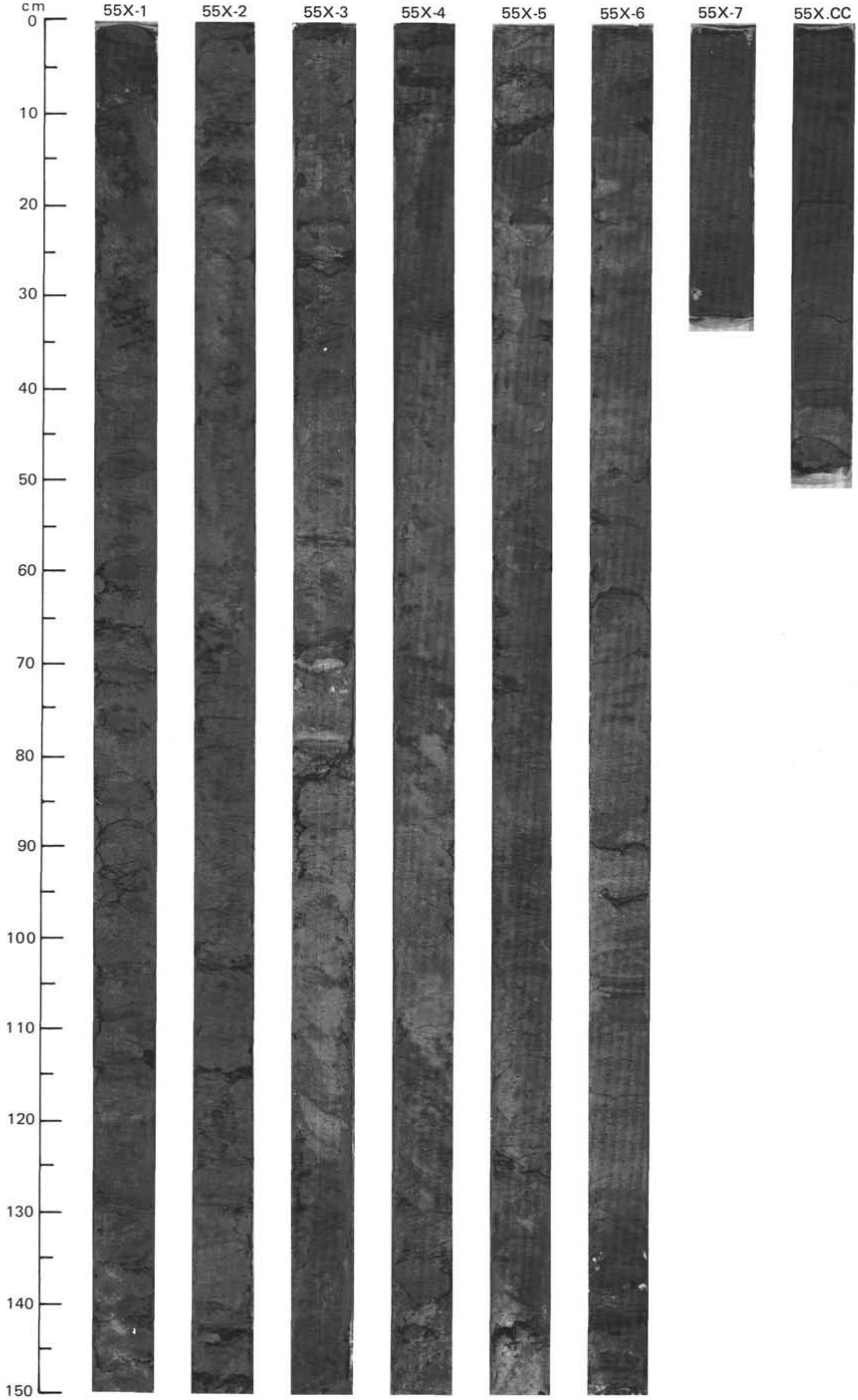
cm
0
10
20
30
40
50
60
70
80
90
100
110
120
130
140
150
55X-1
55X-2
55X-3
55X-4
55X-5
55X-6
55X-7
55X.CC

SITE 643 HOLE A CORE 56X CORED INTERVAL 3305.8-3315.4 mbsl; 526.0-535.6 mbsf

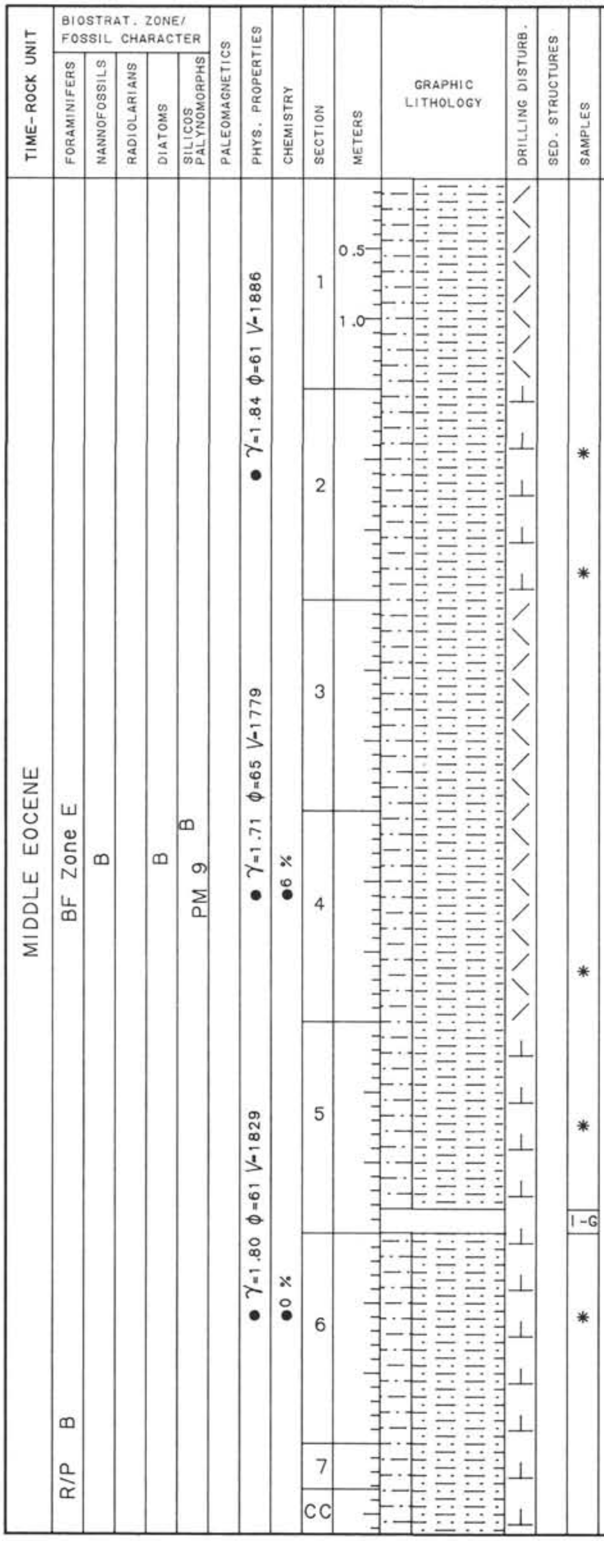

LITHOLOGIC DESCRIPTION

MUDSTONE TO SANDY MUDSTONE

Sections 1, 3, and 4 are highly fragmented. Sections 2 and 5 to CC are moderately fragmented.

Major lithologies:
a. Mudstone to sandy mudstone, dark brown (7.5YR 3/2) to dark reddish gray (5YR 4/2), with rare to abundant compaction laminations, common to abundant mottling, and minor color banding. Section 1, 20 cm, to Section 2, 2 cm; Section 2, 7–15, 32–56, 58–80, and 90–126 cm; Section 2, 139 cm, to Section 3, 30 cm; Section 3, 59–117 cm; Section 4, 30–60 and 118–130 cm; CC, 0–17 cm.
b. Mudstone to sandy mudstone, greenish gray (5GY 5/1) to grayish green (5G 4/2), with abundant compaction laminations. Section 1, 0–20 cm; Section 2, 2–7 cm; Section 3, 30–59 cm; Section 3, 117 cm, to Section 4, 30 cm; Section 4, 60–118 cm; Section 4, 130 cm, to Section 5, 150 cm; CC, 17–33 cm.
c. Mudstone to sandy mudstone, color banded in greenish gray (5GY 5/1) and dark reddish gray (5YR 4/2), or gradational. Contain common compaction laminations. Section 6 to Section 7.

Minor lithology: Mudstone to sandy mudstone, dark bluish gray (5B 4/1). Possible altered volcanic ash. Section 2, 15–32, 56–58, 80–90, and 126–139 cm.

SMEAR SLIDE SUMMARY (%):

	2, 52 D	2, 133 M	4, 113 D	5, 75 D	6, 60 M
TEXTURE:					
Sand	1	1	1	10	50
Silt	13	4	8	10	5
Clay	86	95	91	80	45
COMPOSITION:					
Quartz	2	2	2	—	5
Clay	86	95	91	80	45
Volcanic glass	10	—	1	—	—
Calcite/dolomite	1	—	—	—	50
Accessory minerals	—	—	1	—	—
Glauconite	1	1	—	10	—
Pyrite	—	2	—	—	—
Zeolites	—	5	—	10	—

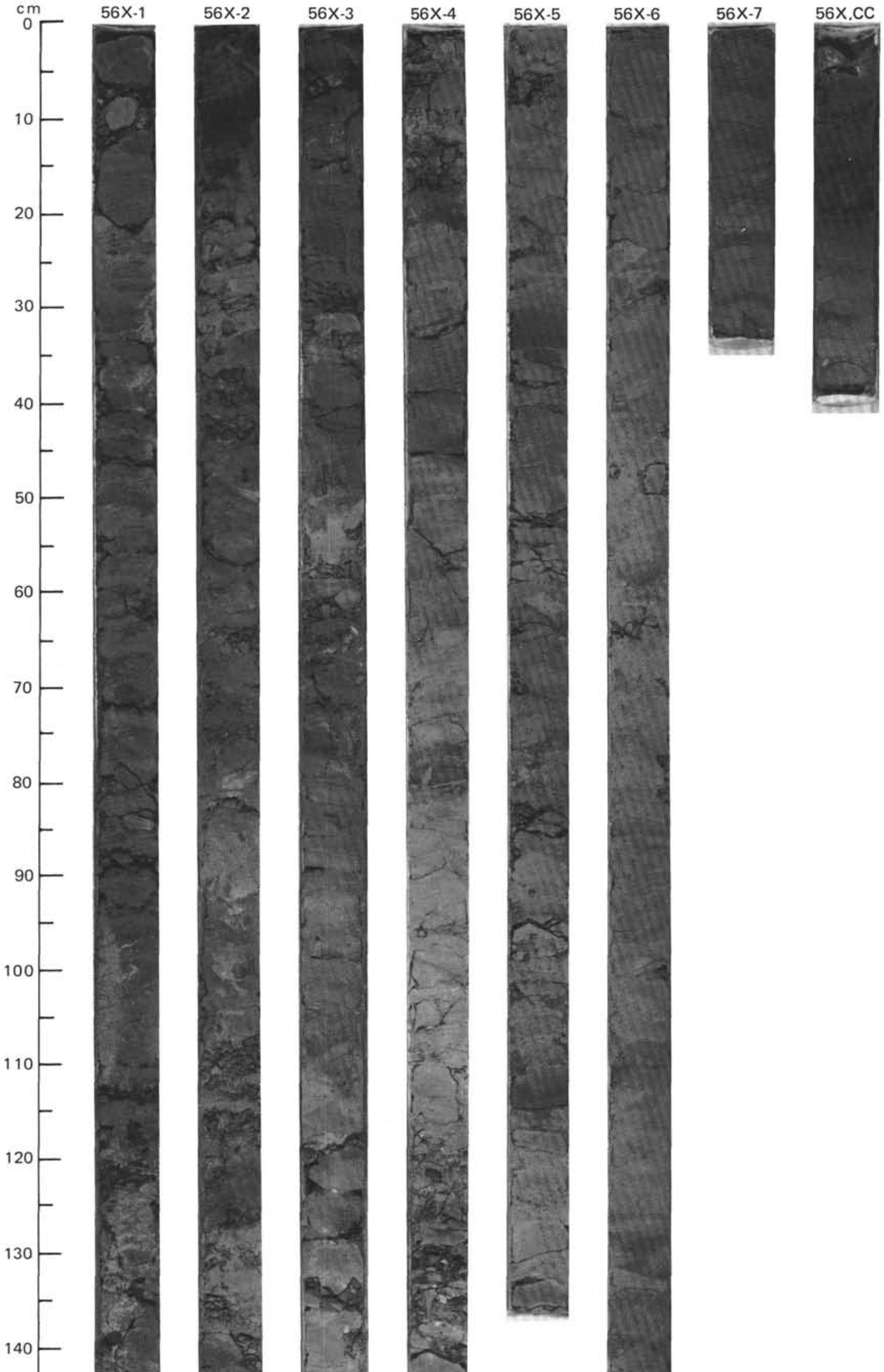
cm
0
10
20
30
40
50
60
70
80
90
100
110
120
130
140
150
56X-1
56X-2
56X-3
56X-4
56X-5
56X-6
56X-7
56X,CC

SITE 643 HOLE A CORE 57X CORED INTERVAL 3315.4-3325.0 mbsl; 535.6-545.2 mbsf

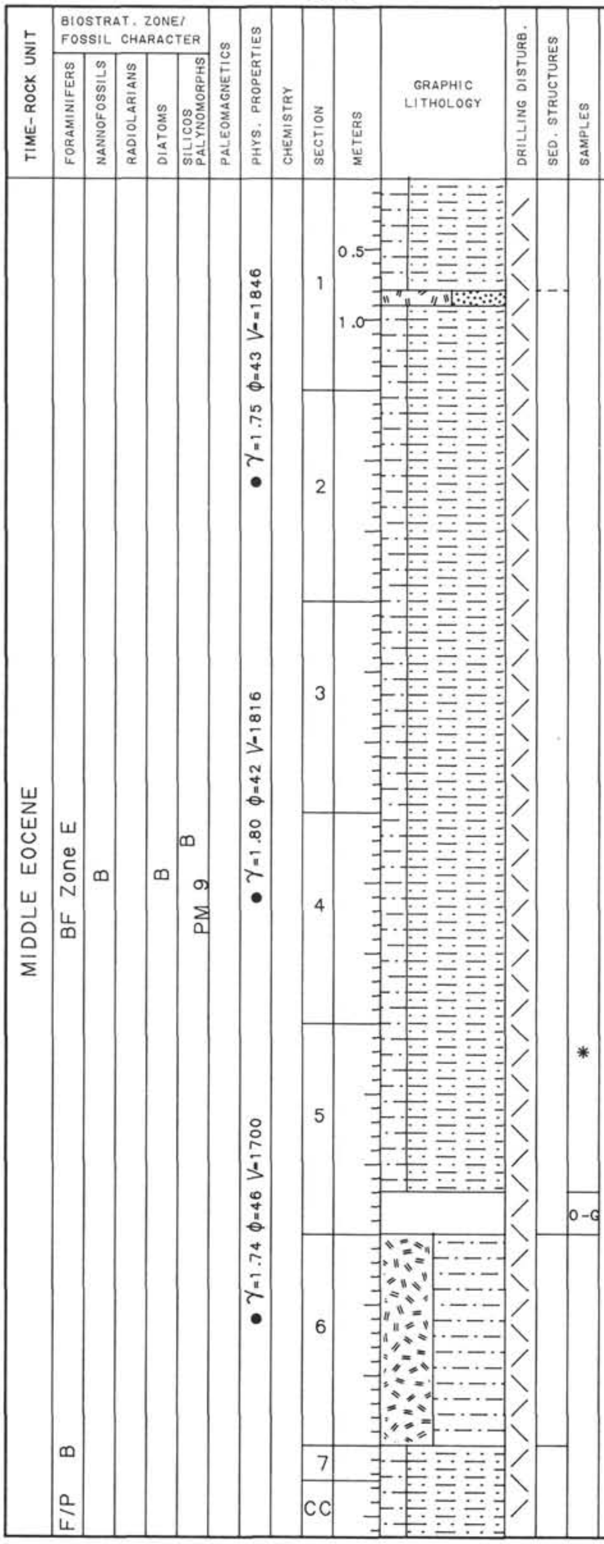

LITHOLOGIC DESCRIPTION

MUDSTONE TO SANDY MUDSTONE

Entire core is moderately to highly fragmented.

Major lithologies:
a. Mudstone to sandy mudstone, greenish gray (5G 5/1) to grayish green (5GY 5/1), with variable reddish gray (5YR 5/2) coloration. Common to abundant compaction lamination, and minor relict depositional structures (wavy, discontinuous lamination; horizontal stratification). Possibly rich in altered volcanic ash. Section 1, 0–80 cm; Section 1, 87 cm, to Section 5; Section 7 to CC.
b. Mudstone to sandy mudstone, greenish gray (5G 5/1) to dusky red (2.5YR 3/2). Compacted pyroclastic sediments, faintly laminated with possible reworked pyroclastic sediments. Section 6.

c. Minor lithology: Sandstone, greenish gray (5G 5/1). Volcaniclastic, fine to coarse grained. Section 1, 80–87 cm.

SMEAR SLIDE SUMMARY (%):

	5, 26 M
TEXTURE:	
Sand	20
Silt	17
Clay	63
COMPOSITION:	
Quartz	5
Clay	63
Accessory minerals	2
Glauconite	25
Zeolites	5

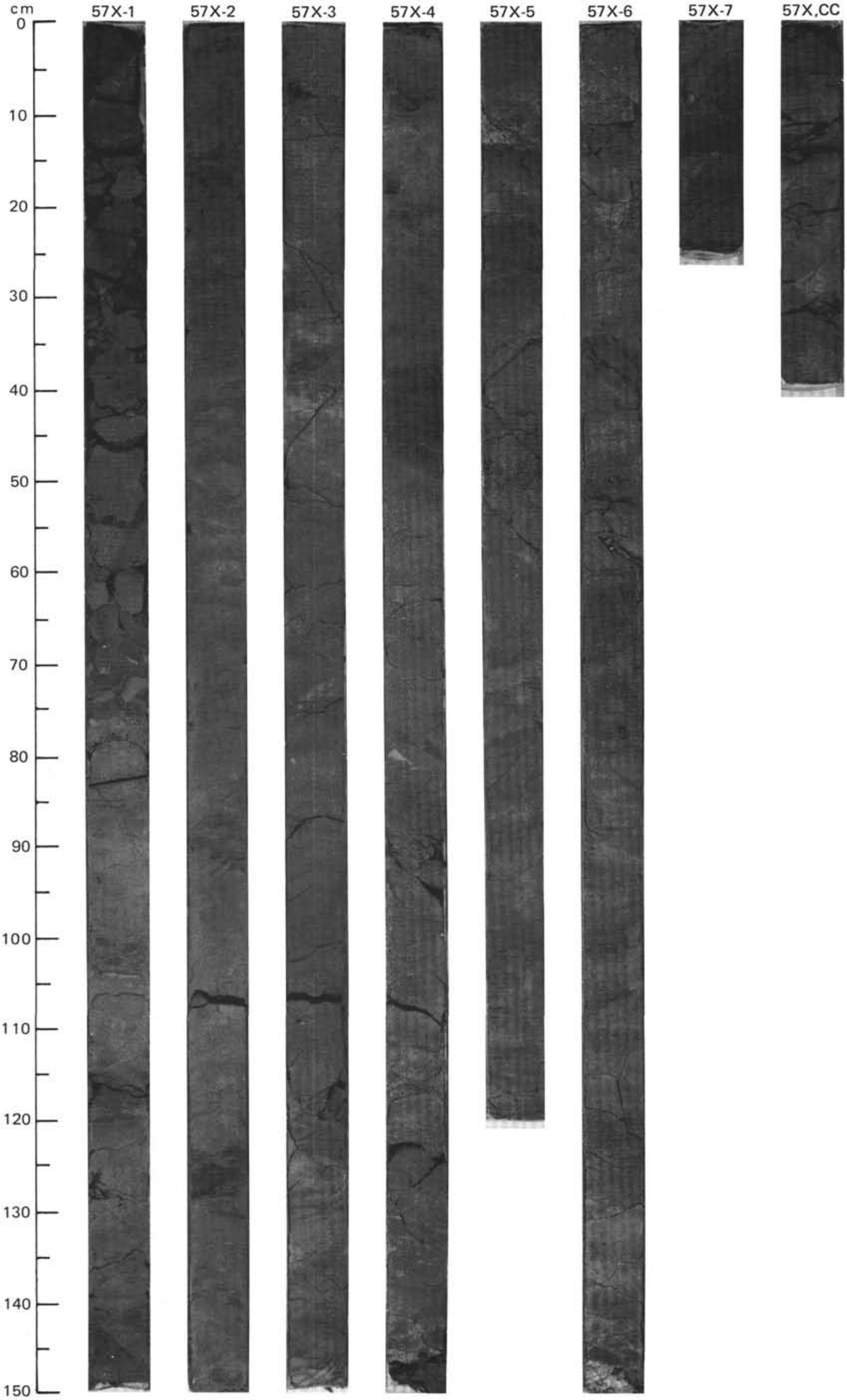
cm
0
10
20
30
40
50
60
70
80
90
100
110
120
130
140
150
57X-1
57X-2
57X-3
57X-4
57X-5
57X-6
57X-7
57X,CC

SITE 643 HOLE A CORE 58M CORED INTERVAL 3325.0-3325.0 mbsl; 545.2-545.2 mbsf

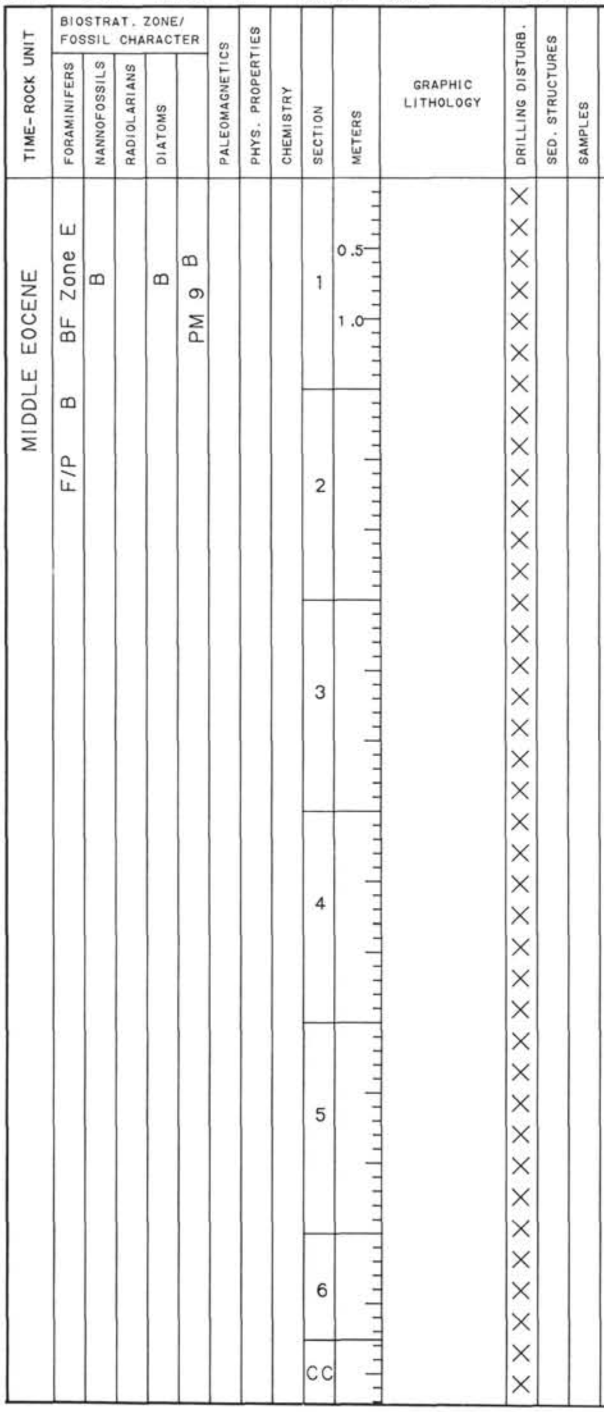

LITHOLOGIC DESCRIPTION

MISCELLANEOUS FILL

Entire core is highly fragmented to drilling breccia.

Sediments consist of a mixture of lithologies contained as fill in hole. Core depth is same as depth of 643A-57.

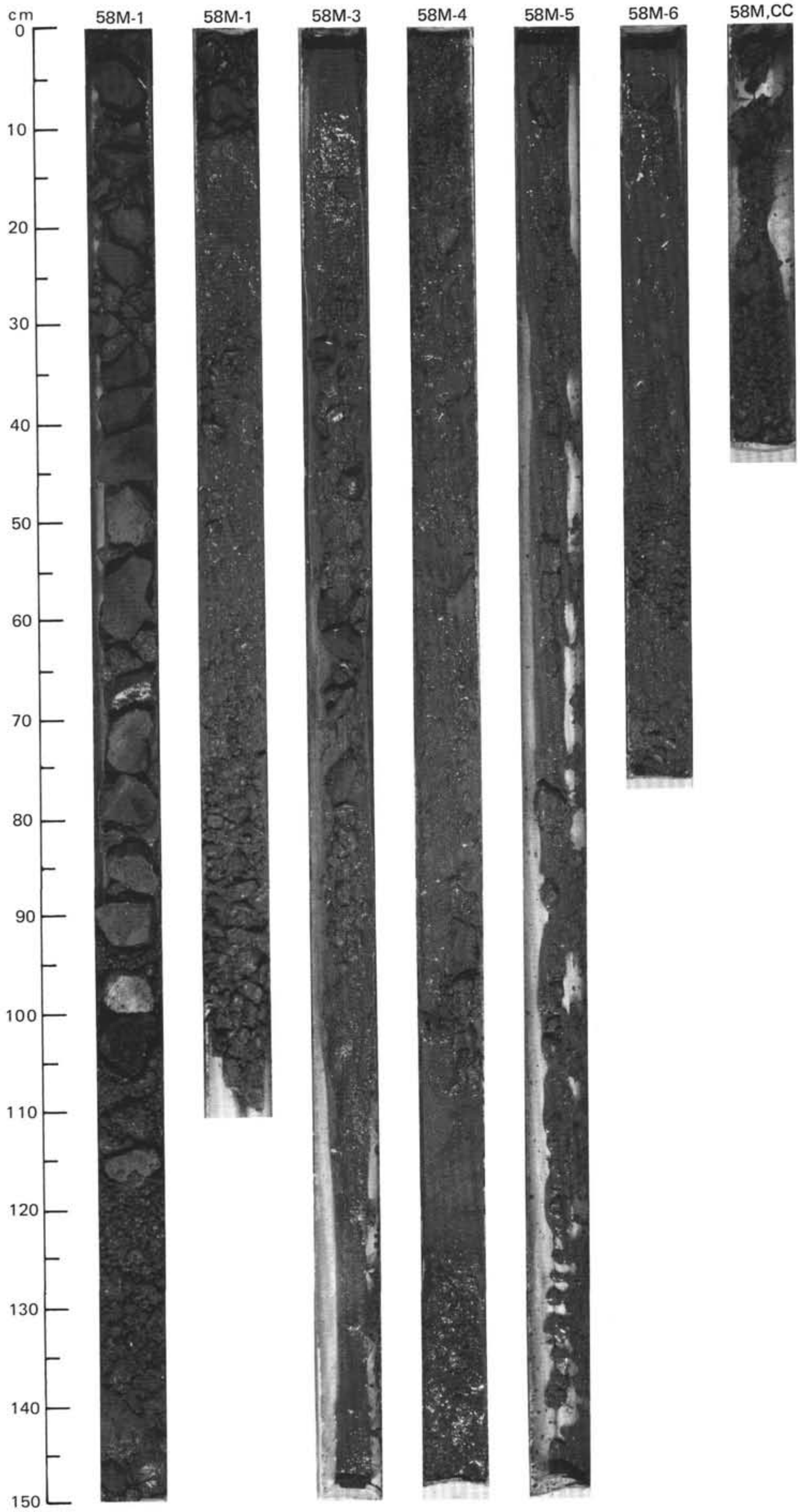
cm
0
10
20
30
40
50
60
70
80
90
100
110
120
130
140
150
58M-1
58M-1
58M-3
58M-4
58M-5
58M-6
58M,CC

SITE 643 HOLE A CORE 59X CORED INTERVAL 3325.0-3334.7 mbsl; 545.2-554.9 mbsf

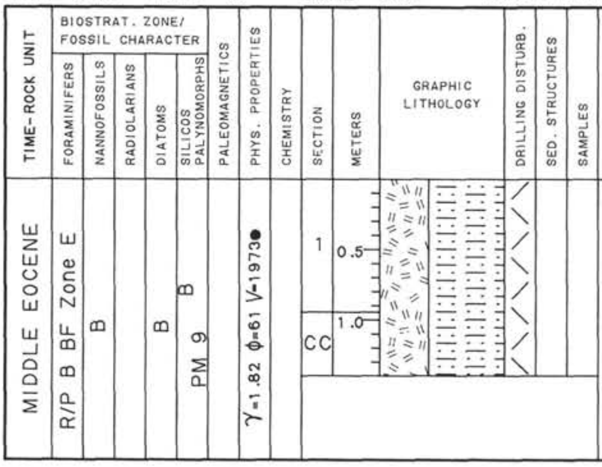

LITHOLOGIC DESCRIPTION

MUDSTONE TO PYROCLASTIC MUDSTONE

Entire core is highly fragmented.

Major lithology: Mudstone to pyroclastic mudstone, greenish gray (5GY 5/1) to reddish gray (5YR 5/2), mottled.

SITE 643 HOLE A CORE 60X CORED INTERVAL 3334.7-3341.0 mbsl; 554.9-561.2 mbsf

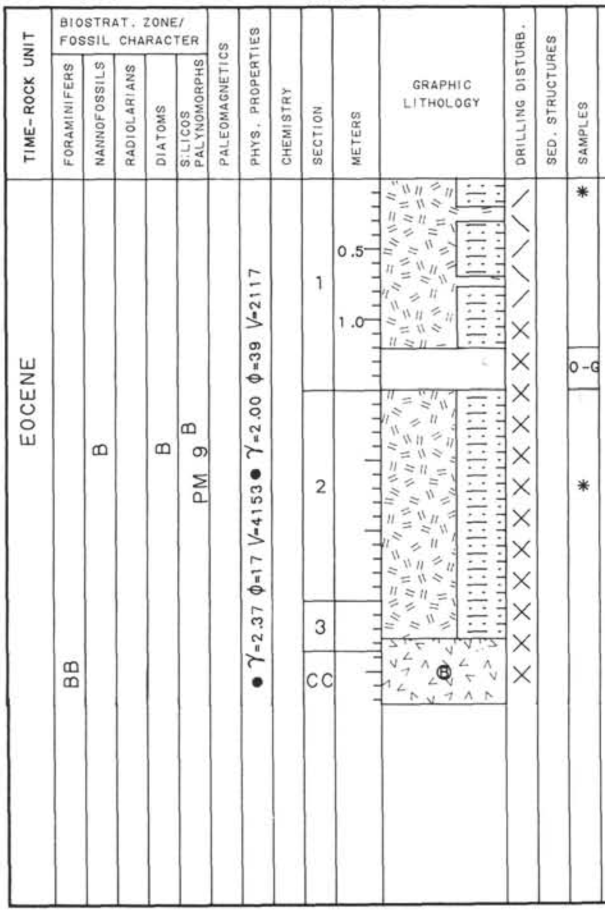

LITHOLOGIC DESCRIPTION

PYROCLASTIC MUDSTONES AND BASALT

Entire core is highly fragmented to completely disturbed (drilling breccia).

Major lithologies:
a. Pyroclastic mudstone, dark olive gray (5Y 3/2), bluish gray (5B 4/2), and greenish gray (5GY 5/1). Coherent blocks ("drilling biscuits") contain some sedimentary structures (parallel laminations; discontinuous, nonparallel laminations, etc.). Section 1 to Section 3, 30 cm.
b. Basalt, dark gray (5Y 4/1), moderately phyric, with filled vesicles. Section 3, 30 cm, to CC.

Minor lithology: Volcanic ash, sandy. Best developed as massive coarse, dark grayish brown (2.5Y 4/2) ash in piece at Section 1, 20–27 cm, and as graded ash bed in piece at Section 1, 70–76 cm.

SMEAR SLIDE SUMMARY (%):

	1, 15 D	2, 61 D
TEXTURE:		
Silt	5	10
Clay	95	90
COMPOSITION:		
Quartz	2	3
Feldspar	3	—
Mica	—	5
Clay	90	90
Volcanic glass	—	2

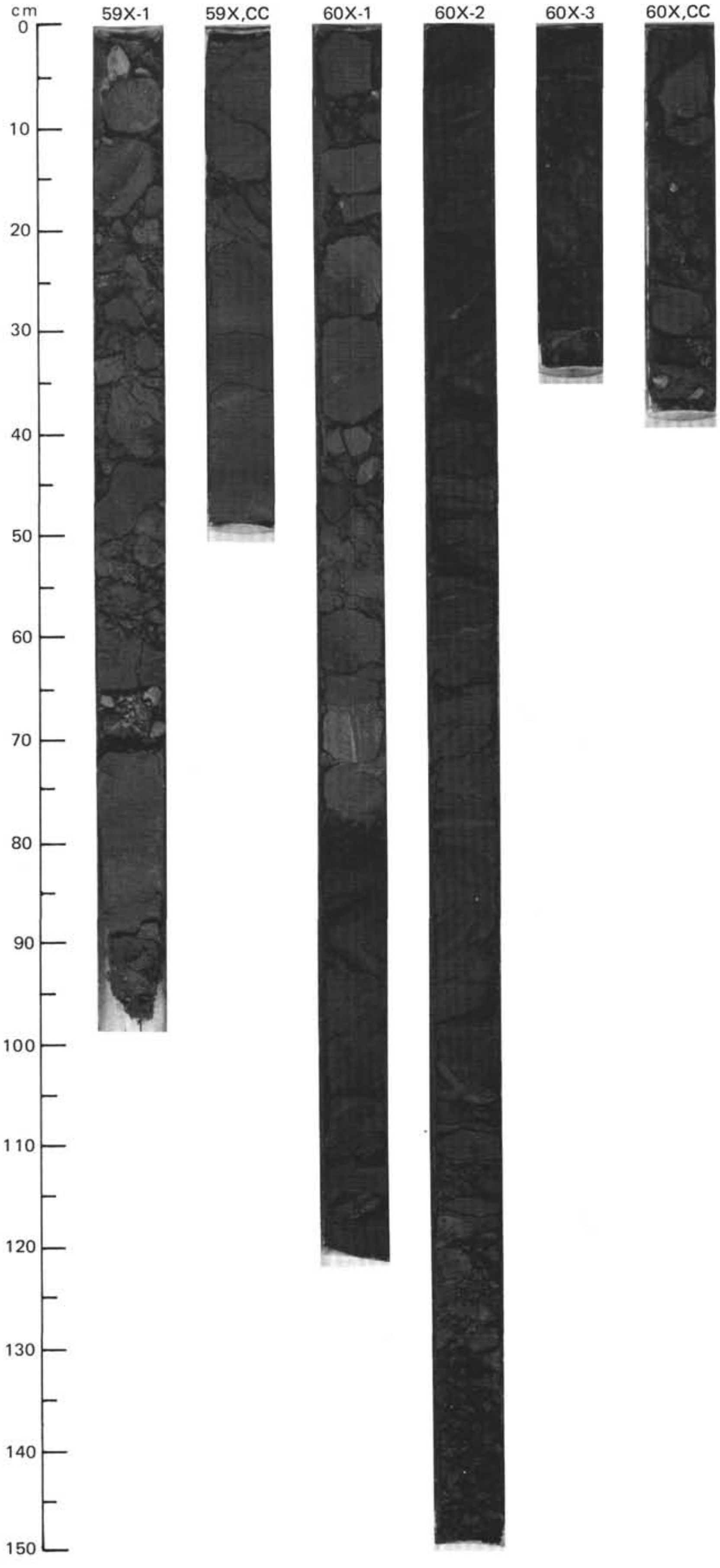
cm
0
10
20
30
40
50
60
70
80
90
100
110
120
130
140
150
59X-1
59X,CC
60X-1
60X-2
60X-3
60X,CC

SITE 643 HOLE A CORE 61X CORED INTERVAL 3341.0-3343.5 mbsl; 561.2-563.7 mbsf

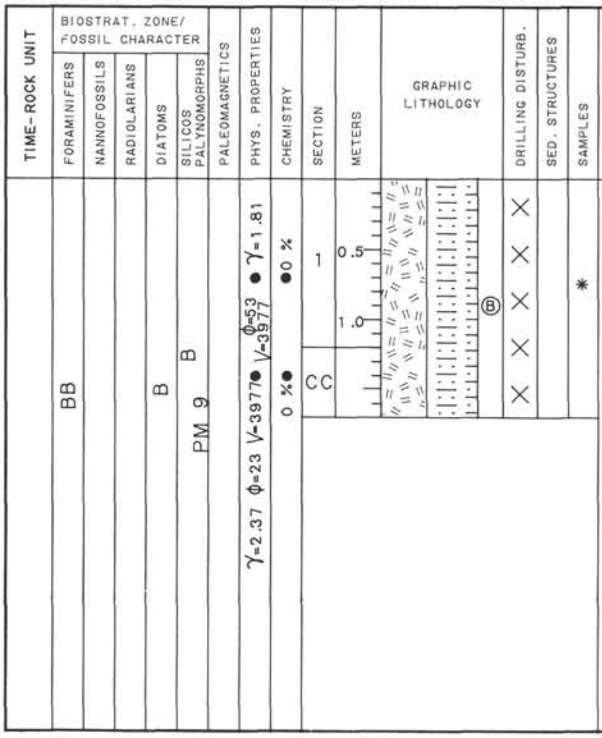

LITHOLOGIC DESCRIPTION

PYROCLASTIC MUDSTONE AND BASALT

Entire core is a drilling breccia.

Major lithologies:
a. Pyroclastic mudstone, dark olive gray (5Y 3/2) to dark greenish gray (5GY 4/1), present as drilling breccia.
b. Basalt, dark gray (5Y 4/1), moderately phyric. Present as drilling breccia.

SMEAR SLIDE SUMMARY (%):

	1, 75 D
TEXTURE:	
Sand	30
Silt	10
Clay	60
COMPOSITION:	
Quartz	10
Mica	2
Clay	65
Volcanic glass	20
Calcite/dolomite	1
Accessory minerals	2

SITE 643 HOLE A CORE 62X CORED INTERVAL 3343.5-3345.0 mbsl; 563.7-565.2 mbsf

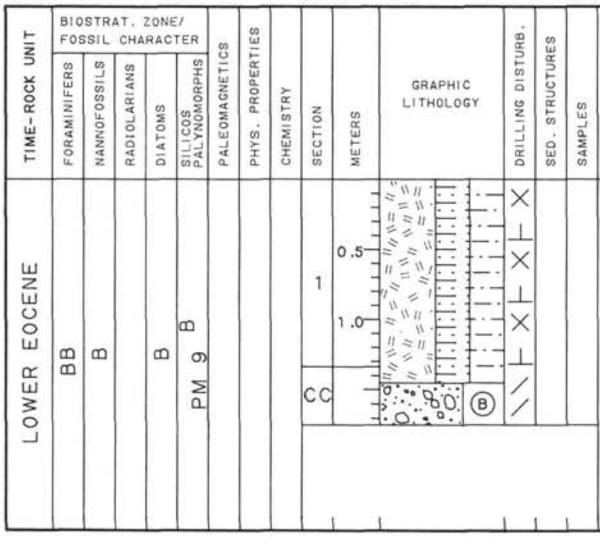

LITHOLOGIC DESCRIPTION

PYROCLASTIC SANDSTONE AND MUDSTONE AND BASALTIC CONGLOMERATE

Section 1, 0–22, 50–77, and 120–135 cm, is drilling breccia. CC, 0–11 cm, is highly fractured. Section 1, 25–50 and 75–100 cm, is moderately fractured. CC, 11–37 cm, is slightly fractured.

Major lithologies:
a. Pyroclastic sandstones and mudstones, dark gray (5Y 4/1) to dark greenish gray (5GY 4/1), moderately to intensely altered. Mudstones show minor mottling, and are commonly overlain by sandstones along sharp, erosional contacts. Sandy mudstones contain a variety of primary structures, including flame structures, cross-lamination, and discontinuous, nonparallel laminations. Sandstones are fine to medium grained, poorly sorted, with abundant matrix. Section 1 to CC, 11 cm.
b. Basaltic conglomerate, dark greenish gray (5GY 4/1) to dusky green (5G 3/2). Clasts are weathered and well rounded, with an average diameter of approximately 2 cm. Clasts are predominantly (~ 80%) basaltic, although one pyroclastic mudstone clast was also observed. Matrix appears to be basaltic in composition, crushed and weathered.

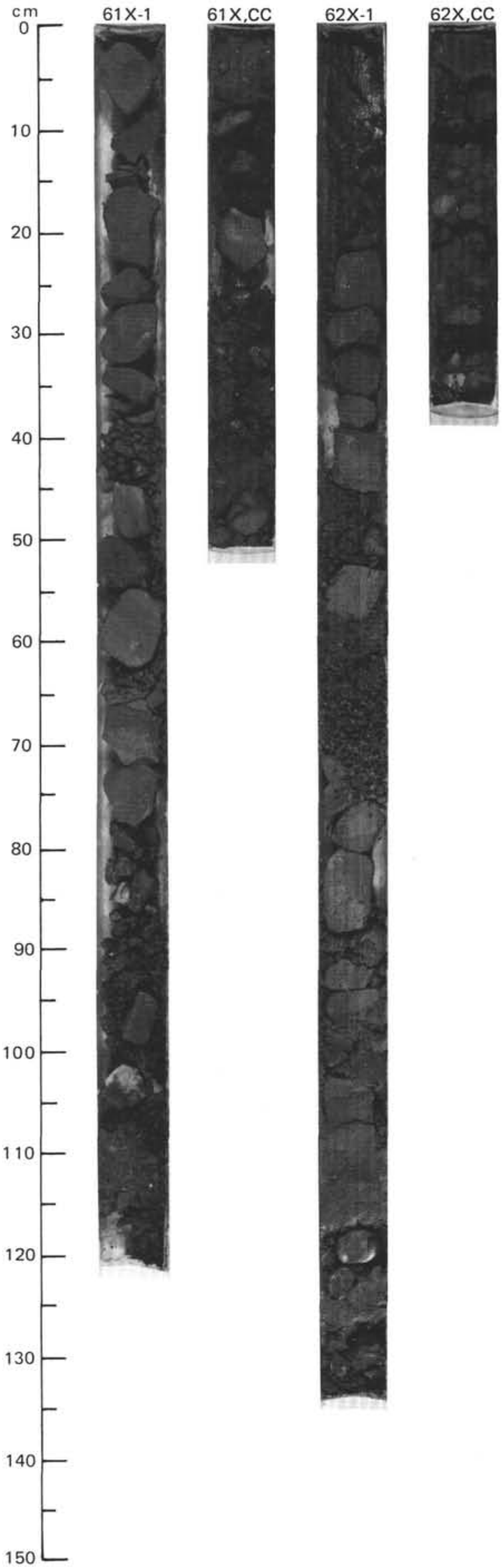
cm
0
10
20
30
40
50
60
70
80
90
100
110
120
130
140
150
61X-1
61X,CC
62X-1
62X,CC